Competitive Grant Program II Projects

Final Report

Project Title: : Production of High Value Cellulase from Tobacco
Award Number: DE-FG-36-05G085013

Recipient: University of Louisville
Project Location: UofL Belknap, HSC, and Owensboro Cancer Center Campuses

Reporting Period: October 15, 2009 – April 15, 2011
Date of Report: June 15, 2011
Written by: R. Eric Berson and Keith Davis

The objectives of this project were to: (1) Develop a plant-based expression system, using tobacco as the host, to produce enhanced, lower-cost cellulose–degrading enzymes. (2) Develop an efficient method for scaling up separation of a single cellulase species, CBH1, from a commercial cellulase cocktail using ion-exchange chromatography.

Task number 1: Express the CBH1 gene in tobacco.

Many competing technologies have been developed to produce recombinant proteins in plants using methods that modify the genetic complement of the production plant species, such that prodigy inherits the foreign gene sequence. Although this method has been shown to provide a robust source of foreign protein expression it does have notable drawbacks. The process of genetic transformation is slow, requiring months to years to derived sufficient seed for significant plantings. Horizontal transmission of the recombinant gene is a concern and therefore complex regulations have been developed to prevent pollen transfer or re-growth of transgenic crops through tissue or seed dispersal. Finally, many food or feed crops are often employed as production hosts leaving significant concerns for contamination of the food supply.

The methods tested here offer a powerful, alternative recombinant protein expression strategy, which provide the significant advantages of plant-based bioreactors, but lacks less desirable properties noted above. Advantages include: (1) lack of contamination by mammalian pathogens; (2) relative ease speed and low cost of genetic manipulation; (3) eukaryotic protein modification machinery; (4) economical production; and (5) minimal endotoxin presence.

The two expression platforms tested were GENEWARE®™ and magnICON. These expression systems are based on the RNA virus, tobacco mosaic virus (TMV), and have proven to be extremely useful in producing exogenous proteins in tobacco. These transient systems offer the advantage of allowing a large number of expression constructs to be rapidly produced and tested at the bench-scale, while also being capable of supporting large-scale commercial production. Tobacco as a host offers the advantages of not being a food crop, thus contamination of food sources is not an issue, and being easy to propagate in either greenhouse or field settings.

The magnICON system, developed by Icon Genetics represents a transient expression system composed of a "deconstructed' TMV-based vector system. This system utilizes introduction of two non-replicating TMV component vectors with a plant-expressed recombinase into plant cells. In this system, virus constructs that do not contain a coat protein gene are introduced into *Agrobacterium tumefaciens* and *A. tumefaciens* is infiltrated into the leaves of tobacco plants (magnification). Upon introduction and delivery to the plant nucleus, the recombinase combines the two TMV components into a complete TMV replicon that is then transiently expressed at high levels. Since this expression system does not require systemic movement of the virus or production of viral particles, it is more efficient in producing larger proteins.

The GENEWARE® expression system uses virus-derived vectors based on the rod-shaped plant virus TMV [19]. TMV has a plus sense single stranded RNA genome of approximately 6,400 nucleotides. TMV virions are rigid rod shaped particles of approximately 18 nm in diameter, and 300 nm in length. Each virion is composed of approximately 2,100 copies of the 17.5 kDa coat protein (CP), helically encapsidating the genomic RNA. The viral proteins involved in RNA replication are directly transcribed from the genomic RNA, whereas expression of internal genes is through the production of subgenomic RNAs. The production of subgenomic RNAs, is controlled by sequences in the TMV genome which function as subgenomic promoters. The CP is translated from a subgenomic RNA and is the most abundant protein and RNA produced in the infected cell. In a TMV infected plant there are several mgs of CP produced per gram of infected tissue. GENEWARE® expression vectors take advantage of both the strength and duration of this promoter's activity to reprogram the translational priorities of the plant host cells so that virus-encoded proteins are synthesized at similar high levels as the TMV CP.

MagnICON

- Deconstructed TMV
  - No coat protein
- Use of three different *Agrobacterium* cultures
  - 5' module (apoplast targeting module)
    - Need apoplast targeting module because our protein lacks the ER signal sequence
  - 3' module (Gene of interest)
  - Site specific recombinase
- Mix the three cultures together and infiltrate plants

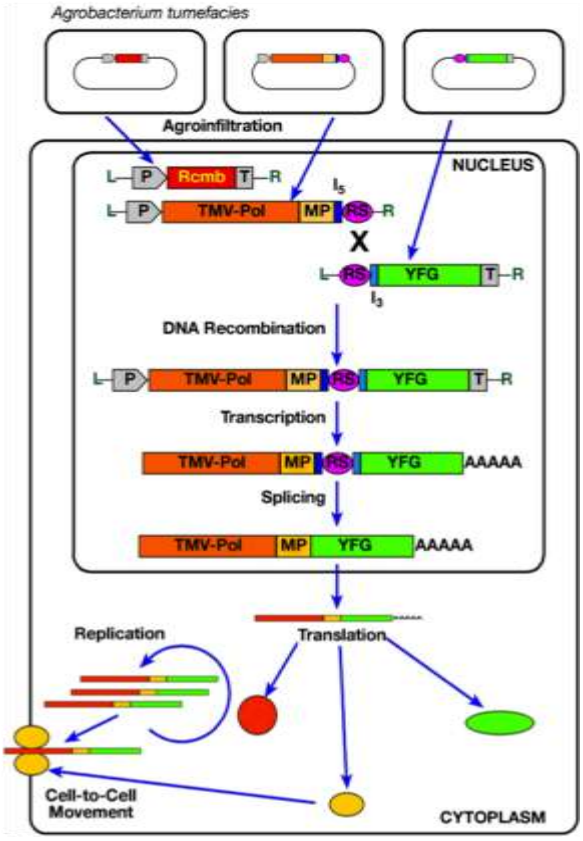

Vacuum Infiltration

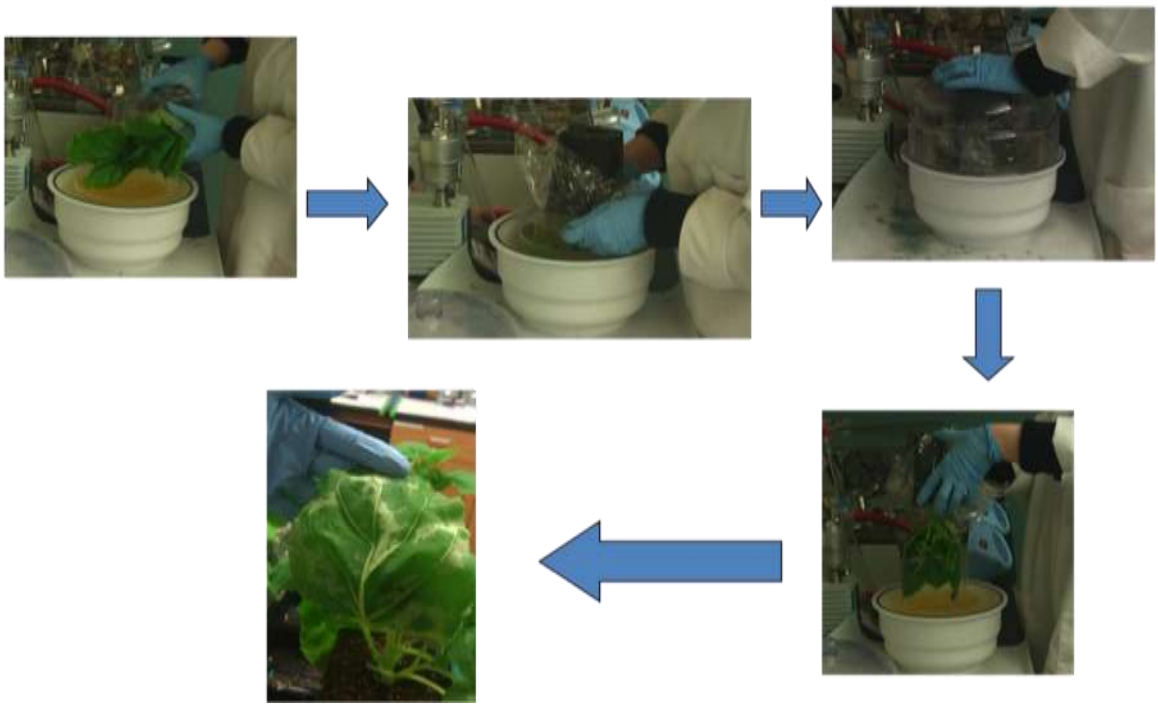

Optimization of Harvest Time and Extraction:

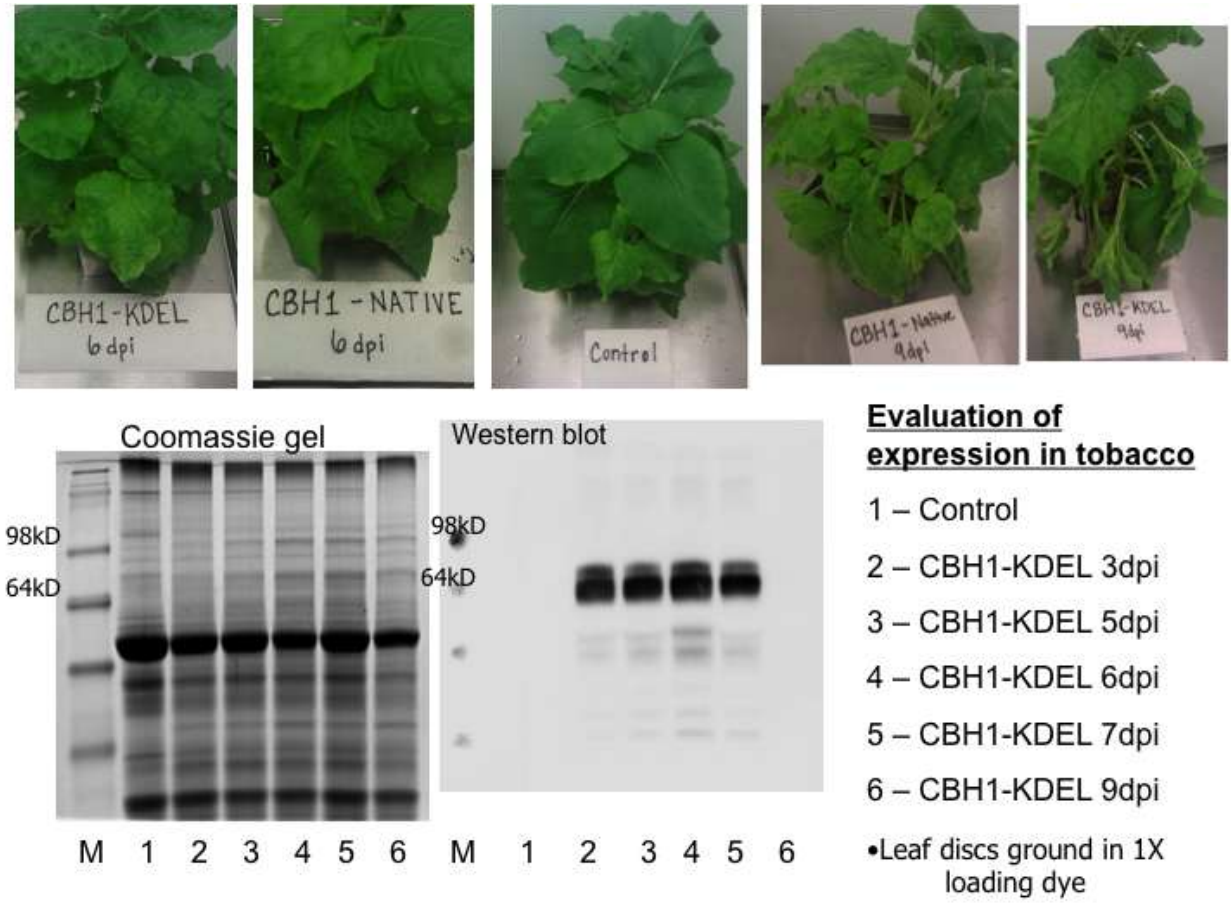

Extraction - Various buffers

- Six buffers at varying pH's tested
- 20mM Acetate buffer, pH 4
- 50mM Citrate buffer, pH 4.8
- 20mM Acetate buffer, pH 5
- PBS, pH 6
- PBS, pH 7.4
- 50mM Tris Base buffer, pH 8

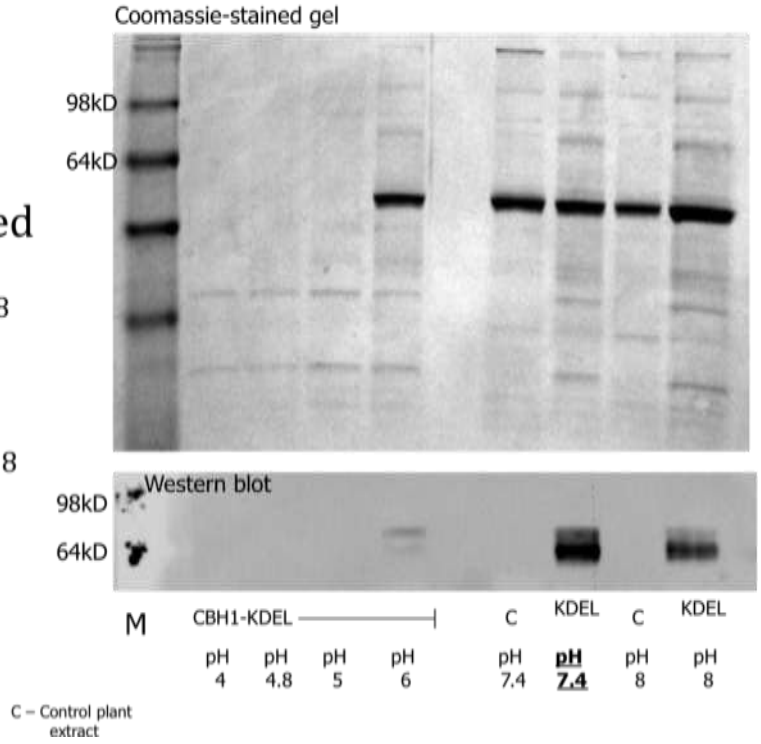

Cellulase Assay:

Concentrated extract for activity assay

- Used 2.5 fold concentrated extract in cellulase assay
- Let samples incubate for longer time periods

- Differences between samples with and without substrate are statistically significant, but the differences between the 8hr and 13hr time point are not.

- Even though there was no time dependence shown between the 8hr and 13hr, there is activity detected within the individual incubations supporting that the plant produced CBH1 is active.

Incubation at 50degC		
Incubation for 8hrs		
Sample	**Avg. Absorbance (400nm)**	
CBH1-KDEL extract	2.9042	**Difference**
		0.39477
CBH1-KDEL extract (no substrate)	2.5095	
CBH1-Native extract	3.4734	
		0.20773
CBH1-Native extract (no substrate)	3.2657	
Incubation for 13hrs		
CBH1-KDEL extract	3.0244	
		0.41683
CBH1-KDEL extract (no substrate)	2.6076	
CBH1-Native extract	3.4609	
		0.20310
CBH1-Native extract (no substrate)	3.2590	

GENEWARE (performed by KBP):

KBP

1. Digested CBH1-KDEL and CBH1-Native genes out of GeneArt synthesized plasmid DNA.
2. Digested aprotinin out of GENEWARE to obtain the GENEWARE backbone alone.
3. Ligated each CBH1 gene into the GENEWARE vector to generate desired construct.

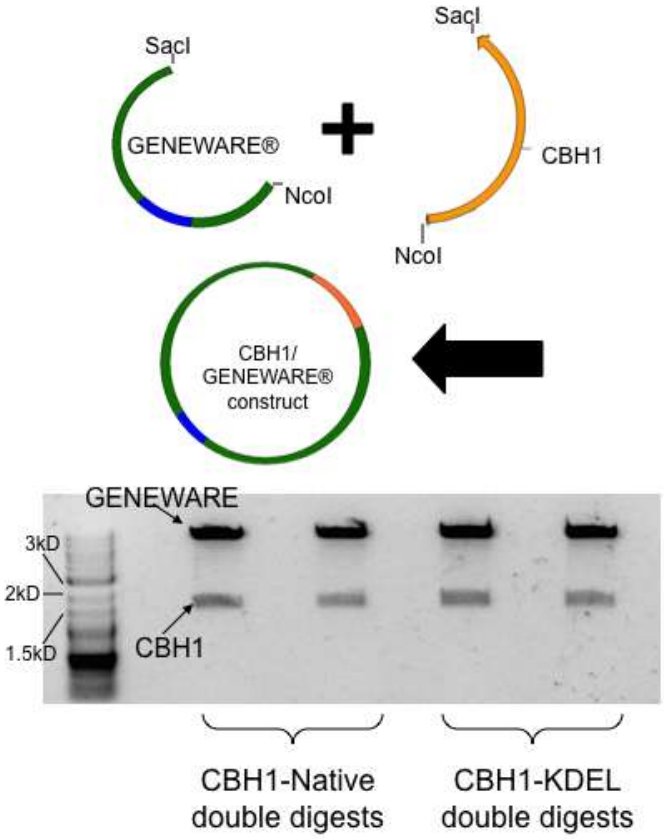

KBP

- Our data suggests that attempting to express CBH1-KDEL using the GENEWARE® system induces a hypersensitivity response from the plant. By observing characteristics of the plant after inoculation and no detection in extract by Western blot, expressing CBH1 using the GENEWARE® system will not be beneficial.

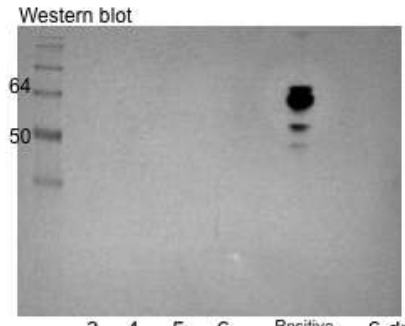

6dpi CBH1-KDEL N.benth GENEWARE®

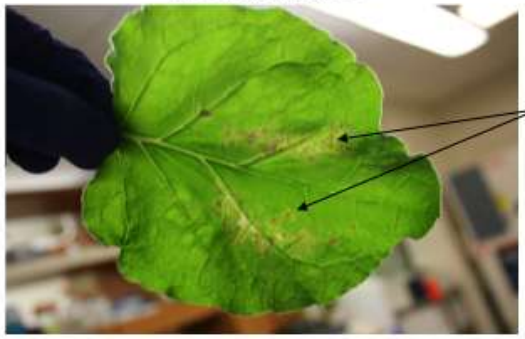

N.benth Control plant

7dpi CBH1-KDEL N.benth GENEWARE®

Summary:

With the magnICON system, CBH1 was successfully reproduced at scale in the tobacco leaves. The extracted enzyme showed significant activity towards pNPC substrate.

The GENEWARE system induce a hypersensitivity response in the plant. The enzyme was not detected in the extract.

Task number 2: Scaled-up separation of CBH1 from a commercial cellulase cocktail.

Enzymatic hydrolysis of cellulose often involves cellulases produced by *Trichoderma reesei* (*T. reesei*), of which Cellobiohydrolase1 (CBH1) is the most abundant (about 60% of total cellulases) and plays an important role in the hydrolysis of crystalline cellulose. A method for separating sufficient quantities from the bulk cellulase cocktail is highly desirable for many studies, such as those that aim to characterize binding and hydrolysis kinetics of CBH1. In this work, CBH1 was separated from other Spezyme CP cellulases by ion exchange chromatography using an efficient modification of a smaller scale process. The ion exchange column was connected to a vacuum manifold system to provide a steady flow through parallel columns and thus achieve scale-up for enzyme separation.

The modification here employed a straightforward way to scale up the process by maintaining the same column length while increasing the effective cross-sectional area by operating multiple columns in parallel. The process is easily further scalable by adding more columns in parallel. To test the feasibility of this scale-up method, the purity and specific p-nitrophenyl-β-D-cellobioside (pNPC) activity of CBH1 were examined and compared to CBH1 separated conventionally with a FPLC system. Stability was also tested, and adsorption and hydrolysis of bacterial microcrystalline cellulose (BMCC) were performed with the CBH1 separated from the scaled-up process.

The ion exchange column (5 ml HiTrap Q HP column) was connected to a VM 20 vacuum manifold (Sigma-Aldrich Co.; St. Louis, MO) to achieve a pressure differential for enzyme separation. A flow route of the separation system is shown in Figure 1 (a) on the following page.

This manifold system required step elution in place of the continuous gradient. Following loading of 29 mg of CBH1 (in 10 mM TEA-HCl pH 7.6 buffer) onto each anion column, 10 ml of 0.1 M, 15 ml of 0.25 M, or 8 ml of 0.33 M sodium chloride in 20 mM TEA-HCl pH 7.0 buffer were applied to elute the protein successively following a wash of the column with 20 ml of 20 mM TEA-HCl pH 7.0 buffer. The purified CBH1 was collected in the fraction eluted with the buffer containing 0.33 M salt. The protocol is summarized in the following Table. With this manifold system (Figure 1b), scale-up can be easily achieved by simply connecting several columns in parallel (5 columns were connected to vacuum manifold in this study).

Step	Species	Quantity (per column)
1	Spezyme CP cellulases	~30 mg
2	20 mM TEA-HCl pH 7.0 buffer (to wash column)	20 ml
3	0.1M salt in 20 mM TEA-HCl pH 7.0 buffers	10 ml
4	0.25 M salt in 20 mM TEA-HCl pH 7.0 buffers	15 ml
5	0.33 M salt in 20 mM TEA-HCl pH 7.0 buffers	8 ml

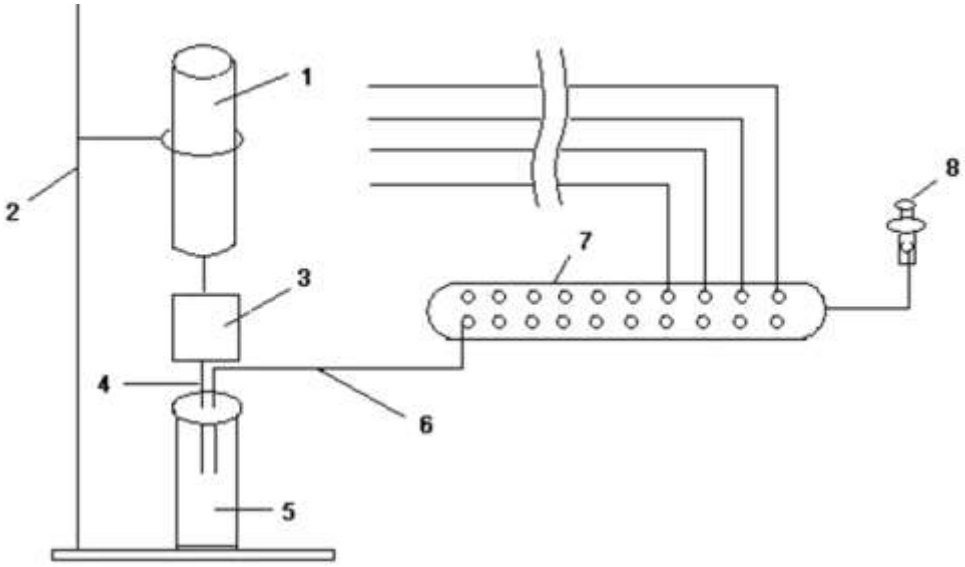

1. syringe 2. holder 3. column 4. sample loop
5. fraction collector 6. vacumn loop 7. VM 20 vacumn manifold
8. vacumn pump

(a)

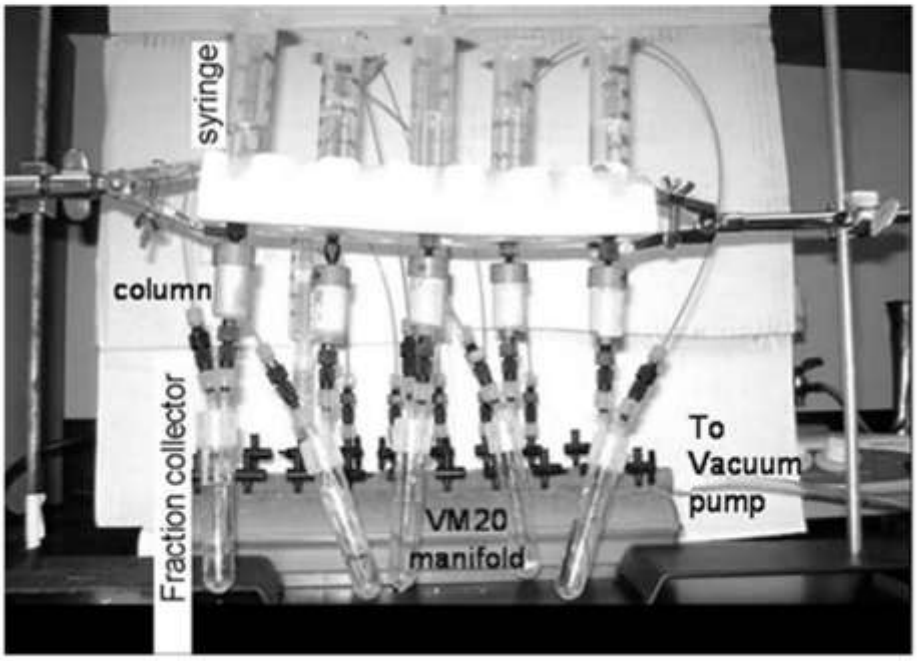

(b)

Figure 1. (Description on the following page)

Figure 1. Scaled-up separation by a vacuum manifold system. (a) Flow route of the system. The syringe is used to store buffers and is connected to a column by a 1/16" female luer syringe fitting (GE Healthcare Bio Sciences AB; Uppsala, Sweden). The column connects to the fraction collector by a sample loop consisting of a 1/16 female/M6 male union (GE Healthcare Bio Sciences AB; Uppsala, Sweden) and Luer lock adapter, M6 female-male (Sigma-Aldrich Co.; St. Louis, MO) and needle in that order. Any well sealed sterile tubes can be used as fraction collectors (For example, 15 ml centrifuge tube). They are connected to the VM 20 vacuum manifold by the vacuum loop consisting of a needle, Luer lock adapter, 1/16 female/M6 male union, 10-32 thread (Sigma-Aldrich Co.; St. Louis, MO), 1/16 IN O.D., 0.03 In I.D peek tubing (Sigma-Aldrich Co.; St. Louis, MO), M6 female-male Pk10 peek one piece finger-tight fittings, 1/16 female/M6 male union and Luer lock adapter in that order. (b) Experimental set up of the scaled-up vacuum manifold separation system.

Task 2 Summary:

CBH1 separation from Spezyme CP cellulases was successfully scaled-up by incorporating a vacuum manifold system and step elution to an ionic chromatography method. The CBH1 separated by this technique exhibited comparable purity and yield to CBH1 separated on a smaller scale by a conventional FPLC system. With five columns running in parallel, about 55 mg CBH1 was separated from 145 mg Spezyme CP cellulases at once, and the system can be easily scaled-up further by adding additional columns. Separated CBH1 was identified as a single band on the SDS-PAGE gel, and showed good stability during a 2-day incubation at 50 ^{o}C. It had a maximum adsorption on BMCC of about 4 μmol/g, and a K_a of 5.55 μM^{-1}. The activity of CBH1 towards pNPC from the scaled-up system (0.052 U/mg) was comparable to that measured in a FPLC (0.047 U/mg) and as reported elsewhere. The degradation of BMCC by CBH1 was fast as determined by real-time imaging with an AFM. The maximum of fiber height was reduced from 45 nm initially to about 8 nm after enzymatic hydrolysis of 2.5 hour, which is about 80% reduction. The results suggest that CBH1 separated by this system is of good quality for studying CBH1/substrate interactions, and this separation protocol can facilitate research in the investigation of CBH1 interactions with cellulose by providing large-scale quantities of purified CBH1, which is an important component in the study of enzymatic hydrolysis of cellulose. Moreover, the vacuum manifold system can be setup for less than 10% of the cost of a FPLC system.

Publications / Presentations:

1. Manuscript on scaled-up separations accepted for publication in *Biotechnology Progress.* Expected in print late summer of early fall 2011.

2. Manuscript for enzyme expression in tobacco plant in preparation.

3. Material presented at the 2011 Symposium on Biotechnology for Fuels and Chemicals, May 2011, Seattle WA.

Cost Effective Energy Efficient School Design –Applied Research

FUNDED UNDER KREC

FINAL REPORT

W. Mark McGinley, Ph. D., PE, FASTM 502-852-4068 – m.mcginley@louisville.edu
Department of Civil and Environmental Engineering, University of Louisville

July 2011

ABSTRACT: Cost Effective Energy Efficient School Design –Applied Research

Significant effort has been focused on the sustainable and energy efficient design of school buildings over the past few years. This effort has culminated in a number of design guidelines such as Leadership in Energy and Environmental Design (LEED) for Schools-New Construction and Major Renovations, and the Kentucky Green and Healthy Schools Design Guidelines. These design provisions go a long way in providing guidance to design professionals and school officials on what areas in the facility design might be addressed to improve the performance of the facility. However, there appears to be a reluctance to embrace these "Green" or "Energy Efficient" designs, partially due to the perception that these designs will cost a lot more than traditional systems. For instance, we typically build schools with concrete and brick masonry walls. This is done since the masonry is relatively low cost, durable and easy to maintain. Recent developments in energy efficient school design has been moving schools to the use of higher first cost building systems that may have higher maintenance costs and are being questioned relative to their fire resistance and indoor environmental impact.

The goal of this project was to use the design guidelines discussed above and develop a list of low life cycle cost systems that can be used to meet the energy efficiency and sustainability goals of the State of Kentucky. Specially, the study focused on evaluating building envelope systems, day-lighting, and heating and cooling system configurations that have, or could be, incorporated into school designs. For each system, a sample design was developed and used to compile a construction cost estimate. Each of the systems will be incorporated into a typical prototype middle school configuration and the effects each system has on the overall energy used over the life cycle of the building was determined using the eQuest analysis program, for five typical Kentucky climates. This data will be used to develop a relationship between each of the systems described above, their life cycle costs and the effect each has on energy use. Variation in each system design will be performed in an effort to minimize lifecycle costs with as little reduction in energy efficiency as possible. Conventional materials and construction practices where used where feasible.

The results show that most significant energy savings can be achieved using more efficient mechanical equipment, control systems and lighting systems. Increases in thermal resistance of the building envelope beyond code minimums, both for opaque walls and fenestrations, does not produce significant reductions in the yearly energy use of the prototype building evaluated in this investigation, at least for the range of climates experienced in Kentucky. Large increases in thermal resistance do not correspond to similar reductions in energy use, and the simple payback periods for these improvements are typically in excess of 100 years. It should be noted that the above conclusions are restricted to mass exterior wall systems and the thermal resistance of light gauge steel faring walls must be quite high (in excess of R = 35) to produce similar results.

Using conventional mass masonry wall systems and roof systems insulated to the code prescriptive minimums, conventional gas fired boilers, a conventional VAV HVAC System with chiller and efficient lighting, and aggressive control strategies result in EUI reductions from 50% to 60% from code minimum performance. Almost 80% reductions in energy use are achieved when ground source heat pumps are used with similar configurations

The economic analysis suggests that simple payback using the conventional HVAC systems with aggressive controls are less than 3 years and this is only slightly increased when interest and typical energy cost increases are accounted for. Use of ground source heat pumps increase the payback period to over 25 years. Improvements in the building envelopes generally have long payback periods (over 100 years) and do not appear to improve the payback periods of the ground source heat pump systems.).

Table of Contents

Cost Effective Energy Efficient School Design

1.0 Introduction

1.1 Problem Statement

I was reported in 2008, that Kentucky uses significant amounts of energy, well above the national average in all segments of the State's economy. Much of this high energy use is being attributed to State's low energy costs resulting in there being little economic incentive to conserve energy [Bashear, 2008]. Bashear goes on to report that Kentucky's energy use is expected to rise to more than 40 percent over current levels by the year 2025. This significant increase in energy demand will likely not only increase energy costs, but could potentially result in a large increase in green-house gas emissions in the State, significantly impacting quality of life and the State's economic health. To address this projected energy and environmental concern, the government of Kentucky has developed a seven point strategic plan that calls for 25 percent of the energy needs of the state in the year 2025 to be met by energy conservation efforts and renewable energy sources. In fact, Strategy 1 of this plan is to reduce protected energy needs by 18 percent through increased energy efficiencies.

Although the commercial sector only accounts for about 17 % of the state's energy consumption and only about 30 percent of this energy use is associated with education institutions [Iyer, et-al, 2007], a significant amount of effort has been focused on improving the energy efficiencies of K-12 institutions. In fact, the recently passed House Bill 2 has mandated that all K-12 schools in Kentucky enroll in the Kentucky

Energy Efficiency Program for Schools (KEEPS) by January 2010. Kentucky state government has also allocated significant funding for this effort and the programmed goal is to reduce energy consumption in this sector by 10 %. This focus on energy use in schools is due in part to the fact that, next to personnel, K-12 school systems spend more on energy that any other operating expense [USDOE-OEERE, 2007]. Reducing energy costs allow more of the tight education budgets to be spent in class room enhancing the education experience.

In support of this effort, the Kentucky education cabinet has developed a design manual for Green and Healthy Schools that addresses criteria similar to those in the Leadership in Energy and Environmental Design (LEED) design provisions for schools. Approximately 20 design criteria are addressed in this manual and about a third of these provisions are directed to reducing the energy used by school facilities [KEEC, 2008].

In addition to the benefits that lower energy use has for the state economy and environment, studies have found that there is a strong relationship between building condition and student performance. Schools with better interior environments substantially increase student achievement and less absenteeism [Evans, 2004], [ASHRAE,2008], [USDOE,2003].

Although significant effort has been focused on the sustainable and energy efficient design of school buildings over the past few years, there appears to be a reluctance to embrace these “Green” or “Energy Efficient” designs, partially due to the perception that these designs will cost a lot more than traditional systems. For instance, we typically

build schools with concrete and brick masonry walls. This is done since the masonry is relatively low cost, durable and there is a long history of its use with these types of structures. Recent developments in energy efficient school design has been moving schools to the use of higher first cost building systems that may have higher maintenance costs and are being questioned relative to their fire resistance and indoor environmental impact. Higher construction costs are a concern on the part of some designers and school officials where traditional school construction costs range from \$80 to \$125/ ft^2. In addition, the relatively low cost of energy in Kentucky and resulting long payback periods, appears to be impacting wide spread adoption of these energy efficient building systems in new school designs. This concern appears to be, in part at least, why school buildings are exempt from the new high performance building design provisions that were recently adopted in Kentucky House Bill 2.

Finally, analysis and field measurements show that majority of the energy used in school facilities is associated with the heating, cooling and lighting [USDOE,2003]. Since the interior heating and cooling loads depend on the building envelop characteristics, in combination with external and internal environmental loads, the building design needs to address all in a holistic manner. In fact, most building systems interact with one another so that optimum building system design must address the holistic behavior of the school facility if it is to be effective [ASHRAE, 2008][USDOE,2003]. However, designs are often not evaluated in a holistic manner due to the nature of the traditional design process.

2.0 Proposed Investigation

In an effort to improve the adoption of energy-efficient strategies in new school designs, a research investigation was conducted. The goals of this investigation are discussed in the following sections. In addition to the project objectives and anticipated benefits the work plan is also presented.

2.1 Project Objectives

The goal of this project is to develop a list of low life cycle cost systems (both first cost and maintenance costs) that can be used to meet, at least in part, the energy efficiency and sustainability goals of the State of Kentucky. This effort is to produce a list of sample building system designs, their costs, their relative advantages and disadvantages, and their impact with respect to the energy performance and the sustainability of schools. This list is to be presented in a format that can be reviewed by designers and school officials to quickly assess which systems might be implemented to reduce energy use, at the least cost, and thereby increase the adoption of energy saving, sustainable building systems into new school construction. In support of this list will be short summaries that discuss each building system, strategies on how to optimize the first cost while maintaining energy efficiency, system durability and expected maintenance performance.

Additional benefits of this investigation are:

1. To provide a holistic evaluation of the energy efficient technologies in typical Kentucky school applications.

2. To compare the cost of implementation versus energy use reduction savings so that not only can payback periods be reduced, but so the greatest reduction in energy use can be achieved with the least amount of capital and/or life cycle costs.
3. Provide recommendations for design and system development for cost effective energy efficient building system for schools.

2.2 Plan of Work

Specially, the study focuses on evaluating building envelope systems, day-lighting and heating and cooling system configurations that have, or could be, incorporated into school designs. A prototype school design was developed with a limited number of sample building system designs and used to compile a construction cost estimates. A variety of energy efficient systems/measures were incorporated into the typical "prototype" middle school building configuration and the effects each system had on the overall energy used over the life cycle of the building was determined using the eQuest energy analysis program.

This prototype school was selected from published prototype designs such as the School Design Clearing house developed by the North Carolina School Planning Section of the North Carolina Department of Public Instruction [NC SPS, 2008]. This clearing house was developed to assist North Carolina school districts, architects and designers in the planning and design of high quality schools in this state. The prototype school was selected so that it had both single story and two story sections and thus

enabled some of the investigation results to be applied to high school and elementary school configurations as well.

The maintenance costs of each system were also estimated over the life of the facility. This data was used to develop capital and life cycle cost of each system configuration and the effect each has on energy use. Where appropriate, a variety of system characteristics were used to look at the effect these characteristics had on the energy use in an effort to optimize the energy performance with costs.

To achieve the goals described above, the following tasks were conducted:

1. A survey of school boards, designers, manufactures, and contractors was conducted to determine the state of the art with respect to energy efficient design for education structures in similar climatic regions of the United States. It was expected that these technologies would include, ground source heat pump systems, day-lighting, thermal mass and high R building envelope systems, thermal storage systems, ariable illumination controls and occupancy sensors on lights and HVAC systems, night- time ventilation and others. The objective of this task was to establish a list of mature energy efficient technologies that have, or could be, applied to educational facility construction.
2. A survey of school systems, education officials, contractors and designers was conducted where energy efficient building systems have been used to determine how these systems are performing and to develop a data base of actual

construction costs. This effort was directed at developing a data base of maintenance costs and expected life cycle for each of technologies investigated.

3. A typical (prototype) one and two story middle school facility was developed. This task built on earlier efforts of the Kentucky Department of Education and others [NC SPS, 2008].
4. The typical middle school design was developed sufficiently using conventional systems designed to the code allowed prescriptive minimum values. The energy use performance of this facility was then analyzed using the DOE 2.0 based eQuest analysis program. These energy analyses were conducted using a range of environmental loads representative of the range expected for these facilities in the state of Kentucky. This energy data was also used to develop operating costs for each facility. The results from this analysis were compared/calibrated against national averages for buildings of similar type using American Society of Heating, Refrigerating and Air-Conditioning Engineers (ASHRAE) and Department of Energy (DOE) publications. This was done to establish a base line energy use estimate for the prototype school facility in each location.
5. The results from Steps 4 was compared to ASHRAE and DOE data for similar facilities and the models were adjusted as necessary to bring the results in line with average expected energy performance.
6. A construction cost estimate was compiled for the facility.
7. The list of technologies/ building configurations developed in Step 1 were evaluated and a number of technologies/ configurations most likely to impact

energy use (with the least cost) were developed sufficiently to conduct both an energy analysis and an incremental construction cost estimate for each of the building prototypes and environmental loadings.

8. Variations on the technology/ building configurations analyzed in Step 7 were done to attempt to optimize each system with respect to energy efficiency and costs. These system variations focused on using conventional systems wherever possible due to the lower costs associated with these systems. For each variation, an energy analysis and incremental cost estimate was conducted for each of the the building configurations. Since lighting uses 25- 40 % of the energy in school construction and produces a significant thermal load [DOE, 2003], a specific focus of this effort was to optimize the application of day-lighting into the classrooms using systems that minimize overall system costs, reduce thermal loading and envelope effects, and increase the beneficial effects of natural light on the teaching environment (ASHRAE, 2008],[DOE 2003].
9. Based on the construction cost estimates, energy use data, and estimates of the maintenance costs, a total relative cost was developed for each building configuration and system variation. Both a 50 and 75 year design life was evaluated. This evaluation was conducted using a both simple pay back and cash flow analyses.
10. Using the data developed in Steps 1 through 9, relationships were established between capital costs and yearly energy saved, and between relative costs and total energy saved over the same period. This analysis was also used to

establish payback periods for each technology and building configuration based on the base line established in Steps 4 through 6.

11. An evaluation of the relationships established in Step 10 was conducted to establish the most cost effective energy saving technologies
12. Tables were developed comparing the energy efficient technologies, their performance in a typical school, their overall effectiveness and their costs.

3.0 Identification of Energy Conservation Measures/Systems

The purpose of the first two tasks in the work plan was to identify mature technologies and systems that have been applied to the design of school facilities. Using the guidelines established by the US Department of Energy, ASHRAE and others [Evans, 2004], [ASHRAE,2008], [USDOE,2003], [KEEC, 2008], a list of mature energy efficient technologies and strategies that could, or had been used, to improve the energy efficiency of School facilities was developed. This list was used to develop two survey forms (see Appendix A) that were used to solicit input from the design, construction and facility management communities in Kentucky and surrounding areas. These forms were distributed at a number of seminars on energy efficient design of wall systems given by the principal investigator to architectural design offices, AIA continuing education seminars and workshops. These forms were also distributed to select energy designers and school facility managers. It was felt that this direct approach would improve the feed-back obtained during the survey. It also allowed information to be solicited directly and verbally from the seminar attendees. A list of seminars given and attended by the Principal Investigator is shown in Table 1.

Due to poor response to the written survey forms (only two were completed and turned in) the principal investigator contacted select school facility managers to solicit their input. Further, individuals at the Kentucky Energy Efficiency Program for Schools (KEEPS) were also contacted and solicited for their input. KEEPS is a center that is housed at the University of Louisville that was created to help Kentucky school districts reduce energy consumption and lower operating expenses.

Finally, two students in the Mechanical Engineering department at the University of Louisville were hired to support the project efforts. These two students work part time for a Kentucky consulting engineering firm, Ameresco Inc. in Louisville, KY. This firm specializes in energy management and energy efficiency investigations on facilities, including schools. The two students were able to engage the input from a team of engineers with significant experience in the application of energy conservation measures as well as input from contractors who routinely install these energy efficient building systems.

Table 1 – Information Gathering Efforts

Venue	Location	Date	Attendees
High Efficiency Wall Design Seminar– AIA Lunch and Learn-Sherman Carter Barnhart	Louisville, KY	Nov. 5, 2009	Architects, Engineers
High Efficiency Wall Design Seminar– AIA Lunch and Learn-Sherman Carter Barnhart	Lexington KY	Jan. 13th, 2010	Architects, Engineers
High Efficiency Wall Design Seminar– AIA Lunch and Learn-SHP Design Group	Cincinnati OH,	Jan 29. 2010	Architects- project managers
High Performance Exterior Wall Design Seminar - AIA Educational Seminar-OMA Annual Meeting	Dublin OH	Feb. 10, 2010	Architects, School Facility Managers
High Performance Sustainable School Work Shop, NEEDS	Lexington KY	March 24, 2010	Architects, School Facility Managers, Engineers, Suppliers
High Performance Wall Designs AIA East Kentucky CSI EKC Trade Show	Lexington KY	June 2, 2010	Architects, Project Managers, Construction Specifiers
High Efficiency Exterior Wall Design Seminar - AIA Learn to Earn Seminar	Lexington KY	June 22, 2010	Architects
Meeting at Kovert Hawkins Architects	Jefferson, IN	June 16, 2010	Architects
High Efficiency Exterior Wall Design - AIA Learn to Earn	Louisville KY	June 23, 2010	Architects
High Performance Wall Design Seminar–AIA Lunch and Learn-Luckett and Farley Design Group	Louisville KY	Oct. 4, 2010	Architects
High Efficiency Exterior Wall Design Seminar - AIA Educational Seminar	Indianapolis IN	March 5, 2010	Architects, Contractors

Based on the input from this group a list of common energy saving technologies and systems were identified. In addition, the range of characteristics typical for these systems such as thermal resistance, efficiencies, etc., were developed. These systems and characteristic ranges are believed to encompass the range of systems routinely considered during the design of school systems in the state of Kentucky. Table 2 lists the general type of energy saving technologies and systems identified during this effort. These systems included higher efficiency thermal building envelop systems, higher

efficiency heating ventilating and air conditioning (HVAC) systems, higher efficiency lighting systems, day lighting, occupancy sensors used to control lights and a variety of control strategies and systems.

Table 2 Common Types of Energy Efficient Building Systems used in School Systems in Kentucky

Building Systems	**Remarks/ Variations**
Wall System Type	Highly insulated masonry cavity walls, Insulated Concrete form Walls, Highly insulated brick veneer
Exterior Window	A variety of high efficiency windows are used.
Day lighting	Use of day lighting with sensor controls
High Efficiency Lighting	Standard and High output T8 fluorescent lamps are commonly used.
Air Barriers	Use of controlled ventilation and airtight construction.
High thermal Resistance Building Envelopes	Both Roof and Walls with varying thermal resistance are used, up to R 26
High efficiency HVAC systems	Use of high efficient HVAC systems, higher efficiency VAV systems, energy recovery systems, ground source heat pumps
Advanced controls and Sensors	Use of sensors and control systems to reduce HVAC run time, increase set-backs and improve HVAC efficiency.
Building Orientation	Placement of elevation with fewer openings in the northern direction.

Note that there have been a few recently designed and constructed schools that have designed to reduce the use of energy to levels that could be supported using wind power, photovoltaic power systems and a variety of less common heating and cooling systems. These systems, while growing in acceptance in the industry, are not routinely adopted due to their relatively high capital costs and the lack of familiarity of the

designers with these systems. As a result, these systems were not deemed sufficiently mature to be addressed in this study.

The above list was used to develop a number of alternative designs for the base school design described in the subsequent sections of this report.

4.0 Prototype Base School Design

Figure 1 shows an aerial view of the Wakefield Middle School that is posted on the School Design Clearing House [NC SPS, 2008] web site. The posted plans for this facility were used as the basis for the prototype school facility evaluated in this investigation. Figures 2 through 8 show the plans, elevation ad typical wall/roof section of a 158,000 ft^2 prototype structure that was used as the base school design.

Figure 1 Aerial View of the Wakefield Middle School

This design was selected since it contained a two story classroom section, a one story administration section, a gymnasium, a cafeteria and an auditorium. The design also contains two major axes of symmetry and has fewer windows on the north elevation.

The facility design also used exterior masonry brick and block cavity walls, and both sloped metal and flat membrane roofing systems. Many of these elements are also common in elementary and high school designs and would thus allow the results of this investigation to be applied to these types of buildings as well. It should be noted that the Wakefield Middle School facility was actually constructed in 1997 in North Carolina for a bid price of $14,500,000, at a cost of approximately $92/ft^2.

Figure 2 First Floor Plan of Prototype Base Building

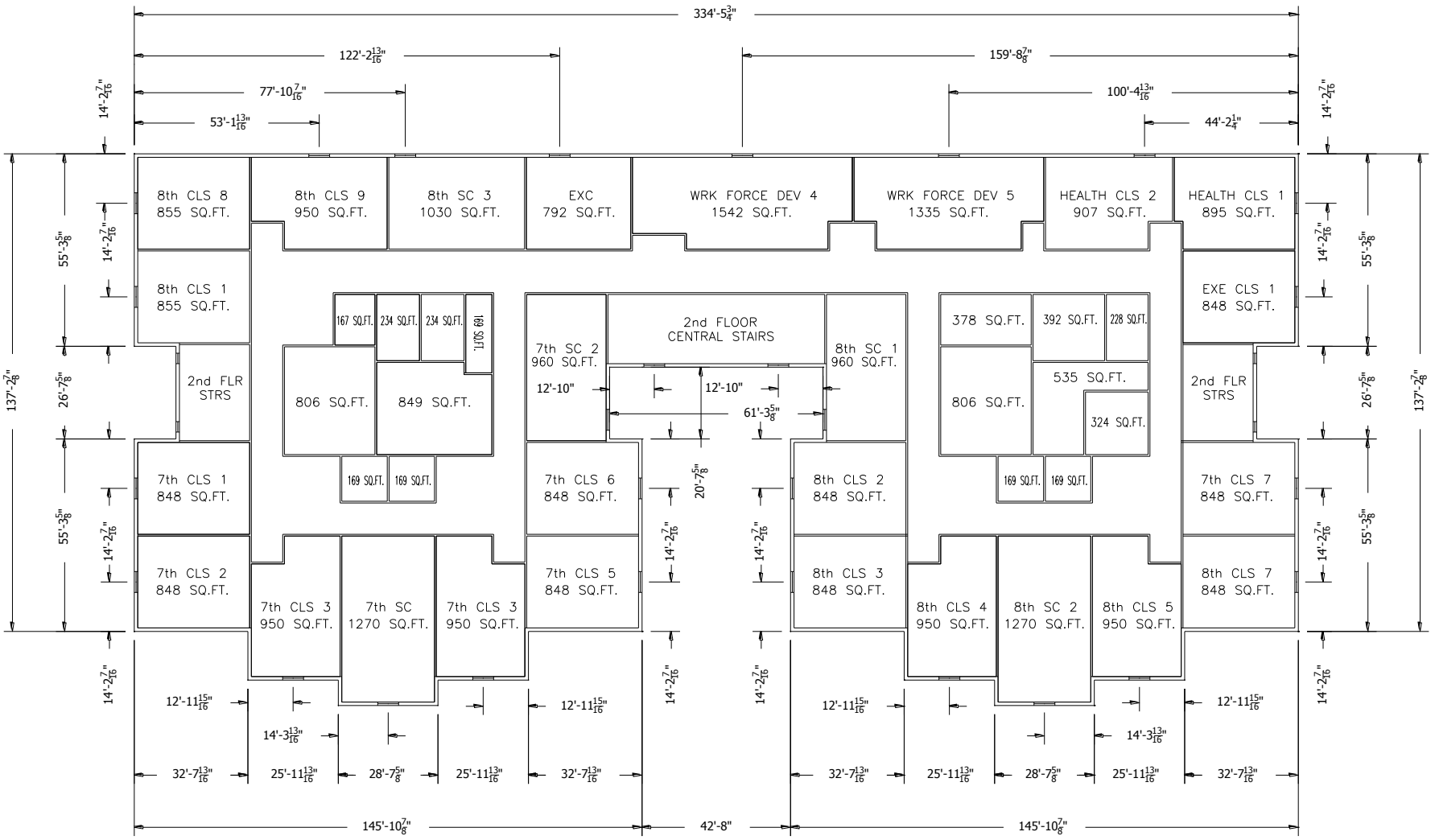

Figure 3 Second Floor Plan of Prototype Base Building

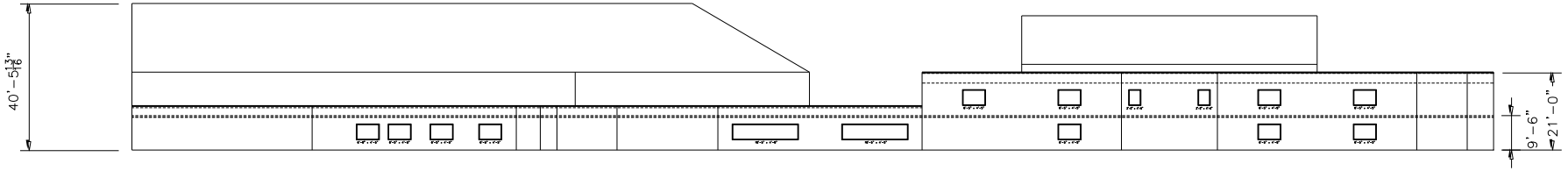

Figure 4 West Elevation of Prototype Base Building

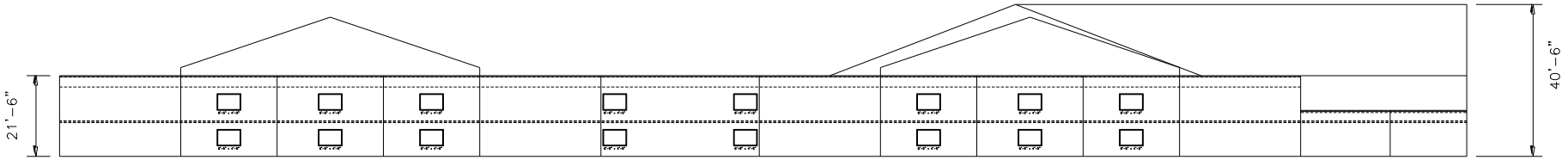

Figure 5 South Elevation of Prototype Base Building

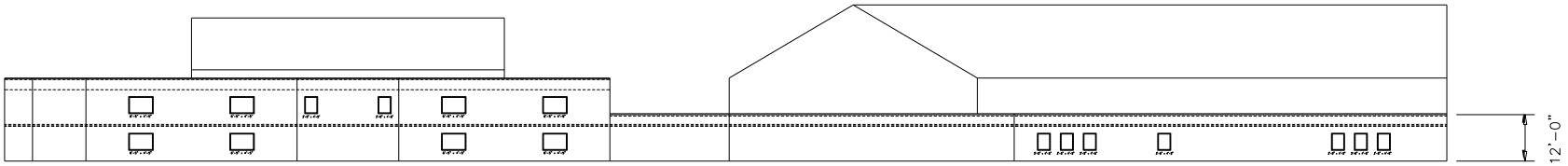

Figure 6 East Elevation of Prototype Base Building

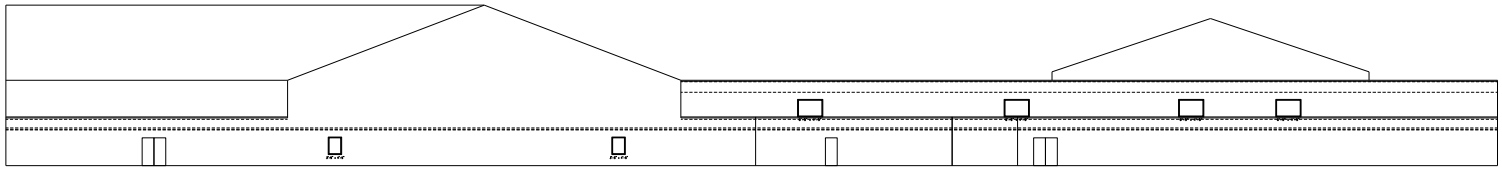

Figure 7 North Elevation of Prototype Base Building

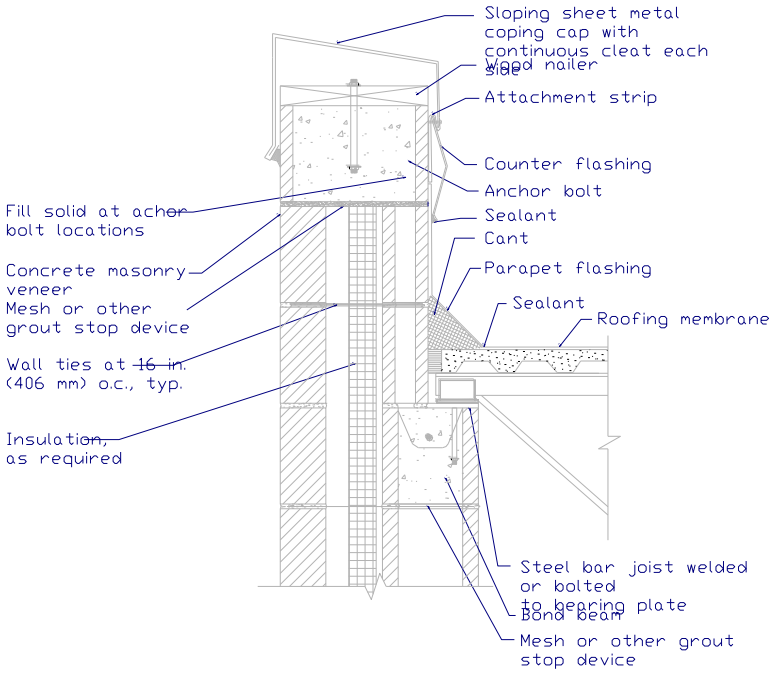

Figure 8 Typical Flat Roof and Exterior Masonry Cavity Wall

Section4.1 Design of Baseline Model

Since most school construction in Kentucky has traditionally used masonry construction for its wall systems, it was felt that an exterior masonry cavity wall system would be representative of construction for most schools and was therefore used for the base line building.

To provide a reasonable base line to compare the performance of various energy conservation strategies in a typical school design, the base building was designed to the minimums allowed in the prescriptive requirements described in the ASHRAE 90.1 ANSI/ASHRAE/IESNA Standard 90.1-2007 Energy Standards for Buildings; Except Low-Rise Residential Buildings. This design approach was chosen since it was assumed that it would be the minimum standard that the facility would be typically designed for. It should be noted that the ASHRAE standard is listed as one of the design alternatives allowed by the energy code (IECC) referenced by the International Building code [IBC,2009], [IEEC, 2009] and the prescriptive provisions in both documents are similar.

To meet the prescriptive thermal properties listed in the ASHRAE standard, the exterior wall construction from outside to inside was assumed to consist of 4" red masonry brick, a 1" air space, 1 ¼" polystyrene rigid insulation, and a 8" concrete masonry unit backing wall (CMU). It was also assumed that all the interior walls were 8" CMU's, since this is quite common for school design due to the high fire resistance of these systems, durability, low maintenance and low sound transmittance. The sloped roof construction

from outside to inside was assumed to consist of a standing seam metal roof system, building paper felt, 3” polyisocyanurate insulation, and steel framing at 2’ spacing. The flat roofing construction from outside to inside was assumed to be a white single ply roofing material, 3” polyisocyanurate insulation, 5/8” plywood sheathing, and steel framing at a 2’ spacing. The ceiling was assumed to consist of a lay-in acoustic tile with no batt insulation. It was also assumed that there are two types of doors, steel urethane foam core and single pane glass doors. The windows are assumed to be clear double pane operable windows with the code minimum allowed thermal transmittance (U) values.

As prescribed in ASHRAE 90.1, it was assumed that the HVAC system in the baseline building was a Variable Air Volume (VAV) system, with hot water reheat at the VAV boxes. A VAV HVAC system is efficient and modulates air flow based on load and temperature set-points. This type of system is also capable of running on a preset thermostat set-point schedule which will reduce or increase the temperatures outside comfort levels during expected unoccupied times. The ASHRAE 90.1 standard states that the baseline HVAC system must be capable of supporting temperature set-backs. This temperature reduction/increase is known as a temperature set-back (TSB) schedule. For the baseline configuration, the TSB schedule is based on a heating temperature of 72°F and a cooling temperature of 74°F during the occupied times and during the unoccupied times, the heating temperature is set to 64°F and the cooling temperature is set to 80°F.

Using traditional design approaches and systems, the base HVAC system was designed and consisted of six standard variable air volume (VAV) units that are used to serve various areas of the school. Each VAV unit was assumed to have multiple VAV boxes, serving individual zones. Hot and cold air was mixed at each VAV box to maintain room temperature within the comfort zone. Cooling was provided by chilled water that was produced from a water cooled, electric centrifugal hermetic chiller. Heating was provided by a forced draft natural gas boiler. The base line HVAC system controls were set up to send out 55°F air to each VAV box and the hot water coils in the VAV box were designed to heat up the air, if local heating is required. If cooling is required, the hot water coil valve at the VAV box is closed. This operation allows simultaneous heating and cooling year round in different areas of the building, and is found in many school facilities today because it provides very good comfort and has relatively low construction costs.

Finally, even though the most new school designs use the more efficient T8 fluorescent lighting fixtures with electronic ballasts, the effect of using these more efficient lights was investigated by using T 12 fluorescent lamp with magnetic ballasts as the main lighting systems for the baseline building. A standard W/ft^2 is used to define the lighting loads for a given area type (eQquest default values were used). It was also assumed that the Gym used metal halide pendant lamp systems. For the cost estimates, typical lamp wattages were used to determine the total number of fixtures in a given area.

5.0 Energy Analysis

The eQuest 3.64 Energy Analysis program [DOE, 2010] was used to analyze the school building. This program uses the DOE 2.0 analysis engine to simulate the yearly energy use in building systems using typical external weather conditions and interior loading schedules.

For all analyses, the eQuest default school occupancy schedules were used. This placed the primary building use during week days, between 8:00 am and 3:00 pm. The school year is typically between September through June and very low occupancy loads were assumed for the summer months of July and August.

To simulate the range of climates that a school designed in Kentucky might experience, the base school and each change in the facility configuration was analyzed assuming the structure was sited either in Louisville, Lexington, Covington, Paducah or Corbin/Williamsburg.

The following section of this report describes the base school energy analyses. Subsequent sections describe the modifications made in the building systems to address potential energy conservation measures and the effects that these modifications have on the energy consumption of the facility.

5.1 Design of Baseline Model and Analysis Results

The baseline heating and cooling system was set up to maintain a constant temperature between 72°F and 74°F during occupied hours. During unoccupied periods in the winter the temperature is allowed to lower to 64°F and during unoccupied periods in the summer the temperature is allowed to raise to 82°F. The HVAC systems were assumed to operate 24 hours a day, 7 days a week, even though the occupancy on the week days is assumed to be from 8 a.m. to 3 p.m., and 9 a.m. to 2 p.m. through the summer. The VAV boxes are equipped with dampers so that when the room temperature demand is satisfied they are allowed to close down to 40% for the core zones and 30% for the perimeter zones. The VAV boxes aren't allowed to fully close because CO_2 levels may rise to unacceptably high levels during occupied periods. Code provisions require that outside air must be supplied to each area of the building during occupied periods of the day. Economizers are installed on each VAV system to provide cooling when the outside air temperature is below 65°F. Domestic hot water is provided by a 940 gallon natural gas water heater.

The baseline building information was entered into eQuest, program using the information described previously and an energy simulation was performed to determine the yearly energy consumption of the facility. Figure 9 shows the graphical representation of the eQest base model and Table 3 summarizes additional critical building systems information. The building energy use performance was simulated using the average hourly weather data for each of the five cities in Kentucky.

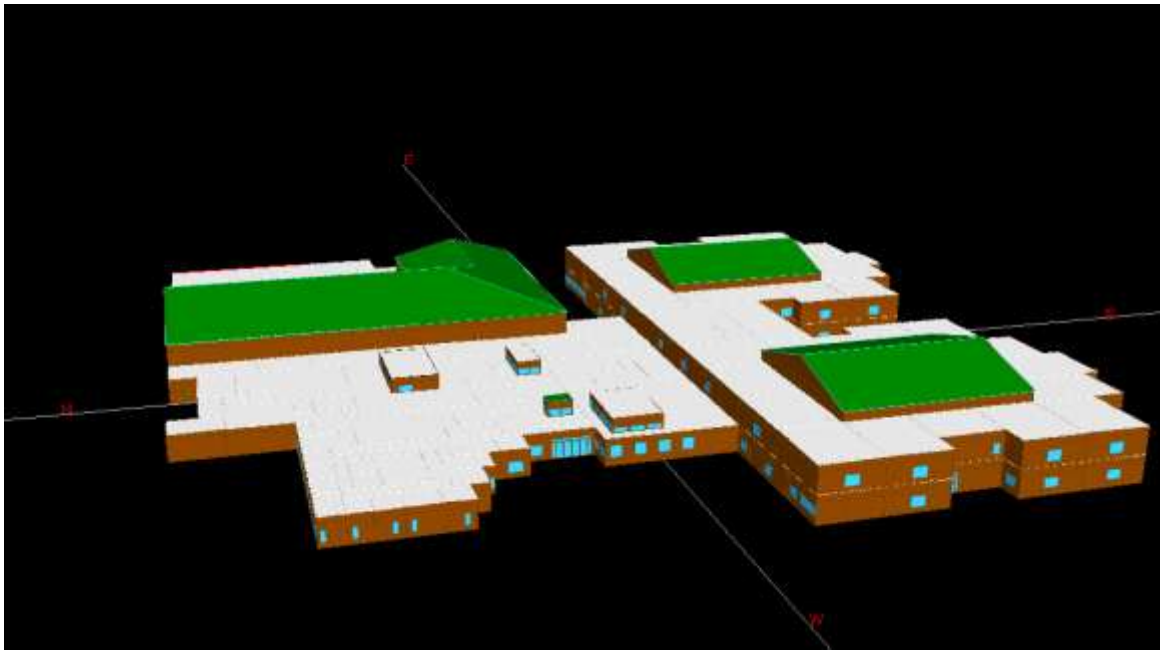

Figure 9. Image of the Base Middle School eQuest Model.

Table 3 Additional Base Building Configuration Information (R in ft^2°F-h/Btu, U Btu/ ft^2°F-h)

Building System	Description
Exterior walls	R=9.09, layers: outside air film, 4" brick, air space, 1-1/4" polystyrene 8"CMU MW hollow, air film
Pitched Roof	R-22.22, layers: outside air film, steel siding, Bldg paper felt, 3" polyisocyanerate, steel siding, inside air film
Built Up Roof	R-26.3, layers: outside air film, Built up roof, 3" polyisocyanerate, 5/8" plywood, metal decking
Ceilings	R-1.95, layers: 1/2" Acoustic tile
Interior walls	R-3.75, layers: inside air film, 8"CMU MW hollow, inside air film
Interior floor	R=1.94, layers: inside air film, 6" MW Conc
Ground floor	R-2.59, layers: inside air film, linoleum, 6" MW conc, inside air film, Stone
Sub floor (in Mechanical areas in Gabled Sections)	R-16.67, layers: AFlr Cons Mat 1, Acoustic tile
Exterior Wall Infiltration	0.5 Air changes per hour
Window/Frame U values	0.54/0.64
VAV HVAC Unit 1 -	22 tons
VAV HVAC Unit 2	129 tons
VAV HVAC Unit 3	127 tons
VAV HVAC Unit 4	174 tons
VAV HVAC Unit 5	178 tons
VAV HVAC Unit 6	25 tons
VAV – Fan Coil Units (boxes)	178 units

Figure 10 shows the monthly electrical energy use predicted by the eQuest analysis for the base building configuration located in Louisville. Figure 11 shows the natural gas usage for the same conditions. Figure 12 shows how the typical electrical usage brakes down with specific device use. It is clear from this figure that the vast majority of the electrical energy is used by the HVAC system and lighting.

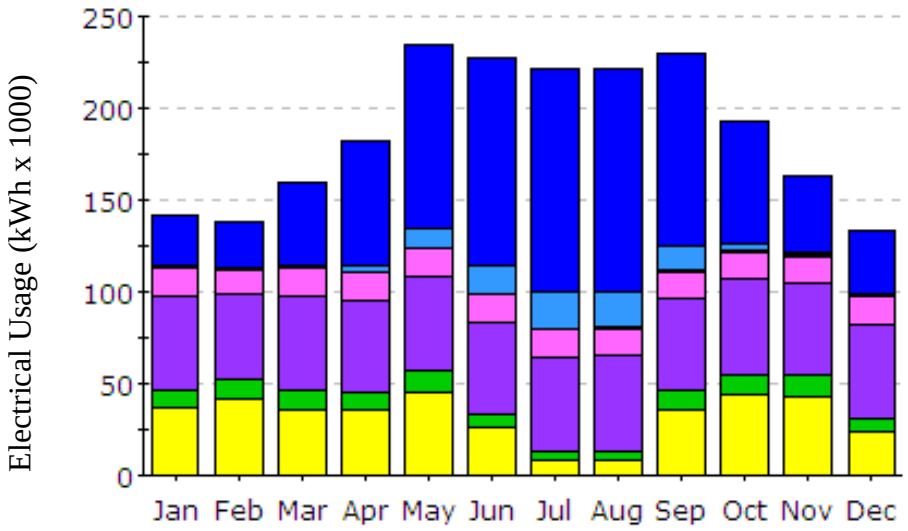

Figure 10. The Baseline Monthly Electrical Usage Profile (Louisville)

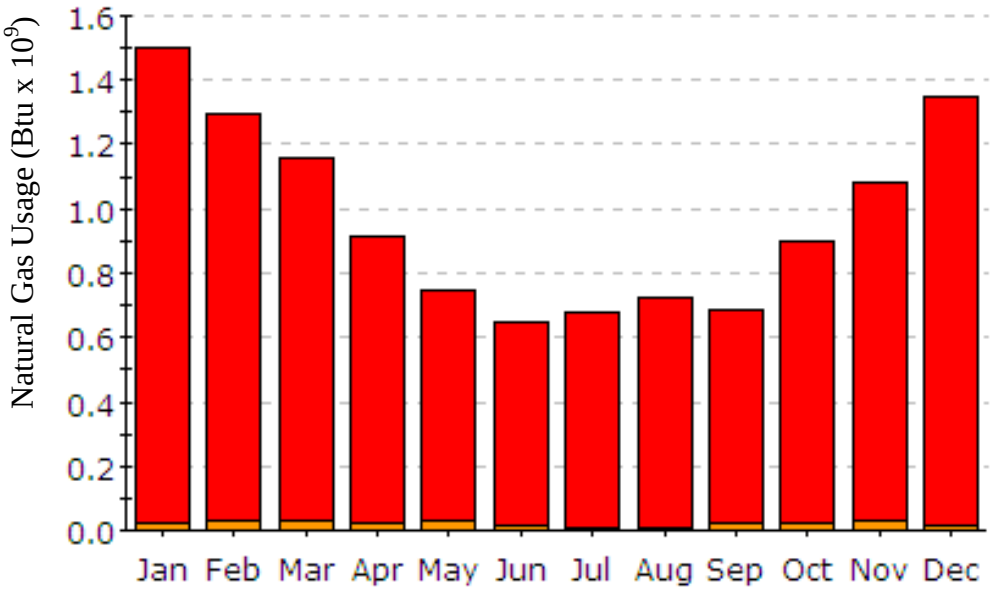

Figure 11. The Baseline Monthly Natural Gas Usage (Louisville)

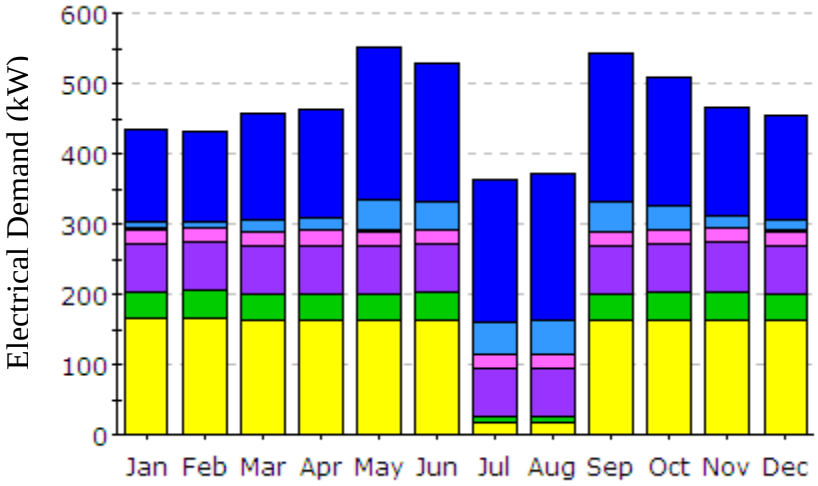

Figure 12. The Baseline Monthly Electrical Demand by Loads.

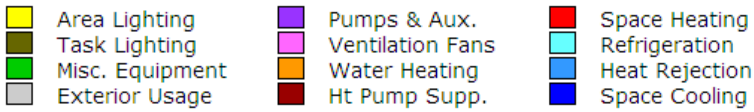

Table 4 lists the predicted annual energy consumption for the base building. The energy use index (EUI) of the facility was calculated to be 132 kBtu/SF. If temperature

set-backs were not used, the analysis would predict an EUI of 173 kBtu/SF for the base configuration. These results compare quite favorably with the average yearly EUI of 169 kBtu/SF for K-12 facilities obtained from a 2003 survey [DOE-EnergyStar,2003], and suggest that the model and simulation are producing energy use values that are typical for educational facilities. Since the code now mandates set-back capabilities and the climate of Kentucky would suggest an energy use that would likely be on the lower side of the national average, the base energy use index was taken to be the lower 132 KBtu/SF, at least for the purposes of this investigation. This index value was predicted for the base building configuration using the minimum setback schedule described in the previous sections for the Louisville location.

The cost of the electricity and gas were calculated using the LG&E/KU commercial utility rate structure (both demand and consumption costs) and are also listed in Table 4.

Table 4. Annual Energy Consumption and Annual Energy Cost per Utility for the Base Building in Louisville.

	Utility	Energy Consumption	Utility Cost	Energy Cost
Baseline Model	Electrical Usage	2,253,991 kWh	$0.0748 / kWh	$ 168,598
	Electrical Demand	5,622 kW	$12.00 / kW	$ 67,463
	Natural Gas Usage	11,645,294 kBtu	$0.01 / kBtu	$ 116,453
Total				$ 352,515

The base building model was also analyzed using average hourly weather data for Lexington, Covington, Paducah and Corbin/Williamsburg. The results of these analyses are shown in Table 5. Table 5 shows that the EUI ranges from 130 to 135 kBtu/SF, with Paducah having the highest energy demand. This is likely due to the higher cooling degree days in Paducah. Table 5 also lists the total energy cost for the base building.

Select energy use output plots from the eQuest analyses are listed in Appendix B. It should be noted that the Kitchen loads were included in miscellaneous equipment loads and were not varied. These loads were assumed to be consistent in all the configurations and not part of the evaluation addressed in this investigation, even though kitchen loads can be substantial. Kitchen energy loads and the need to control these can be addressed by limiting the type of foods prepared, and the appropriate selection of high efficiency appliances; thus were thought to be beyond the scope of this study.

Table 5 Energy use and Cost for Base School Building

Rerun status	multiplier	Corbin/Williamsburg	Covington	Lexington	Louisville	Paducah	Corbin	Covington	Lexington	Louisville	Paducah
	3.412	kWh	kWh	kWh	kWh	kWh					
		kW	kW	kW	kW	kW					
CM #	1	kBtu	kBtu	kBtu	kBtu	kBtu					
Baseline	Electric	2,324,765	2,155,194	2,186,284	2,253,991	2,312,572	$ 78,716.51	$ 72,974.85	$ 74,027.56	$ 76,320.12	$ 78,303.70
	Demand	5,630	5,272	5,368	5,622	5,688	$ 63,550.60	$ 59,618.51	$ 60,452.39	$ 63,465.52	$ 64,342.73
	Gas	11,080,212	12,327,792	12,216,803	11,645,294	11,916,435	$ 82,952.01	$ 92,291.99	$ 91,461.10	$ 87,182.49	$ 89,212.40
	Baseline EUI	130	134	134	132	135	$ 225,219.12	$ 224,885.35	$ 225,941.05	$ 226,968.13	$ 231,858.82
Baseline_NO_TSB	Electric	2,358,757	2,182,066	2,214,492	2,285,573	2,342,593	$ 79,867.48	$ 73,884.74	$ 74,982.69	$ 77,389.52	$ 79,320.22
	Demand	5,672	5,305	5,411	5,669	5,731	$ 64,042.45	$ 60,006.77	$ 60,952.80	$ 64,010.88	$ 64,834.44
	Gas	17,279,282	18,516,056	18,430,562	17,814,514	18,104,882	$ 129,361.36	$ 138,620.46	$ 137,980.42	$ 133,368.37	$ 135,542.17
	Baseline_NO_TSB EUI	173 / -33.2 %	177 / -31.9 %	177 / -32.1 %	175 / -32.5 %	178 / -31.8 %	$273,271 / -21.3 %	$272,512 / -21.2 %	$273,916 / -21.2 %	$274,769 / -21.1 %	$279,697 / -20.6 %

5.2 Energy Conservation Measures and Analysis Results

Utilizing the energy simulation software, eQuest, numerous energy conservation measures, or ECM's, were simulated to determine the effectiveness of each measure.

The following energy conservation measures were addressed as variations in the base school eQuest model configuration:

Building Structure Components

1. Vary roofing insulation: use 3", 4" and 5" thick polyisocyanurate foam board.
2. Vary the exterior masonry cavity wall insulation: 1 ¼" thick polystyrene, 1 ½" thick polystyrene, 2" thick polyisocyanurate foam board, 3" polyisocyanurate foam board. (see Figure 8.)
3. Change the exterior CMU wall structure to an insulated concrete form (ICF) wall system; from outside to inside the wall components consist of 4" face brick, air space, 1 ½" polyurethane, 6" 140lb concrete, 1 ½" polyurethane, and ½" gypsum board. (see Figure 13).
4. Change the exterior CMU wall system to a steel stud wall system; from outside to inside the wall components consist of 4" face brick, air space, 1 ½" thick polystyrene foam insulation board, 2" x 6" steel studs spaced at 16" on center with R-19 batt insulation in between the studs, and ½" interior gypsum board (code minimum). (see Figure 14).

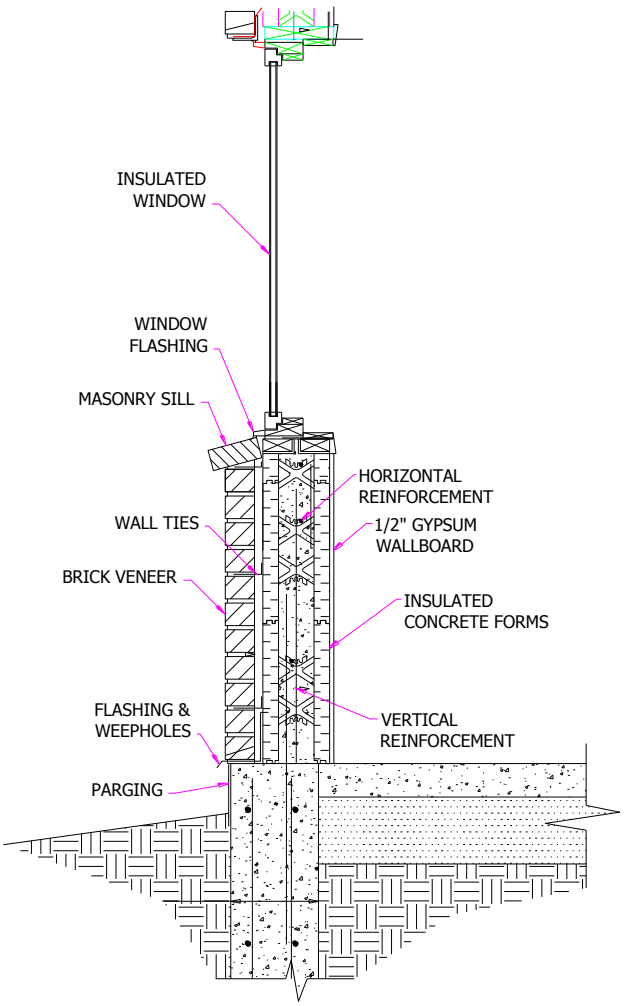

Figure 13 Typical Exterior ICF Wall System

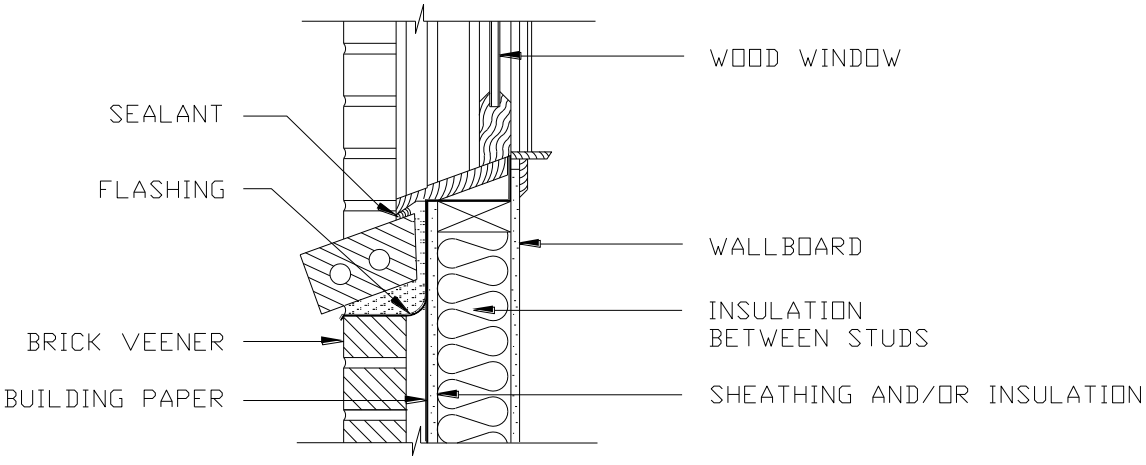

Figure 14 Typical Exterior Brick Veneer Steel Stud Wall System

5. Modify the brick veneer steel stud wall systems to include 1 ½" polystyrene insulation in the air cavity, then 2" and 3 ½" polyisocyanurate board insulation in the air cavity.

6. Change the brick veneer steel stud wall system, from outside to inside the wall components consist of 4" face brick, air space, 3" polystyrene, 2" x 6" steel stud spaced 16" on center with no batt insulation in between the studs, and ½" gypsum board.

7. This is a combination ECM configuration. Change the exterior CMU wall structure to an exterior ICF wall system and change all roofing insulation from 3" of polyisocyanurate to 5" of polyisocyanurate insulation board.

8. This is a combination ECM configuration. Change the exterior masonry cavity wall system insulation from 1 ¼" polystyrene to 2" of polyisocyanurate insulation board and change all roofing insulation from 3" polyisocyanurate to 5" of polyisocyanurate insulation board. (Higher R envelope)

9. This is a combination ECM configuration. Change the exterior masonry cavity wall system insulation from 1 ¼" polystyrene to 3" polyisocyanurate insulation board and change all roofing insulation from 3" polyisocyanurate to 5" of polyisocyanurate insulation board. (Higher R envelope)

10. Vary the base exterior wall infiltration rate of 0.5 air changes per hour to 0.2, 0.15 and 0.1 air changes per hour. This was done to simulate the effect of higher air tightness on energy usage.

11. Vary the thermal transmission coefficient (U) of the windows. Window U Values: U value/Window U value (glass and aluminum frame with thermal break) Baseline - .54/.64, Type 1 (C.18) - .67/.69. Type 2 (C.19) - .23/.31.

Building Structure Orientation

1. Vary the orientation of the building axis from 45° off true to 315° at 45° intervals. This will allow the effects of building orientation on energy use to be quantified.

Building Lighting Components

1. Change all the lighting systems from 34 watt T12 lights with magnetic ballasts to 28 watt T8 lamps with electronic ballasts. This modification theoretically reduces the electrical area lighting load by 30%.

2. Install day-lighting controls that will either turn off half of the lamps or all of the lamps depending on measured lighting levels in rooms with windows.

Building Heating, Ventilation, and Air Conditioning Components

1. During the occupied periods the room temperature is maintained between 72 and 74. If the sensed temperature falls below 72, the system enters heating mode and if the sensed temperature rises above 74 degrees, the system enters cooling mode. During unoccupied periods in the cooling season, the controls will be changed to allow the room temperature to rise to 80°F and during the heating season the temperature is allowed to lower to 64°F. This can be accomplished with a stand-alone 7-day programmable thermostat or with a direct digital control system that has control over all of the thermostats in one location.

2. In manner similar to the previous option the room temperatures during unoccupied periods in the cooling season are allowed to increase to 90°F and during the heating season the room temperatures are allowed to lower to 55°F.

3. Minimum Outside Air Schedule: This control schedule allows the outside air damper at the air handler to fully close during unoccupied periods in the building. If there is a cooling load in the building and the outside air temperature is below 65°F (dry bulb) the control schedule will be overridden and the air handler unit will enter economizer mode. Economizer mode fully opens the outside air damper bringing in 100% outside air and exhausting 100% of the return air. This economizer setting is efficient because it reduces the amount of energy needed to remove heat from the space. This can be accomplished with a schedule that is programmed into the direct digital control system. The outside air dampers should already have an electrical servo motor that controls the operation of the damper.

4. Modified Fan Schedule: The air handler units are shut down during the unoccupied periods. If any zone falls below the heating set point the unit will cycle on for 1 hour.

5. A variable frequency drive mortar (VFD) is used for the cooling tower fan: A variable frequency drive is installed on the cooling tower fan in order to control the speed of the fan based on cooling load demand.

6. VFD mortars used on circulating pumps and reset of loop temperature: Two-way valves are installed instead of 3-way valves along with variable frequency drives on the chilled water and hot water circulating pumps. The two-way valves will modulate depending on heating and/or cooling load. The flow rate of the pumps will be reduced depending on static pressure sensors in the water loop. The boiler water loop temperature is adjusted based on outside air temperature. The chilled water loop temperature is adjusted based on outside air temperature.

7. ERV on AHUs: An enthalpy wheel energy recovery ventilator (ERV) will be installed on each of the air handler units. The exhaust air is used to pre-heat or pre-cool the outside air before entering the air handler without contaminating the air.

8. VAV Box Minimum Air Flow Schedule: Allows the damper controlling the minimum air flow in a VAV box to fully close during unoccupied periods if the room temperature is satisfied.

9. Boiler Water Loop Operation: The boiler water loop operation is based on demand not standby.

10. Chilled Water Loop Operation: The chilled water loop operation is based on demand not standby.

11. The VAV system is changed to a geothermal system. The geothermal system uses multiple heat pump units that serve individual zones. Simultaneous heating and cooling is still available but the source of heating and cooling is the ground which remains at a constant temperature year round. In this system a boiler, chiller, and cooling tower are not needed. Control strategies will also be implemented on the geothermal system to optimize the system. It was assumed that the geothermal system heat pump system will replace the existing base HVAC system and this system utilizes heat pumps to control the individual zones instead of the VAV distribution boxes A vertical well field using l ¾" polyethylene tubing was used in the design and an iterative process was used to size the well to match the load of the building. The initial design had constant flow circulating pumps and three-way valves at each of the heat pump units to bypass the heat pump if the space is at set point. An alternate design evaluated whether two-way valves could be installed instead of three way valves and these valves

used with a variable frequency drive that is installed on the circulation pump to vary the flow.

12. The VAV system is changed to a water source heat pump system. This system uses multiple heat pump units that serve individual zones. Simultaneous heating and cooling is still available but the source of heating and cooling is a water loop. A boiler and fluid cooler are attached to the water loop to add or remove heat if necessary. Control strategies will also be implemented on the water source heat pump system to optimize the system.

13. Minimum Outside Air Schedule with geothermal heat pump: This control schedule allows the outside air damper at the air handler to fully close during unoccupied periods in the building. If there is a cooling load in the building and the outside air temperature is below 65 F (dry bulb) the control schedule will be overridden and the air handler unit will enter economizer mode. Economizer mode fully opens the outside air damper bringing in 100% outside air and exhausting 100% of return air. The economizer reduces the amount of energy needed to remove heat from the space. This can be accomplished with a schedule that is programmed into the direct digital control system. The outside air dampers should already have an electrical servo motor that controls the operation of the damper.

14. Modified Fan Schedule with geothermal heat pump HVAC system: The air handler units are shut down during the unoccupied periods. If any zone falls below the heating set point the unit will cycle on for 1 hour.

15. Variable speed pumps on each geothermal heat pump HVAC system: The variable speed pumps will allow the flow rate of the fluid to vary depending upon the

load. Load resets are also included in this ECM. The load reset allows the heating deck to reset its temperature based on the coolest room in the zone, and the cooling deck to reset its temperature based on the warmest zone.

16. Increase the boiler efficiency from 80 to 90%.

17. This is a combination ECM configuration. Use the ICF exterior wall and 5" of polyisocyanurate insulation board on the roof and a geothermal heat pump HVAC system.

18. This is a combination ECM configuration. Use the highest insulated CMU exterior wall and 5" of polyisocyanurate insulation board on the roof and a geothermal heat pump HVAC system.

Building Domestic Water Heating Components

1. The domestic hot water is provided by an electric water heater instead of a natural gas water heater.

2. The domestic hot water is provided by an electric heat pump instead of a natural gas water heater.

Note that it was assumed that the geothermal heat pump system will replace the existing base HVAC system and utilizes heat pumps to control the individual zones instead of the VAV distribution boxes. In the ground source geothermal system, a chiller or boiler is not needed to make up the remaining load.

A water source heat pump system was also evaluated in place of the geothermal heat pump system to determine the difference in energy savings and upfront capital costs. The water source heat pump system will be slightly cheaper because the system utilizes an existing pond or well as the heat exchanger instead of drilling a well field. The system won't be as efficient due to the larger fluctuations in water temperature versus the ground temperature.

The energy conservation measures were simulated separately to determine the effects that each had on the building energy use. Some of the more effective measures were then combined and their combined effects determined. It was clear from the analyses that savings of each ECM cannot simply be added together. For each change in building configuration, the yearly energy use in Louisville, Lexington, Covington, Corbin/Williamsburg, and Paducah were simulated. Tables 6 through 11 summarize the results of these analyses. These tables also list the total EUI, the percentage change in EUI and the total energy costs for each configuration.

Table 6 Yearly Energy Use for Envelope Related ECM's and Energy Costs

Rerun status	Energy Efficiency Measure	Construction Data	multiplier	Corbin/Williamsburg	Covington	Lexington	Louisville	Paducah	Corbin	Covington	Lexington	Louisville	Paducah
			3.412	kWh	kWh	kWh	kWh	kWh					
				kW	kW	kW	kW	kW					
CM #	description1	Changes	1	kBtu	kBtu	kBtu	kBtu	kBtu					
C.1	Pitched Roof R-25.64 Built Up Roof R-29.41	Change 3" exterior Polyisocyanurate to 3.5" exterior Polyisocyanurate	Electric	2,324,003	2,154,543	2,185,691	2,253,298	2,311,966	$ 78,691	$ 72,953	$ 74,008	$ 76,297	$ 78,283
			Demand	5,628	5,270	5,367	5,620	5,687	$ 63,531	$ 59,601	$ 60,436	$ 63,448	$ 64,324
			Gas	11,057,305	12,280,164	12,171,872	11,610,529	11,877,451	$ 82,781	$ 91,935	$ 91,125	$ 86,922	$ 88,921
			C.1 EUI	130 / .1 %	134 / .3 %	134 / .2 %	132 / .2 %	135 / .2 %	$225,002 / .1 %	$224,490 / .2 %	$225,568 / .2 %	$226,667 / .1 %	$231,528 / .1 %
C.2	Pitched Roof R-29.41 Built Up Roof R-33.33	Change 3" exterior Polyisocyanurate to 4" exterior Polyisocyanurate	Electric	2,323,392	2,154,063	2,185,232	2,252,749	2,311,495	$ 78,670	$ 72,937	$ 73,992	$ 76,278	$ 78,267
			Demand	5,627	5,269	5,366	5,619	5,685	$ 63,515	$ 59,588	$ 60,423	$ 63,435	$ 64,309
			Gas	11,039,218	12,242,390	12,136,838	11,582,843	11,847,062	$ 82,645	$ 91,653	$ 90,862	$ 86,715	$ 88,693
			C.2 EUI	130 / .2 %	134 / .5 %	134 / .4 %	132 / .3 %	135 / .4 %	$224,830 / .2 %	$224,178 / .3 %	$225,277 / .3 %	$226,428 / .2 %	$231,270 / .3 %
C.3	Pitched Roof R-37.04 Built Up Roof R-40.00	Change 3" exterior Polyisocyanurate to 5" exterior Polyisocyanurate	Electric	2,322,535	2,153,377	2,184,581	2,251,926	2,310,792	$ 78,641	$ 72,913	$ 73,970	$ 76,250	$ 78,243
			Demand	5,625	5,267	5,364	5,618	5,684	$ 63,491	$ 59,569	$ 60,403	$ 63,415	$ 64,287
			Gas	11,011,239	12,186,213	12,083,807	11,540,309	11,800,659	$ 82,436	$ 91,232	$ 90,465	$ 86,397	$ 88,346
			C.3 EUI	129 / .4 %	133 / .8 %	133 / .7 %	131 / .6 %	134 / .6 %	$224,568 / .3 %	$223,715 / .5 %	$224,839 / .5 %	$226,061 / .4 %	$230,876 / .4 %
C.4	ICF walls R-21.74	ICF Wall: air film, 4" brick, air space, 1.5" Polyurethane, 6" 140lb conc., 1.5" Polyurethane, 1/2" gyp board, air film	Electric	2,324,371	2,154,839	2,163,009	2,253,728	2,312,122	$ 78,703	$ 72,963	$ 73,240	$ 76,311	$ 78,288
			Demand	5,631	5,272	5,329	5,623	5,689	$ 63,565	$ 59,617	$ 60,004	$ 63,472	$ 64,348
			Gas	11,045,692	12,151,629	12,052,720	11,546,113	11,798,442	$ 82,694	$ 90,973	$ 90,233	$ 86,440	$ 88,329
			C.4 EUI	130 / .2 %	133 / .9 %	133 / 1.2 %	131 / .5 %	134 / .6 %	$224,961 / .1 %	$223,553 / .6 %	$223,476 / 1.1 %	$226,224 / .3 %	$230,965 / .4 %
C.5	CMU walls R-25	Changed 1-1/4" Polystyrene to 3" ployiso	Electric	2,324,081	2,154,614	2,162,782	2,253,297	2,311,822	$ 78,693	$ 72,955	$ 73,232	$ 76,297	$ 78,278
			Demand	5,629	5,271	5,327	5,621	5,687	$ 63,543	$ 59,605	$ 59,987	$ 63,452	$ 64,328
			Gas	11,042,519	12,133,630	12,036,631	11,536,908	11,791,807	$ 82,670	$ 90,838	$ 90,112	$ 86,371	$ 88,279
			C.5 EUI	130 / .2 %	133 / 1.0 %	133 / 1.3 %	131 / .6 %	134 / .6 %	$224,906 / .1 %	$223,399 / .7 %	$223,331 / 1.2 %	$226,120 / .4 %	$230,886 / .4 %
C.6	CMU walls R-18.18	Changed 1-1/4" Polystyrene to 2" ployiso	Electric	2,324,223	2,154,749	2,185,776	2,253,456	2,311,991	$ 78,698	$ 72,960	$ 74,010	$ 76,302	$ 78,284
			Demand	5,629	5,271	5,367	5,621	5,687	$ 63,545	$ 59,608	$ 60,443	$ 63,455	$ 64,331
			Gas	11,050,622	12,177,489	12,081,000	11,560,328	11,819,560	$ 82,730	$ 91,167	$ 90,444	$ 86,546	$ 88,487
			C.6 EUI	130 / .2 %	133 / .8 %	133 / .7 %	131 / .4 %	135 / .5 %	$224,973 / .1 %	$223,735 / .5 %	$224,898 / .5 %	$226,304 / .3 %	$231,103 / .3 %
C.7	CMU walls R-13.33	Changed 1-1/4" Polystyrene to 1 1/2" polyurethane	Electric	2,324,423	2,154,918	2,185,999	2,253,659	2,312,189	$ 78,705	$ 72,965	$ 74,018	$ 76,309	$ 78,291
			Demand	5,629	5,271	5,368	5,621	5,688	$ 63,547	$ 59,612	$ 60,447	$ 63,459	$ 64,336
			Gas	11,061,140	12,233,706	12,131,544	11,590,998	11,855,189	$ 82,809	$ 91,588	$ 90,823	$ 86,776	$ 88,754
			C.7 EUI	130 / .1 %	134 / .5 %	134 / .4 %	132 / .3 %	135 / .3 %	$225,061 / .1 %	$224,165 / .3 %	$225,288 / .3 %	$226,544 / .2 %	$231,380 / .2 %
C.8	Steel Stud Walls R-34.5	Steel wall stud layers: air film, 4" face brick, air space, 3.5" polyiso, 2x6 steel wall 16 O.C. R-19 batt insul, gypsum board air film	Electric	2,324,466	2,154,917	2,163,217	2,253,852	2,312,212	$ 78,706	$ 72,965	$ 73,247	$ 76,315	$ 78,291
			Demand	5,631	5,272	5,329	5,623	5,689	$ 63,568	$ 59,625	$ 60,010	$ 63,475	$ 64,352
			Gas	11,040,827	12,117,113	12,021,283	11,529,392	11,781,746	$ 82,657	$ 90,715	$ 89,997	$ 86,315	$ 88,204
			C.8 EUI	130 / .2 %	133 / 1.1 %	133 / 1.4 %	131 / .6 %	134 / .7 %	$224,932 / .1 %	$223,305 / .7 %	$223,254 / 1.2 %	$226,105 / .4 %	$230,848 / .4 %
C.9	Steel Stud Walls R-23.08	Steel wall stud layers: air film, 4" face brick, air space, 2" polyiso, 2x6 steel wall 16 O.C. R-19 batt insul, gypsum board air film	Electric	2,324,597	2,155,034	2,163,319	2,253,977	2,312,348	$ 78,711	$ 72,969	$ 73,250	$ 76,320	$ 78,296
			Demand	5,631	5,272	5,329	5,623	5,689	$ 63,571	$ 59,627	$ 60,012	$ 63,477	$ 64,355
			Gas	11,046,803	12,145,689	12,046,930	11,545,084	11,799,834	$ 82,702	$ 90,929	$ 90,189	$ 86,432	$ 88,339
			C.9 EUI	130 / .2 %	133 / .9 %	133 / 1.3 %	131 / .5 %	134 / .6 %	$224,983 / .1 %	$223,525 / .6 %	$223,451 / 1.1 %	$226,229 / .3 %	$230,990 / .4 %
C.10	Steel Stud Walls R-16.4	Steel wall stud layers: air film, 4" face brick, air space, 1.5" Polystyrene, 2x6 steel wall 16 O.C. R-19 batt insul, 1/2" GYP board, air film	Electric	2,324,756	2,155,163	2,186,289	2,254,126	2,312,528	$ 78,716	$ 72,974	$ 74,028	$ 76,325	$ 78,302
			Demand	5,631	5,273	5,370	5,623	5,690	$ 63,572	$ 59,630	$ 60,467	$ 63,480	$ 64,358
			Gas	11,058,984	12,201,785	12,102,814	11,575,661	11,838,826	$ 82,793	$ 91,349	$ 90,608	$ 86,661	$ 88,631
			C.10 EUI	130 / .1 %	134 / .6 %	134 / .6 %	132 / .4 %	135 / .4 %	$225,081 / .1 %	$223,953 / .4 %	$225,102 / .4 %	$226,466 / .2 %	$231,291 / .2 %
C.11	Steel Stud Walls R-16.67	Steel wall stud layers: air film, 4" face brick, air space, 3" Polystyrene, 2x6 steel wall 16 O.C. No batt insul, 1/2" GYP board, air film	Electric	2,324,755	2,155,154	2,186,267	2,254,108	2,312,518	$ 78,716	$ 72,973	$ 74,027	$ 76,324	$ 78,302
			Demand	5,631	5,273	5,369	5,623	5,689	$ 63,571	$ 59,630	$ 60,466	$ 63,479	$ 64,357
			Gas	11,058,907	12,201,197	12,102,294	11,575,330	11,838,529	$ 82,793	$ 91,344	$ 90,604	$ 86,659	$ 88,629
			C.11 EUI	130 / .1 %	134 / .6 %	134 / .6 %	132 / .4 %	135 / .4 %	$225,080 / .1 %	$223,947 / .4 %	$225,097 / .4 %	$226,462 / .2 %	$231,288 / .2 %

Table 7 Yearly Energy Use For Envelope Related and Combined ECM's and Energy Costs

Rerun status	Energy Efficiency Measure	Construction Data	multiplier	Corbin/Williamsburg	Covington	Lexington	Louisville	Paducah	Corbin	Covington	Lexington	Louisville	Paducah
			3.412	kWh	kWh	kWh	kWh	kWh					
				kW	kW	kW	kW	kW					
CM #	description1	Changes	1	kBtu	kBtu	kBtu	kBtu	kBtu					
C.12	10% air infiltration rate	Change all A-C air change rates to .10 air changes/hour	Electric	2,325,254	2,155,410	2,186,654	2,254,430	2,313,034	$ 78,733	$ 72,982	$ 74,040	$ 76,335	$ 78,319
			Demand	5,631	5,272	5,369	5,623	5,689	$ 63,563	$ 59,625	$ 60,462	$ 63,478	$ 64,356
			Gas	11,097,347	12,347,417	12,236,464	11,663,269	11,935,081	$ 83,080	$ 92,439	$ 91,608	$ 87,317	$ 89,352
			C.12 EUI	130 / -.1 %	135 / -.1 %	135 / -.1 %	132 / -.1 %	135 / -.1 %	$225,376 / -.1 %	$225,046 / -.1 %	$226,110 / -.1 %	$227,130 / -.1 %	$232,027 / -.1 %
C.13	15% air infiltration rate	Change all A-C air change rates to .15 air changes/hour	Electric	2,321,278	2,152,409	2,183,320	2,250,902	2,308,755	$ 78,598	$ 72,881	$ 73,927	$ 76,216	$ 78,174
			Demand	5,622	5,266	5,362	5,614	5,679	$ 63,464	$ 59,549	$ 60,379	$ 63,375	$ 64,238
			Gas	11,038,169	12,260,001	12,153,581	11,591,638	11,859,080	$ 82,637	$ 91,784	$ 90,988	$ 86,781	$ 88,783
			C.13 EUI	129 / .3 %	134 / .4 %	134 / .4 %	132 / .3 %	135 / .4 %	$224,700 / .2 %	$224,214 / .3 %	$225,294 / .3 %	$226,372 / .3 %	$231,196 / .3 %
C.14	20% air infiltration rate	Change all A-C air change rates to .20 air changes/hour	Electric	2,317,499	2,149,638	2,180,254	2,247,549	2,304,498	$ 78,471	$ 72,787	$ 73,823	$ 76,102	$ 78,030
			Demand	5,614	5,260	5,355	5,606	5,669	$ 63,371	$ 59,480	$ 60,303	$ 63,278	$ 64,124
			Gas	10,982,564	12,177,339	12,075,338	11,525,407	11,786,948	$ 82,221	$ 91,166	$ 90,402	$ 86,285	$ 88,243
			C.14 EUI	129 / .6 %	133 / .9 %	133 / .8 %	131 / .7 %	134 / .8 %	$224,062 / .5 %	$223,432 / .6 %	$224,528 / .6 %	$225,664 / .6 %	$230,397 / .6 %
C.15	ICF R-21.74, Pitched Roof R-37.04 Built Up Roof R-40.00	Wall: air film, 4" brick, air space, 1.5" Polyurethane, 6" 140lb conc., 1.5" Polyurethane, 1/2" gyp board, air film; for roof: Changed 3" exterior Polyisocyanurate to 5" exterior Polyisocyanurate	Electric	2,322,224	2,153,080	2,161,200	2,251,740	2,310,401	$ 78,630	$ 72,903	$ 73,178	$ 76,244	$ 78,230
			Demand	5,626	5,267	5,324	5,618	5,684	$ 63,503	$ 59,568	$ 59,951	$ 63,421	$ 64,291
			Gas	10,985,502	12,055,125	11,960,755	11,466,418	11,714,064	$ 82,243	$ 90,251	$ 89,544	$ 85,843	$ 87,697
			C.15 EUI	129 / .5 %	133 / 1.4 %	132 / 1.7 %	131 / 1.0 %	134 / 1.1 %	$224,376 / .4 %	$222,722 / 1.0 %	$222,673 / 1.4 %	$225,509 / .6 %	$230,218 / .7 %
C.16	CMU walls R-18.18 Pitched Roof R-37.04 Built Up Roof R-40.00	for wall Changed 1-1/4" Polystyrene to 2" polyiso, for roof Changed 3" exterior Polyisocyanurate to 5" exterior Polyisocyanurate	Electric	2,323,801	2,154,315	2,162,577	2,253,024	2,311,536	$ 78,684	$ 72,945	$ 73,225	$ 76,287	$ 78,269
			Demand	5,629	5,270	5,327	5,620	5,686	$ 63,538	$ 59,598	$ 59,981	$ 63,446	$ 64,321
			Gas	11,035,409	12,067,056	11,977,556	11,503,068	11,751,035	$ 82,617	$ 90,340	$ 89,670	$ 86,118	$ 87,974
			C.16 EUI	130 / .3 %	133 / 1.3 %	132 / 1.6 %	131 / .8 %	134 / .9 %	$224,838 / .2 %	$222,883 / .9 %	$222,876 / 1.4 %	$225,851 / .5 %	$230,564 / .6 %
C.17	CMU walls R-25 Pitched Roof R-37.04 Built Up Roof R-40.00	for wall Changed 1-1/4" Polystyrene to 3" ployiso, for roof Changed 3" exterior Polyisocyanurate to 5" exterior Polyisocyanurate	Electric	2,321,832	2,152,783	2,160,938	2,251,232	2,310,044	$ 78,617	$ 72,893	$ 73,169	$ 76,227	$ 78,218
			Demand	5,624	5,266	5,323	5,617	5,682	$ 63,483	$ 59,556	$ 59,935	$ 63,401	$ 64,272
			Gas	10,974,749	11,991,213	11,903,001	11,433,142	11,675,963	$ 82,162	$ 89,772	$ 89,112	$ 85,594	$ 87,412
			C.17 EUI	129 / .6 %	132 / 1.8 %	132 / 2.0 %	131 / 1.1 %	134 / 1.3 %	$224,263 / .4 %	$222,221 / 1.2 %	$222,216 / 1.6 %	$225,222 / .8 %	$229,903 / .8 %
C.18	Window Option 1	Higher U value	Electric	2,324,562	2,155,062	2,186,118	2,253,741	2,312,224	$ 78,710	$ 72,970	$ 74,022	$ 76,312	$ 78,292
			Demand	5,629	5,271	5,368	5,621	5,688	$ 63,547	$ 59,616	$ 60,449	$ 63,460	$ 64,336
			Gas	11,082,455	12,333,715	12,222,249	11,648,839	11,920,555	$ 82,969	$ 92,336	$ 91,502	$ 87,209	$ 89,243
			C.18 EUI	130 / .0 %	134 / .0 %	134 / .0 %	132 / .0 %	135 / .0 %	$225,225 / .0 %	$224,923 / .0 %	$225,973 / .0 %	$226,981 / .0 %	$231,871 / .0 %
C.19	Window Option 2	Lower U value	Electric	2,323,961	2,154,652	2,185,759	2,253,076	2,311,750	$ 78,689	$ 72,956	$ 74,010	$ 76,289	$ 78,276
			Demand	5,628	5,271	5,367	5,620	5,687	$ 63,535	$ 59,608	$ 60,442	$ 63,447	$ 64,325
			Gas	11,061,751	12,259,951	12,155,823	11,601,794	11,870,052	$ 82,814	$ 91,784	$ 91,005	$ 86,857	$ 88,865
			C.19 EUI	130 / .1 %	134 / .4 %	134 / .3 %	132 / .2 %	135 / .2 %	$225,038 / .1 %	$224,348 / .2 %	$225,456 / .2 %	$226,593 / .2 %	$231,466 / .2 %

Table 8 Yearly Energy Use For Building Orientation and Lighting ECM's and Energy Costs

Rerun status	Energy Efficiency Measure	Construction Data	multiplier	Corbin/Williamsburg	Covington	Lexington	Louisville	Paducah	Corbin	Covington	Lexington	Louisville	Paducah
			3.412	kWh	kWh	kWh	kWh	kWh					
				kW	kW	kW	kW	kW					
CM #	description1	Changes	1	kBtu	kBtu	kBtu	kBtu	kBtu					
			Electric	2,324,727	2,155,292	2,186,165	2,253,805	2,312,598	$ 78,715	$ 72,978	$ 74,024	$ 76,314	$ 78,305
A.45	45° Orientation		Demand	5,629	5,272	5,368	5,622	5,688	$ 63,549	$ 59,621	$ 60,450	$ 63,463	$ 64,342
			Gas	11,069,990	12,319,086	12,207,030	11,634,374	11,905,235	$ 82,875	$ 92,227	$ 91,388	$ 87,101	$ 89,129
			A.45 EUI	130 / .1 %	134 / .0 %	134 / .1 %	132 / .1 %	135 / .1 %	$225,140 / .0 %	$224,826 / .0 %	$225,862 / .0 %	$226,878 / .0 %	$231,775 / .0 %
			Electric	2,326,252	2,156,600	2,187,593	2,255,280	2,314,386	$ 78,767	$ 73,022	$ 74,072	$ 76,364	$ 78,365
A.90	90° Orientation		Demand	5,632	5,274	5,371	5,625	5,692	$ 63,582	$ 59,648	$ 60,482	$ 63,496	$ 64,383
			Gas	11,064,819	12,314,061	12,200,978	11,627,392	11,899,792	$ 82,837	$ 92,189	$ 91,343	$ 87,048	$ 89,088
			A.90 EUI	130 / .1 %	134 / .0 %	134 / .1 %	132 / .1 %	135 / .1 %	$225,186 / .0 %	$224,860 / .0 %	$225,896 / .0 %	$226,908 / .0 %	$231,836 / .0 %
			Electric	2,326,415	2,156,706	2,187,473	2,255,853	2,314,337	$ 78,772	$ 73,026	$ 74,068	$ 76,383	$ 78,363
A.135	135° Orientation		Demand	5,633	5,274	5,371	5,626	5,692	$ 63,586	$ 59,650	$ 60,481	$ 63,510	$ 64,383
			Gas	11,048,876	12,299,402	12,187,651	11,614,524	11,882,912	$ 82,717	$ 92,079	$ 91,243	$ 86,952	$ 88,961
			A.135 EUI	130 / .1 %	134 / .1 %	134 / .1 %	132 / .1 %	135 / .1 %	$225,076 / .1 %	$224,755 / .1 %	$225,791 / .1 %	$226,845 / .1 %	$231,707 / .1 %
			Electric	2,327,613	2,157,071	2,187,889	2,256,793	2,313,738	$ 78,813	$ 73,038	$ 74,082	$ 76,415	$ 78,343
A.180	180° Orientation		Demand	5,635	5,275	5,371	5,627	5,691	$ 63,612	$ 59,657	$ 60,487	$ 63,527	$ 64,370
			Gas	11,060,082	12,304,143	12,192,308	11,622,990	11,885,472	$ 82,801	$ 92,115	$ 91,278	$ 87,016	$ 88,981
			A.180 EUI	130 / .1 %	134 / .1 %	134 / .1 %	132 / .1 %	135 / .1 %	$225,227 / .0 %	$224,810 / .0 %	$225,847 / .0 %	$226,958 / .0 %	$231,693 / .1 %
			Electric	2,327,503	2,157,164	2,187,817	2,256,844	2,314,906	$ 78,809	$ 73,042	$ 74,079	$ 76,417	$ 78,383
A.225	225° Orientation		Demand	5,635	5,275	5,371	5,627	5,692	$ 63,608	$ 59,659	$ 60,484	$ 63,527	$ 64,390
			Gas	11,063,742	12,311,566	12,195,744	11,628,591	11,894,760	$ 82,829	$ 92,171	$ 91,303	$ 87,057	$ 89,050
			A.225 EUI	130 / .0 %	134 / .0 %	134 / .1 %	132 / .0 %	135 / .1 %	$225,246 / .0 %	$224,871 / .0 %	$225,867 / .0 %	$227,001 / .0 %	$231,823 / .0 %
			Electric	2,326,711	2,156,993	2,187,484	2,255,925	2,314,815	$ 78,782	$ 73,036	$ 74,068	$ 76,386	$ 78,380
A.270	270° Orientation		Demand	5,633	5,275	5,371	5,626	5,692	$ 63,591	$ 59,656	$ 60,478	$ 63,507	$ 64,389
			Gas	11,076,833	12,327,311	12,210,490	11,641,027	11,912,888	$ 82,927	$ 92,288	$ 91,414	$ 87,151	$ 89,186
			A.270 EUI	130 / .0 %	134 / .0 %	134 / .0 %	132 / .0 %	135 / .0 %	$225,300 / .0 %	$224,980 / .0 %	$225,960 / .0 %	$227,043 / .0 %	$231,954 / .0 %
			Electric	2,324,617	2,155,251	2,186,129	2,254,120	2,312,743	$ 78,712	$ 72,977	$ 74,022	$ 76,325	$ 78,309
A.315	315° Orientation		Demand	5,629	5,272	5,368	5,622	5,688	$ 63,547	$ 59,620	$ 60,449	$ 63,469	$ 64,346
			Gas	11,073,357	12,323,050	12,209,451	11,640,039	11,908,519	$ 82,901	$ 92,257	$ 91,406	$ 87,143	$ 89,153
			A.315 EUI	130 / .0 %	134 / .0 %	134 / .0 %	132 / .0 %	135 / .0 %	$225,159 / .0 %	$224,853 / .0 %	$225,878 / .0 %	$226,936 / .0 %	$231,808 / .0 %
			Electric	2,207,939	2,038,436	2,069,607	2,136,992	2,195,818	$ 74,761	$ 69,021	$ 70,077	$ 72,359	$ 74,350
L.1	T8 Lighting	Change all building lights from T12 to T8,Change ballast from Energy Efficient Magnetic to Rapid Start Electronic	Demand	5,116	4,763	4,855	5,108	5,175	$ 57,881	$ 53,996	$ 54,784	$ 57,792	$ 58,671
			Gas	11,500,783	12,753,427	12,642,829	12,066,841	12,340,375	$ 86,101	$ 95,479	$ 94,651	$ 90,338	$ 92,386
			L.1 EUI	130 / -.1 %	135 / -.1 %	135 / -.1 %	132 / -.1 %	135 / -.1 %	$218,742 / 2.9 %	$218,496 / 2.8 %	$219,511 / 2.8 %	$220,488 / 2.9 %	$225,408 / 2.8 %
			Electric	2,231,810	2,062,348	2,093,461	2,161,117	2,219,689	$ 75,569	$ 69,831	$ 70,885	$ 73,175	$ 75,159
L.2	Modified Lighting Schedule	Occupancy Sensors	Demand	5,629	5,271	5,368	5,622	5,688	$ 63,548	$ 59,616	$ 60,450	$ 63,464	$ 64,341
			Gas	11,382,382	12,636,979	12,527,116	11,949,399	12,224,473	$ 85,214	$ 94,607	$ 93,784	$ 89,459	$ 91,519
			L.2 EUI	130 / .1 %	134 / .0 %	134 / .0 %	132 / .1 %	135 / .0 %	$224,331 / .4 %	$224,054 / .4 %	$225,119 / .4 %	$226,098 / .4 %	$231,019 / .4 %

Table 9 Yearly Energy Use for Building HVAC Systems and Controls ECM's and Energy Costs

				Energy Consumption					Energy Cost				
Rerun status	Energy Efficiency Measure	Construction Data	multiplier	Corbin/Williamsburg	Covington	Lexington	Louisville	Paducah	Corbin	Covington	Lexington	Louisville	Paducah
			3.412	kWh	kWh	kWh	kWh	kWh					
				kW	kW	kW	kW	kW					
CM #	description1	Changes	1	kBtu	kBtu	kBtu	kBtu	kBtu					
M.1	90% Boiler Efficiency		Electric	2,324,765	2,155,194	2,186,284	2,253,991	2,312,572	$ 78,717	$ 72,975	$ 74,028	$ 76,320	$ 78,304
			Demand	5,630	5,272	5,368	5,622	5,688	$ 63,551	$ 59,619	$ 60,452	$ 63,466	$ 64,343
			Gas	9,876,676	10,987,248	10,888,370	10,379,653	10,620,913	$ 73,942	$ 82,256	$ 81,516	$ 77,707	$ 79,513
			M.1 EUI	122 / 6.3 %	125 / 6.8 %	125 / 6.8 %	123 / 6.5 %	126 / 6.5 %	$216,209 / 4.0 %	$214,849 / 4.5 %	$215,996 / 4.4 %	$217,493 / 4.2 %	$222,160 / 4.2 %
M.2	Large Temperature Setback	Cooling Unoccupied - 90 F Heating Unoccupied - 55 F	Electric	2,310,047	2,143,611	2,174,275	2,241,089	2,300,129	$ 78,218	$ 72,583	$ 73,621	$ 75,883	$ 77,882
			Demand	5,624	5,277	5,362	5,615	5,684	$ 63,483	$ 59,669	$ 60,375	$ 63,390	$ 64,294
			Gas	7,410,173	8,609,121	8,528,811	8,075,958	8,199,456	$ 55,476	$ 64,452	$ 63,851	$ 60,461	$ 61,385
			M.2 EUI	104 / 19.6 %	109 / 19.1 %	109 / 19.0 %	107 / 18.7 %	110 / 19.0 %	$197,178 / 12.5 %	$196,704 / 12.5 %	$197,847 / 12.4 %	$199,734 / 12.0 %	$203,561 / 12.2 %
M.3	Daylighting	Using light sensors to change lighting levels	Electric	2,317,186	2,147,723	2,178,771	2,246,527	2,305,107	$ 78,460	$ 72,722	$ 73,773	$ 76,067	$ 78,051
			Demand	5,574	5,218	5,316	5,567	5,637	$ 62,933	$ 59,020	$ 59,870	$ 62,858	$ 63,772
			Gas	11,106,359	12,353,895	12,243,149	11,670,696	11,942,769	$ 83,148	$ 92,487	$ 91,658	$ 87,373	$ 89,410
			M.3 EUI	130 / .0 %	134 / .0 %	134 / .0 %	132 / .0 %	135 / .0 %	$224,541 / .3 %	$224,229 / .3 %	$225,301 / .3 %	$226,298 / .3 %	$231,233 / .3 %
M.4	Water Side Economizer	Install heat exchanger that uses free cooling	Electric	2,622,678	2,443,120	2,476,611	2,550,008	2,622,113	$ 88,804	$ 82,724	$ 83,858	$ 86,343	$ 88,785
			Demand	6,104	5,700	5,790	6,072	6,179	$ 69,012	$ 64,501	$ 65,243	$ 68,613	$ 69,981
			Gas	11,080,212	12,327,792	12,216,803	11,645,294	11,916,435	$ 82,952	$ 92,292	$ 91,461	$ 87,182	$ 89,212
			M.4 EUI	137 / -5.3 %	141 / -5.0 %	141 / -5.0 %	139 / -5.2 %	142 / -5.3 %	$240,768 / -6.9 %	$239,517 / -6.5 %	$240,562 / -6.5 %	$242,139 / -6.7 %	$247,978 / -7.0 %
M.5	Minimum OA Schedule	Closes OA Damper during unoccupied periods unless when calling for economizer mode	Electric	2,260,468	2,113,638	2,143,032	2,199,054	2,259,090	$ 76,539	$ 71,568	$ 72,563	$ 74,460	$ 76,493
			Demand	5,630	5,272	5,368	5,622	5,688	$ 63,550	$ 59,618	$ 60,452	$ 63,465	$ 64,342
			Gas	11,096,300	12,230,868	12,124,794	11,579,176	11,797,079	$ 83,072	$ 91,566	$ 90,772	$ 86,688	$ 88,319
			M.5 EUI	128 / 1.1 %	133 / 1.2 %	133 / 1.2 %	130 / 1.3 %	133 / 1.5 %	$223,162 / .9 %	$222,752 / .9 %	$223,787 / 1.0 %	$224,612 / 1.0 %	$229,154 / 1.2 %
M.6	Modified Fan Schedule	HVAC Systems shut down during the period of 7PM and 6 AM. If any zone falls below heating setpoint the unit will cycle on for 1 hour.	Electric	1,913,418	1,799,622	1,814,150	1,881,953	1,932,836	$ 64,788	$ 60,935	$ 61,427	$ 63,723	$ 65,446
			Demand	5,634	5,276	5,372	5,629	5,694	$ 63,605	$ 59,675	$ 60,501	$ 63,545	$ 64,405
			Gas	8,030,401	9,669,016	9,500,514	8,829,274	9,186,772	$ 60,120	$ 72,387	$ 71,126	$ 66,100	$ 68,777
			M.6 EUI	99 / 23.4 %	108 / 19.7 %	107 / 20.3 %	104 / 21.1 %	108 / 20.3 %	$188,513 / 16.3 %	$192,998 / 14.2 %	$193,053 / 14.6 %	$193,368 / 14.8 %	$198,627 / 14.3 %
M.7	VFD on Cooling Tower Fan	Install variable frequency drive on cooling tower fan that will control the fan fan speed based on the load	Electric	2,255,734	2,103,676	2,133,087	2,192,615	2,248,044	$ 76,379	$ 71,230	$ 72,226	$ 74,242	$ 76,119
			Demand	5,447	5,095	5,180	5,411	5,482	$ 61,425	$ 57,524	$ 58,250	$ 60,989	$ 61,925
			Gas	11,080,212	12,327,792	12,216,803	11,645,294	11,916,435	$ 82,952	$ 92,292	$ 91,461	$ 87,182	$ 89,212
			M.7 EUI	128 / 1.2 %	133 / .9 %	133 / .9 %	131 / 1.1 %	134 / 1.1 %	$220,757 / 2.0 %	$221,047 / 1.7 %	$221,937 / 1.8 %	$222,414 / 2.0 %	$227,256 / 2.0 %
M.8	3-Way to 2-Way Valves and VFD on Pumps Combine with CHW & HW Reset Temps	Installing 2-way valves instead of 3-way valves allows the pump to be controlled based on demand by a variable frequency drive	Electric	1,995,585	1,831,460	1,858,679	1,922,553	1,969,102	$ 67,570	$ 62,013	$ 62,935	$ 65,098	$ 66,674
			Demand	5,237	4,878	4,970	5,231	5,281	$ 59,177	$ 55,235	$ 55,998	$ 59,113	$ 59,808
			Gas	11,183,029	12,433,487	12,321,928	11,749,275	12,021,145	$ 83,722	$ 93,083	$ 92,248	$ 87,961	$ 89,996
			M.8 EUI	123 / 5.4 %	128 / 5.1 %	127 / 5.1 %	125 / 5.3 %	128 / 5.4 %	$210,469 / 6.5 %	$210,331 / 6.5 %	$211,181 / 6.5 %	$212,172 / 6.5 %	$216,478 / 6.6 %
M.9	ERV on AHUs	Enthalphy wheel energy recovery ventilator installed on each air handler unit	Electric	2,899,647	2,801,934	2,827,415	2,861,021	2,929,345	$ 98,182	$ 94,874	$ 95,736	$ 96,874	$ 99,188
			Demand	5,876	5,702	5,729	5,855	5,991	$ 66,109	$ 64,119	$ 64,313	$ 65,868	$ 67,445
			Gas	10,616,985	11,684,794	11,590,138	11,074,329	11,294,736	$ 79,484	$ 87,478	$ 86,770	$ 82,908	$ 84,558
			M.9 EUI	140 / -7.9 %	145 / -7.9 %	145 / -7.9 %	142 / -7.8 %	145 / -7.5 %	$243,775 / -8.2 %	$246,471 / -9.6 %	$246,819 / -9.2 %	$245,650 / -8.2 %	$251,191 / -8.3 %

Table 10 Yearly Energy Use for Building HVAC Systems, Controls and Combined ECM's, and Energy Costs

				Energy Consumption					Energy Cost				
Rerun status	Energy Efficiency Measure	Construction Data	multiplier	Corbin/Williamsburg	Covington	Lexington	Louisville	Paducah	Corbin	Covington	Lexington	Louisville	Paducah
			3.412	kWh	kWh	kWh	kWh	kWh					
				kW	kW	kW	kW	kW					
CM #	description1	Changes	1	kBtu	kBtu	kBtu	kBtu	kBtu					
M.10	VAV Box Minimum Air Flow Schedule	Allows the minimum air flow through a VAV box to go down to 0% during unoccupied periods	Electric	1,848,459	1,778,740	1,794,073	1,832,281	1,889,383	$ 62,589	$ 60,228	$ 60,747	$ 62,041	$ 63,975
			Demand	5,641	5,287	5,378	5,644	5,705	$ 63,694	$ 59,803	$ 60,577	$ 63,734	$ 64,543
			Gas	4,767,941	6,703,362	6,527,761	5,873,445	6,218,153	$ 35,695	$ 50,185	$ 48,870	$ 43,972	$ 46,552
			M.10 EUI	76 / 41.7 %	87 / 35.1 %	86 / 35.7 %	83 / 37.3 %	87 / 36.1 %	$161,978 / 28.1 %	$170,216 / 24.3 %	$170,195 / 24.7 %	$169,747 / 25.2 %	$175,070 / 24.5 %
M.11	DHW using Electricity	Domestic Hot Water is provided by an electric water heater	Electric	2,377,938	2,211,474	2,242,138	2,308,469	2,367,529	$ 80,517	$ 74,881	$ 75,919	$ 78,165	$ 80,165
			Demand	5,882	5,540	5,634	5,881	5,950	$ 66,321	$ 62,564	$ 63,373	$ 66,309	$ 67,213
			Gas	10,831,716	12,064,771	11,955,778	11,390,696	11,659,600	$ 81,092	$ 90,323	$ 89,507	$ 85,276	$ 87,290
			M.11 EUI	129 / .4 %	134 / .4 %	134 / .4 %	132 / .4 %	135 / .3 %	$227,930 / -1.2 %	$227,767 / -1.3 %	$228,798 / -1.3 %	$229,750 / -1.2 %	$234,668 / -1.2 %
M.12	DHW using Heat Pump	Domestic Hot Water is provided by an electric heat pump	Electric	2,470,861	2,304,235	2,334,907	2,401,315	2,460,351	$ 83,663	$ 78,021	$ 79,060	$ 81,309	$ 83,307
			Demand	5,959	5,617	5,711	5,958	6,027	$ 67,211	$ 63,454	$ 64,262	$ 67,198	$ 68,103
			Gas	10,831,716	12,064,771	11,955,778	11,390,696	11,659,600	$ 81,092	$ 90,323	$ 89,507	$ 85,276	$ 87,290
M.16	Chilled Water Loop Operation	Chilled Water loop operation is based on demand not standby	Electric	2,036,309	1,786,918	1,830,683	1,927,530	1,953,059	$ 68,949	$ 60,505	$ 61,987	$ 65,266	$ 66,131
			Demand	5,630	5,277	5,378	5,622	5,597	$ 63,552	$ 59,674	$ 60,554	$ 63,466	$ 63,405
			Gas	11,080,209	12,327,791	12,216,800	11,645,297	11,916,431	$ 82,952	$ 92,292	$ 91,461	$ 87,183	$ 89,212
			M.16 EUI	123 / 5.2 %	126 / 6.4 %	126 / 6.2 %	124 / 5.8 %	127 / 6.2 %	$215,454 / 4.3 %	$212,471 / 5.5 %	$214,002 / 5.3 %	$215,914 / 4.9 %	$218,748 / 5.7 %
VAV.ALL	VAV: Combination of ...C.3 - L.1 - M.1 - A.45 - M.2 - M.3 - M.6 - M.7 - M.8 - M.10		Electric	1,128,241	1,081,818	1,098,859	1,132,120	1,158,875	$ 38,202	$ 36,630	$ 37,207	$ 38,334	$ 39,239
			Demand	4,482	4,142	4,210	4,453	4,512	$ 50,735	$ 46,964	$ 47,491	$ 50,378	$ 51,179
			Gas	3,560,816	4,653,454	4,503,837	4,157,817	4,275,444	$ 26,658	$ 34,838	$ 33,718	$ 31,127	$ 32,008
			VAV.ALL EUI	51 / 61.0 %	57 / 57.6 %	56 / 58.1 %	55 / 58.5 %	56 / 58.5 %	$115,595 / 48.7 %	$118,432 / 47.3 %	$118,416 / 47.6 %	$119,839 / 47.2 %	$122,426 / 47.2 %
G.M.17	Geothermal Heat Pump System	Change HVAC System from VAV to Geothermal	Electric	1,452,819	1,560,733	1,531,237	1,518,665	1,576,518	$ 49,192	$ 52,846	$ 51,848	$ 51,422	$ 53,381
			Demand	5,984	5,932	5,800	6,085	6,204	$ 66,721	$ 65,658	$ 64,156	$ 67,864	$ 69,252
			Gas	246,508	261,358	259,308	252,698	255,045	$ 1,845	$ 1,957	$ 1,941	$ 1,892	$ 1,909
			G.M.17 EUI	36 / 72.6 %	38 / 71.6 %	37 / 72.1 %	37 / 71.9 %	38 / 71.6 %	$117,759 / 47.7 %	$120,461 / 46.4 %	$117,945 / 47.8 %	$121,178 / 46.6 %	$124,542 / 46.3 %
G.M.19	Minimum OA Schedule		Electric	1,334,538	1,381,344	1,362,143	1,368,240	1,417,766	$ 45,187	$ 46,772	$ 46,122	$ 46,329	$ 48,006
			Demand	5,657	5,754	5,661	5,811	6,126	$ 63,587	$ 64,044	$ 62,960	$ 65,205	$ 68,649
			Gas	246,084	260,964	258,911	252,314	254,671	$ 1,842	$ 1,954	$ 1,938	$ 1,889	$ 1,907
			G.M.19 EUI	33 / 74.8 %	34 / 74.7 %	34 / 75.1 %	34 / 74.6 %	35 / 74.3 %	$110,617 / 50.9 %	$112,770 / 49.9 %	$111,020 / 50.9 %	$113,422 / 50.0 %	$118,562 / 48.9 %

Table 11 Yearly Energy Use for Building Controls and Combined ECM's, and Energy Costs

Rerun status	Energy Efficiency Measure	Construction Data	multiplier	Corbin/Williamsburg	Covington	Lexington	Louisville	Paducah	Corbin	Covington	Lexington	Louisville	Paducah
			3.412	kWh	kWh	kWh	kWh	kWh					
				kW	kW	kW	kW	kW					
CM #	description1	Changes	1	kBtu	kBtu	kBtu	kBtu	kBtu					
G.M.20	Modified Fan Schedule		Electric	1,200,843	1,312,111	1,290,174	1,273,244	1,326,557	$ 40,661	$ 44,428	$ 43,685	$ 43,112	$ 44,917
			Demand	5,820	5,873	5,738	5,975	6,145	$ 65,004	$ 65,010	$ 63,507	$ 66,662	$ 68,590
			Gas	246,537	261,381	259,311	252,713	255,039	$ 1,846	$ 1,957	$ 1,941	$ 1,892	$ 1,909
			G.M.20 EUI	30 / 77.2 %	32 / 75.9 %	32 / 76.3 %	31 / 76.2 %	33 / 75.9 %	$107,510 / 52.3 %	$111,395 / 50.5 %	$109,133 / 51.7 %	$111,666 / 50.8 %	$115,416 / 50.2 %
G.M.21	Variable Speed Pumps, Load Reset on Heating Side, and Load Reset on Cooling Side		Electric	1,393,491	1,498,899	1,471,579	1,456,177	1,512,340	$ 47,184	$ 50,753	$ 49,828	$ 49,306	$ 51,208
			Demand	5,737	5,642	5,539	5,806	5,969	$ 63,965	$ 62,481	$ 61,283	$ 64,773	$ 66,616
			Gas	246,513	261,370	259,319	252,707	255,051	$ 1,846	$ 1,957	$ 1,941	$ 1,892	$ 1,909
			G.M.21 EUI	34 / 73.7 %	37 / 72.7 %	36 / 73.2 %	36 / 73.0 %	37 / 72.7 %	$112,995 / 49.8 %	$115,191 / 48.8 %	$113,052 / 50.0 %	$115,971 / 48.9 %	$119,733 / 48.4 %
G.M.24	Water or Well for HX		Electric	1,578,236	1,665,396	1,639,331	1,636,555	1,702,825	$ 53,439	$ 56,390	$ 55,508	$ 55,414	$ 57,658
			Demand	6,925	6,817	6,842	6,882	7,222	$ 76,756	$ 75,356	$ 75,710	$ 76,194	$ 80,015
			Gas	246,762	261,794	259,726	253,039	255,379	$ 1,847	$ 1,960	$ 1,944	$ 1,894	$ 1,912
			G.M.24 EUI	38 / 70.4 %	41 / 69.8 %	40 / 70.3 %	40 / 69.8 %	41 / 69.4 %	$132,043 / 41.4 %	$133,706 / 40.5 %	$133,162 / 41.1 %	$133,502 / 41.2 %	$139,584 / 39.8 %
G.C.3	Pitched Roof R-37.04 Built Up Roof R-40.00	Change 3" exterior Polyisocyanurate to 5" exterior Polyisocyanurate	Electric	1,439,467	1,543,096	1,514,571	1,503,018	1,559,588	$ 48,740	$ 52,249	$ 51,283	$ 50,892	$ 52,808
			Demand	5,924	5,897	5,763	6,056	6,161	$ 66,083	$ 65,284	$ 63,765	$ 67,540	$ 68,772
			Gas	246,521	261,320	259,277	252,684	255,022	$ 1,846	$ 1,956	$ 1,941	$ 1,892	$ 1,909
			G.C.3 EUI	35 / 72.9 %	38 / 71.9 %	37 / 72.4 %	37 / 72.2 %	38 / 71.8 %	$116,669 / 48.2 %	$119,490 / 46.9 %	$116,989 / 48.2 %	$120,324 / 47.0 %	$123,489 / 46.7 %
G.C.8	Steel Stud Walls R-34.5	Steel wall stud layers: air film, 4" face brick, air space, 3.5" polyiso, 2x6 steel wall 16 O.C. R-19 batt insul, gypsum board air film	Electric	1,432,225	1,533,744	1,496,904	1,495,121	1,548,149	$ 48,495	$ 51,933	$ 50,685	$ 50,625	$ 52,420
			Demand	5,900	5,852	5,692	6,015	6,115	$ 65,791	$ 64,785	$ 62,957	$ 67,050	$ 68,233
			Gas	246,447	261,262	259,215	252,625	254,983	$ 1,845	$ 1,956	$ 1,941	$ 1,891	$ 1,909
			G.C.8 EUI	35 / 73.0 %	38 / 72.1 %	37 / 72.7 %	37 / 72.3 %	38 / 72.0 %	$116,131 / 48.4 %	$118,673 / 47.2 %	$115,583 / 48.8 %	$119,566 / 47.3 %	$122,563 / 47.1 %
G.C.15	ICF R-21.74, Pitched Roof R-37.04 Built Up Roof R-40.00	Wall: air film, 4" brick, air space, 1.5" Polyurethane, 6" 140lb conc., 1.5" Polyurethane, 1/2" gyp board, air film; for roof: Changed 3"	Electric	1,427,408	1,526,047	1,491,046	1,488,408	1,542,085	$ 48,332	$ 51,672	$ 50,487	$ 50,397	$ 52,215
			Demand	5,847	5,808	5,657	5,969	6,070	$ 65,241	$ 64,320	$ 62,588	$ 66,568	$ 67,742
			Gas	246,497	261,273	259,232	252,652	254,995	$ 1,845	$ 1,956	$ 1,941	$ 1,891	$ 1,909
			G.C.15 EUI	35 / 73.1 %	37 / 72.2 %	37 / 72.8 %	36 / 72.4 %	38 / 72.1 %	$115,418 / 48.8 %	$117,948 / 47.6 %	$115,015 / 49.1 %	$118,857 / 47.6 %	$121,866 / 47.4 %
G.C.17	CMU walls R-25 Pitched Roof R-37.04 Built Up Roof R-40.00	for wall Changed 1-1/4" Polystyrene to 3" ployiso, for roof Changed 3" exterior Polyisocyanurate to 5" exterior Polyisocyanurate	Electric	1,416,066	1,512,897	1,477,694	1,475,611	1,529,540	$ 47,948	$ 51,227	$ 50,035	$ 49,964	$ 51,790
			Demand	5,855	5,821	5,662	5,982	6,082	$ 65,320	$ 64,448	$ 62,635	$ 66,709	$ 67,864
			Gas	246,487	261,250	259,208	252,634	254,979	$ 1,845	$ 1,956	$ 1,941	$ 1,891	$ 1,909
			G.C.17 EUI	35 / 73.3 %	37 / 72.4 %	36 / 73.1 %	36 / 72.7 %	37 / 72.4 %	$115,114 / 48.9 %	$117,630 / 47.7 %	$114,611 / 49.3 %	$118,565 / 47.8 %	$121,563 / 47.6 %
G.Option1	G.C.15, M.17, M.19, M.20, M.21	Combination of ECMs with ICF wall construction	Electric	1,059,416	1,110,013	1,085,608	1,090,433	1,133,887	$ 35,872	$ 37,585	$ 36,759	$ 36,922	$ 38,393
			Demand	5,240	5,346	5,187	5,383	5,648	$ 58,722	$ 59,333	$ 57,531	$ 60,202	$ 63,079
			Gas	246,451	261,223	259,167	252,598	254,939	$ 1,845	$ 1,956	$ 1,940	$ 1,891	$ 1,909
			G.Option1 EUI	26 / 79.7 %	28 / 79.4 %	27 / 79.9 %	27 / 79.5 %	28 / 79.2 %	$96,439 / 57.2 %	$98,874 / 56.0 %	$96,230 / 57.4 %	$99,016 / 56.4 %	$103,381 / 55.4 %
G.Option2	G.C.17, M.17, M.19, M.20, M.21	Combination of ECMs with CMU construction	Electric	1,046,560	1,094,627	1,071,354	1,076,905	1,118,109	$ 35,437	$ 37,064	$ 36,276	$ 36,464	$ 37,859
			Demand	5,224	5,342	5,176	5,374	5,644	$ 58,549	$ 59,287	$ 57,400	$ 60,095	$ 63,036
			Gas	246,427	261,181	259,131	252,570	254,914	$ 1,845	$ 1,955	$ 1,940	$ 1,891	$ 1,908
			G.Option2 EUI	26 / 79.9 %	27 / 79.7 %	27 / 80.1 %	27 / 79.7 %	28 / 79.5 %	$95,830 / 57.5 %	$98,307 / 56.3 %	$95,617 / 57.7 %	$98,450 / 56.6 %	$102,803 / 55.7 %
G.Option3	G.C.3,G.C.8, M.17, M.19, M.20, M.21	Combination of ECMs with Steel Stud construction	Electric	1,050,112	1,097,568	1,073,871	1,080,187	1,121,160	$ 35,557	$ 37,164	$ 36,361	$ 36,575	$ 37,962
			Demand	5,218	5,326	5,165	5,358	5,631	$ 58,474	$ 59,116	$ 57,297	$ 59,924	$ 62,897
			Gas	246,404	261,158	259,108	252,549	254,899	$ 1,845	$ 1,955	$ 1,940	$ 1,891	$ 1,908
			G.Option3 EUI	26 / 79.9 %	27 / 79.6 %	27 / 80.1 %	27 / 79.6 %	28 / 79.4 %	$95,875 / 57.4 %	$98,235 / 56.3 %	$95,598 / 57.7 %	$98,390 / 56.7 %	$102,768 / 55.7 %

5.3 Energy Conservation Measures Discussion of Analyses Results

Review of Tables 5 through Table 7 shows that, in general, large increases in the thermal resistance of the building envelope reduce the yearly energy use in the building by less than 1.0 %. The highest reduction of energy use was shown when the cavity wall insulation was increased to 3" of polyisocyanerate foam board (Wall R of 25). The performance of the ICF wall system and the masonry cavity wall systems with comparable insulation is quite similar. The low mass, brick veneer steel stud wall system needed much higher R values to give comparable performance. Relatively large changes in roof insulation only changed the energy use in the building by less than 0.8%. Figure 15 shows the variation of the yearly energy savings (as total cost savings) as a function of R value for three envelope systems.

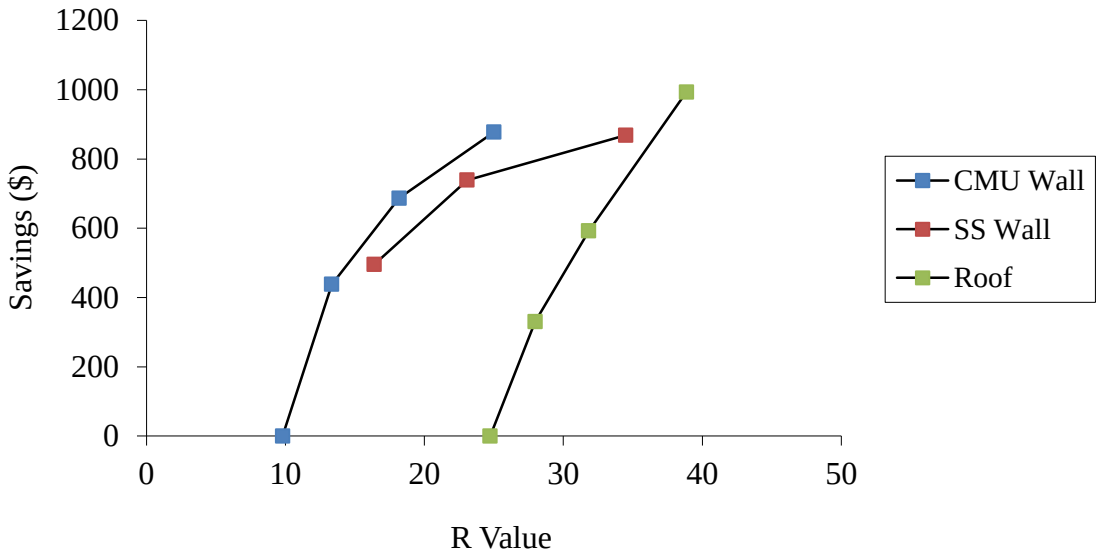

Figure 15 Variation of Yearly Energy Cost Savings with Wall and Roof R values (SS is the Brick Veneer steel Stud Wall, CMU is the CMU cavity wall)

It appears that the prescriptive thermal resistance requirements (R) in the code are high enough that increases in thermal resistance in the walls are less effective at higher values. This phenomenon was also seen in study of mass wall systems by Oakridge National Laboratory [Kosny et-la, 2001], where increasing the thermal resistance of mass wall systems to reduce energy use becomes significantly less effective past a certain point. The R value where increases become less effective changes with climate and mass of the wall, the higher the mass, or hotter the climate, the lower the R value where the insulation becomes less effective.

These tables also show when you combine significant increases in envelop resistance in the walls and roof the effects cannot be directly added, there are obviously interactions. Furthermore there is relatively low impact on energy use with relatively large changes in window U values, at least for the building configuration investigated. Larger window areas will likely produce larger effects.

The tabled values also show that making the exterior walls more airtight does result in a small energy savings (less than 1%) but the results of the analyses suggests that making it too airtight can be detrimental. It appears that, for low infiltration rates, a significant amount of energy is needed to provide mechanical ventilation for all the exterior spaces and this significantly reduces the net energy savings (In one case, this actually takes more energy than the base line configuration).

Examination of Table 8, shows that building orientation has a very minor effect on energy usage. This is probably due to the fact that, although the one face of the building has fewer windows, the total area of fenestrations is low. Structures with larger window areas will likely show higher orientation effects on energy usage.

Table 8 also shows that changing out the T 12 lamps for T 8 lamps does reduce the overall electrical energy used by about 5%. However, the reduction in waste heat energy provided by the lights increases the heating load and increases the gas heat energy demand by about 3%. Thus, the overall effect on the building energy use index is minimal (about 0.1%), but the overall energy cost savings was about 3%. This same effect can be seen when occupancy sensors are used on the lights.

Examination of the results listed in Tables 9 through 11 show that changes in the mechanical systems and control strategies produce the greatest effects on the energy used by the facility. Using a higher efficiency boiler greatly reduced the gas energy used and lowers the EUI by about 6.5 %. Modified fan scheduling (general shut down at night) and large set-backs can save a significant amount of energy, resulting in reductions in EUI of approximately 20%. Allowing the VAV boxes to close fully during unoccupied periods also can significantly reduce energy use, with reductions in EUI's of over 30%. Finally changing the HVAC system out for a ground source heat pump system provides the greatest reduction in energy use, an EUI reduction of approximately 72%. Even using the less efficient water source heat pump produces a reduction in EUI of about 70%.

In an effort to evaluate how much energy could be saved in the building, select energy conservation measures (ECM) were combined. One group of ECM's were applied to the base building configuration and restricted to the conventional VAV HVAC systems. This was done in an attempt to see how far you could reasonably reduce the energy consumption of a conventional HVAC system and was expected to produce the lowest capital costs (ECM – All - in Table 10). The second group used a ground source heat pump for the HVAC system and a variety of wall systems, and control strategies (The G option configurations).

The ECM's addressed in the ECM-all group were selected in an effort to produce the greatest reduction in energy use at the least cost. An exterior CMU cavity wall was used with a high R, a roof with 5" polyisocyanerate insulation,T8 lighting, 90% efficient condensing boiler, daylighting, a larger temperature setback schedule, modified fan schedule, VFD mortars on cooling tower fan, 2-way valves with a VFD on the chilled water pumps, and a VAV box minimum air flow schedule. The total reduction in energy use was in excess of 57%. Figure 16 shows the amount of electrical energy used through the year in the ECM all building configuration. Also shown on this graph is the electrical energy used by the base building. A significant reduction in energy use can be seen, especially in the peak cooling months. Figure 17 shows a similar comparison for the gas energy use for both ECM and base building configurations. There is a more uniform reduction across the year, with a slight increase in December. It should be noted that reductions in energy use near 50% could be achieved without increases in the building envelope.

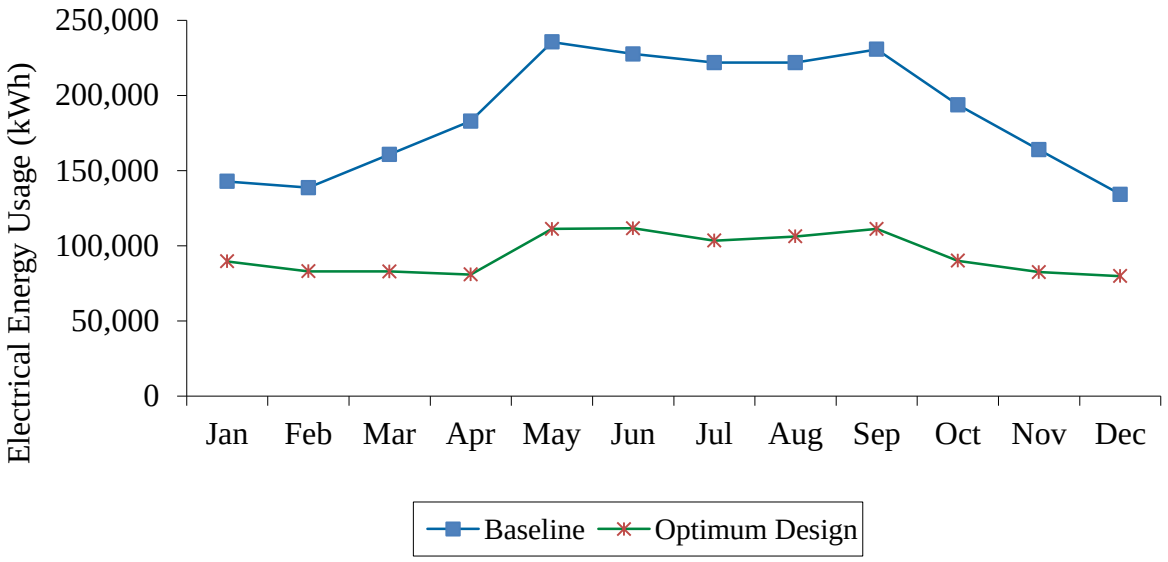

Figure 16 ECM-all Configuration Yearly Electrical Energy Use

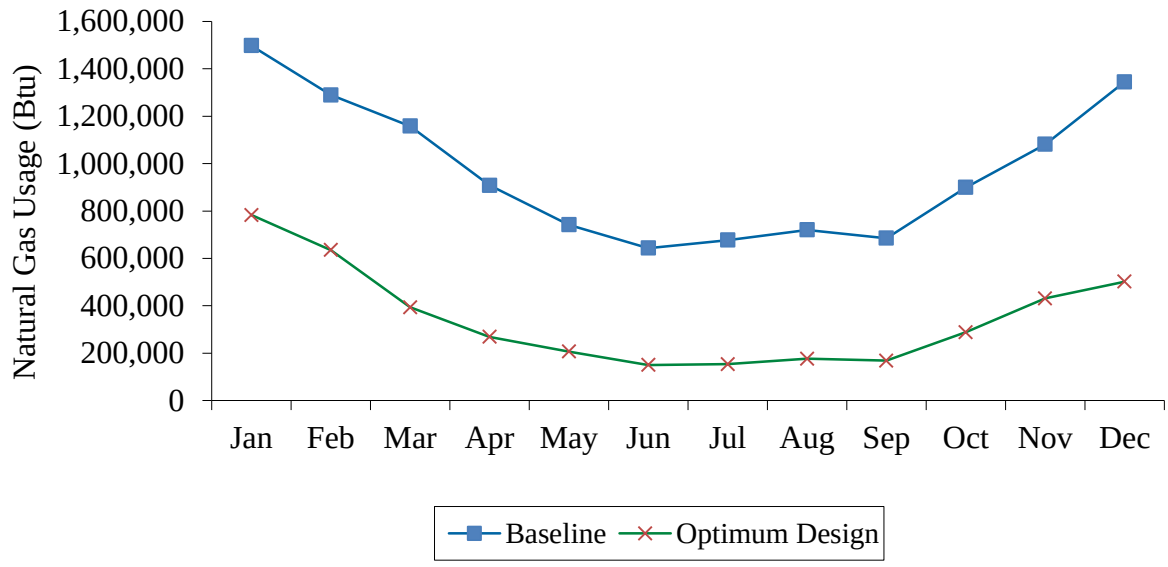

Figure 17 ECM-all Configuration Yearly Gas Energy Use

For the ground source heat pump configurations with loop operation on demand, variable speed fans and pumps, a modified fan schedule and OA Schedule, and some

of the higher R envelope systems, the reduction in yearly energy use based on EUI is approximately 80%.

It is clear that, while the use of ground source heat pumps will significantly reduce the energy used in school facilities, significant reduction in energy use can be realized using conventional VAV systems, efficient boilers, mortars and lights and an aggressive control strategy that turns the HVAC system off when the spaces are not occupied (see Figure 18). It should be noted that care must be exercised when using low ventilation rates that sufficient conditioned air is brought into spaces so that mold and mildew (or other moisture related) problems do not occur.

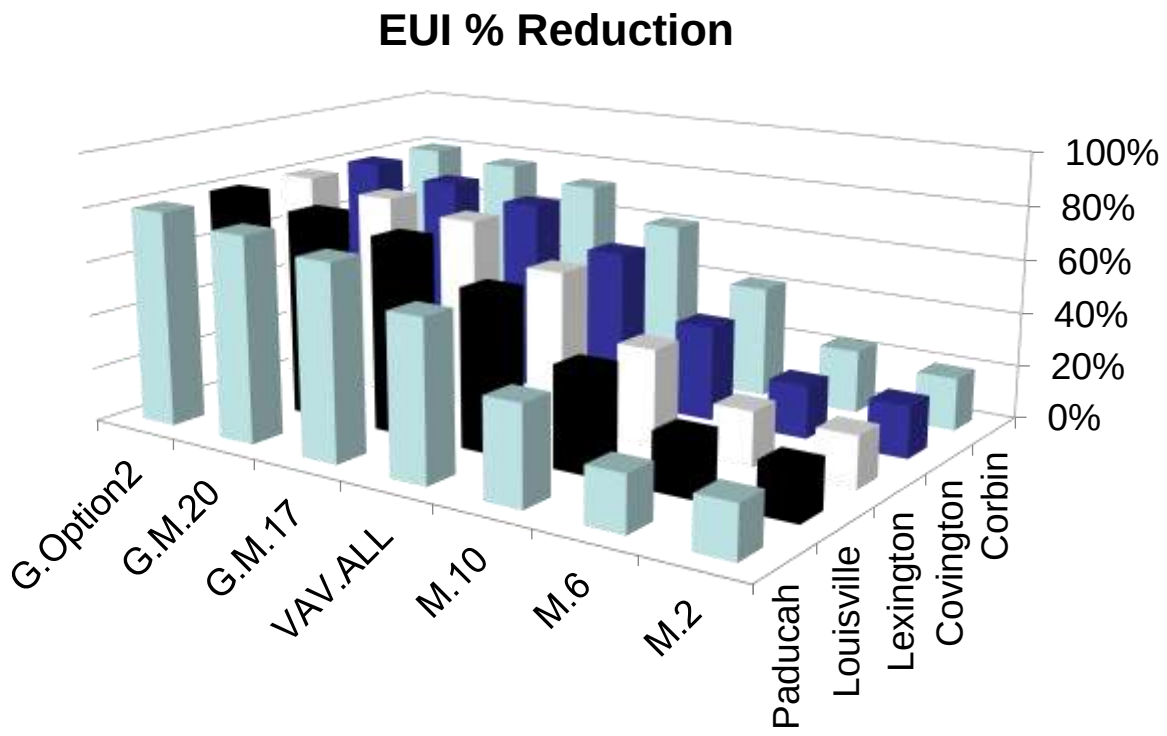

Figure 18 Energy Savings for Select ECM's Based EUI Reduction

5.0 Economic Analysis

The base school building cost was estimated using a square foot cost of $111/ft^2. This unit cost was obtained from the RSMEANS Building Construction Cost Data Manual, for a 158,000 ft^2 middle school in Louisville, KY [RSMEANS-BC, 2011]. This unit cost resulted in a total construction cost (excluding fees and land) of $17,540,000. The unit cost value was confirmed by a construction estimator as being a reasonable value for school construction costs in Kentucky.

In an effort to evaluate the economic viability of the various energy conservation measures described in the previous sections, an economic analysis was conducted. This analysis involved determining the incremental costs associated with changes in building configuration needed to support each ECM. These costs were generated by first estimating the quantity and configuration of the affected systems in the base building configuration. The quantity and configuration of the systems in the new building system configuration was then estimated. Unit costs for the original and modified systems were estimated for the five Kentucky cities using the RSMEANS Building Construction Cost Data Manual, the RSMEANS Building Mechanical Cost Data Manual, the RSMEANS Electrical Construction Cost Data Manual, input from a certified construction estimator [RsMeans, 2011], and input from mechanical contractors and HVAC engineers familiar with design and construction of the systems

being evaluated. The incremental costs were then determined for each ECM by simply subtracting the new system cost from the base configuration.

For instance, the total opaque wall area for the base school was obtained from the CAD plans and totaled 48,900 ft^2. The incremental cost of using 2" polyosicyanerate foam insulation over using the 1-1/4" polystyrene foam was $\$0.18.ft^2$ for Louisville. This produced a total capital cost increase $8,923 for this ECM in Louisville. There are slight differences in the cost for each city. It should be noted that only differences in costs were addressed, not total building costs.

For ECM's that required additional equipment or sensors, the number of these items were estimated and added to the total cost of the ECM. The total incremental cost of each ECM was tabulated in Tables 12 through 16. For each ECM, an estimate on maintenance (and/or replacement) costs was attempted and where it was expected to be different from the base system, these costs were added to the costs of the ECM as a yearly cost. For instance, the use of gypsum wall board on the interior face of the exterior walls on the brick veneer steel stud walls and the ICF systems will require additional maintenance compared to the masonry cavity wall systems. It was expected that approximately 10% more of the wall area will have to be patched and painted for these systems each year, compared to other wall systems. A cost for this painting and patching was estimated using the values in the MEANS Cost Manuals and a yearly maintenance cost was developed. Each city has slightly different costs so are tabulated separately. Note that some ECM's had no additional cost associated with

them, such as changing the orientation of the building. These ECM's are identified as no cost ECM's.

Also shown in each of these tables is the simple pay-back period (SPB) for each ECM. This was obtained by dividing incremental capital costs by the yearly energy cost savings. Maintenance costs, interest and energy price increases were not included.

Examination of the tables show that envelope improvements have long simple payback periods, in general, in excess of 100 years and well beyond the design life of a typical school facility. There are some ECM's, such as the use of T 8 lamp with electronic ballasts, where the cost are actually slight lower the base configuration cost. These ECM's save both capital costs and energy costs and should always be considered in design.

It should be noted that there are some ECM's that show lower capital cost, such as the use of brick veneer steel stud exterior wall systems that should be adapted with care. While the capital costs are significantly lower and they can be insulated to give comparable energy performance, the other performance characteristics of these systems may not be equivalent to the traditional masonry cavity wall systems. The durability, fire resistance and sound transmission characteristics of the brick veneer steel stud systems are not comparable to the masonry cavity wall systems, nor the ICF systems.

It is also evident in the examination of the tables that the lowest simple payback periods are for those ECM's that address control strategies. These ECM's usually have very low capital costs and provide significant energy savings. In fact, the ECM that combined the conventional VAV HVAC systems, an efficient boiler and aggressive control strategies, efficient lights, etc. (ECM-ALL), reduced the EUI by over 50% and had a simple payback of about 2.5 years.

The paybacks for the ECM's that incorporated the ground source, or water source heat pumps, are much longer than those where the conventional HVAC system was used. All the simple payback periods exceeded 25 years. The cost for the VAV systems were based on unit cost of $7000/ton, the ground source heat pump systems at $14,000/ ton and the water source heat pumps at $13,000/ton. These values are based on averages experienced by a design engineers with over 20 years of experience in the Kentucky. It should be noted that better paybacks might be possible if the tonnage of the heat pumps is reduced by reducing demand. However, the demand reduction costs (ECM's) must be incorporated in the analysis and for this investigation, the HVAC tonnage was kept consistent.

The previous discussion is represented in the graph in Figure 19. On this plot selected ECM's are shown and it is clear that the most cost effective ECM's are those that incorporated higher efficiency conventional systems, and aggressive control strategies. Significantly, higher payback periods are shown for ECM's that incorporate ground and

water source heat pumps and building envelope improvements much beyond the code minimums have very long payback periods.

Table 12a Louisville Economic Analysis of ECM's

ECM	Description	Cost	Savings	SPB (Years)	SF In Year
A.45	Varying the Orientation - No Cost	$ -	$ 98.72	0.0	NO Cost ECM
A.90	Varying the Orientation - No Cost	$ -	$ 5.69	0.0	NO Cost ECM
A.135	Varying the Orientation - No Cost	$ -	$ 44.71	0.0	NO Cost ECM
A.180	Varying the Orientation - No Cost	$ -	$ (107.78)	0.0	NO IMPROVEMENT
A.225	Varying the Orientation - No Cost	$ -	$ (152.90)	0.0	NO IMPROVEMENT
A.270	Varying the Orientation - No Cost	$ -	$ (156.24)	0.0	NO IMPROVEMENT
A.315	Varying the Orientation - No Cost	$ -	$ 26.39	0.0	NO Cost ECM
C.1	Change 3" exterior Polyisocyanurate to 3.5" exterior	$ 84,274.71	$ 330.02	255.4	-
C.2	Change 3" exterior Polyisocyanurate to 4" exterior	$ 94,678.99	$ 592.28	159.9	-
C.3	Change 3" exterior Polyisocyanurate to 5" exterior	$ 187,277.13	$ 993.39	188.5	-
C.4	ICF Wall: air film, 4" brick, air space, 1.5" Polyurethane, 6"	$ 252,986.52	$ 755.20	335.0	-
C.5	Changed 1-1/4" Polystyrene to 3" ploiyso	$ 66,031.59	$ 877.44	75.3	-
C.6	Changed 1-1/4" Polystyrene to 2" ploiyso	$ 8,923.19	$ 686.98	13.0	17
C.7	Changed 1-1/4" Polystyrene to 1 1/2" polyurethane	$ -	$ 438.10	0.0	NO Cost ECM
C.8	Steel wall stud layers: air film, 4" face brick, air space, 3.5" polyiso, 2x6 steel wall 16 O.C. R-19 batt insul, gypsum board air film	$ (255,556.89)	$ 868.51	-294.2	NO Cost ECM
C.9	Steel wall stud layers: air film, 4" face brick, air space, 2" polyiso, 2x6 steel wall 16 O.C. R-19 batt insul, gypsum board air film	$ (309,542.18)	$ 739.09	-418.8	NO Cost ECM
C.10	Steel wall stud layers: air film, 4" face brick, air space, 1.5" Polystyrene, 2x6 steel wall 16 O.C. R-19 batt insul, 1/2" GYP board, air film	$ (326,942.39)	$ 495.87	-659.3	NO Cost ECM
C.11	Steel wall stud layers: air film, 4" face brick, air space, 3" Polystyrene, 2x6 steel wall 16 O.C. No batt insul, 1/2" GYP board, air film	$ (313,557.61)	$ 500.51	-626.5	NO Cost ECM
C.12	Light Vapor Barrior	$ -	$ (180.49)	0.0	NO IMPROVEMENT
C.13	Medium Vapor Barrior	$ 42,385.14	$ 725.60	58.4	-
C.14	Heavy Vapor Barrier	$ 84,770.28	$ 1,573.12	53.9	-
C.15	Wall: air film, 4" brick, air space, 1.5" Polyurethane, 6" 140lb conc., 1.5" Polyurethane, 1/2" gyp board, air film; for roof: Changed 3" exterior Polyisocyanurate to 5" exterior Polyisocyanurate	$ 440,263.65	$ 1,553.44	283.4	-
C.16	for wall Changed 1-1/4" Polystyrene to 2" polyiso, for roof Changed 3" exterior Polyisocyanurate to 5" exterior Polyisocyanurate	$ 196,200.32	$ 1,157.86	169.5	-
C.17	for wall Changed 1-1/4" Polystyrene to 3" ploiyso, for roof Changed 3" exterior Polyisocyanurate to 5" exterior Polyisocyanurate	$ 253,308.71	$ 1,862.18	136.0	-
C.18	Window Type 1	$ (10,770.88)	$ (2.22)	4841.1	-
C.19	Window Type 2	$ 16,156.32	$ 414.00	39.0	-
L.1	Energy Efficient Lighting	$ (100.43)	$ 11,755.75	0.0	NO Cost ECM
L.2	Modified Lighting Schedule	$ 17,113.27	$ 4,668.15	3.7	4

Table 12b Louisville Economic Analysis of ECM's

ECM	Description	Cost	Savings	SPB (Years)	SF In Year
M.1	Condensing Boiler	$ 2,264.60	$ 9,492.31	0.2	1
M.2	Large Temperature Setbacks	$ -	$ 27,813.53	0.0	NO Cost ECM
M.3	Daylighting	$ 17,113.27	$ 1,021.24	16.8	24
M.4	Water Side Economizer	$ -	$ (27,538.22)	0.0	NO IMPROVEMENT
M.5	Minimum OA Schedule	$ 169,990.00	$ 4,605.77	36.9	-
M.6	Modified Fan Schedule	$ 169,990.00	$ 48,868.29	3.5	4
M.7	VFD on Cooling Tower Fan	$ 11,869.00	$ 7,123.72	1.7	2
M.8	3-Way to 2-Way Valves and VFD on Pumps Combine with CHW & HW Reset Temps	$ 15,886.20	$ 28,698.77	0.6	1
M.9	ERV on AHUs	$ -	$ (43,919.85)	0.0	NO IMPROVEMENT
M.10	VAV Box Minimum Air Flow Schedule	$ 169,990.00	$ 74,569.17	2.3	3
M.11	DHW using Electricity	$ 30,500.00	$ (5,272.99)	-5.8	NO IMPROVEMENT
M.12	DHW using Heat Pump	$ -	$ (13,144.90)	0.0	NO IMPROVEMENT
M.16	Chilled Water Loop Operation	$ -	$ 24,419.14	0.0	NO Cost ECM
ECM.ALL	VAV: Combination of …C.3 - L.1 - M.1 - A.45 - M.2 - M.3 - M.6 - M.7 - M.8 - M.10	$ 404,299.77	$ 154,101.99	2.6	3
G.M.17	Geothermal Heat Pump System	$ 3,787,000.00	$ 134,895.07	28.1	64
G.M.19	Minimum OA Schedule	$ 3,956,990.00	$ 149,432.38	26.5	55
G.M.20	Modified Fan Schedule	$ 3,956,990.00	$ 154,565.65	25.6	51
G.M.21	Variable Speed Pumps, Load Reset on Heating Side, and Load Reset on Cooling Side	$ -	$ 142,908.80	0.0	NO Cost ECM
G.M.24	Water or Well for HX	$ 3,189,000.00	$ 116,499.94	27.4	60
G.C.3	Change 3" exterior Polyisocyanurate to 5" exterior Polyisocyanurate	$ 187,277.13	$ 136,411.53	1.4	2
G.C.8	Steel wall stud layers: air film, 4" face brick, air space, 3.5" polyiso, 2x6 steel wall 16 O.C. R-19 batt insul, gypsum board air film	$ (309,542.18)	$ 137,493.37	-2.3	NO Cost ECM
G.C.15	Wall: air film, 4" brick, air space, 1.5" Polyurethane, 6" 140lb conc., 1.5" Polyurethane, 1/2" gyp board, air film; for roof: Changed 3" exterior Polyisocyanurate to 5" exterior Polyisocyanurate	$ 440,263.65	$ 138,545.01	3.2	4
G.C.17	for wall Changed 1-1/4" Polystyrene to 3" ployiso, for roof Changed 3" exterior Polyisocyanurate to 5" exterior Polyisocyanurate	$ 253,308.71	$ 139,343.34	1.8	2
G.Option1	G.C.15, M.17, M.19, M.20, M.21	$ 12,141,243.65	$ 175,344.16	69.2	-
G.Option2	G.C.17, M.17, M.19, M.20, M.21	$ 11,954,288.71	$ 176,471.24	67.7	-
G.Option3	G.C.3,G.C.8, M.17, M.19, M.20, M.21	$ 11,578,714.95	$ 176,409.63	65.6	-

Table 13a Lexington Economic Analysis of ECM's

ECM	Description	Cost	Savings	SPB (Years)	SF In Year
A.45	Varying the Orientation - No Cost	$ -	$ 84.70	0.0	NO Cost ECM
A.90	Varying the Orientation - No Cost	$ -	$ (9.95)	0.0	NO IMPROVEMENT
A.135	Varying the Orientation - No Cost	$ -	$ 99.87	0.0	NO Cost ECM
A.180	Varying the Orientation - No Cost	$ -	$ 26.66	0.0	NO Cost ECM
A.225	Varying the Orientation - No Cost	$ -	$ 9.38	0.0	NO Cost ECM
A.270	Varying the Orientation - No Cost	$ -	$ (69.27)	0.0	NO IMPROVEMENT
A.315	Varying the Orientation - No Cost	$ -	$ 70.25	0.0	NO Cost ECM
C.1	Change 3" exterior Polyisocyanurate to 3.5" exterior	$ 80,213.28	$ 398.30	201.4	-
C.2	Change 3" exterior Polyisocyanurate to 4" exterior	$ 90,116.15	$ 708.69	127.2	-
C.3	Change 3" exterior Polyisocyanurate to 5" exterior	$ 178,251.73	$ 1,174.61	151.8	-
C.4	ICF Wall: air film, 4" brick, air space, 1.5" Polyurethane, 6"	$ 240,794.40	$ 3,445.19	69.9	-
C.5	Changed 1-1/4" Polystyrene to 3" ploYiso	$ 62,849.34	$ 3,600.79	17.5	26
C.6	Changed 1-1/4" Polystyrene to 2" ploYiso	$ 8,493.15	$ 1,065.97	8.0	10
C.7	Changed 1-1/4" Polystyrene to 1 1/2" polyurethane	$ -	$ 665.81	0.0	NO Cost ECM
C.8	Steel wall stud layers: air film, 4" face brick, air space, 3.5" polyiso, 2x6 steel wall 16 O.C. R-19 batt insul, gypsum board air film	$ (243,240.90)	$ 3,659.41	-66.5	NO Cost ECM
C.9	Steel wall stud layers: air film, 4" face brick, air space, 2" polyiso, 2x6 steel wall 16 O.C. R-19 batt insul, gypsum board air film	$ (294,624.48)	$ 3,457.38	-85.2	NO Cost ECM
C.10	Steel wall stud layers: air film, 4" face brick, air space, 1.5" Polystyrene, 2x6 steel wall 16 O.C. R-19 batt insul, 1/2" GYP board, air film	$ (311,186.13)	$ 839.19	-370.8	NO Cost ECM
C.11	Steel wall stud layers: air film, 4" face brick, air space, 3" Polystyrene, 2x6 steel wall 16 O.C. No batt insul, 1/2" GYP board, air film	$ (298,446.40)	$ 845.31	-353.1	NO Cost ECM
C.12	Light Vapor Barrior	$ -	$ (184.67)	0.0	NO IMPROVEMENT
C.13	Medium Vapor Barrior	$ 40,342.48	$ 772.22	52.2	-
C.14	Heavy Vapor Barrier	$ 80,684.96	$ 1,667.37	48.4	-
C.15	Wall: air film, 4" brick, air space, 1.5" Polyurethane, 6" 140lb conc., 1.5" Polyurethane, 1/2" gyp board, air film; for roof: Changed 3" exterior Polyisocyanurate to 5" exterior Polyisocyanurate	$ 419,046.12	$ 4,324.34	96.9	-
C.16	for wall Changed 1-1/4" Polystyrene to 2" polyiso, for roof Changed 3" exterior Polyisocyanurate to 5" exterior Polyisocyanurate	$ 186,744.88	$ 4,064.38	45.9	-
C.17	for wall Changed 1-1/4" Polystyrene to 3" ploYiso, for roof Changed 3" exterior Polyisocyanurate to 5" exterior Polyisocyanurate	$ 241,101.07	$ 4,793.64	50.3	-
C.18	Window Type 1	$ (10,251.80)	$ (24.84)	412.6	-
C.19	Window Type 2	$ 15,377.70	$ 507.52	30.3	83
L.1	Energy Efficient Lighting	$ (95.59)	$ 11,692.46	0.0	NO Cost ECM
L.2	Modified Lighting Schedule	$ 16,288.54	$ 4,618.11	3.5	4

Table 13b Lexington Economic Analysis of ECM's

ECM	Description	Cost	Savings	SPB (Years)	SF In Year
M.1	Condensing Boiler	$ 2,155.46	$ 9,963.25	0.2	1
M.2	Large Temperature Setbacks	$ -	$ 28,637.68	0.0	NO Cost ECM
M.3	Daylighting	$ 16,288.54	$ 993.72	16.4	24
M.4	Water Side Economizer	$ -	$ (26,780.55)	0.0	NO IMPROVEMENT
M.5	Minimum OA Schedule	$ 161,797.71	$ 3,925.49	41.2	-
M.6	Modified Fan Schedule	$ 161,797.71	$ 48,159.35	3.4	4
M.7	VFD on Cooling Tower Fan	$ 11,297.00	$ 6,236.17	1.8	2
M.8	3-Way to 2-Way Valves and VFD on Pumps Combine with CHW & HW Reset Temps	$ 15,120.60	$ 28,495.25	0.5	1
M.9	ERV on AHUs	$ -	$ (47,583.43)	0.0	NO IMPROVEMENT
M.10	VAV Box Minimum Air Flow Schedule	$ 161,797.71	$ 71,882.54	2.3	3
M.11	DHW using Electricity	$ 29,030.12	$ (5,410.70)	-5.4	NO IMPROVEMENT
M.12	DHW using Heat Pump	$ -	$ (13,277.16)	0.0	NO IMPROVEMENT
M.16	Chilled Water Loop Operation	$ -	$ 26,480.87	0.0	NO Cost ECM
ECM.ALL	VAV: Combination of …C.3 - L.1 - M.1 - A.45 - M.2 - M.3 - M.6 - M.7 - M.8 - M.10	$ 384,815.44	$ 153,083.45	2.5	3
G.M.17	Geothermal Heat Pump System	$ 3,604,493.98	$ 133,499.50	27.0	58
G.M.19	Minimum OA Schedule	$ 3,766,291.69	$ 147,818.38	25.5	50
G.M.20	Modified Fan Schedule	$ 3,766,291.69	$ 152,271.04	24.7	47
G.M.21	Variable Speed Pumps, Load Reset on Heating Side, and Load Reset on Cooling Side	$ -	$ 141,087.11	0.0	NO Cost ECM
G.M.24	Water or Well for HX	$ 3,035,313.25	$ 112,906.07	26.9	57
G.C.3	Change 3" exterior Polyisocyanurate to 5" exterior Polyisocyanurate	$ 178,251.73	$ 135,186.17	1.3	2
G.C.8	Steel wall stud layers: air film, 4" face brick, air space, 3.5" polyiso, 2x6 steel wall 16 O.C. R-19 batt insul, gypsum board air film	$ (294,624.48)	$ 137,362.30	-2.1	NO Cost ECM
G.C.15	Wall: air film, 4" brick, air space, 1.5" Polyurethane, 6" 140lb conc., 1.5" Polyurethane, 1/2" gyp board, air film; for roof: Changed 3" exterior Polyisocyanurate to 5" exterior Polyisocyanurate	$ 419,046.12	$ 138,216.97	3.0	4
G.C.17	for wall Changed 1-1/4" Polystyrene to 3" ployiso, for roof Changed 3" exterior Polyisocyanurate to 5" exterior Polyisocyanurate	$ 241,101.07	$ 139,154.69	1.7	2
G.Option1	G.C.15, M.17, M.19, M.20, M.21	$ 11,556,123.47	$ 174,186.74	66.3	-
G.Option2	G.C.17, M.17, M.19, M.20, M.21	$ 11,378,178.42	$ 175,392.04	64.9	-
G.Option3	G.C.3,G.C.8, M.17, M.19, M.20, M.21	$ 11,020,704.59	$ 175,330.22	62.9	-

Table 14a Covington Economic Analysis of ECM's

ECM	Description	Cost	Savings	SPB (Years)	SF In Year
A.45	Varying the Orientation - No Cost	$ -	$ 55.58	0.0	NO Cost ECM
A.90	Varying the Orientation - No Cost	$ -	$ (33.15)	0.0	NO IMPROVEMENT
A.135	Varying the Orientation - No Cost	$ -	$ 66.98	0.0	NO Cost ECM
A.180	Varying the Orientation - No Cost	$ -	$ (3.13)	0.0	NO IMPROVEMENT
A.225	Varying the Orientation - No Cost	$ -	$ (67.81)	0.0	NO IMPROVEMENT
A.270	Varying the Orientation - No Cost	$ -	$ (169.92)	0.0	NO IMPROVEMENT
A.315	Varying the Orientation - No Cost	$ -	$ 29.57	0.0	NO Cost ECM
C.1	Change 3" exterior Polyisocyanurate to 3.5" exterior	$ 87,782.31	$ 423.38	207.3	-
C.2	Change 3" exterior Polyisocyanurate to 4" exterior	$ 98,619.63	$ 755.68	130.5	-
C.3	Change 3" exterior Polyisocyanurate to 5" exterior	$ 195,071.80	$ 1,247.67	156.3	-
C.4	ICF Wall: air film, 4" brick, air space, 1.5" Polyurethane, 6"	$ 263,516.08	$ 1,349.20	195.3	-
C.5	Changed 1-1/4" Polystyrene to 3" ploy iso	$ 68,779.89	$ 1,513.06	45.5	-
C.6	Changed 1-1/4" Polystyrene to 2" ploy iso	$ 9,294.58	$ 1,170.95	7.9	10
C.7	Changed 1-1/4" Polystyrene to 1 1/2" polyurethane	$ -	$ 732.70	0.0	NO Cost ECM
C.8	Steel wall stud layers: air film, 4" face brick, air space, 3.5" polyiso, 2x6 steel wall 16 O.C. R-19 batt insul, gypsum board air film	$ (266,193.44)	$ 1,593.53	-167.0	NO Cost ECM
C.9	Steel wall stud layers: air film, 4" face brick, air space, 2" polyiso, 2x6 steel wall 16 O.C. R-19 batt insul, gypsum board air film	$ (322,425.64)	$ 1,368.20	-235.7	NO Cost ECM
C.10	Steel wall stud layers: air film, 4" face brick, air space, 1.5" Polystyrene, 2x6 steel wall 16 O.C. R-19 batt insul, 1/2" GYP board, air film	$ (340,550.07)	$ 934.66	-364.4	NO Cost ECM
C.11	Steel wall stud layers: air film, 4" face brick, air space, 3" Polystyrene, 2x6 steel wall 16 O.C. No batt insul, 1/2" GYP board, air film	$ (326,608.20)	$ 940.22	-347.4	NO Cost ECM
C.12	Light Vapor Barrior	$ -	$ (169.86)	0.0	NO IMPROVEMENT
C.13	Medium Vapor Barrior	$ 44,149.25	$ 787.51	56.1	-
C.14	Heavy Vapor Barrier	$ 88,298.51	$ 1,686.59	52.4	-
C.15	Wall: air film, 4" brick, air space, 1.5" Polyurethane, 6" 140lb conc., 1.5" Polyurethane, 1/2" gyp board, air film; for roof: Changed 3" exterior Polyisocyanurate to 5" exterior Polyisocyanurate	$ 458,587.87	$ 2,254.57	203.4	-
C.16	for wall Changed 1-1/4" Polystyrene to 2" polyiso, for roof Changed 3" exterior Polyisocyanurate to 5" exterior Polyisocyanurate	$ 204,366.38	$ 2,042.37	100.1	-
C.17	for wall Changed 1-1/4" Polystyrene to 3" ploy iso, for roof Changed 3" exterior Polyisocyanurate to 5" exterior Polyisocyanurate	$ 263,851.68	$ 2,768.40	95.3	-
C.18	Window Type 1	$ (11,219.18)	$ (32.04)	350.1	-
C.19	Window Type 2	$ 16,828.76	$ 560.83	30.0	80
L.1	Energy Efficient Lighting	$ (104.61)	$ 11,646.78	0.0	NO Cost ECM
L.2	Modified Lighting Schedule	$ 17,825.54	$ 4,628.32	3.9	5

Table 14b Covington Economic Analysis of ECM's

ECM	Description	Cost	Savings	SPB (Years)	SF In Year
M.1	Condensing Boiler	$ 2,358.85	$ 10,054.08	0.2	1
M.2	Large Temperature Setbacks	$ -	$ 28,690.82	0.0	NO Cost ECM
M.3	Daylighting	$ 17,825.54	$ 1,011.06	17.6	26
M.4	Water Side Economizer	$ -	$ (26,675.30)	0.0	NO IMPROVEMENT
M.5	Minimum OA Schedule	$ 177,065.16	$ 3,836.06	46.2	-
M.6	Modified Fan Schedule	$ 177,065.16	$ 46,480.40	3.8	5
M.7	VFD on Cooling Tower Fan	$ 12,363.00	$ 5,972.46	2.1	3
M.8	3-Way to 2-Way Valves and VFD on Pumps Combine with CHW & HW Reset Temps	$ 16,547.40	$ 28,144.55	0.6	1
M.9	ERV on AHUs	$ -	$ (48,712.83)	0.0	NO IMPROVEMENT
M.10	VAV Box Minimum Air Flow Schedule	$ 177,065.16	$ 70,159.82	2.5	3
M.11	DHW using Electricity	$ 31,769.44	$ (5,455.96)	-5.8	NO IMPROVEMENT
M.12	DHW using Heat Pump	$ -	$ (13,322.62)	0.0	NO IMPROVEMENT
M.16	Chilled Water Loop Operation	$ -	$ 27,482.99	0.0	NO Cost ECM
ECM.ALL	VAV: Combination of …C.3 - L.1 - M.1 - A.45 - M.2 - M.3 - M.6 - M.7 - M.8 - M.10	$ 421,127.14	$ 151,396.88	2.8	3
G.M.17	Geothermal Heat Pump System	$ 3,944,618.84	$ 127,045.00	31.0	93
G.M.19	Minimum OA Schedule	$ 4,121,684.00	$ 142,601.24	28.9	70
G.M.20	Modified Fan Schedule	$ 4,121,684.00	$ 146,339.42	28.2	64
G.M.21	Variable Speed Pumps, Load Reset on Heating Side, and Load Reset on Cooling Side	$ -	$ 135,144.55	0.0	NO Cost ECM
G.M.24	Water or Well for HX	$ 3,321,729.46	$ 108,590.14	30.6	86
G.C.3	Change 3" exterior Polyisocyanurate to 5" exterior Polyisocyanurate	$ 195,071.80	$ 128,779.55	1.5	2
G.C.8	Steel wall stud layers: air film, 4" face brick, air space, 3.5" polyiso, 2x6 steel wall 16 O.C. R-19 batt insul, gypsum board air film	$ (322,425.64)	$ 130,018.73	-2.5	NO Cost ECM
G.C.15	Wall: air film, 4" brick, air space, 1.5" Polyurethane, 6" 140lb conc., 1.5" Polyurethane, 1/2" gyp board, air film; for roof: Changed 3" exterior Polyisocyanurate to 5" exterior Polyisocyanurate	$ 458,587.87	$ 131,120.33	3.5	4
G.C.17	for wall Changed 1-1/4" Polystyrene to 3" ployiso, for roof Changed 3" exterior Polyisocyanurate to 5" exterior Polyisocyanurate	$ 263,851.68	$ 131,953.75	2.0	3
G.Option1	G.C.15, M.17, M.19, M.20, M.21	$ 12,646,574.71	$ 167,784.15	75.4	-
G.Option2	G.C.17, M.17, M.19, M.20, M.21	$ 12,451,838.52	$ 168,984.55	73.7	-
G.Option3	G.C.3,G.C.8, M.17, M.19, M.20, M.21	$ 12,060,632.99	$ 168,960.82	71.4	-

Table 15a Corbin/Williamsburg Economic Analysis of ECM's

ECM	Description	Cost	Savings	SPB (Years)	SF In Year
A.45	Varying the Orientation - No Cost	$ -	$ 80.88	0.0	NO Cost ECM
A.90	Varying the Orientation - No Cost	$ -	$ (28.99)	0.0	NO IMPROVEMENT
A.135	Varying the Orientation - No Cost	$ -	$ 74.22	0.0	NO Cost ECM
A.180	Varying the Orientation - No Cost	$ -	$ (127.47)	0.0	NO IMPROVEMENT
A.225	Varying the Orientation - No Cost	$ -	$ (141.52)	0.0	NO IMPROVEMENT
A.270	Varying the Orientation - No Cost	$ -	$ (162.56)	0.0	NO IMPROVEMENT
A.315	Varying the Orientation - No Cost	$ -	$ 66.57	0.0	NO Cost ECM
C.1	Change 3" exterior Polyisocyanurate to 3.5" exterior	$ 73,290.38	$ 248.97	294.4	-
C.2	Change 3" exterior Polyisocyanurate to 4" exterior	$ 82,338.58	$ 446.57	184.4	-
C.3	Change 3" exterior Polyisocyanurate to 5" exterior	$ 162,867.51	$ 744.21	218.8	-
C.4	ICF Wall: air film, 4" brick, air space, 1.5" Polyurethane, 6"	$ 220,012.37	$ 273.47	804.5	-
C.5	Changed 1-1/4" Polystyrene to 3" ploysio	$ 57,425.06	$ 341.19	168.3	-
C.6	Changed 1-1/4" Polystyrene to 2" ploysio	$ 7,760.14	$ 268.06	28.9	70
C.7	Changed 1-1/4" Polystyrene to 1 1/2" polyurethane	$ -	$ 172.18	0.0	NO Cost ECM
C.8	Steel wall stud layers: air film, 4" face brick, air space, 3.5" polyiso, 2x6 steel wall 16 O.C. R-19 batt insul, gypsum board air film	$ (222,247.73)	$ 298.60	-744.3	NO Cost ECM
C.9	Steel wall stud layers: air film, 4" face brick, air space, 2" polyiso, 2x6 steel wall 16 O.C. R-19 batt insul, gypsum board air film	$ (269,196.59)	$ 241.71	-1113.7	NO Cost ECM
C.10	Steel wall stud layers: air film, 4" face brick, air space, 1.5" Polystyrene, 2x6 steel wall 16 O.C. R-19 batt insul, 1/2" GYP board, air film	$ (284,328.87)	$ 137.51	-2067.7	NO Cost ECM
C.11	Steel wall stud layers: air film, 4" face brick, air space, 3" Polystyrene, 2x6 steel wall 16 O.C. No batt insul, 1/2" GYP board, air film	$ (272,688.66)	$ 138.52	-1968.6	NO Cost ECM
C.12	Light Vapor Barrior	$ -	$ (177.93)	0.0	NO IMPROVEMENT
C.13	Medium Vapor Barrior	$ 36,860.68	$ 665.06	55.4	-
C.14	Heavy Vapor Barrier	$ 73,721.36	$ 1,460.93	50.5	-
C.15	Wall: air film, 4" brick, air space, 1.5" Polyurethane, 6" 140lb conc., 1.5" Polyurethane, 1/2" gyp board, air film; for roof: Changed 3" exterior Polyisocyanurate to 5" exterior Polyisocyanurate	$ 382,879.89	$ 948.12	403.8	-
C.16	for wall Changed 1-1/4" Polystyrene to 2" polyiso, for roof Changed 3" exterior Polyisocyanurate to 5" exterior Polyisocyanurate	$ 170,627.66	$ 420.72	405.6	-
C.17	for wall Changed 1-1/4" Polystyrene to 3" ploysio, for roof Changed 3" exterior Polyisocyanurate to 5" exterior Polyisocyanurate	$ 220,292.57	$ 1,078.28	204.3	-
C.18	Window Type 1	$ (9,367.01)	$ 2.64	-3548.2	-
C.19	Window Type 2	$ 14,050.51	$ 214.89	65.4	-
L.1	Energy Efficient Lighting	$ (87.34)	$ 11,745.89	0.0	NO Cost ECM
L.2	Modified Lighting Schedule	$ 14,882.74	$ 4,689.88	3.2	4

Table 15b Corbin/Williamsburg Economic Analysis of ECM's

ECM	Description	Cost	Savings	SPB (Years)	SF In Year
M.1	Condensing Boiler	$ 1,969.43	$ 9,026.52	0.2	1
M.2	Large Temperature Setbacks	$ -	$ 28,695.67	0.0	NO Cost ECM
M.3	Daylighting	$ 14,882.74	$ 1,042.97	14.3	20
M.4	Water Side Economizer	$ -	$ (27,971.92)	0.0	NO IMPROVEMENT
M.5	Minimum OA Schedule	$ 147,833.58	$ 4,688.97	31.5	101
M.6	Modified Fan Schedule	$ 147,833.58	$ 53,587.19	2.8	3
M.7	VFD on Cooling Tower Fan	$ 10,322.00	$ 7,354.17	1.4	2
M.8	3-Way to 2-Way Valves and VFD on Pumps Combine with CHW & HW Reset Temps	$ 13,815.60	$ 28,562.41	0.5	1
M.9	ERV on AHUs	$ -	$ (42,479.28)	0.0	NO IMPROVEMENT
M.10	VAV Box Minimum Air Flow Schedule	$ 147,833.58	$ 82,827.31	1.8	2
M.11	DHW using Electricity	$ 26,524.64	$ (5,140.23)	-5.2	NO IMPROVEMENT
M.12	DHW using Heat Pump	$ -	$ (13,018.15)	0.0	NO IMPROVEMENT
M.16	Chilled Water Loop Operation	$ -	$ 21,574.40	0.0	NO Cost ECM
ECM.ALL	VAV: Combination of …C.3 - L.1 - M.1 - A.45 - M.2 - M.3 - M.6 - M.7 - M.8 - M.10	$ 351,603.52	$ 159,669.18	2.2	3
G.M.17	Geothermal Heat Pump System	$ 3,293,404.16	$ 142,220.99	23.2	41
G.M.19	Minimum OA Schedule	$ 3,441,237.74	$ 154,990.47	22.2	38
G.M.20	Modified Fan Schedule	$ 3,441,237.74	$ 163,037.04	21.1	35
G.M.21	Variable Speed Pumps, Load Reset on Heating Side, and Load Reset on Cooling Side	$ -	$ 149,618.04	0.0	NO Cost ECM
G.M.24	Water or Well for HX	$ 2,773,347.21	$ 121,543.03	22.8	40
G.C.3	Change 3" exterior Polyisocyanurate to 5" exterior Polyisocyanurate	$ 162,867.51	$ 143,936.13	1.1	2
G.C.8	Steel wall stud layers: air film, 4" face brick, air space, 3.5" polyiso, 2x6 steel wall 16 O.C. R-19 batt insul, gypsum board air film	$ (269,196.59)	$ 144,766.42	-1.9	NO Cost ECM
G.C.15	Wall: air film, 4" brick, air space, 1.5" Polyurethane, 6" 140lb conc., 1.5" Polyurethane, 1/2" gyp board, air film; for roof: Changed 3" exterior Polyisocyanurate to 5" exterior Polyisocyanurate	$ 382,879.89	$ 145,760.52	2.6	3
G.C.17	for wall Changed 1-1/4" Polystyrene to 3" ployiso, for roof Changed 3" exterior Polyisocyanurate to 5" exterior Polyisocyanurate	$ 220,292.57	$ 146,515.53	1.5	2
G.Option1	G.C.15, M.17, M.19, M.20, M.21	$ 10,558,759.54	$ 180,579.07	58.5	-
G.Option2	G.C.17, M.17, M.19, M.20, M.21	$ 10,396,172.22	$ 181,724.25	57.2	-
G.Option3	G.C.3,G.C.8, M.17, M.19, M.20, M.21	$ 10,069,550.57	$ 181,533.73	55.5	-

Table 16b Paducah Economic Analysis of ECM's

ECM	Description	Cost	Savings	SPB (Years)	SF In Year
A.45	Varying the Orientation - No Cost	$ -	$ 82.82	0.0	NO Cost ECM
A.90	Varying the Orientation - No Cost	$ -	$ (52.67)	0.0	NO IMPROVEMENT
A.135	Varying the Orientation - No Cost	$ -	$ 77.83	0.0	NO Cost ECM
A.180	Varying the Orientation - No Cost	$ -	$ 116.55	0.0	NO Cost ECM
A.225	Varying the Orientation - No Cost	$ -	$ (61.72)	0.0	NO IMPROVEMENT
A.270	Varying the Orientation - No Cost	$ -	$ (189.81)	0.0	NO IMPROVEMENT
A.315	Varying the Orientation - No Cost	$ -	$ 43.64	0.0	NO Cost ECM
C.1	Change 3" exterior Polyisocyanurate to 3.5" exterior	$ 82,797.82	$ 356.33	232.4	-
C.2	Change 3" exterior Polyisocyanurate to 4" exterior	$ 93,019.78	$ 634.52	146.6	-
C.3	Change 3" exterior Polyisocyanurate to 5" exterior	$ 183,995.16	$ 1,057.23	174.0	-
C.4	ICF Wall: air film, 4" brick, air space, 1.5" Polyurethane, 6"	$ 248,553.02	$ 913.18	272.2	-
C.5	Changed 1-1/4" Polystyrene to 3" ploYiso	$ 64,874.41	$ 1,005.27	64.5	-
C.6	Changed 1-1/4" Polystyrene to 2" ploYiso	$ 8,766.81	$ 781.34	11.2	15
C.7	Changed 1-1/4" Polystyrene to 1 1/2" polyurethane	$ -	$ 495.17	0.0	NO Cost ECM
C.8	Steel wall stud layers: air film, 4" face brick, air space, 3.5" polyiso, 2x6 steel wall 16 O.C. R-19 batt insul, gypsum board air film	$ (251,078.35)	$ 1,026.88	-244.5	NO Cost ECM
C.9	Steel wall stud layers: air film, 4" face brick, air space, 2" polyiso, 2x6 steel wall 16 O.C. R-19 batt insul, gypsum board air film	$ (304,117.56)	$ 878.42	-346.2	NO Cost ECM
C.10	Steel wall stud layers: air film, 4" face brick, air space, 1.5" Polystyrene, 2x6 steel wall 16 O.C. R-19 batt insul, 1/2" GYP board, air film	$ (321,212.84)	$ 569.40	-564.1	NO Cost ECM
C.11	Steel wall stud layers: air film, 4" face brick, air space, 3" Polystyrene, 2x6 steel wall 16 O.C. No batt insul, 1/2" GYP board, air film	$ (308,062.63)	$ 573.07	-537.6	NO Cost ECM
C.12	Light Vapor Barrior	$ -	$ (187.95)	0.0	NO IMPROVEMENT
C.13	Medium Vapor Barrior	$ 41,642.35	$ 822.68	50.6	-
C.14	Heavy Vapor Barrier	$ 83,284.71	$ 1,799.79	46.3	-
C.15	Wall: air film, 4" brick, air space, 1.5" Polyurethane, 6" 140lb conc., 1.5" Polyurethane, 1/2" gyp board, air film; for roof: Changed 3" exterior Polyisocyanurate to 5" exterior Polyisocyanurate	$ 432,548.18	$ 1,732.69	249.6	-
C.16	for wall Changed 1-1/4" Polystyrene to 2" polyiso, for roof Changed 3" exterior Polyisocyanurate to 5" exterior Polyisocyanurate	$ 192,761.98	$ 1,339.51	143.9	-
C.17	for wall Changed 1-1/4" Polystyrene to 3" ploYiso, for roof Changed 3" exterior Polyisocyanurate to 5" exterior Polyisocyanurate	$ 248,869.57	$ 2,063.26	120.6	-
C.18	Window Type 1	$ (10,582.12)	$ 2.48	-4273.9	NO Cost ECM
C.19	Window Type 2	$ 15,873.19	$ 427.53	37.1	-
L.1	Energy Efficient Lighting	$ (98.67)	$ 11,716.26	0.0	NO Cost ECM
L.2	Modified Lighting Schedule	$ 16,813.37	$ 4,638.75	3.6	4

Table 16b Paducah Economic Analysis of ECM's

ECM	Description	Cost	Savings	SPB (Years)	SF In Year
M.1	Condensing Boiler	$ 2,224.91	$ 9,716.42	0.2	1
M.2	Large Temperature Setbacks	$ -	$ 28,853.10	0.0	NO Cost ECM
M.3	Daylighting	$ 16,813.37	$ 975.23	17.2	25
M.4	Water Side Economizer	$ -	$ (29,047.87)	0.0	NO IMPROVEMENT
M.5	Minimum OA Schedule	$ 167,010.99	$ 4,896.32	34.1	-
M.6	Modified Fan Schedule	$ 167,010.99	$ 48,812.90	3.4	4
M.7	VFD on Cooling Tower Fan	$ 11,661.00	$ 7,303.75	1.6	2
M.8	3-Way to 2-Way Valves and VFD on Pumps Combine with CHW & HW Reset Temps	$ 15,607.80	$ 29,788.01	0.5	1
M.9	ERV on AHUs	$ -	$ (45,107.32)	0.0	NO IMPROVEMENT
M.10	VAV Box Minimum Air Flow Schedule	$ 167,010.99	$ 74,193.19	2.3	3
M.11	DHW using Electricity	$ 29,965.50	$ (5,321.04)	-5.6	NO IMPROVEMENT
M.12	DHW using Heat Pump	$ -	$ (13,192.45)	0.0	NO IMPROVEMENT
M.16	Chilled Water Loop Operation	$ -	$ 27,981.15	0.0	NO Cost ECM
ECM.ALL	VAV: Combination of …C.3 - L.1 - M.1 - A.45 - M.2 - M.3 - M.6 - M.7 - M.8 - M.10	$ 397,214.56	$ 157,718.71	2.5	3
G.M.17	Geothermal Heat Pump System	$ 3,720,634.17	$ 136,333.17	27.3	59
G.M.19	Minimum OA Schedule	$ 3,887,645.16	$ 149,142.76	26.1	53
G.M.20	Modified Fan Schedule	$ 3,887,645.16	$ 155,736.14	25.0	48
G.M.21	Variable Speed Pumps, Load Reset on Heating Side, and Load Reset on Cooling Side	$ -	$ 143,952.68	0.0	NO Cost ECM
G.M.24	Water or Well for HX	$ 3,133,113.91	$ 114,662.64	27.3	59
G.C.3	Change 3" exterior Polyisocyanurate to 5" exterior Polyisocyanurate	$ 183,995.16	$ 138,114.74	1.3	2
G.C.8	Steel wall stud layers: air film, 4" face brick, air space, 3.5" polyiso, 2x6 steel wall 16 O.C. R-19 batt insul, gypsum board air film	$ (304,117.56)	$ 139,523.51	-2.2	NO Cost ECM
G.C.15	Wall: air film, 4" brick, air space, 1.5" Polyurethane, 6" 140lb conc., 1.5" Polyurethane, 1/2" gyp board, air film; for roof: Changed 3" exterior Polyisocyanurate to 5" exterior Polyisocyanurate	$ 432,548.18	$ 140,512.05	3.1	4
G.C.17	for wall Changed 1-1/4" Polystyrene to 3" ployiso, for roof Changed 3" exterior Polyisocyanurate to 5" exterior Polyisocyanurate	$ 248,869.57	$ 141,308.35	1.8	2
G.Option1	G.C.15, M.17, M.19, M.20, M.21	$ 11,928,472.67	$ 176,110.52	67.7	-
G.Option2	G.C.17, M.17, M.19, M.20, M.21	11744794.06	177334.0821	66.2	-
G.Option3	G.C.3,G.C.8, M.17, M.19, M.20, M.21	11375802.09	177260.7163	64.2	-

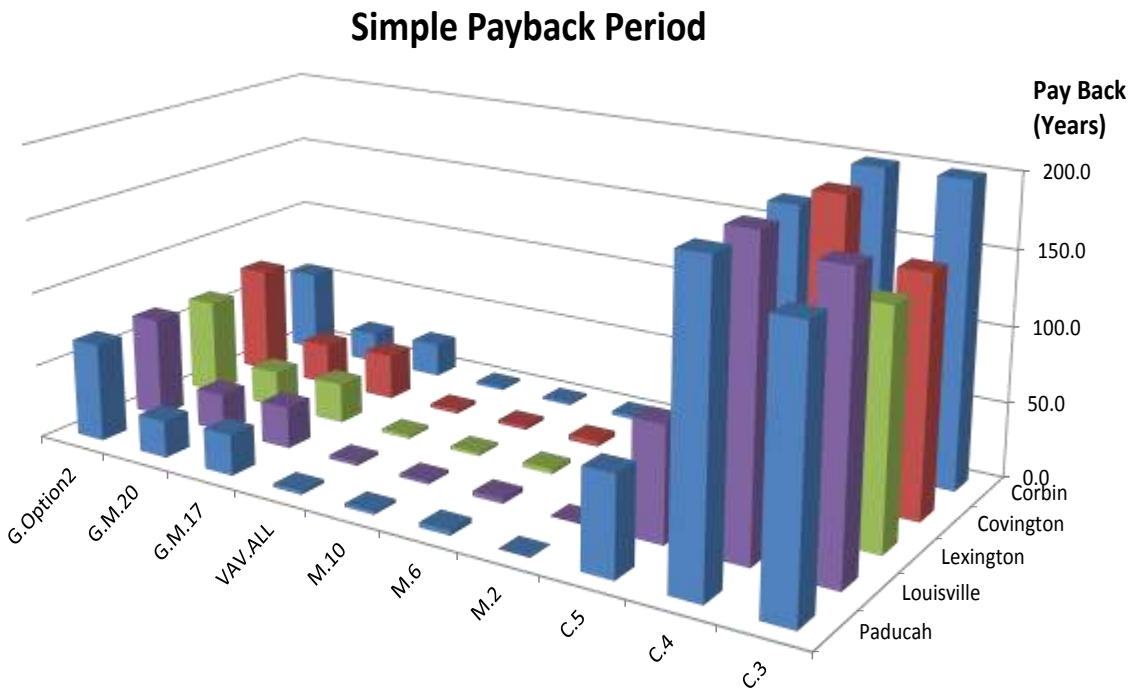

Figure 19 Simple Payback Periods for Selected ECM's

To account for incremental changes in maintenance costs that might be associated with an ECM, interest and increases in energy costs, a cash flow analysis was performed. This analysis assumed that interest rates were a constant 4.5% per year, and energy costs would increase at a constant rate of 1.5 % per year. The incremental capital costs and interest of the ECM was assumed to be paid off by the yearly energy savings generated by the ECM, (generally over a 25 year amortization period). Any incremental maintenance cost associated with the ECM was deducted from the energy savings. The number of years that were needed to pay off the capital costs and interest were calculated. This time period was referred to as the year where the ECM was self-funding (SF). Tables 12 through 16 also show the self-

funding year for each ECM. If a there is no entry in the table, that the net energy savings generated by the ECM was not able to pay off the capital and interest costs over a 300 year period. In general, the results from the cash flow analyses supported the conclusions described previously for the simple payback analyses, control and high efficiency conventional systems are the most cost effective.

6.0 Design Optimization and Recommendations

It is evident from the previous analysis that significant reduction in the energy used by school facilities can be attained using a number of technologies and design strategies readily available in the field. It is also clear that, for the school building configuration investigated, in the range of climates in Kentucky, significant energy savings can be achieved using a conventionally designed building with, T-8 fluorescent lights, masonry cavity walls with code minimum R values (~9 ft^2°F-h/Btu), a high R value for the roof (~37- 40 ft^2°F-h/Btu), code minimum U values for the fenestrations and a conventional VAV HVAC (with chiller and a high efficiency gas fired boiler). Use of aggressive set-backs, occupancy controlled ventilation and lights, and variable speed mortars with 2-way valves allowed a reduction in energy use in excess of 50%, with simple payback period of about 2.5 years. This is a significant finding.

It should be noted that the roof insulation improvements addressed in the above configuration do not improve the energy efficiency of the building a large amount and have a significant cost (simple payback is in excess of 100 years). Thus, it may be more cost effective to leave the roof insulation values at the code prescribed minimum values, in many cases.

It also appears that the mass masonry cavity wall or ICF systems will perform about the same with respect to energy use, although a lower cavity insulation value is required for the masonry wall systems to give comparable performance. The ICF wall systems have a higher wall costs so traditional masonry cavity wall systems appear to be the most cost effect exterior wall systems when comparing these two wall systems.

According to the cost and energy analysis, the most cost effective exterior wall system is the highly insulated brick veneer wall system. However, the brick veneer steel stud wall system does not give comparable performance in other characteristics such as durability, sound transmission, passive fire resistance, nor structural support. In this investigation, it was assumed that all wall systems were infill walls and used the same post and beam steel framing system for support. Thus, these wall system performance characteristics were not account for in the investigation and should be addressed before the brick veneer steel stud wall system is adopted generally in design. It is likely that the much lower capital cost of the brick veneer, steel stud wall system will be increased relative to the cost of load bearing masonry or ICF wall systems, when the steel framing systems are accounted for. There is also the concern of durability of the steel stud systems, since they very susceptible to moisture damage, corrosion and thermal bridging issues.

However, the ICF and masonry wall systems can be used for structural support, in much the same manner, and provide similar sound transmission characteristics. Thus, these systems comparisons are likely valid over a range building configurations.

With the conventional facility configurations, the primary reduction in energy use is obtained with the aggressive use of set-backs and occupancy controlled ventilation. These account for the greatest reduction in energy use. Care must be exercised in applying this strategy since there is a potential of creating areas were the air in spaces my build up significant amounts of humidity, and have surface temperatures that are below the dew point. This can create conditions where moisture can collect on surfaces, creating conditions for mold or mildew growth and potential damage to the building systems.

The greatest single reduction in yearly energy use predicted for the prototype building in the Kentucky climate was obtained when the conventional HVAC system was replaced with a ground source heat pump system. However, the large capital cost of the heat pump system makes the payback period quite large (over 25 years). Changes in set-back schedules and occupancy control of ventilation and lights improve this payback period slightly and should be pursued when this system is used for HVAC. Envelope improvements appear to lengthen the pay-back periods and are not as effective when ground source heat pumps are used.

7.0 Summary and Conclusions

This investigation evaluated the cost effectiveness of a variety of mature energy conservation measures (ECM's) based on the energy performance of a prototype school building in five typical Kentucky climates. An economic analysis was also conducted to estimate the cost of each ECM, and both a simple payback and cash flow analysis was conducted.

The results show that most significant energy savings can be achieved using more efficient mechanical equipment, control systems and lighting systems. Increases in thermal resistance of the building envelope beyond code minimums, both for opaque walls and fenestrations, does not produce significant reductions in the yearly energy use of the prototype building evaluated in this investigation, at least for the range of climates experienced in Kentucky. Large increases in thermal resistance do not correspond to similar reductions in energy use, and the simple payback periods for these improvements are typically in excess of 100 years. It should be noted that the above conclusions are restricted to mass exterior wall systems and the thermal resistance of light gauge steel faring walls must be quite high (in excess of R = 35) to produce similar results.

Using conventional mass masonry wall systems and roof systems insulated to the code prescriptive minimums, conventional gas fired boilers, a conventional VAV HVAC System with chiller and efficient lighting, and aggressive control strategies result in EUI reductions from 50% to 60% from code minimum performance. Almost 80% reductions in energy use are achieved when ground source heat pumps are used with similar configurations

The economic analysis suggests that simple payback using the conventional HVAC systems with aggressive controls are less than 3 years and this is only slightly increased when interest and typical energy cost increases are accounted for. Use of ground source heat pumps increase the payback period to over 25 years. Improvements in the building envelopes generally have long payback periods (over 100 years) and do not appear to improve the payback periods of the ground source heat pump systems.

6.0 REFERENCES:

1. American Society of Heating Refrigeration and Air-Conditioning Engineers, ”Advanced Energy Design Guide for K- 12 Buildings., American Society of Heating Refrigeration and Air-Conditioning Engineers, Atlanta, GA, USA, 2008.

2. American Society of Heating Refrigeration and Air-Conditioning Engineers, ”ANSI/ASHRAE/IESNA Standard 90.1-2007Energy Standard for Buildings Except Low-Rise Residential Buildings”, American Society of Heating Refrigeration and Air-Conditioning Engineers, Atlanta, GA, USA, 2007.

3. Governor Steven L. Bashear, “Intelligent Energy Choices for Kentucky’s Future- Kentucky’s 7-Point Strategy for Energy Independence”, Kentucky Department for Development and Energy Independence, November 2008, Web published - http://www.energy.ky.gov/.

4. Deane Evans, High-Performance School Buildings Resource and Strategy Guide, Sustainable Buildings Industry Council, New York State Energy Research and Development Authority, Albany, NY, 2nd edition, 2004 .

5. Kentucky Environmental Education Council, “Kentucky Green Schools Design Manual”, Kentucky Education Cabinet, 2008.

6. J. Kosny, T. Petrie, D. Gawin, P. Childs, A Desjarlais, and J.Christian, “Thermal Mass - Energy Savings Potential in Residential Buildings, Buildings Technology Center, ORNL August , 2001.

7. North Carolina School Planning Section of the North Carolina Department of Public Instruction, Prortype Design Clearing House , http://www.schoolclearinghouse.org/, 2008

8. RsMEANS, Building Construction Cost Data, RsMeans, Norwell MA, 2011.

9. RsMEANS, Building Electrical Cost Data, RsMeans, Norwell MA, 2011.

10. RsMEANS, Building Mechanical Cost Data, RsMeans, Norwell MA, 2011.

11. Sri Iyer, Sieglinde Kinne and Don Douglass, “An Overview of Kentucky’s Energy Consumption and Energy Efficiency Potential, Kentucky Pollution Prevention Center for the Kentucky Governor’s Office of Energy Policy, August 2007, University of Louisville.

12. The International Code Council, International Building Code (IBC), 500 New Jersey Avenue, NW, 6th Floor, Washington, DC 20001, 2009.

13. The International Code Council, International Energy Conservation Code (IECC), 500 New Jersey Avenue, NW, 6th Floor, Washington, DC 20001, 2009

14. US Department of Energy, Office of Energy Efficiency and Renewable Energy, Building Technologies, January 2008.

15. US Department of Energy, Office of Building Technology, "Energy Design Guidelines- For High Performance Schools in Temperate and Humid Climates, 2003.

16. US Department of Energy -Energy Star Program, Energy indexes, http://www.energystar.gov/index.cfm?fuseaction=buildingcontest.eui, 2003.

17. US Department of Energy, Energy Analysis programs, http://doe2.com/equest/ 2010.

Appendix A Survey Forms

SURVEY OF ENERGY EFFICIENCY IN SCHOOLS

Significant effort has been focused on the design of sustainable and energy efficient school buildings over the past few years. This effort has culminated in a number of design guidelines such as Leadership in Energy and Environmental Design (LEED) for Schools-New Construction and Major Renovations, and the Kentucky Green and Healthy Schools Design Guidelines. These design provisions go a long way in providing guidance to design professionals and school officials on what areas in the facility design might be addressed to improve the performance of the facility. However, there appears to be a reluctance to embrace these "Green" or "Energy Efficient" designs, partially due to the perception that these designs will cost a lot more than traditional systems.

The goal of this project is to use the design guidelines discussed above and develop a list of low life cycle cost systems (both first cost and maintenance costs) that can be used to meet, at least in part, the energy efficiency and sustainability goals of the State of Kentucky. Each of the systems will be incorporated into a typical prototype configuration and the effects each system has on the

overall energy used over the life cycle of the building will be determined using an analysis program. This data will be used to develop a relationship between each of the systems described above, their life cycle costs and the effect each has on energy use. Each system design will be performed in an effort to minimize lifecycle costs with as little reduction in energy efficiency as possible.

The effort above will result in a matrix of sample building system designs that can be reviewed by designers and school officials to quickly assess which systems might be implemented to reduce energy use, at the least cost.

The purpose of this survey is to twofold:
1 To help establish typical design practice in Kentucky for energy efficient schools.
2. To attempt to develop a partial data base of effective design practices and costs.
We ask that you complete the following form and email us m.mcginley@louisville.edu. If you provide an email address we will ensure that you receive a PDF version of the final report when it is ready.

Designers Survey

K-12 School Energy Efficiency Survey

Please take a few moments to complete the following survey, being as specific and accurate as possible. If you are reporting on more than one school or building please complete a separate survey for each building or school. Questions should be answered based on current configurations in use in Kentucky's schools. Please feel free to add any additional comments that you may feel are relevant or specific to your individual situation. If you are unsure or a question does not apply please skip that question and move on to the next question.

Contact Name: _Click here to enter text.
Contact Email:Click here to enter text.
Contact Telephone No.:Click here to enter text.

Name of school _ Click here to enter text. **County of school Location** Click here to enter text.

1. What type of school are you reporting about?

Elementary school	Middle school	High school
☐	☐	☐

2. What is the primary use of your building?

Main school with gym attached	Main School	Gym	Other Click here to enter text.
☐	☐	☐	☐

3. How many stories is your building?

One story in all areas	One and two stories	Two Stories	O Other Click here to enter text.
☐	☐	☐	☐

4. How many square feet are in your building? Click here to enter text.

5. What is the floor to floor height in your building? Click here to enter text.

6. What is the primary building structure construction?

Steel frame ☐ High mass ☐

7. What was the cost per square foot for the walls? Click here to enter text.

8. What was the cost per square foot for the roof? Click here to enter text.

9. What is the design life of the buildings structure?

0-25 years	26-45 years	46-60 years	61-75 years	76+ years
☐	☐	☐	☐	☐

10. What is the design R-value for the building's wall system?

8-11	12-13	14-16	17-19	20-22
☐	☐	☐	☐	☐

11. What is the R-value of the roof system?

13-19	20-23	24-28	29-32	33-38
☐	☐	☐	☐	☐

12. For high mass wall systems where is the insulation located?

Inside wall mass	Outside wall mass	On both sides of wall mass
☐	☐	☐

13. What direction is the major axis of the building?

North / South	East / West	Northeast / Southwest	Northwest / Southeast
☐	☐	☐	☐

14. What color is the exposed roof surface?

White	A light color besides white	Black	A dark color besides black	A medium color such as tan
☐	☐	☐	☐	☐

15. What is the fenestration area for doors per side of the building?

	North	**South**	**East**	**West**
Double door with center post	Click here to enter text.	Click here to enter text.	Click here to enter text.	Click here to enter text.
Double door without center post	Click here to enter text.	Click here to enter text.	Click here to enter text.	Click here to enter text.
Single door single swing	Click here to enter text.	Click here to enter text.	Click here to enter text.	Click here to enter text.
Single door double swing	Click here to enter text.	Click here to enter text.	Click here to enter text.	Click here to enter text.
Overhead or roll-up	Click here to enter text.	Click here to enter text.	Click here to enter text.	Click here to enter text.

16. What is the average U-value for each door type in the building?

	.2 - .4	**.5 - .6**	**.7 - .8**	**.9 - 1**
Double door with center post	☐	☐	☐	☐
Double door without center post	☐	☐	☐	☐
Single door single swing	☐	☐	☐	☐
Single door double swing	☐	☐	☐	☐

Overhead or roll-up	☐	☐	☐	☐

17. What was the cost per door for the exterior doors?

Double door with center post	Click here to enter text.
Double door without center post	Click here to enter text.
Single door single swing	Click here to enter text.
Single door double swing	Click here to enter text.
Overhead or roll-up	Click here to enter text.

18. What is the design life of the building's exterior doors?

0-10 years	11-15 years	16-20 years	21-30 years	31-50 years
☐	☐	☐	☐	☐

19. What is the total window area per side of the building?

	North	**South**	**East**	**West**
Single pane	Click here to enter text.	Click here to enter text.	Click here to enter text.	Click here to enter text.
Double pane	Click here to enter text.	Click here to enter text.	Click here to enter text.	Click here to enter text.
Triple pane	Click here to	Click here to	Click here to	Click here to

enter text. enter text. enter text. enter text.

20. What is the average U-value for each window type in the building?

21. What was the cost per window?

Single Pane Click here to enter text.

Double Pane Click here to enter text.

Triple Pane Click here to enter text.

22. What is the design life of the building's windows?

0-10 years	11-15 years	16-20 years	21-30 years	31-50 years
☐	☐	☐	☐	☐

23. Where are overhangs used above windows on your building?

No overhangs	South Side	East Side	North Side	West Side
☐	☐	☐	☐	☐

24. What was the cost/ft for the window overhangs? Click here to enter text.

25. What tonnage of HVAC system(s) is/are used in your building?

HSHP	DX System	WSHP.5 - .6	VAV System	Fan Coil and Chiller System
Click here to enter text.	Click here to enter text.	Click here to enter text.	Click here to enter text.	Click here to enter text.

26. What is the cooling efficiency rating of your HVAC system at 77^{o} F?

	SEER 9-10.8 EER 7.9-9.4 COP 2.3-2.8	SEER 10.9-12.5 EER 9.5-10.9 COP 2.9-3.2	SEER 12.6-14.3 EER 11.0-12.5 COP 3.3-3.7	SEER 14.4-16 EER 12.6-14 COP 3.8-4.1
GSHP	☐	☐	☐	☐
DX system	☐	☐	☐	☐
WSHP	☐	☐	☐	☐
VAV system	☐	☐	☐	☐
Fan coil and chiller system	☐	☐	☐	☐

27. What is the heating efficiency rating of your HVAC system at 32^{o} F?

GSHP	WSHP	VAV system	SEER 9-10.8 EER 7.9-9.4 COP 2.3-2.8
DX system		Fan coil and chiller system	

	SEER 10.9-12.5 EER 9.5-10.9 COP 2.9-3.2	SEER 12.6-14.3 EER 11.0-12.5 COP 3.3-3.7	SEER 14.4-16 EER 12.6-14 COP 3.8-4.1
☐	☐	☐	☐
☐	☐	☐	☐
☐	☐	☐	☐
☐	☐	☐	☐
☐	☐	☐	☐

28. What was the cost for your HVAC system? Click here to enter text.

29. What is the design life of the building's HVAC system?

0-10 years	11-15 years	16-20 years	21-30 years	31-50 years
☐	☐	☐	☐	☐

30. What type of Domestic Hot Water system (DHW) is used in the building?

Gas storage	Gas Instantaneous	Electric storage	Electric instantaneous	Solar
☐	☐	☐	☐	☐

31. For solar DHW systems what backup system is used?

Gas storage	Gas Instantaneous	Electric storage	Electric instantaneous
☐	☐	☐	☐

32. What is the efficiency rating of your DHW system?

	Gas storage	Gas Instantaneous

	70-80%	81-90%	91-95%	96-100%
Electric storage	☐	☐	☐	☐
Electric instantaneous	☐	☐	☐	☐
	☐	☐	☐	☐
	☐	☐	☐	☐

33. What was the cost for the DHW system? Click here to enter text.

34. What is the design life of the building's DHW system?

0-10 years	11-15 years	16-20 years	21-30 years	31-50 years
☐	☐	☐	☐	☐

35. Does your building use day lighting technologies? (If day lighting is not provided please skip to question # 59)

☐Yes ☐No

36. What types of day lighting technologies are used, check all that apply?

Side lighting	Skylights	Roof Monitors	Clerestories
☐	☐	☐	☐

37. What percentage of your building is lit with side lighting? (If side lighting is not used please skip to question # 40)

0-10 ☐ 11-20 ☐ 21-30 ☐ 31-40 ☐

41-50 ☐ 51-60 ☐ 61-80 ☐ 81-100 ☐

38. What is the total window area per side of the building used for side lighting?

North	South	East	West
Click here to enter text.	Click here to enter text.	Click here to enter text.	Click here to enter text.

39. Does your side lighting system incorporate any of the following? (Check all that apply)

Light shelves	Overhangs	Separate view windows
☐	☐	☐

40. What percentage of your building is lit with skylights? (If skylights are not used please skip to question # 45)

0-10 ☐ 21-30 ☐ 41-50 ☐ 61-80 ☐

11-20 ☐ 31-40 ☐ 51-60 ☐ 81-100 ☐

41. What is the fenestration area to lit floor area percentage for the skylights?

1-2% ☐ 4% ☐ 6% ☐ 8% ☐

3% ☐ 5% ☐ 7% ☐ 9% ☐

42. What areas of your building are lit by skylights? (Check all that apply)

Gym ☐ Corridors ☐

Classrooms ☐ Other Click here to enter text. ☐

43. Do your sky lights use reflective glazing?

Yes ☐ No ☐

44. What was your cost per square foot of fenestration area for skylights? Click here to enter text.

45. What percentage of your building is lit with roof monitors? (If roof monitors are not used please skip to question # 50)

0-10 ☐ 21-30 ☐ 41-50 ☐ 61-80 ☐

11-20 ☐ 31-40 ☐ 51-60 ☐ 81-100 ☐

46. What is the fenestration area to lit floor area percentage for roof monitors?

1-2% ☐ 4% ☐ 6% ☐ 8% ☐

3% ☐ 5% ☐ 7% ☐ 9% ☐

47. What areas of your buildings are lit by roof monitors? (Check all that apply)

Gym ☐ Corridors ☐

Classrooms ☐ Other Click here to enter text. ☐

48. What direction do your roof monitors face?

South side ☐ East side ☐ West side ☐ North side ☐

49. What was your cost per square foot of fenestration area for roof monitors? Click here to enter text.

50. What percentage of your building is lit with clerestories? (If clerestories are not used please skip to question # 57)

0-10 ☐ 21-30 ☐ 41-50 ☐ 61-80 ☐

11-20 ☐ 31-40 ☐ 51-60 ☐ 81-100 ☐

51. What is the fenestration area to lit floor area percentage for clerestories?

1-2% ☐ 4% ☐ 6% ☐ 8% ☐

3% ☐ 5% ☐ 7% ☐ 9% ☐

52. What areas of your buildings are lit by clerestories? (Check all that apply)

Gym ☐ Corridors ☐

Classrooms	☐	Other Click here to enter text.	☐

53. What type of clerestory systems are in your buildings?

Top and side lit	Top lit only	Side lit only
☐	☐	☐

54. For side lit clerestories are overhangs used?

Yes ☐ No ☐

55. For side lit clerestories what direction do your clerestories receive light from? (check all that apply)

South side	East side	West side	North side
☐	☐	☐	☐

56. What was your cost per square foot of fenestration area for clerestories? Click here to enter text.

57. Are the artificial lights equipped with an automatic dimming system in areas with day lighting?

Yes ☐ No ☐

58. What was your cost for automatic dimmers? Click here to enter text.

59. What type of fluorescent artificial lighting is used in the building?

T12	T8	T5	T5HO
☐	☐	☐	☐

60. What type of room lighting controls are used in the building?

Manual on/off	Manual on/auto off (timers)	Automatic on automatic off (occupancy sensors)
☐	☐	☐

SURVEY OF ENERGY EFFICIENCY IN SCHOOLS

Significant effort has been focused on the design of sustainable and energy efficient school buildings over the past few years. This effort has culminated in a number of design guidelines such as Leadership in Energy and Environmental Design (LEED) for Schools-New Construction and Major Renovations, and the Kentucky Green and Healthy Schools Design Guidelines. These design provisions go a long way in providing guidance to design professionals and school officials on what areas in the facility design might be addressed to improve the performance of the facility. However, there appears to be a reluctance to embrace these "Green" or "Energy Efficient" designs, partially due to the perception that these designs will cost a lot more than traditional systems.

The goal of this project is to use the design guidelines discussed above and develop a list of low life cycle cost systems (both first cost and maintenance costs) that can be used to meet, at least in part, the energy efficiency and sustainability goals of the State of Kentucky. Each of the systems will be incorporated into a typical prototype configuration and the effects each system has on the overall energy used over the life cycle of the building will be determined using an analysis program. This data will be used to develop a relationship between each of the systems described above, their life cycle costs and the effect each has on energy use. Each system design will be performed in an effort to minimize lifecycle costs with as little reduction in energy efficiency as possible.

The effort above will result in a matrix of sample building system designs that can be reviewed by designers and school officials to quickly assess which systems might be implemented to reduce energy use, at the least cost.

The purpose of this survey is to twofold:
1 To help establish typical design practice in Kentucky for energy efficient schools.
2. To attempt to develop a partial data base of effective design practices and costs.
We ask that you complete the following form and email us m.mcginley@louisville.edu. If you provide an email address we will ensure that you receive a PDF version of the final report when it is ready.

Facility Managers/Contracters

K-12 School Energy Efficiency Survey

Please take a few moments to complete the following survey, being as specific and accurate as possible. If you are reporting on more than one school or building please complete a

separate survey for each building or school. Questions should be answered based on current configurations in use in Kentucky's schools. Please feel free to add any additional comments that you may feel are relevant or specific to your individual situation. If you are unsure or a question does not apply please skip that question and move on to the next question.

Contact Name: _Click here to enter text.
Contact Email:Click here to enter text.
Contact Telephone No.:Click here to enter text.

Name of school _ Click here to enter text. **County of school Location** Click here to enter text.

61. What type of school are you reporting about?

Elementary school	Middle school	High school
☐	☐	☐

62. What is the primary use of your building?

Main school with gym attached	Main School	Gym	Other Click here to enter text.
☐	☐	☐	☐

63. How many stories is your building?

One story in all areas	One and two stories	Two Stories	O Other Click here to enter text.
☐	☐	☐	☐

64. How many square feet are in your building? Click here to enter text.

65. What is the floor to floor height in your building? Click here to enter text.

66. What is the age of your building?

0-5 years	☐	11-15 years	☐	21-25 years	☐
6-10 years	☐	16-20 years	☐	26+ years	☐

67. What is the annual electricity use in your building? Click here to enter text. **KW**

68. What is the annual natural gas use in your building? Click here to enter text. **CCF**

69. What is the primary building structure construction?

Steel frame ☐ High mass ☐

70. What is the annual maintenance cost for the walls? Click here to enter text.

71. What is the annual maintenance cost for the roof? Click here to enter text.

72. Please rate your building structures durability. (1-Excellent 5-Very Poor)

1	2	3	4	5
☐	☐	☐	☐	☐

73. Please rate your building structures effectiveness. (1-Excellent 5-Very Poor)

1	2	3	4	5
☐	☐	☐	☐	☐

74. What is the design life of the buildings structure?

0-25 years	26-45 years	46-60 years	61-75 years	76+ years
☐	☐	☐	☐	☐

75. What is the design R-value for the building's wall system?

8-11	12-13	14-16	17-19	20-22
☐	☐	☐	☐	☐

76. What is the R-value of the roof system?

13-19	20-23	24-28	29-32	33-38
☐	☐	☐	☐	☐

77. For high mass wall systems where is the insulation located?

Inside wall mass	Outside wall mass	On both sides of wall mass
☐	☐	☐

78. What direction is the major axis of the building?

North / South	East / West	Northeast / Southwest	Northwest / Southeast
☐	☐	☐	☐

79. What color is the exposed roof surface?

White	A light color besides white	Black	A dark color besides black	A medium color such as tan
☐	☐	☐	☐	☐

80. What is the fenestration area for doors per side of the building?

	North	South	East	West
Double door with center post	Click here to enter text.	Click here to enter text.	Click here to enter text.	Click here to enter text.
Double door without center post	Click here to enter text.	Click here to enter text.	Click here to enter text.	Click here to enter text.
Single door single swing	Click here to enter text.	Click here to enter text.	Click here to enter text.	Click here to enter text.
Single door double swing	Click here to enter text.	Click here to enter text.	Click here to enter text.	Click here to enter text.
Overhead or roll-up	Click here to enter text.	Click here to enter text.	Click here to enter text.	Click here to enter text.

81. What is the average U-value for each door type in the building?

	.2 - .4	.5 - .6	.7 - .8	.9 - 1
Double door with center post	☐	☐	☐	☐

Double door without center post	☐	☐	☐	☐
Single door single swing	☐	☐	☐	☐
Single door double swing	☐	☐	☐	☐
Overhead or roll-up	☐	☐	☐	☐

82. What is the maintenance cost per year for the exterior doors?

Double door with center post	Click here to enter text.
Double door without center post	Click here to enter text.
Single door single swing	Click here to enter text.
Single door double swing	Click here to enter text.
Overhead or roll-up	Click here to enter text.

83. Please rate the durability of your building's exterior doors. (1-Excellent 5-Very Poor)

1	2	3	4	5
☐	☐	☐	☐	☐

84. Please rate the effectiveness of your building's exterior doors. (1-Excellent 5-Very Poor)

1	2	3	4	5
☐	☐	☐	☐	☐

85. What is the design life of the building's exterior doors?

0-10 years	11-15 years	16-20 years	21-30 years	31-50 years
☐	☐	☐	☐	☐

86. What is the total window area per side of the building?

	North	**South**	**East**	**West**
Single pane	Click here to enter text.	Click here to enter text.	Click here to enter text.	Click here to enter text.
Double pane	Click here to enter text.	Click here to enter text.	Click here to enter text.	Click here to enter text.
Triple pane	Click here to enter text.	Click here to enter text.	Click here to enter text.	Click here to enter text.

	.2 - .4	.5 - .6	0.7-0.8	0.9 – 1.0
Single pane	☐	☐	☐	☐
Double pane	☐	☐	☐	☐
Triple pane	☐	☐	☐	☐

87. What is the average U-value for each window type in the building?

88. What is the annual maintenance cost per year for the windows? Click here to enter text.

89. Please rate the durability of your building's windows. (1-Excellent 5-Very Poor)

1	2	3	4	5
☐	☐	☐	☐	☐

90. Please rate the effectiveness of your building's windows. (1-Excellent 5-Very Poor)

1	2	3	4	5
☐	☐	☐	☐	☐

91. What is the design life of the building's windows?

0-10 years	11-15 years	16-20 years	21-30 years	31-50 years
☐	☐	☐	☐	☐

92. Where are overhangs used above windows on your building?

No overhangs	South Side	East Side	North Side	West Side
☐	☐	☐	☐	☐

93. What tonnage of HVAC system(s) is/are used in your building?

HSHP	DX System	WSHP	VAV System	Fan Coil and Chiller System
Click here to enter text.	Click here to enter text.	Click here to enter text.	Click here to enter text.	Click here to enter text.

94. What is the cooling efficiency rating of your HVAC system at 77^{o} F?

	SEER 9-10.8 EER 7.9-9.4 COP 2.3-2.8	SEER 10.9-12.5 EER 9.5-10.9 COP 2.9-3.2	SEER 12.6-14.3 EER 11.0-12.5 COP 3.3-3.7	SEER 14.4-16 EER 12.6-14 COP 3.8-4.1
GSHP	☐	☐	☐	☐
DX system	☐	☐	☐	☐
WSHP	☐	☐	☐	☐
VAV system	☐	☐	☐	☐
Fan coil and chiller system	☐	☐	☐	☐

95. What is the heating efficiency rating of your HVAC system at 32^{o} F?

	SEER 9-10.8 EER 7.9-9.4 COP 2.3-2.8	SEER 10.9-12.5 EER 9.5-10.9 COP 2.9-3.2	SEER 12.6-14.3 EER 11.0-12.5 COP 3.3-3.7
GSHP	☐	☐	☐
DX system	☐	☐	☐
WSHP	☐	☐	☐
VAV system	☐	☐	☐
Fan coil and chiller system	☐	☐	☐

SEER 14.4-16 ☐ ☐
EER 12.6-14 ☐
COP 3.8-4.1 ☐
☐

96. What is the annual maintenance cost for your HVAC system? Click here to enter text.

97. Please rate the durability of your building's HVAC system. (1-Excellent 5-Very Poor)

1	2	3	4	5
☐	☐	☐	☐	☐

98. Please rate the effectiveness of your building's HVAC system. (1-Excellent 5-Very Poor)

1	2	3	4	5
☐	☐	☐	☐	☐

99. What is the design life of the building's HVAC system?

0-10 years	11-15 years	16-20 years	21-30 years	31-50 years
☐	☐	☐	☐	☐

100. What type of Domestic Hot Water system (DHW) is used in the building?

Gas storage	Gas Instantaneous	Electric storage	Electric instantaneous	Solar
☐	☐	☐	☐	☐

101. For solar DHW systems what backup system is used?

Gas storage	Gas Instantaneous	Electric storage	Electric instantaneous
☐	☐	☐	☐

102. What is the efficiency rating of your DHW system?

	70-80%	81-90%	91-95%	96-100%
Gas storage	☐	☐	☐	☐
Gas Instantaneous	☐	☐	☐	☐
Electric storage	☐	☐	☐	☐
Electric instantaneous	☐	☐	☐	☐

103. What is the annual maintenance cost for the DHW system? Click here to enter text.

104. Please rate the durability of your building's DHW system. (1-Excellent 5-Very Poor)

1	2	3	4	5
☐	☐	☐	☐	☐

105. Please rate the effectiveness of your building's DHW system. (1-Excellent 5-Very Poor)

1	2	3	4	5
☐	☐	☐	☐	☐

106. What is the design life of the building's DHW system?

0-10 years	11-15 years	16-20 years	21-30 years	31-50 years
☐	☐	☐	☐	☐

107. Does your building use day lighting technologies? (If day lighting is not provided please skip to question # 73)

☐Yes ☐No

108. What types of day lighting technologies are used, check all that apply?

Side lighting	Skylights	Roof Monitors	Clerestories
☐	☐	☐	☐

109. What percentage of your building is lit with side lighting? (If side lighting is not used please skip to question # 52)

0-10 ☐	21-30 ☐	41-50 ☐	61-80 ☐
11-20 ☐	31-40 ☐	51-60 ☐	81-100 ☐

110. What is the total window area per side of the building used for side lighting?

North	South	East	West
Click here to enter text.	Click here to enter text.	Click here to enter text.	Click here to enter text.

111. Does your side lighting system incorporate any of the following? (Check all that apply)

Light shelves	☐	Overhangs

☐ Separate view windows ☐

112. What percentage of your building is lit with skylights? (If skylights are not used please skip to question # 57)

0-10 ☐	21-30 ☐	41-50 ☐	61-80 ☐
11-20 ☐	31-40 ☐	51-60 ☐	81-100 ☐

113. What is the fenestration area to lit floor area percentage for the skylights?

1-2% ☐	4% ☐	6% ☐	8% ☐
3% ☐	5% ☐	7% ☐	9% ☐

114. What areas of your building are lit by skylights? (Check all that apply)

Gym	Corridors	Classrooms	Other Click here to enter text.
☐	☐	☐	☐

115. Do your sky lights use reflective glazing?

Yes ☐ No ☐

116. What is your annual maintenance cost for skylights? Click here to enter text.

117. What percentage of your building is lit with roof monitors? (If roof monitors are not used please skip to question # 62)

0-10 ☐	21-30 ☐	41-50 ☐	61-80 ☐
11-20 ☐	31-40 ☐	51-60 ☐	81-100 ☐

118. What is the fenestration area to lit floor area percentage for roof monitors?

1-2% ☐	4% ☐	6% ☐	8% ☐
3% ☐	5% ☐	7% ☐	9% ☐

119. What areas of your buildings are lit by roof monitors? (Check all that apply)

Gym	Corridors	Classrooms	Other Click here to enter text.
☐	☐	☐	☐

120. What direction do your roof monitors face?

South side	East side	West side	North side
☐	☐	☐	☐

121. What is your annual maintenance cost for roof monitors? Click here to enter text.

122. What percentage of your building is lit with clerestories? (If clerestories are not used please skip to question # 69)

0-10 ☐	21-30 ☐	41-50 ☐	61-80 ☐
11-20 ☐	31-40 ☐	51-60 ☐	81-100 ☐

123. What is the fenestration area to lit floor area percentage for clerestories?

1-2% ☐	4% ☐	6% ☐	8% ☐
3% ☐	5% ☐	7% ☐	9% ☐

124. What areas of your buildings are lit by clerestories? (Check all that apply)

Gym	Corridors	Classrooms	Other Click here to enter text.
☐	☐	☐	☐

125. What type of clerestory systems are in your buildings?

Top and side lit	Top lit only	Side lit only
☐	☐	☐

126. For side lit clerestories are overhangs used?

Yes ☐ No ☐

127. For side lit clerestories what direction do your clerestories receive light from? (check all that apply)

South side	East side	West side	North side
☐	☐	☐	☐

128. What is your annual maintenance cost for clerestories? Click here to enter text.

129. Please rate the durability of your building's day lighting system. (1-Excellent 5-Very Poor)

1	2	3	4	5
☐	☐	☐	☐	☐

130. Please rate the effectiveness of your building's day lighting system. (1-Excellent 5-Very Poor)

1	2	3	4	5
☐	☐	☐	☐	☐

131. Are the artificial lights equipped with an automatic dimming system in areas with day lighting?

Yes ☐ No ☐

132. What is your annual maintenance cost for automatic dimmers? Click here to enter text.

133. What type of fluorescent artificial lighting is used in the building?

T12	T8	T5	T5HO
☐	☐	☐	☐

134. What type of room lighting controls are used in the building?

Manual on/off	Manual on/auto off (timers)	Automatic on automatic off (occupancy sensors)
☐	☐	☐

Appendix B

Select eQuest Energy use Summaries

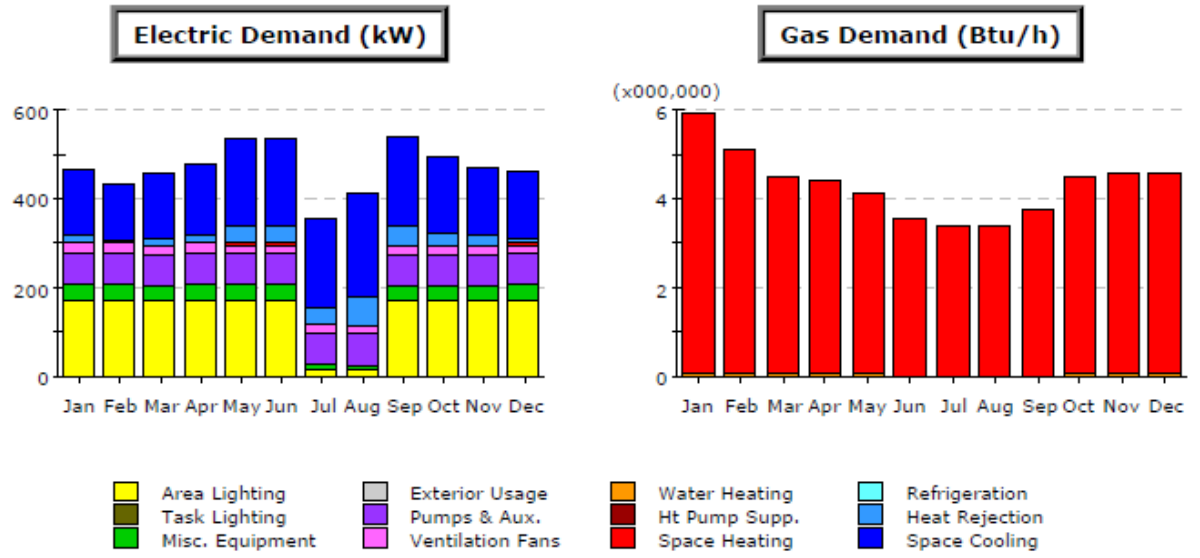

Electric Demand (kW)

	Jan	Feb	Mar	Apr	May	Jun	Jul	Aug	Sep	Oct	Nov	Dec	Total
Space Cool	150.2	125.7	145.4	160.1	197.7	197.7	197.5	238.0	206.0	170.3	154.9	148.9	2,092.5
Heat Reject.	15.1	6.0	12.8	18.3	38.1	38.2	39.0	62.4	40.8	25.8	17.6	14.8	329.1
Refrigeration	-	-	-	-	-	-	-	-	-	-	-	-	-
Space Heat	1.0	1.2	1.0	1.1	0.9	0.9	1.1	0.1	0.8	0.9	0.9	1.0	11.0
HP Supp.	-	-	-	-	-	-	-	-	-	-	-	-	-
Hot Water	-	-	-	-	-	-	-	-	-	-	-	-	-
Vent. Fans	20.3	20.3	20.3	20.3	20.3	20.3	20.3	20.3	20.3	20.3	20.3	20.3	243.3
Pumps & Aux.	69.8	69.8	69.8	69.8	69.8	69.8	69.8	69.8	69.8	69.8	69.8	69.8	837.1
Ext. Usage	-	-	-	-	-	-	-	-	-	-	-	-	-
Misc. Equip.	39.9	40.3	36.6	39.1	37.9	37.9	7.7	7.6	36.6	36.6	36.6	37.9	394.6
Task Lights	-	-	-	-	-	-	-	-	-	-	-	-	-
Area Lights	168.8	168.8	168.8	168.8	168.8	168.8	17.4	16.5	168.8	168.8	168.8	168.8	1,722.0
Total	465.1	432.0	454.7	477.4	533.4	533.6	352.8	414.6	543.1	492.5	468.9	461.5	5,629.6

Gas Demand (Btu/h x000,000)

	Jan	Feb	Mar	Apr	May	Jun	Jul	Aug	Sep	Oct	Nov	Dec	Total
Space Cool	-	-	-	-	-	-	-	-	-	-	-	-	-
Heat Reject.	-	-	-	-	-	-	-	-	-	-	-	-	-
Refrigeration	-	-	-	-	-	-	-	-	-	-	-	-	-
Space Heat	5.88	5.04	4.40	4.30	4.08	3.55	3.37	3.34	3.76	4.45	4.47	4.51	51.16
HP Supp.	-	-	-	-	-	-	-	-	-	-	-	-	-
Hot Water	0.07	0.07	0.07	0.07	0.07	0.01	0.01	0.01	0.01	0.06	0.06	0.07	0.58
Vent. Fans	-	-	-	-	-	-	-	-	-	-	-	-	-
Pumps & Aux.	-	-	-	-	-	-	-	-	-	-	-	-	-
Ext. Usage	-	-	-	-	-	-	-	-	-	-	-	-	-
Misc. Equip.	-	-	-	-	-	-	-	-	-	-	-	-	-
Task Lights	-	-	-	-	-	-	-	-	-	-	-	-	-
Area Lights	-	-	-	-	-	-	-	-	-	-	-	-	-
Total	5.95	5.11	4.48	4.38	4.15	3.56	3.37	3.35	3.77	4.51	4.54	4.58	51.74

Figure B1. Monthly Energy Demand Profile – Baseline- Corbin

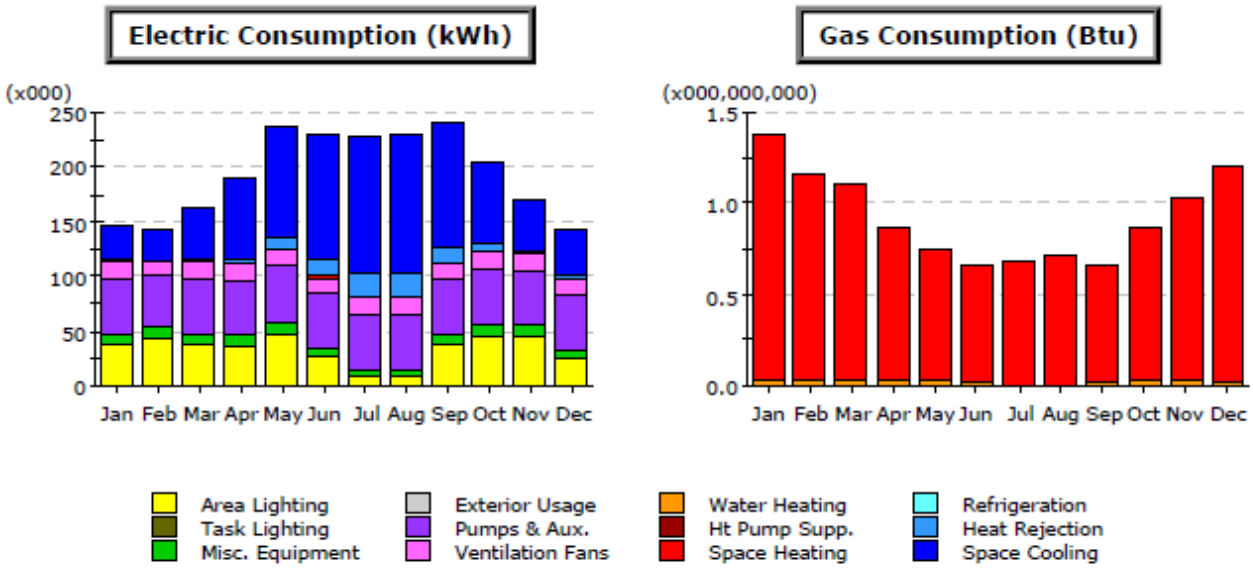

Electric Consumption (kWh x000)

	Jan	Feb	Mar	Apr	May	Jun	Jul	Aug	Sep	Oct	Nov	Dec	Total
Space Cool	32.4	28.1	46.7	74.2	100.4	115.0	126.3	126.8	113.1	75.7	46.4	42.8	927.8
Heat Reject.	0.5	0.1	1.4	4.3	11.2	16.3	21.3	21.4	15.3	5.3	1.6	1.4	100.0
Refrigeration	-	-	-	-	-	-	-	-	-	-	-	-	-
Space Heat	0.8	0.7	0.7	0.6	0.5	0.4	0.4	0.4	0.4	0.5	0.6	0.7	6.7
HP Supp.	-	-	-	-	-	-	-	-	-	-	-	-	-
Hot Water	-	-	-	-	-	-	-	-	-	-	-	-	-
Vent. Fans	15.1	13.6	15.1	14.6	15.1	14.6	15.1	15.1	14.6	15.1	14.6	15.1	177.6
Pumps & Aux.	51.9	46.9	51.9	50.2	51.9	50.2	51.9	51.9	50.2	51.9	50.2	51.9	611.1
Ext. Usage	-	-	-	-	-	-	-	-	-	-	-	-	-
Misc. Equip.	10.0	10.8	10.0	9.9	11.9	7.9	4.5	4.6	10.0	11.5	11.4	7.4	109.9
Task Lights	-	-	-	-	-	-	-	-	-	-	-	-	-
Area Lights	36.9	41.8	36.9	36.7	46.2	26.4	8.7	8.9	37.0	44.3	44.1	23.9	391.6
Total	147.6	141.9	162.6	190.5	237.1	230.8	228.2	229.1	240.6	204.3	168.9	143.2	2,324.8

Gas Consumption (Btu x000,000,000)

	Jan	Feb	Mar	Apr	May	Jun	Jul	Aug	Sep	Oct	Nov	Dec	Total
Space Cool	-	-	-	-	-	-	-	-	-	-	-	-	-
Heat Reject.	-	-	-	-	-	-	-	-	-	-	-	-	-
Refrigeration	-	-	-	-	-	-	-	-	-	-	-	-	-
Space Heat	1.35	1.14	1.08	0.84	0.72	0.64	0.67	0.70	0.64	0.85	1.01	1.19	10.83
HP Supp.	-	-	-	-	-	-	-	-	-	-	-	-	-
Hot Water	0.03	0.03	0.03	0.03	0.03	0.02	0.01	0.00	0.02	0.02	0.03	0.02	0.25
Vent. Fans	-	-	-	-	-	-	-	-	-	-	-	-	-
Pumps & Aux.	-	-	-	-	-	-	-	-	-	-	-	-	-
Ext. Usage	-	-	-	-	-	-	-	-	-	-	-	-	-
Misc. Equip.	-	-	-	-	-	-	-	-	-	-	-	-	-
Task Lights	-	-	-	-	-	-	-	-	-	-	-	-	-
Area Lights	-	-	-	-	-	-	-	-	-	-	-	-	-
Total	1.38	1.16	1.11	0.87	0.75	0.66	0.68	0.70	0.66	0.87	1.03	1.21	11.08

Figure B2. Monthly Energy Use Profile – Baseline- Corbin

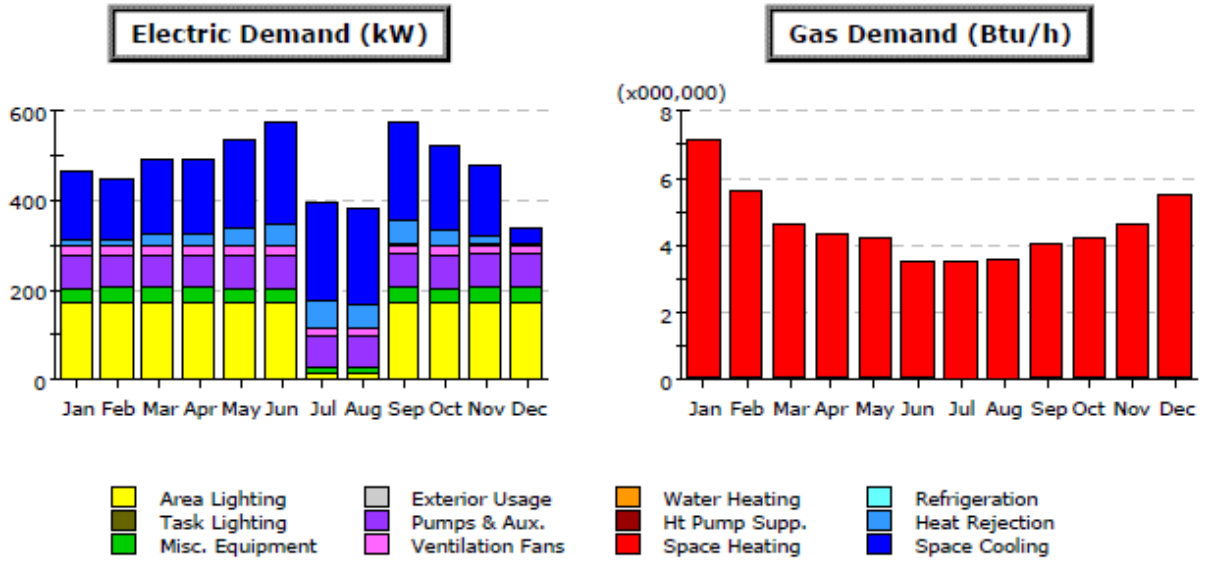

Electric Demand (kW)

	Jan	Feb	Mar	Apr	May	Jun	Jul	Aug	Sep	Oct	Nov	Dec	Total
Space Cool	152.1	140.7	165.5	166.0	199.9	225.6	223.3	213.6	220.6	185.2	155.9	36.4	2,085.0
Heat Reject.	14.0	8.8	22.2	22.3	37.1	49.7	55.4	47.0	48.5	33.0	16.2	-	354.1
Refrigeration	-	-	-	-	-	-	-	-	-	-	-	-	-
Space Heat	1.1	1.1	1.1	0.9	0.9	0.9	1.1	1.1	0.9	0.9	1.0	1.7	12.6
HP Supp.	-	-	-	-	-	-	-	-	-	-	-	-	-
Hot Water	-	-	-	-	-	-	-	-	-	-	-	-	-
Vent. Fans	20.3	20.3	20.3	20.3	20.3	20.3	20.3	20.3	20.3	20.3	20.3	20.3	243.4
Pumps & Aux.	72.5	72.5	72.5	72.5	72.5	72.5	72.5	72.5	72.5	72.5	72.5	72.5	869.7
Ext. Usage	-	-	-	-	-	-	-	-	-	-	-	-	-
Misc. Equip.	36.6	37.9	39.9	39.9	36.6	36.6	7.8	7.7	40.3	36.6	40.3	40.3	400.4
Task Lights	-	-	-	-	-	-	-	-	-	-	-	-	-
Area Lights	168.8	168.8	168.8	168.8	168.8	168.8	17.4	17.4	168.8	168.8	168.8	168.8	1,723.0
Total	465.3	450.1	490.2	490.7	536.1	574.3	397.8	379.6	571.9	517.2	474.9	340.0	5,688.2

Gas Demand (Btu/h x000,000)

	Jan	Feb	Mar	Apr	May	Jun	Jul	Aug	Sep	Oct	Nov	Dec	Total
Space Cool	-	-	-	-	-	-	-	-	-	-	-	-	-
Heat Reject.	-	-	-	-	-	-	-	-	-	-	-	-	-
Refrigeration	-	-	-	-	-	-	-	-	-	-	-	-	-
Space Heat	7.06	5.54	4.54	4.30	4.16	3.41	3.52	3.57	4.02	4.13	4.56	5.44	54.25
HP Supp.	-	-	-	-	-	-	-	-	-	-	-	-	-
Hot Water	0.07	0.08	0.08	0.08	0.07	0.07	0.01	0.01	0.06	0.06	0.06	0.07	0.71
Vent. Fans	-	-	-	-	-	-	-	-	-	-	-	-	-
Pumps & Aux.	-	-	-	-	-	-	-	-	-	-	-	-	-
Ext. Usage	-	-	-	-	-	-	-	-	-	-	-	-	-
Misc. Equip.	-	-	-	-	-	-	-	-	-	-	-	-	-
Task Lights	-	-	-	-	-	-	-	-	-	-	-	-	-
Area Lights	-	-	-	-	-	-	-	-	-	-	-	-	-
Total	7.13	5.61	4.61	4.37	4.24	3.48	3.53	3.58	4.07	4.19	4.63	5.51	54.96

Figure B3. Monthly Energy Demand Profile – Baseline- Paducha

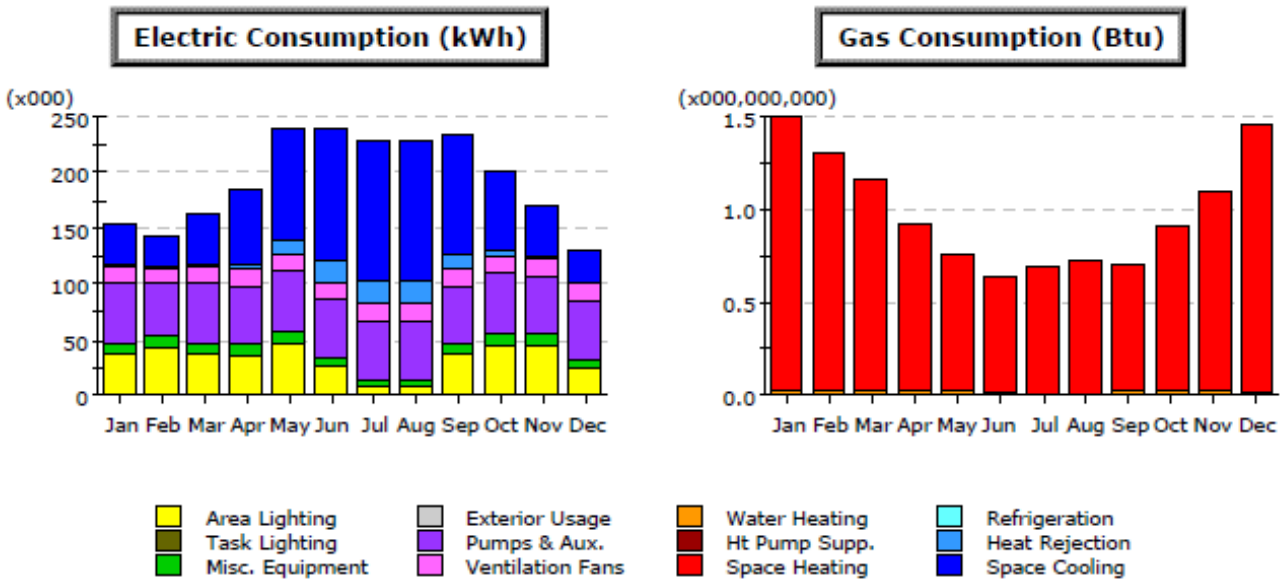

Electric Consumption (kWh x000)

	Jan	Feb	Mar	Apr	May	Jun	Jul	Aug	Sep	Oct	Nov	Dec	Total
Space Cool	37.3	26.6	44.4	67.1	100.2	119.4	126.1	126.4	106.7	69.9	44.5	28.9	897.5
Heat Reject.	0.8	0.1	1.3	3.7	10.2	18.1	19.9	19.5	13.9	5.1	1.4	0.0	93.9
Refrigeration	-	-	-	-	-	-	-	-	-	-	-	-	-
Space Heat	0.8	0.7	0.7	0.6	0.5	0.4	0.4	0.5	0.5	0.6	0.6	0.8	7.0
HP Supp.	-	-	-	-	-	-	-	-	-	-	-	-	-
Hot Water	-	-	-	-	-	-	-	-	-	-	-	-	-
Vent. Fans	15.1	13.6	15.1	14.6	15.1	14.6	15.1	15.1	14.6	15.1	14.6	15.1	177.6
Pumps & Aux.	53.9	48.7	53.9	52.2	53.9	52.2	53.9	53.9	52.2	53.9	52.2	53.9	634.9
Ext. Usage	-	-	-	-	-	-	-	-	-	-	-	-	-
Misc. Equip.	10.0	10.8	10.0	9.9	11.9	7.9	4.5	4.6	10.0	11.5	11.4	7.4	109.9
Task Lights	-	-	-	-	-	-	-	-	-	-	-	-	-
Area Lights	36.9	41.8	36.9	36.7	46.2	26.4	8.7	8.9	37.0	44.3	44.1	23.9	391.6
Total	155.0	142.2	162.3	184.7	238.0	238.9	228.6	228.8	234.8	200.4	168.9	130.1	2,312.6

Gas Consumption (Btu x000,000,000)

	Jan	Feb	Mar	Apr	May	Jun	Jul	Aug	Sep	Oct	Nov	Dec	Total
Space Cool	-	-	-	-	-	-	-	-	-	-	-	-	-
Heat Reject.	-	-	-	-	-	-	-	-	-	-	-	-	-
Refrigeration	-	-	-	-	-	-	-	-	-	-	-	-	-
Space Heat	1.47	1.27	1.14	0.90	0.73	0.62	0.69	0.72	0.69	0.89	1.07	1.45	11.66
HP Supp.	-	-	-	-	-	-	-	-	-	-	-	-	-
Hot Water	0.03	0.03	0.03	0.03	0.03	0.02	0.01	0.01	0.02	0.03	0.03	0.02	0.26
Vent. Fans	-	-	-	-	-	-	-	-	-	-	-	-	-
Pumps & Aux.	-	-	-	-	-	-	-	-	-	-	-	-	-
Ext. Usage	-	-	-	-	-	-	-	-	-	-	-	-	-
Misc. Equip.	-	-	-	-	-	-	-	-	-	-	-	-	-
Task Lights	-	-	-	-	-	-	-	-	-	-	-	-	-
Area Lights	-	-	-	-	-	-	-	-	-	-	-	-	-
Total	1.50	1.30	1.17	0.93	0.76	0.64	0.69	0.73	0.72	0.91	1.10	1.46	11.92

Figure B4. Monthly Energy Use Profile – Baseline- Paducah

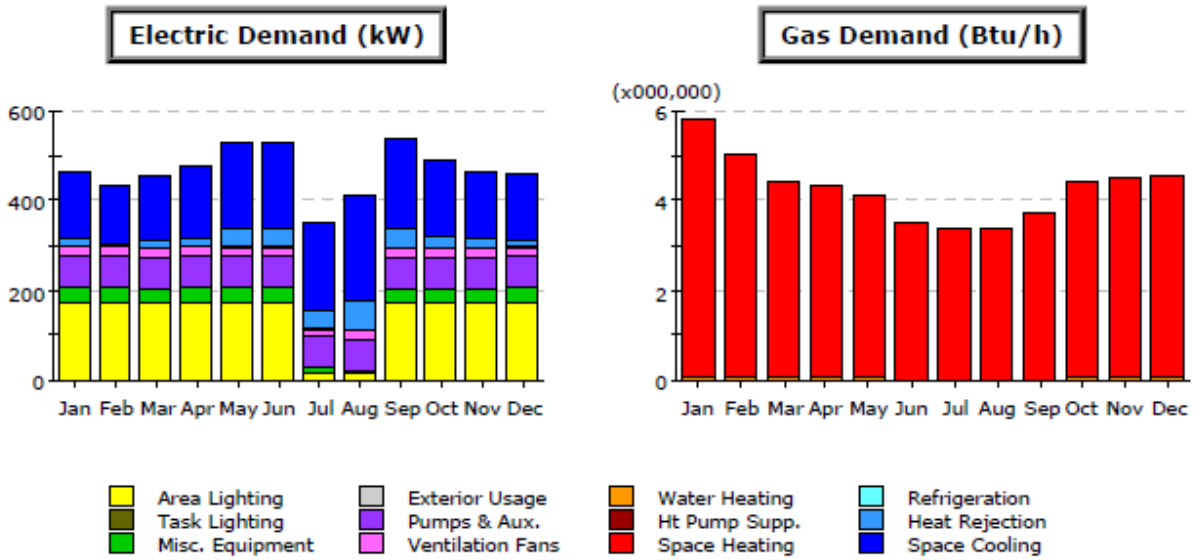

Electric Demand (kW)

	Jan	Feb	Mar	Apr	May	Jun	Jul	Aug	Sep	Oct	Nov	Dec	Total
Space Cool	150.1	125.6	145.3	160.0	197.2	197.2	197.1	237.3	205.6	169.9	154.7	148.8	2,088.9
Heat Reject.	15.1	6.0	12.8	18.2	38.0	38.1	38.9	62.3	40.8	25.8	17.6	14.8	328.5
Refrigeration	-	-	-	-	-	-	-	-	-	-	-	-	-
Space Heat	1.0	1.2	1.0	1.1	0.9	0.9	1.1	0.1	0.8	0.9	0.9	1.0	11.0
HP Supp.	-	-	-	-	-	-	-	-	-	-	-	-	-
Hot Water	-	-	-	-	-	-	-	-	-	-	-	-	-
Vent. Fans	20.3	20.3	20.3	20.3	20.3	20.3	20.3	20.3	20.3	20.3	20.3	20.3	243.3
Pumps & Aux.	69.7	69.7	69.7	69.7	69.7	69.7	69.7	69.7	69.7	69.7	69.7	69.7	836.2
Ext. Usage	-	-	-	-	-	-	-	-	-	-	-	-	-
Misc. Equip.	39.9	40.3	36.6	39.1	37.9	37.9	7.7	7.6	36.6	36.6	36.6	37.9	394.6
Task Lights	-	-	-	-	-	-	-	-	-	-	-	-	-
Area Lights	168.8	168.8	168.8	168.8	168.8	168.8	17.4	16.5	168.8	168.8	168.8	168.8	1,722.0
Total	464.9	431.8	454.6	477.2	532.8	532.9	352.2	413.7	542.5	492.0	468.6	461.3	5,624.6

Gas Demand (Btu/h x000,000)

	Jan	Feb	Mar	Apr	May	Jun	Jul	Aug	Sep	Oct	Nov	Dec	Total
Space Cool	-	-	-	-	-	-	-	-	-	-	-	-	-
Heat Reject.	-	-	-	-	-	-	-	-	-	-	-	-	-
Refrigeration	-	-	-	-	-	-	-	-	-	-	-	-	-
Space Heat	5.75	4.98	4.35	4.27	4.06	3.54	3.37	3.35	3.75	4.41	4.44	4.47	50.74
HP Supp.	-	-	-	-	-	-	-	-	-	-	-	-	-
Hot Water	0.07	0.07	0.07	0.07	0.07	0.01	0.01	0.01	0.01	0.06	0.06	0.07	0.58
Vent. Fans	-	-	-	-	-	-	-	-	-	-	-	-	-
Pumps & Aux.	-	-	-	-	-	-	-	-	-	-	-	-	-
Ext. Usage	-	-	-	-	-	-	-	-	-	-	-	-	-
Misc. Equip.	-	-	-	-	-	-	-	-	-	-	-	-	-
Task Lights	-	-	-	-	-	-	-	-	-	-	-	-	-
Area Lights	-	-	-	-	-	-	-	-	-	-	-	-	-
Total	5.82	5.05	4.42	4.34	4.13	3.55	3.38	3.36	3.76	4.47	4.50	4.54	51.31

Figure B5. Monthly Energy Demand Profile – C3-High Roof R- Corbin

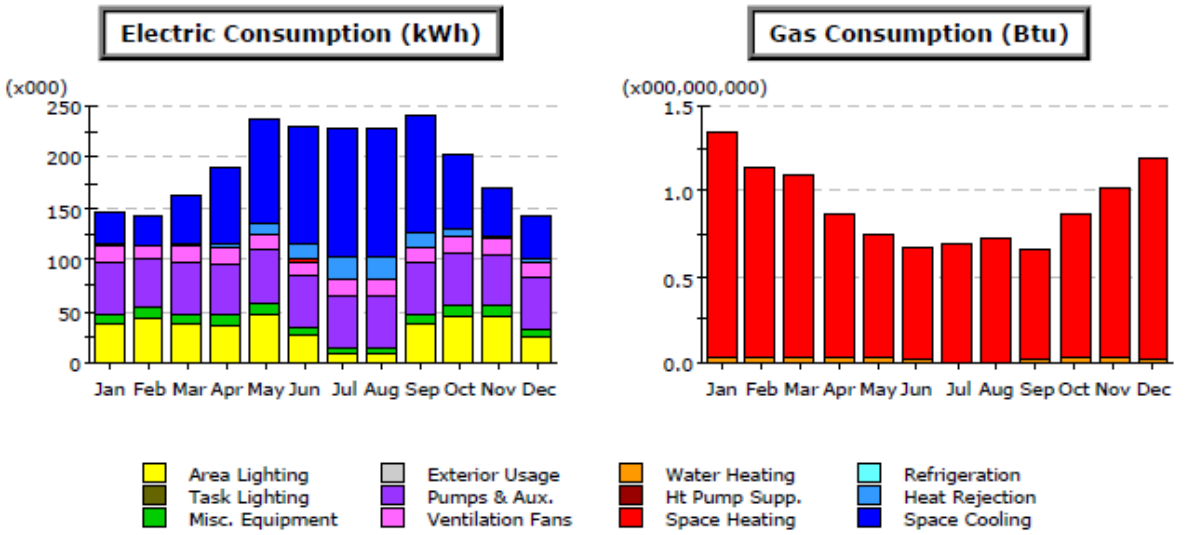

Electric Consumption (kWh x000)

	Jan	Feb	Mar	Apr	May	Jun	Jul	Aug	Sep	Oct	Nov	Dec	Total
Space Cool	32.4	28.1	46.7	74.2	100.3	114.7	126.1	126.5	112.9	75.6	46.3	42.7	926.5
Heat Reject.	0.5	0.1	1.3	4.3	11.2	16.2	21.3	21.4	15.2	5.3	1.6	1.4	99.8
Refrigeration	-	-	-	-	-	-	-	-	-	-	-	-	-
Space Heat	0.8	0.7	0.7	0.6	0.5	0.4	0.4	0.4	0.4	0.5	0.6	0.7	6.7
HP Supp.	-	-	-	-	-	-	-	-	-	-	-	-	-
Hot Water	-	-	-	-	-	-	-	-	-	-	-	-	-
Vent. Fans	15.1	13.6	15.1	14.6	15.1	14.6	15.1	15.1	14.6	15.1	14.6	15.1	177.6
Pumps & Aux.	51.8	46.8	51.8	50.2	51.8	50.2	51.8	51.8	50.2	51.8	50.2	51.8	610.4
Ext. Usage	-	-	-	-	-	-	-	-	-	-	-	-	-
Misc. Equip.	10.0	10.8	10.0	9.9	11.9	7.9	4.5	4.6	10.0	11.5	11.4	7.4	109.9
Task Lights	-	-	-	-	-	-	-	-	-	-	-	-	-
Area Lights	36.9	41.8	36.9	36.7	46.2	26.4	8.7	8.9	37.0	44.3	44.1	23.9	391.6
Total	147.5	141.9	162.5	190.3	236.9	230.5	227.8	228.7	240.4	204.2	168.8	143.1	2,322.5

Gas Consumption (Btu x000,000,000)

	Jan	Feb	Mar	Apr	May	Jun	Jul	Aug	Sep	Oct	Nov	Dec	Total
Space Cool	-	-	-	-	-	-	-	-	-	-	-	-	-
Heat Reject.	-	-	-	-	-	-	-	-	-	-	-	-	-
Refrigeration	-	-	-	-	-	-	-	-	-	-	-	-	-
Space Heat	1.32	1.11	1.07	0.84	0.72	0.65	0.69	0.71	0.64	0.84	0.99	1.17	10.76
HP Supp.	-	-	-	-	-	-	-	-	-	-	-	-	-
Hot Water	0.03	0.03	0.03	0.03	0.03	0.02	0.01	0.01	0.02	0.02	0.03	0.02	0.25
Vent. Fans	-	-	-	-	-	-	-	-	-	-	-	-	-
Pumps & Aux.	-	-	-	-	-	-	-	-	-	-	-	-	-
Ext. Usage	-	-	-	-	-	-	-	-	-	-	-	-	-
Misc. Equip.	-	-	-	-	-	-	-	-	-	-	-	-	-
Task Lights	-	-	-	-	-	-	-	-	-	-	-	-	-
Area Lights	-	-	-	-	-	-	-	-	-	-	-	-	-
Total	1.35	1.14	1.09	0.86	0.75	0.67	0.69	0.72	0.66	0.87	1.02	1.19	11.01

Figure B6. Monthly Energy Use Profile – C3-High Roof R- Corbin

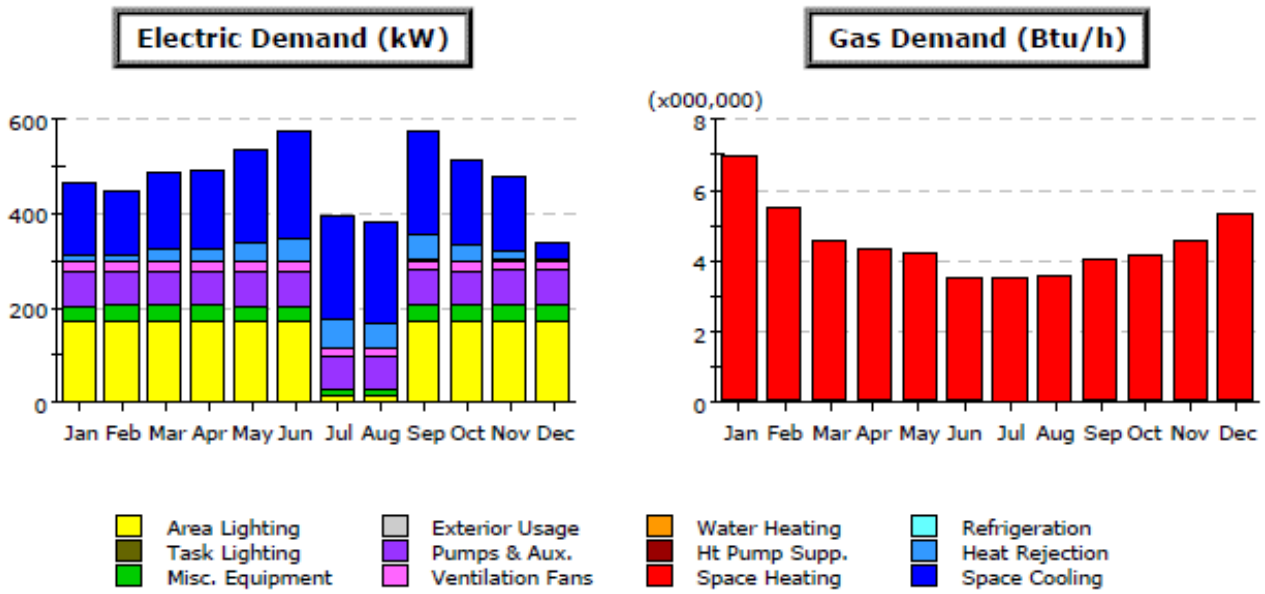

Electric Demand (kW)

	Jan	Feb	Mar	Apr	May	Jun	Jul	Aug	Sep	Oct	Nov	Dec	Total
Space Cool	152.0	140.7	165.4	165.8	199.4	225.1	222.7	213.1	220.2	182.1	155.8	36.4	2,078.9
Heat Reject.	14.0	8.8	22.1	22.2	37.0	49.5	55.2	46.9	48.5	32.3	16.2	-	352.8
Refrigeration	-	-	-	-	-	-	-	-	-	-	-	-	-
Space Heat	1.1	1.1	1.1	0.9	0.9	0.9	1.1	1.1	0.9	0.9	1.0	1.6	12.7
HP Supp.	-	-	-	-	-	-	-	-	-	-	-	-	-
Hot Water	-	-	-	-	-	-	-	-	-	-	-	-	-
Vent. Fans	20.3	20.3	20.3	20.3	20.3	20.3	20.3	20.3	20.3	20.3	20.3	20.3	243.4
Pumps & Aux.	72.4	72.4	72.4	72.4	72.4	72.4	72.4	72.4	72.4	72.4	72.4	72.4	869.1
Ext. Usage	-	-	-	-	-	-	-	-	-	-	-	-	-
Misc. Equip.	36.6	37.9	39.9	39.9	36.6	36.6	7.8	7.7	40.3	39.9	40.3	40.3	403.7
Task Lights	-	-	-	-	-	-	-	-	-	-	-	-	-
Area Lights	168.8	168.8	168.8	168.8	168.8	168.8	17.4	17.4	168.8	168.8	168.8	168.8	1,723.0
Total	465.2	450.0	490.1	490.4	535.5	573.6	397.0	379.0	571.4	516.8	474.8	339.9	5,683.6

Gas Demand (Btu/h x000,000)

	Jan	Feb	Mar	Apr	May	Jun	Jul	Aug	Sep	Oct	Nov	Dec	Total
Space Cool	-	-	-	-	-	-	-	-	-	-	-	-	-
Heat Reject.	-	-	-	-	-	-	-	-	-	-	-	-	-
Refrigeration	-	-	-	-	-	-	-	-	-	-	-	-	-
Space Heat	6.86	5.43	4.50	4.26	4.13	3.41	3.52	3.57	3.99	4.10	4.52	5.30	53.59
HP Supp.	-	-	-	-	-	-	-	-	-	-	-	-	-
Hot Water	0.07	0.08	0.08	0.08	0.07	0.07	0.01	0.01	0.06	0.06	0.06	0.07	0.71
Vent. Fans	-	-	-	-	-	-	-	-	-	-	-	-	-
Pumps & Aux.	-	-	-	-	-	-	-	-	-	-	-	-	-
Ext. Usage	-	-	-	-	-	-	-	-	-	-	-	-	-
Misc. Equip.	-	-	-	-	-	-	-	-	-	-	-	-	-
Task Lights	-	-	-	-	-	-	-	-	-	-	-	-	-
Area Lights	-	-	-	-	-	-	-	-	-	-	-	-	-
Total	6.93	5.51	4.57	4.34	4.20	3.47	3.52	3.58	4.05	4.16	4.59	5.37	54.29

Figure B7. Monthly Energy Demand Profile – C3-High Roof R- Paducah

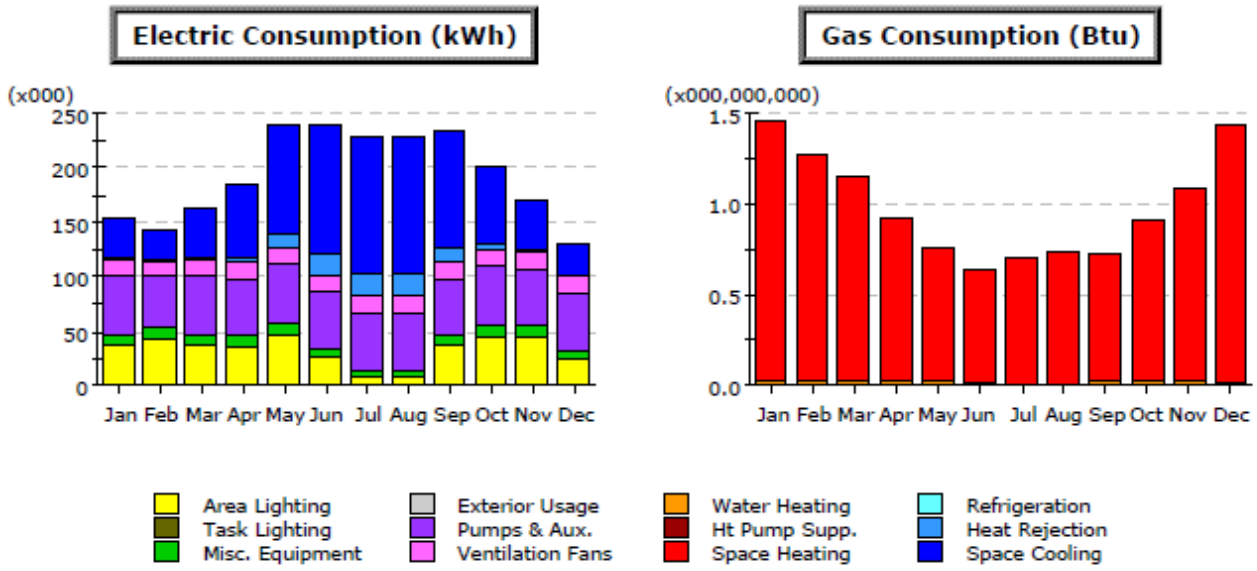

Electric Consumption (kWh x000)

	Jan	Feb	Mar	Apr	May	Jun	Jul	Aug	Sep	Oct	Nov	Dec	Total
Space Cool	37.3	26.5	44.4	67.1	100.1	119.2	125.9	126.1	106.6	69.9	44.5	28.8	896.4
Heat Reject.	0.8	0.1	1.3	3.7	10.1	18.0	19.8	19.5	13.9	5.1	1.4	0.0	93.8
Refrigeration	-	-	-	-	-	-	-	-	-	-	-	-	-
Space Heat	0.8	0.7	0.7	0.6	0.5	0.4	0.4	0.5	0.5	0.6	0.6	0.8	7.0
HP Supp.	-	-	-	-	-	-	-	-	-	-	-	-	-
Hot Water	-	-	-	-	-	-	-	-	-	-	-	-	-
Vent. Fans	15.1	13.6	15.1	14.6	15.1	14.6	15.1	15.1	14.6	15.1	14.6	15.1	177.6
Pumps & Aux.	53.9	48.7	53.9	52.1	53.9	52.1	53.9	53.9	52.1	53.9	52.1	53.9	634.4
Ext. Usage	-	-	-	-	-	-	-	-	-	-	-	-	-
Misc. Equip.	10.0	10.8	10.0	9.9	11.9	7.9	4.5	4.6	10.0	11.5	11.4	7.4	109.9
Task Lights	-	-	-	-	-	-	-	-	-	-	-	-	-
Area Lights	36.9	41.8	36.9	36.7	46.2	26.4	8.7	8.9	37.0	44.3	44.1	23.9	391.6
Total	154.9	142.2	162.2	184.6	237.8	238.6	228.3	228.5	234.7	200.3	168.8	130.0	2,310.8

Gas Consumption (Btu x000,000,000)

	Jan	Feb	Mar	Apr	May	Jun	Jul	Aug	Sep	Oct	Nov	Dec	Total
Space Cool	-	-	-	-	-	-	-	-	-	-	-	-	-
Heat Reject.	-	-	-	-	-	-	-	-	-	-	-	-	-
Refrigeration	-	-	-	-	-	-	-	-	-	-	-	-	-
Space Heat	1.43	1.24	1.13	0.90	0.73	0.63	0.70	0.74	0.70	0.88	1.06	1.41	11.54
HP Supp.	-	-	-	-	-	-	-	-	-	-	-	-	-
Hot Water	0.03	0.03	0.03	0.03	0.03	0.02	0.01	0.01	0.02	0.03	0.03	0.02	0.26
Vent. Fans	-	-	-	-	-	-	-	-	-	-	-	-	-
Pumps & Aux.	-	-	-	-	-	-	-	-	-	-	-	-	-
Ext. Usage	-	-	-	-	-	-	-	-	-	-	-	-	-
Misc. Equip.	-	-	-	-	-	-	-	-	-	-	-	-	-
Task Lights	-	-	-	-	-	-	-	-	-	-	-	-	-
Area Lights	-	-	-	-	-	-	-	-	-	-	-	-	-
Total	1.46	1.27	1.15	0.92	0.77	0.65	0.71	0.74	0.72	0.90	1.08	1.43	11.80

Figure B8. Monthly Energy Use Profile – C3-High Roof R- Paducah

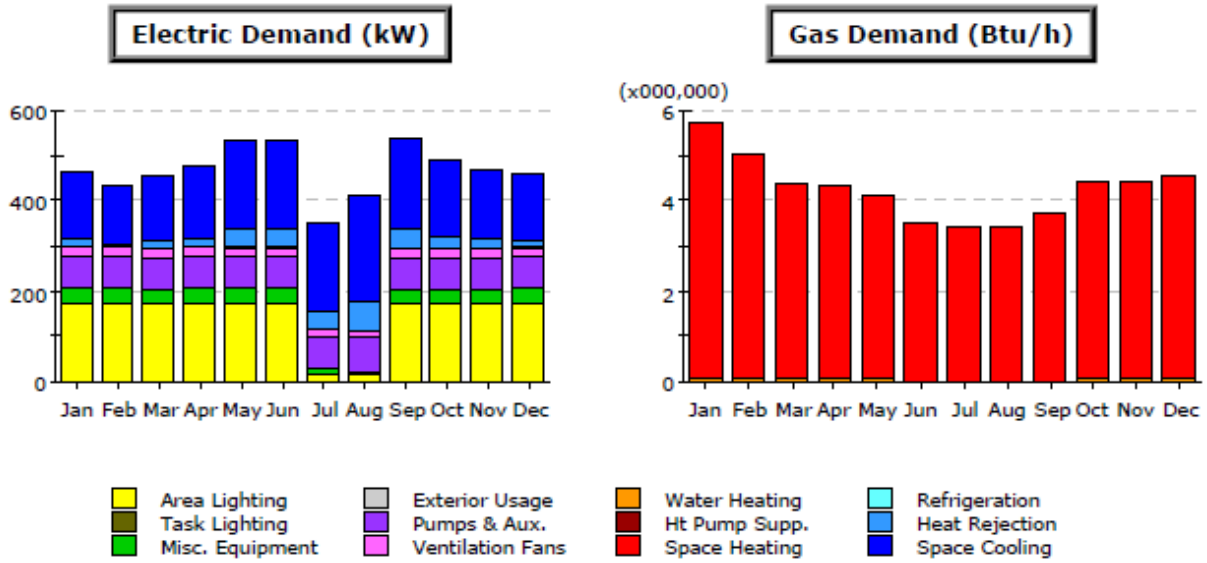

Electric Demand (kW)

	Jan	Feb	Mar	Apr	May	Jun	Jul	Aug	Sep	Oct	Nov	Dec	Total
Space Cool	150.3	125.7	145.5	160.1	197.8	197.8	197.5	238.1	206.2	170.4	155.0	149.2	2,093.6
Heat Reject.	15.2	6.0	12.9	18.3	38.1	38.2	39.0	62.4	40.9	25.9	17.7	14.9	329.3
Refrigeration	-	-	-	-	-	-	-	-	-	-	-	-	-
Space Heat	1.0	1.1	1.0	1.1	0.9	0.9	1.1	0.1	0.8	0.9	0.9	1.0	10.8
HP Supp.	-	-	-	-	-	-	-	-	-	-	-	-	-
Hot Water	-	-	-	-	-	-	-	-	-	-	-	-	-
Vent. Fans	20.3	20.3	20.3	20.3	20.3	20.3	20.3	20.3	20.3	20.3	20.3	20.3	243.3
Pumps & Aux.	69.8	69.8	69.8	69.8	69.8	69.8	69.8	69.8	69.8	69.8	69.8	69.8	837.1
Ext. Usage	-	-	-	-	-	-	-	-	-	-	-	-	-
Misc. Equip.	39.9	40.3	36.6	39.1	37.9	37.9	7.7	7.6	36.6	36.6	36.6	37.9	394.6
Task Lights	-	-	-	-	-	-	-	-	-	-	-	-	-
Area Lights	168.8	168.8	168.8	168.8	168.8	168.8	17.4	16.5	168.8	168.8	168.8	168.8	1,722.0
Total	465.2	431.9	454.8	477.4	533.6	533.7	352.9	414.7	543.2	492.7	469.0	461.8	5,630.8

Gas Demand (Btu/h x000,000)

	Jan	Feb	Mar	Apr	May	Jun	Jul	Aug	Sep	Oct	Nov	Dec	Total
Space Cool	-	-	-	-	-	-	-	-	-	-	-	-	-
Heat Reject.	-	-	-	-	-	-	-	-	-	-	-	-	-
Refrigeration	-	-	-	-	-	-	-	-	-	-	-	-	-
Space Heat	5.67	4.94	4.34	4.26	4.05	3.55	3.41	3.40	3.74	4.37	4.37	4.47	50.56
HP Supp.	-	-	-	-	-	-	-	-	-	-	-	-	-
Hot Water	0.07	0.07	0.07	0.07	0.07	0.01	0.01	0.01	0.01	0.06	0.06	0.07	0.58
Vent. Fans	-	-	-	-	-	-	-	-	-	-	-	-	-
Pumps & Aux.	-	-	-	-	-	-	-	-	-	-	-	-	-
Ext. Usage	-	-	-	-	-	-	-	-	-	-	-	-	-
Misc. Equip.	-	-	-	-	-	-	-	-	-	-	-	-	-
Task Lights	-	-	-	-	-	-	-	-	-	-	-	-	-
Area Lights	-	-	-	-	-	-	-	-	-	-	-	-	-
Total	5.74	5.01	4.41	4.33	4.12	3.56	3.42	3.40	3.74	4.43	4.44	4.53	51.14

Figure B9. Monthly Energy Demand Profile –C4- ICF- Corbin

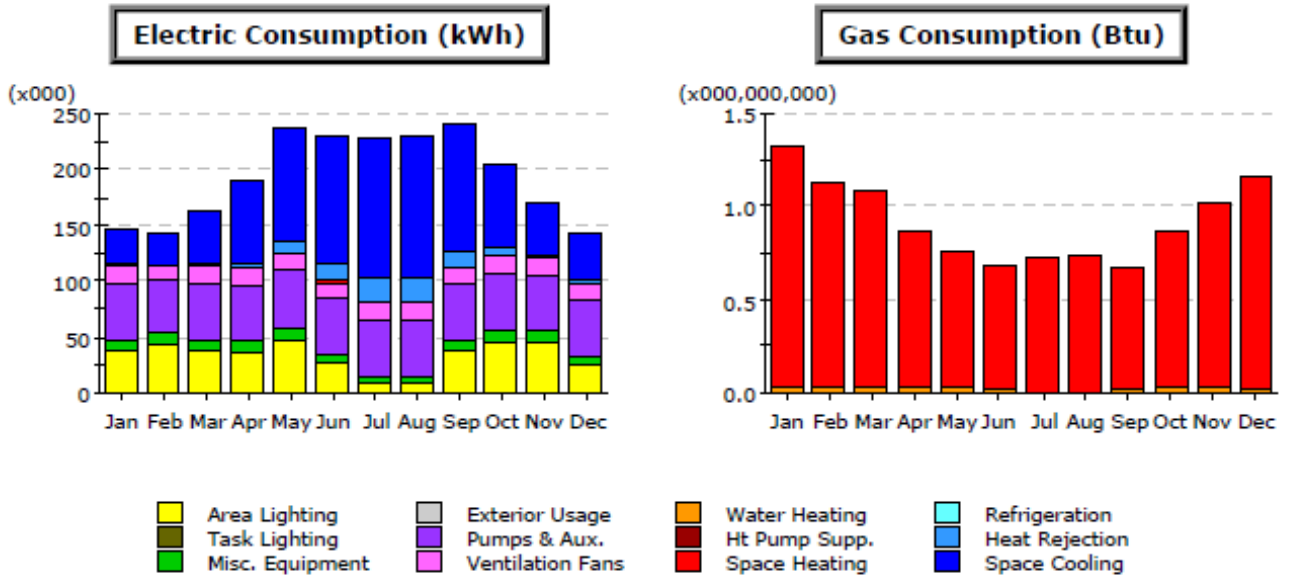

Electric Consumption (kWh x000)

	Jan	Feb	Mar	Apr	May	Jun	Jul	Aug	Sep	Oct	Nov	Dec	Total
Space Cool	32.4	28.1	46.7	74.2	100.4	114.9	126.2	126.7	113.0	75.7	46.4	42.8	927.5
Heat Reject.	0.5	0.1	1.4	4.3	11.2	16.3	21.3	21.4	15.2	5.3	1.6	1.4	99.9
Refrigeration	-	-	-	-	-	-	-	-	-	-	-	-	-
Space Heat	0.7	0.6	0.7	0.6	0.5	0.4	0.5	0.5	0.4	0.5	0.6	0.7	6.8
HP Supp.	-	-	-	-	-	-	-	-	-	-	-	-	-
Hot Water	-	-	-	-	-	-	-	-	-	-	-	-	-
Vent. Fans	15.1	13.6	15.1	14.6	15.1	14.6	15.1	15.1	14.6	15.1	14.6	15.1	177.6
Pumps & Aux.	51.9	46.9	51.9	50.2	51.9	50.2	51.9	51.9	50.2	51.9	50.2	51.9	611.1
Ext. Usage	-	-	-	-	-	-	-	-	-	-	-	-	-
Misc. Equip.	10.0	10.8	10.0	9.9	11.9	7.9	4.5	4.6	10.0	11.5	11.4	7.4	109.9
Task Lights	-	-	-	-	-	-	-	-	-	-	-	-	-
Area Lights	36.9	41.8	36.9	36.7	46.2	26.4	8.7	8.9	37.0	44.3	44.1	23.9	391.6
Total	147.5	141.9	162.6	190.5	237.1	230.7	228.1	228.9	240.6	204.3	168.9	143.1	2,324.4

Gas Consumption (Btu x000,000,000)

	Jan	Feb	Mar	Apr	May	Jun	Jul	Aug	Sep	Oct	Nov	Dec	Total
Space Cool	-	-	-	-	-	-	-	-	-	-	-	-	-
Heat Reject.	-	-	-	-	-	-	-	-	-	-	-	-	-
Refrigeration	-	-	-	-	-	-	-	-	-	-	-	-	-
Space Heat	1.31	1.10	1.06	0.84	0.73	0.67	0.71	0.73	0.65	0.84	0.99	1.16	10.80
HP Supp.	-	-	-	-	-	-	-	-	-	-	-	-	-
Hot Water	0.03	0.03	0.03	0.03	0.03	0.02	0.01	0.01	0.02	0.02	0.03	0.02	0.25
Vent. Fans	-	-	-	-	-	-	-	-	-	-	-	-	-
Pumps & Aux.	-	-	-	-	-	-	-	-	-	-	-	-	-
Ext. Usage	-	-	-	-	-	-	-	-	-	-	-	-	-
Misc. Equip.	-	-	-	-	-	-	-	-	-	-	-	-	-
Task Lights	-	-	-	-	-	-	-	-	-	-	-	-	-
Area Lights	-	-	-	-	-	-	-	-	-	-	-	-	-
Total	1.33	1.12	1.09	0.87	0.76	0.69	0.72	0.74	0.67	0.87	1.01	1.17	11.05

Figure B10. Monthly Energy Use Profile – C4- ICF - Corbin

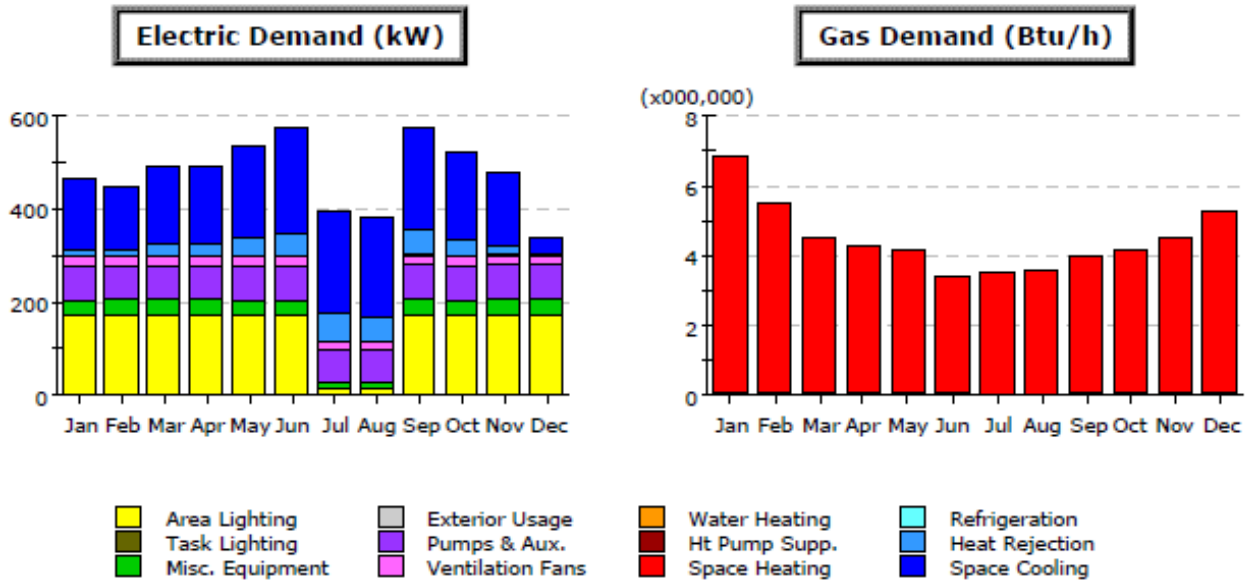

Electric Demand (kW)

	Jan	Feb	Mar	Apr	May	Jun	Jul	Aug	Sep	Oct	Nov	Dec	Total
Space Cool	152.1	141.0	165.6	166.1	200.0	225.8	223.3	213.6	220.6	185.2	155.9	36.4	2,085.5
Heat Reject.	14.0	8.9	22.2	22.3	37.1	49.7	55.4	47.0	48.5	33.0	16.2	-	354.3
Refrigeration	-	-	-	-	-	-	-	-	-	-	-	-	-
Space Heat	1.1	1.0	1.0	0.9	0.9	0.8	1.1	1.1	0.9	0.9	1.0	1.5	12.4
HP Supp.	-	-	-	-	-	-	-	-	-	-	-	-	-
Hot Water	-	-	-	-	-	-	-	-	-	-	-	-	-
Vent. Fans	20.3	20.3	20.3	20.3	20.3	20.3	20.3	20.3	20.3	20.3	20.3	20.3	243.4
Pumps & Aux.	72.5	72.5	72.5	72.5	72.5	72.5	72.5	72.5	72.5	72.5	72.5	72.5	869.7
Ext. Usage	-	-	-	-	-	-	-	-	-	-	-	-	-
Misc. Equip.	36.6	37.9	39.9	39.9	36.6	36.6	7.8	7.7	40.3	36.6	40.3	40.3	400.4
Task Lights	-	-	-	-	-	-	-	-	-	-	-	-	-
Area Lights	168.8	168.8	168.8	168.8	168.8	168.8	17.4	17.4	168.8	168.8	168.8	168.8	1,723.0
Total	465.3	450.3	490.3	490.8	536.2	574.5	397.7	379.6	571.9	517.3	474.9	339.8	5,688.7

Gas Demand (Btu/h x000,000)

	Jan	Feb	Mar	Apr	May	Jun	Jul	Aug	Sep	Oct	Nov	Dec	Total
Space Cool	-	-	-	-	-	-	-	-	-	-	-	-	-
Heat Reject.	-	-	-	-	-	-	-	-	-	-	-	-	-
Refrigeration	-	-	-	-	-	-	-	-	-	-	-	-	-
Space Heat	6.76	5.40	4.46	4.24	4.11	3.39	3.53	3.56	3.97	4.08	4.46	5.19	53.12
HP Supp.	-	-	-	-	-	-	-	-	-	-	-	-	-
Hot Water	0.07	0.08	0.08	0.08	0.07	0.07	0.01	0.01	0.06	0.06	0.06	0.07	0.71
Vent. Fans	-	-	-	-	-	-	-	-	-	-	-	-	-
Pumps & Aux.	-	-	-	-	-	-	-	-	-	-	-	-	-
Ext. Usage	-	-	-	-	-	-	-	-	-	-	-	-	-
Misc. Equip.	-	-	-	-	-	-	-	-	-	-	-	-	-
Task Lights	-	-	-	-	-	-	-	-	-	-	-	-	-
Area Lights	-	-	-	-	-	-	-	-	-	-	-	-	-
Total	6.83	5.47	4.53	4.31	4.18	3.45	3.53	3.56	4.03	4.14	4.52	5.26	53.83

Figure B11. Monthly Energy Demand Profile – C4- ICF - Paducah

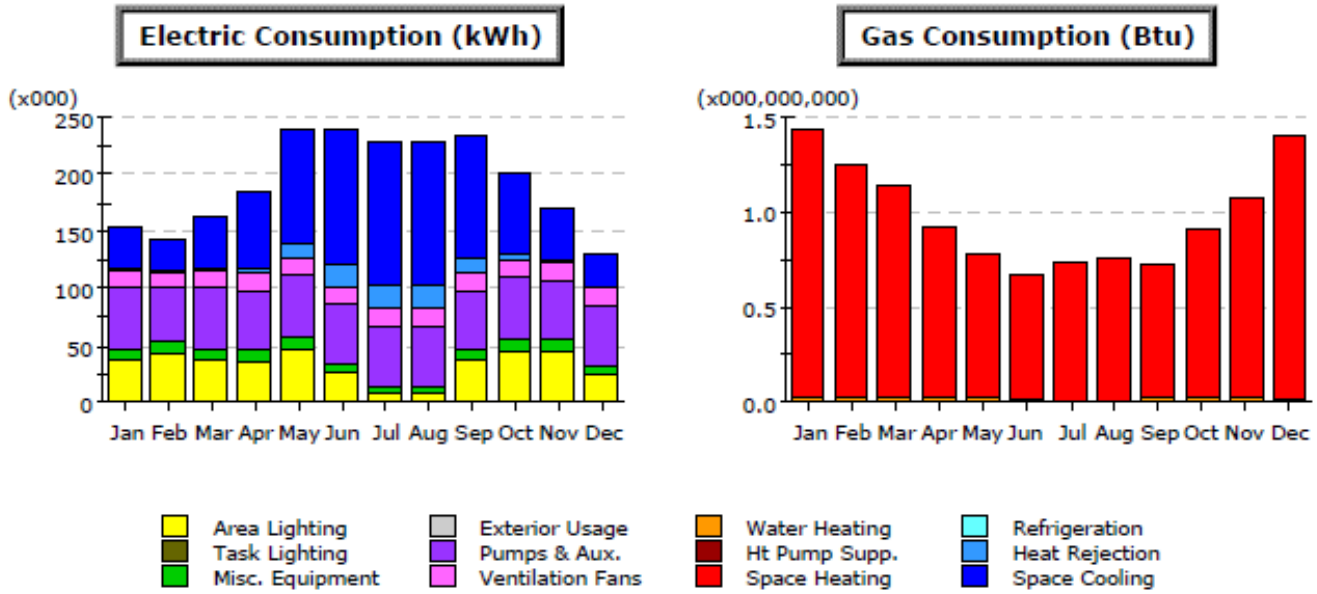

Electric Consumption (kWh x000)

	Jan	Feb	Mar	Apr	May	Jun	Jul	Aug	Sep	Oct	Nov	Dec	Total
Space Cool	37.3	26.6	44.4	67.1	100.2	119.3	126.0	126.3	106.7	69.9	44.5	28.9	897.2
Heat Reject.	0.8	0.1	1.3	3.7	10.2	18.0	19.9	19.5	13.9	5.1	1.4	0.0	93.8
Refrigeration	-	-	-	-	-	-	-	-	-	-	-	-	-
Space Heat	0.8	0.7	0.7	0.6	0.5	0.4	0.5	0.5	0.5	0.6	0.6	0.8	7.0
HP Supp.	-	-	-	-	-	-	-	-	-	-	-	-	-
Hot Water	-	-	-	-	-	-	-	-	-	-	-	-	-
Vent. Fans	15.1	13.6	15.1	14.6	15.1	14.6	15.1	15.1	14.6	15.1	14.6	15.1	177.6
Pumps & Aux.	53.9	48.7	53.9	52.2	53.9	52.2	53.9	53.9	52.2	53.9	52.2	53.9	634.9
Ext. Usage	-	-	-	-	-	-	-	-	-	-	-	-	-
Misc. Equip.	10.0	10.8	10.0	9.9	11.9	7.9	4.5	4.6	10.0	11.5	11.4	7.4	109.9
Task Lights	-	-	-	-	-	-	-	-	-	-	-	-	-
Area Lights	36.9	41.8	36.9	36.7	46.2	26.4	8.7	8.9	37.0	44.3	44.1	23.9	391.6
Total	154.9	142.2	162.3	184.7	238.0	238.8	228.5	228.7	234.8	200.4	168.9	130.0	2,312.1

Gas Consumption (Btu x000,000,000)

	Jan	Feb	Mar	Apr	May	Jun	Jul	Aug	Sep	Oct	Nov	Dec	Total
Space Cool	-	-	-	-	-	-	-	-	-	-	-	-	-
Heat Reject.	-	-	-	-	-	-	-	-	-	-	-	-	-
Refrigeration	-	-	-	-	-	-	-	-	-	-	-	-	-
Space Heat	1.41	1.22	1.12	0.90	0.75	0.65	0.73	0.76	0.71	0.88	1.04	1.38	11.54
HP Supp.	-	-	-	-	-	-	-	-	-	-	-	-	-
Hot Water	0.03	0.03	0.03	0.03	0.03	0.02	0.01	0.01	0.02	0.03	0.03	0.02	0.26
Vent. Fans	-	-	-	-	-	-	-	-	-	-	-	-	-
Pumps & Aux.	-	-	-	-	-	-	-	-	-	-	-	-	-
Ext. Usage	-	-	-	-	-	-	-	-	-	-	-	-	-
Misc. Equip.	-	-	-	-	-	-	-	-	-	-	-	-	-
Task Lights	-	-	-	-	-	-	-	-	-	-	-	-	-
Area Lights	-	-	-	-	-	-	-	-	-	-	-	-	-
Total	1.44	1.25	1.14	0.93	0.78	0.67	0.73	0.76	0.73	0.90	1.07	1.40	11.80

Figure B12. Monthly Energy Use Profile – C4- ICF - Paducah

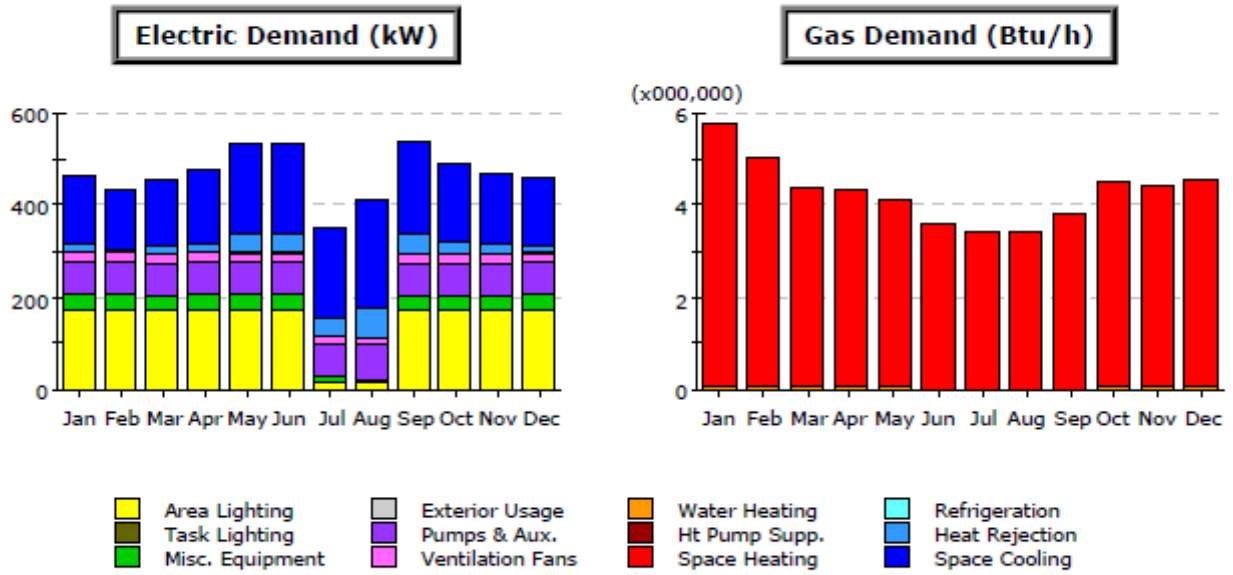

Electric Demand (kW)

	Jan	Feb	Mar	Apr	May	Jun	Jul	Aug	Sep	Oct	Nov	Dec	Total
Space Cool	150.2	125.7	145.4	160.1	197.6	197.6	197.4	237.9	206.0	170.2	154.9	149.0	2,092.0
Heat Reject.	15.1	6.0	12.8	18.3	38.1	38.2	39.0	62.4	40.8	25.8	17.6	14.9	329.0
Refrigeration	-	-	-	-	-	-	-	-	-	-	-	-	-
Space Heat	1.0	1.1	1.0	1.1	0.9	0.9	1.1	0.1	0.8	0.9	0.9	1.0	11.0
HP Supp.	-	-	-	-	-	-	-	-	-	-	-	-	-
Hot Water	-	-	-	-	-	-	-	-	-	-	-	-	-
Vent. Fans	20.3	20.3	20.3	20.3	20.3	20.3	20.3	20.3	20.3	20.3	20.3	20.3	243.3
Pumps & Aux.	69.7	69.7	69.7	69.7	69.7	69.7	69.7	69.7	69.7	69.7	69.7	69.7	837.0
Ext. Usage	-	-	-	-	-	-	-	-	-	-	-	-	-
Misc. Equip.	39.9	40.3	36.6	39.1	37.9	37.9	7.7	7.6	36.6	36.6	36.6	37.9	394.6
Task Lights	-	-	-	-	-	-	-	-	-	-	-	-	-
Area Lights	168.8	168.8	168.8	168.8	168.8	168.8	17.4	16.5	168.8	168.8	168.8	168.8	1,722.0
Total	465.1	431.9	454.7	477.4	533.3	533.5	352.7	414.4	543.0	492.4	468.9	461.6	5,629.0

Gas Demand (Btu/h x000,000)

	Jan	Feb	Mar	Apr	May	Jun	Jul	Aug	Sep	Oct	Nov	Dec	Total
Space Cool	-	-	-	-	-	-	-	-	-	-	-	-	-
Heat Reject.	-	-	-	-	-	-	-	-	-	-	-	-	-
Refrigeration	-	-	-	-	-	-	-	-	-	-	-	-	-
Space Heat	5.71	4.96	4.34	4.29	4.08	3.59	3.44	3.42	3.78	4.42	4.41	4.49	50.91
HP Supp.	-	-	-	-	-	-	-	-	-	-	-	-	-
Hot Water	0.07	0.07	0.07	0.07	0.07	0.01	0.01	0.01	0.01	0.06	0.06	0.07	0.58
Vent. Fans	-	-	-	-	-	-	-	-	-	-	-	-	-
Pumps & Aux.	-	-	-	-	-	-	-	-	-	-	-	-	-
Ext. Usage	-	-	-	-	-	-	-	-	-	-	-	-	-
Misc. Equip.	-	-	-	-	-	-	-	-	-	-	-	-	-
Task Lights	-	-	-	-	-	-	-	-	-	-	-	-	-
Area Lights	-	-	-	-	-	-	-	-	-	-	-	-	-
Total	5.78	5.03	4.41	4.36	4.15	3.59	3.45	3.43	3.79	4.47	4.47	4.55	51.49

Figure B13. Monthly Energy Demand Profile – C5-High R CMU Walls - Corbin

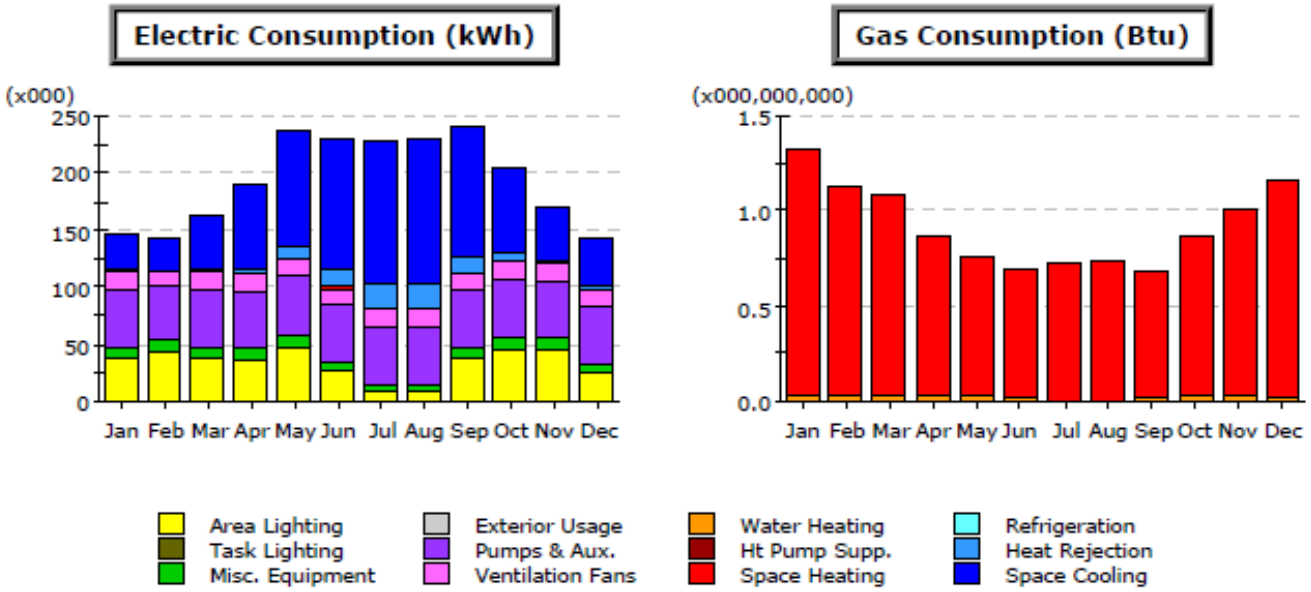

Electric Consumption (kWh x000)

	Jan	Feb	Mar	Apr	May	Jun	Jul	Aug	Sep	Oct	Nov	Dec	Total
Space Cool	32.4	28.1	46.7	74.2	100.4	114.9	126.2	126.7	113.0	75.7	46.4	42.8	927.3
Heat Reject.	0.5	0.1	1.4	4.3	11.2	16.3	21.3	21.4	15.2	5.3	1.6	1.4	99.9
Refrigeration	-	-	-	-	-	-	-	-	-	-	-	-	-
Space Heat	0.7	0.6	0.7	0.6	0.5	0.4	0.5	0.5	0.4	0.5	0.6	0.7	6.7
HP Supp.	-	-	-	-	-	-	-	-	-	-	-	-	-
Hot Water	-	-	-	-	-	-	-	-	-	-	-	-	-
Vent. Fans	15.1	13.6	15.1	14.6	15.1	14.6	15.1	15.1	14.6	15.1	14.6	15.1	177.6
Pumps & Aux.	51.9	46.9	51.9	50.2	51.9	50.2	51.9	51.9	50.2	51.9	50.2	51.9	611.0
Ext. Usage	-	-	-	-	-	-	-	-	-	-	-	-	-
Misc. Equip.	10.0	10.8	10.0	9.9	11.9	7.9	4.5	4.6	10.0	11.5	11.4	7.4	109.9
Task Lights	-	-	-	-	-	-	-	-	-	-	-	-	-
Area Lights	36.9	41.8	36.9	36.7	46.2	26.4	8.7	8.9	37.0	44.3	44.1	23.9	391.6
Total	147.5	141.9	162.6	190.4	237.1	230.7	228.1	228.9	240.5	204.3	168.9	143.1	2,324.1

Gas Consumption (Btu x000,000,000)

	Jan	Feb	Mar	Apr	May	Jun	Jul	Aug	Sep	Oct	Nov	Dec	Total
Space Cool	-	-	-	-	-	-	-	-	-	-	-	-	-
Heat Reject.	-	-	-	-	-	-	-	-	-	-	-	-	-
Refrigeration	-	-	-	-	-	-	-	-	-	-	-	-	-
Space Heat	1.30	1.09	1.06	0.84	0.73	0.67	0.72	0.74	0.66	0.85	0.98	1.15	10.79
HP Supp.	-	-	-	-	-	-	-	-	-	-	-	-	-
Hot Water	0.03	0.03	0.03	0.03	0.03	0.02	0.01	0.01	0.02	0.02	0.03	0.02	0.25
Vent. Fans	-	-	-	-	-	-	-	-	-	-	-	-	-
Pumps & Aux.	-	-	-	-	-	-	-	-	-	-	-	-	-
Ext. Usage	-	-	-	-	-	-	-	-	-	-	-	-	-
Misc. Equip.	-	-	-	-	-	-	-	-	-	-	-	-	-
Task Lights	-	-	-	-	-	-	-	-	-	-	-	-	-
Area Lights	-	-	-	-	-	-	-	-	-	-	-	-	-
Total	1.32	1.12	1.08	0.87	0.76	0.69	0.72	0.74	0.68	0.87	1.01	1.17	11.04

Figure B14. Monthly Energy Use Profile – C5-High R CMU Walls- Corbin

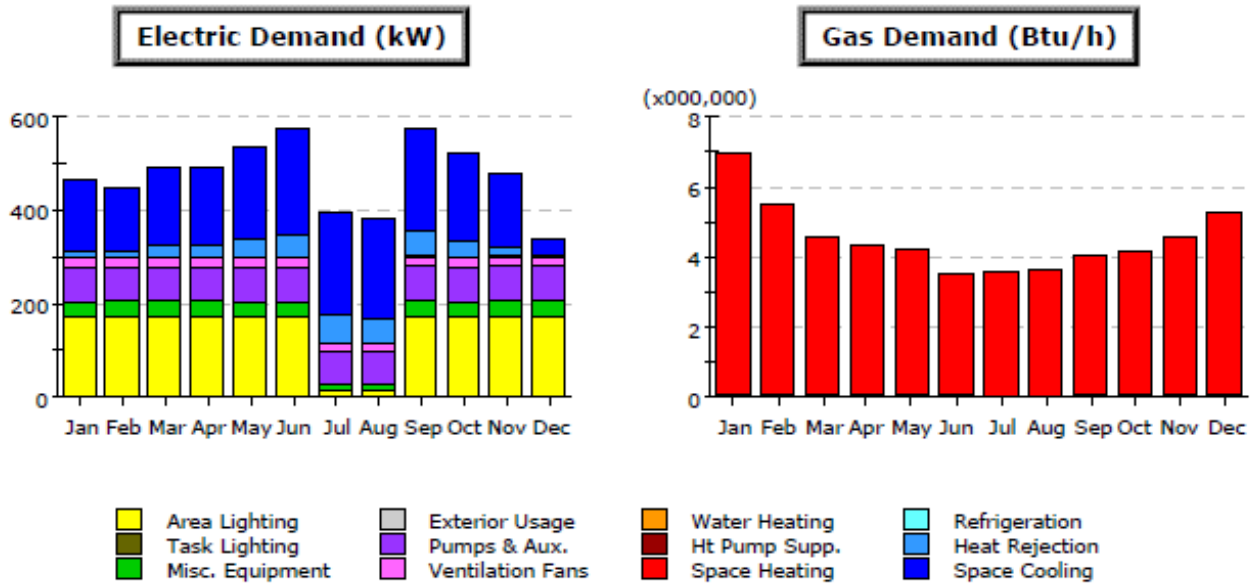

Electric Demand (kW)

	Jan	Feb	Mar	Apr	May	Jun	Jul	Aug	Sep	Oct	Nov	Dec	Total
Space Cool	152.1	140.8	165.5	166.0	199.8	225.6	223.1	213.5	220.4	185.1	155.9	36.4	2,084.1
Heat Reject.	14.0	8.9	22.2	22.3	37.1	49.6	55.3	47.0	48.5	33.0	16.2	-	354.0
Refrigeration	-	-	-	-	-	-	-	-	-	-	-	-	-
Space Heat	1.1	1.1	1.1	1.0	0.9	0.9	1.1	1.1	0.9	0.9	1.0	1.6	12.6
HP Supp.	-	-	-	-	-	-	-	-	-	-	-	-	-
Hot Water	-	-	-	-	-	-	-	-	-	-	-	-	-
Vent. Fans	20.3	20.3	20.3	20.3	20.3	20.3	20.3	20.3	20.3	20.3	20.3	20.3	243.4
Pumps & Aux.	72.5	72.5	72.5	72.5	72.5	72.5	72.5	72.5	72.5	72.5	72.5	72.5	869.6
Ext. Usage	-	-	-	-	-	-	-	-	-	-	-	-	-
Misc. Equip.	36.6	37.9	39.9	39.9	36.6	36.6	7.8	7.7	40.3	36.6	40.3	40.3	400.4
Task Lights	-	-	-	-	-	-	-	-	-	-	-	-	-
Area Lights	168.8	168.8	168.8	168.8	168.8	168.8	17.4	17.4	168.8	168.8	168.8	168.8	1,723.0
Total	465.3	450.2	490.2	490.7	536.0	574.2	397.5	379.4	571.7	517.1	474.9	339.9	5,687.0

Gas Demand (Btu/h x000,000)

	Jan	Feb	Mar	Apr	May	Jun	Jul	Aug	Sep	Oct	Nov	Dec	Total
Space Cool	-	-	-	-	-	-	-	-	-	-	-	-	-
Heat Reject.	-	-	-	-	-	-	-	-	-	-	-	-	-
Refrigeration	-	-	-	-	-	-	-	-	-	-	-	-	-
Space Heat	6.82	5.40	4.48	4.28	4.15	3.43	3.57	3.60	4.01	4.10	4.50	5.23	53.57
HP Supp.	-	-	-	-	-	-	-	-	-	-	-	-	-
Hot Water	0.07	0.08	0.08	0.08	0.07	0.07	0.01	0.01	0.06	0.06	0.06	0.07	0.71
Vent. Fans	-	-	-	-	-	-	-	-	-	-	-	-	-
Pumps & Aux.	-	-	-	-	-	-	-	-	-	-	-	-	-
Ext. Usage	-	-	-	-	-	-	-	-	-	-	-	-	-
Misc. Equip.	-	-	-	-	-	-	-	-	-	-	-	-	-
Task Lights	-	-	-	-	-	-	-	-	-	-	-	-	-
Area Lights	-	-	-	-	-	-	-	-	-	-	-	-	-
Total	6.90	5.48	4.56	4.35	4.22	3.50	3.57	3.61	4.07	4.16	4.56	5.30	54.28

Figure B15. Monthly Energy Demand Profile – C5-High R CMU Walls- Paducah

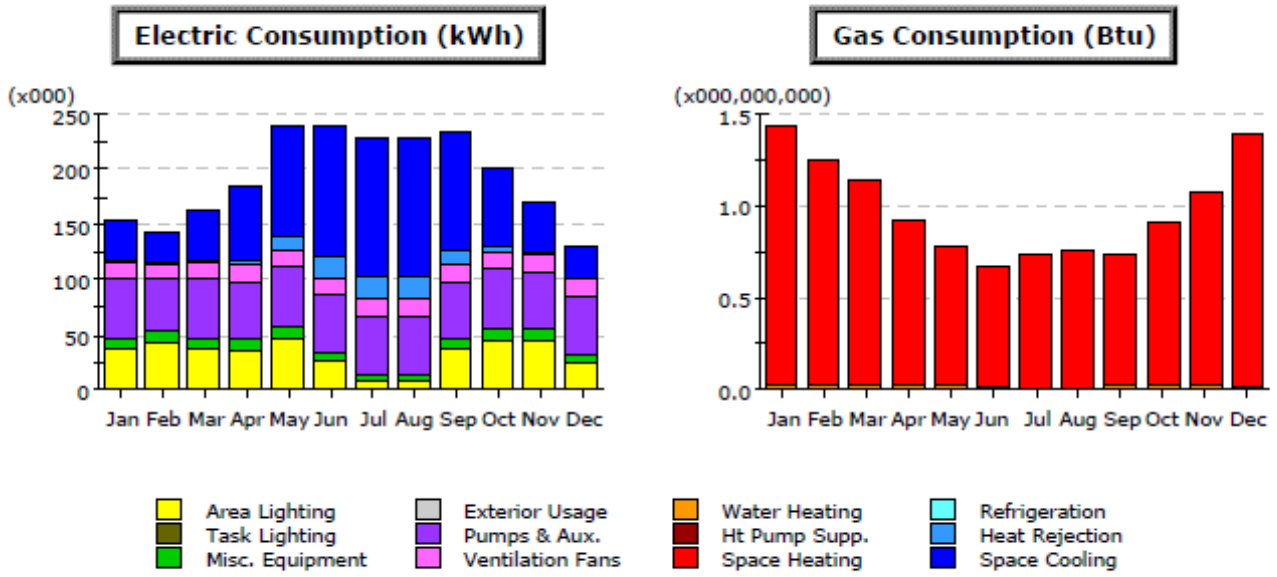

Electric Consumption (kWh x000)

	Jan	Feb	Mar	Apr	May	Jun	Jul	Aug	Sep	Oct	Nov	Dec	Total
Space Cool	37.3	26.6	44.4	67.1	100.2	119.2	126.0	126.2	106.6	69.9	44.5	28.8	897.0
Heat Reject.	0.8	0.1	1.3	3.7	10.2	18.0	19.9	19.5	13.9	5.1	1.4	0.0	93.8
Refrigeration	-	-	-	-	-	-	-	-	-	-	-	-	-
Space Heat	0.8	0.7	0.7	0.6	0.5	0.4	0.5	0.5	0.5	0.6	0.6	0.8	7.0
HP Supp.	-	-	-	-	-	-	-	-	-	-	-	-	-
Hot Water	-	-	-	-	-	-	-	-	-	-	-	-	-
Vent. Fans	15.1	13.6	15.1	14.6	15.1	14.6	15.1	15.1	14.6	15.1	14.6	15.1	177.6
Pumps & Aux.	53.9	48.7	53.9	52.2	53.9	52.2	53.9	53.9	52.2	53.9	52.2	53.9	634.8
Ext. Usage	-	-	-	-	-	-	-	-	-	-	-	-	-
Misc. Equip.	10.0	10.8	10.0	9.9	11.9	7.9	4.5	4.6	10.0	11.5	11.4	7.4	109.9
Task Lights	-	-	-	-	-	-	-	-	-	-	-	-	-
Area Lights	36.9	41.8	36.9	36.7	46.2	26.4	8.7	8.9	37.0	44.3	44.1	23.9	391.6
Total	154.9	142.2	162.3	184.7	237.9	238.8	228.5	228.6	234.8	200.4	168.8	130.0	2,311.8

Gas Consumption (Btu x000,000,000)

	Jan	Feb	Mar	Apr	May	Jun	Jul	Aug	Sep	Oct	Nov	Dec	Total
Space Cool	-	-	-	-	-	-	-	-	-	-	-	-	-
Heat Reject.	-	-	-	-	-	-	-	-	-	-	-	-	-
Refrigeration	-	-	-	-	-	-	-	-	-	-	-	-	-
Space Heat	1.41	1.21	1.11	0.90	0.75	0.65	0.73	0.76	0.71	0.88	1.04	1.38	11.53
HP Supp.	-	-	-	-	-	-	-	-	-	-	-	-	-
Hot Water	0.03	0.03	0.03	0.03	0.03	0.02	0.01	0.01	0.02	0.03	0.03	0.02	0.26
Vent. Fans	-	-	-	-	-	-	-	-	-	-	-	-	-
Pumps & Aux.	-	-	-	-	-	-	-	-	-	-	-	-	-
Ext. Usage	-	-	-	-	-	-	-	-	-	-	-	-	-
Misc. Equip.	-	-	-	-	-	-	-	-	-	-	-	-	-
Task Lights	-	-	-	-	-	-	-	-	-	-	-	-	-
Area Lights	-	-	-	-	-	-	-	-	-	-	-	-	-
Total	1.43	1.24	1.14	0.92	0.78	0.67	0.74	0.77	0.73	0.91	1.07	1.40	11.79

Figure B16. Monthly Energy Use Profile – C5-High R CMU Walls- Paducah

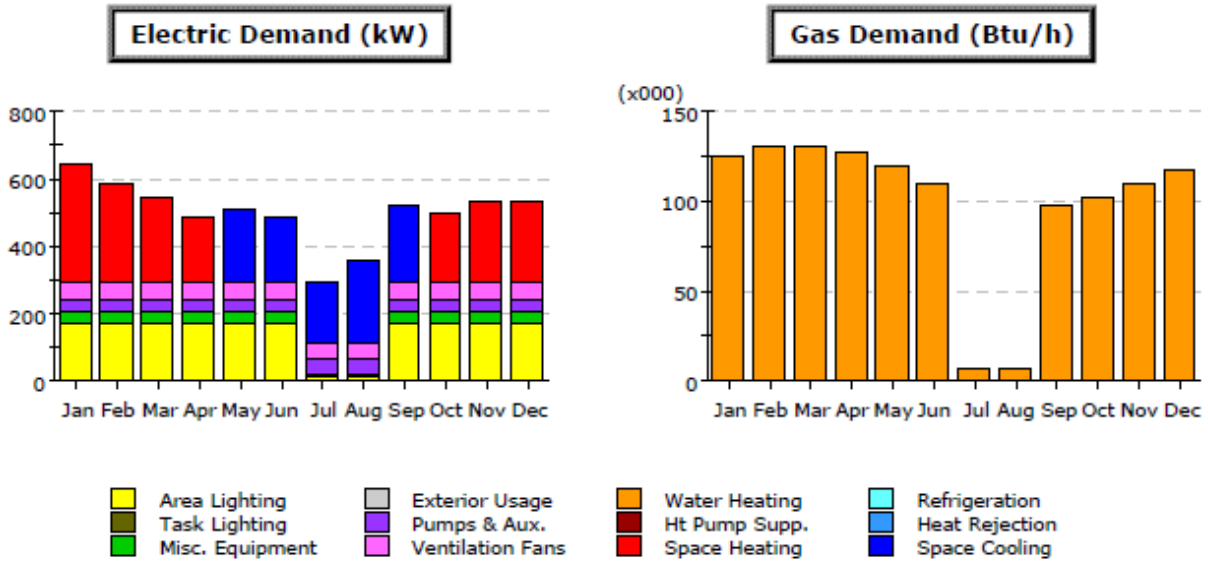

Electric Demand (kW)

	Jan	Feb	Mar	Apr	May	Jun	Jul	Aug	Sep	Oct	Nov	Dec	Total
Space Cool	-	-	-	-	213.3	190.7	178.4	240.7	230.6	-	-	-	1,053.7
Heat Reject.	-	-	-	-	-	-	-	-	-	-	-	-	-
Refrigeration	-	-	-	-	-	-	-	-	-	-	-	-	-
Space Heat	347.1	294.1	249.8	190.2	-	-	-	-	-	205.6	241.6	242.4	1,770.8
HP Supp.	-	-	-	-	-	-	-	-	-	-	-	-	-
Hot Water	-	-	-	-	-	-	-	-	-	-	-	-	-
Vent. Fans	49.4	49.4	49.4	49.4	49.4	49.4	49.4	49.4	49.4	49.4	49.4	49.4	592.2
Pumps & Aux.	38.9	38.9	38.9	38.9	38.9	38.9	38.9	38.9	38.9	38.9	38.9	38.9	467.1
Ext. Usage	-	-	-	-	-	-	-	-	-	-	-	-	-
Misc. Equip.	36.0	36.0	36.0	36.0	36.6	36.6	7.7	7.7	36.6	36.0	36.0	36.0	377.4
Task Lights	-	-	-	-	-	-	-	-	-	-	-	-	-
Area Lights	168.8	168.8	168.8	168.8	168.8	168.8	17.3	17.3	168.8	168.8	168.8	168.8	1,722.8
Total	640.3	587.3	542.9	483.3	507.0	484.4	291.6	354.0	524.3	498.7	534.8	535.5	5,984.0

Gas Demand (Btu/h x000)

	Jan	Feb	Mar	Apr	May	Jun	Jul	Aug	Sep	Oct	Nov	Dec	Total
Space Cool	-	-	-	-	-	-	-	-	-	-	-	-	-
Heat Reject.	-	-	-	-	-	-	-	-	-	-	-	-	-
Refrigeration	-	-	-	-	-	-	-	-	-	-	-	-	-
Space Heat	-	-	-	-	-	-	-	-	-	-	-	-	-
HP Supp.	-	-	-	-	-	-	-	-	-	-	-	-	-
Hot Water	125.1	129.3	129.5	127.3	118.9	110.3	6.6	6.5	98.3	102.4	109.5	117.5	1,181.4
Vent. Fans	-	-	-	-	-	-	-	-	-	-	-	-	-
Pumps & Aux.	-	-	-	-	-	-	-	-	-	-	-	-	-
Ext. Usage	-	-	-	-	-	-	-	-	-	-	-	-	-
Misc. Equip.	-	-	-	-	-	-	-	-	-	-	-	-	-
Task Lights	-	-	-	-	-	-	-	-	-	-	-	-	-
Area Lights	-	-	-	-	-	-	-	-	-	-	-	-	-
Total	125.1	129.3	129.5	127.3	118.9	110.3	6.6	6.5	98.3	102.4	109.5	117.5	1,181.4

Figure B 17. Monthly Energy Demand Profile – GM17-Baseline GSHP- Corbin

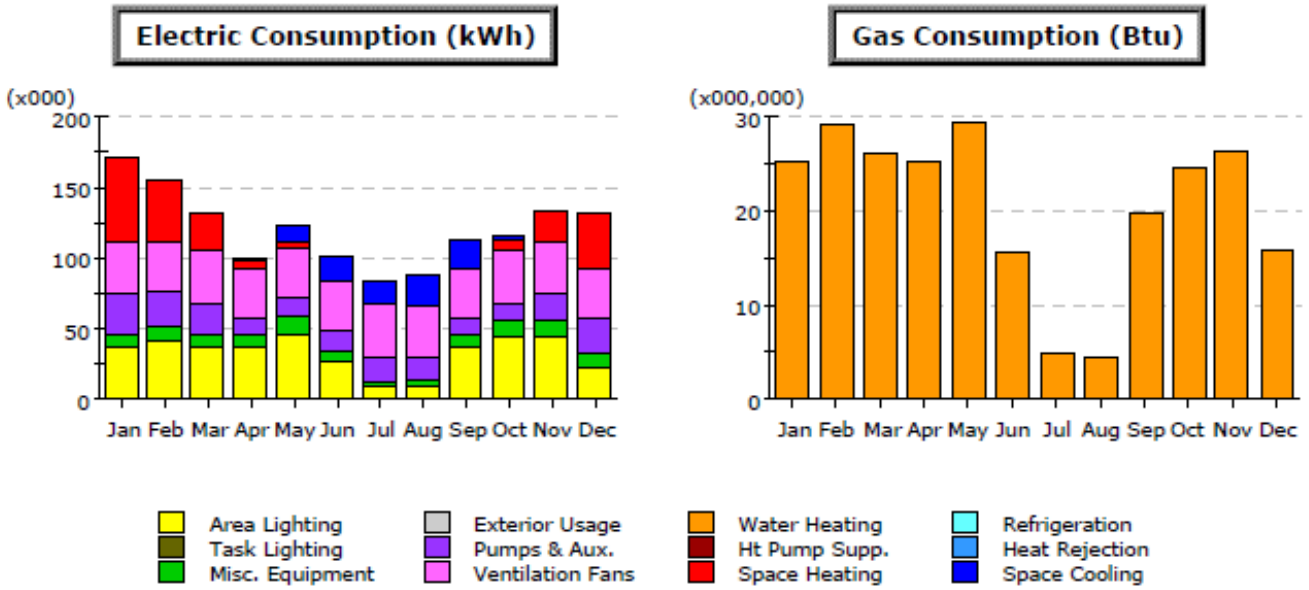

Electric Consumption (kWh x000)

	Jan	Feb	Mar	Apr	May	Jun	Jul	Aug	Sep	Oct	Nov	Dec	Total
Space Cool	0.1	-	0.0	1.3	12.5	17.5	17.5	21.4	19.3	3.8	0.7	0.2	94.3
Heat Reject.	-	-	-	-	-	-	-	-	-	-	-	-	-
Refrigeration	-	-	-	-	-	-	-	-	-	-	-	-	-
Space Heat	60.4	45.7	26.7	5.4	3.0	0.0	-	-	0.3	7.8	22.9	39.4	211.6
HP Supp.	-	-	-	-	-	-	-	-	-	-	-	-	-
Hot Water	-	-	-	-	-	-	-	-	-	-	-	-	-
Vent. Fans	36.7	33.2	36.7	35.5	36.7	35.5	36.7	36.7	35.5	36.7	35.5	36.7	432.3
Pumps & Aux.	27.5	24.4	21.3	11.2	12.9	14.1	17.3	16.2	10.4	12.6	20.3	24.9	213.1
Ext. Usage	-	-	-	-	-	-	-	-	-	-	-	-	-
Misc. Equip.	10.0	10.8	10.0	9.9	11.9	7.9	4.5	4.6	10.0	11.5	11.4	7.4	109.9
Task Lights	-	-	-	-	-	-	-	-	-	-	-	-	-
Area Lights	36.9	41.8	36.9	36.7	46.2	26.4	8.7	8.9	37.0	44.3	44.1	23.9	391.6
Total	171.6	155.8	131.7	100.1	123.1	101.5	84.6	87.7	112.5	116.8	134.8	132.5	1,452.8

Gas Consumption (Btu x000,000)

	Jan	Feb	Mar	Apr	May	Jun	Jul	Aug	Sep	Oct	Nov	Dec	Total
Space Cool	-	-	-	-	-	-	-	-	-	-	-	-	-
Heat Reject.	-	-	-	-	-	-	-	-	-	-	-	-	-
Refrigeration	-	-	-	-	-	-	-	-	-	-	-	-	-
Space Heat	-	-	-	-	-	-	-	-	-	-	-	-	-
HP Supp.	-	-	-	-	-	-	-	-	-	-	-	-	-
Hot Water	25.22	29.15	25.96	25.22	29.46	15.48	4.73	4.64	19.73	24.74	26.28	15.90	246.51
Vent. Fans	-	-	-	-	-	-	-	-	-	-	-	-	-
Pumps & Aux.	-	-	-	-	-	-	-	-	-	-	-	-	-
Ext. Usage	-	-	-	-	-	-	-	-	-	-	-	-	-
Misc. Equip.	-	-	-	-	-	-	-	-	-	-	-	-	-
Task Lights	-	-	-	-	-	-	-	-	-	-	-	-	-
Area Lights	-	-	-	-	-	-	-	-	-	-	-	-	-
Total	25.22	29.15	25.96	25.22	29.46	15.48	4.73	4.64	19.73	24.74	26.28	15.90	246.51

Figure B18. Monthly Energy Use Profile-GM17-Baseline GSHP - Corbin

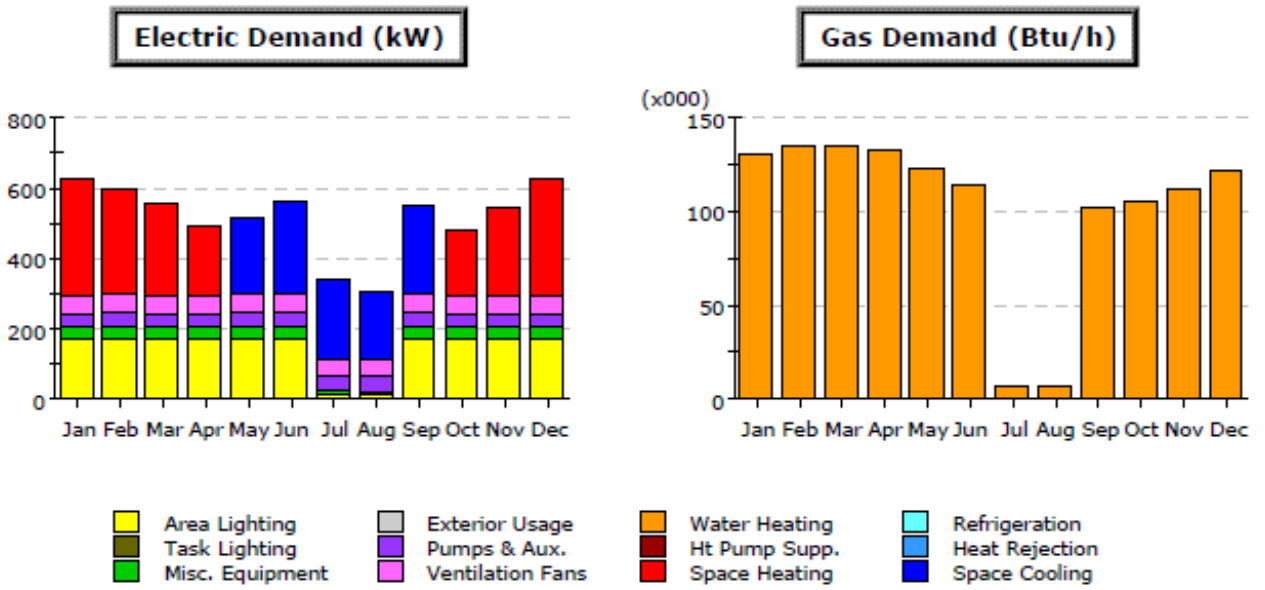

Electric Demand (kW)

	Jan	Feb	Mar	Apr	May	Jun	Jul	Aug	Sep	Oct	Nov	Dec	Total
Space Cool	-	-	-	-	218.6	263.5	225.5	188.7	255.5	-	-	-	1,151.8
Heat Reject.	-	-	-	-	-	-	-	-	-	-	-	-	-
Refrigeration	-	-	-	-	-	-	-	-	-	-	-	-	-
Space Heat	335.7	303.2	261.3	194.6	-	-	-	-	-	180.3	246.7	332.7	1,854.4
HP Supp.	-	-	-	-	-	-	-	-	-	-	-	-	-
Hot Water	-	-	-	-	-	-	-	-	-	-	-	-	-
Vent. Fans	49.6	49.6	49.6	49.6	49.6	49.6	49.6	49.6	49.6	49.6	49.6	49.6	595.2
Pumps & Aux.	41.4	41.4	41.4	41.4	41.4	41.4	41.4	41.4	41.4	41.4	41.4	41.4	497.1
Ext. Usage	-	-	-	-	-	-	-	-	-	-	-	-	-
Misc. Equip.	36.0	36.9	36.0	36.0	36.6	40.3	7.8	7.7	36.6	36.0	36.0	36.0	382.1
Task Lights	-	-	-	-	-	-	-	-	-	-	-	-	-
Area Lights	168.8	168.8	168.8	168.8	168.8	168.8	17.4	17.3	168.8	168.8	168.8	168.8	1,722.9
Total	631.6	599.9	557.2	490.5	515.1	563.6	341.7	304.8	551.9	476.1	542.5	628.6	6,203.5

Gas Demand (Btu/h x000)

	Jan	Feb	Mar	Apr	May	Jun	Jul	Aug	Sep	Oct	Nov	Dec	Total
Space Cool	-	-	-	-	-	-	-	-	-	-	-	-	-
Heat Reject.	-	-	-	-	-	-	-	-	-	-	-	-	-
Refrigeration	-	-	-	-	-	-	-	-	-	-	-	-	-
Space Heat	-	-	-	-	-	-	-	-	-	-	-	-	-
HP Supp.	-	-	-	-	-	-	-	-	-	-	-	-	-
Hot Water	130.5	134.8	134.9	132.5	123.4	114.1	6.8	6.7	101.2	105.4	113.1	122.0	1,225.4
Vent. Fans	-	-	-	-	-	-	-	-	-	-	-	-	-
Pumps & Aux.	-	-	-	-	-	-	-	-	-	-	-	-	-
Ext. Usage	-	-	-	-	-	-	-	-	-	-	-	-	-
Misc. Equip.	-	-	-	-	-	-	-	-	-	-	-	-	-
Task Lights	-	-	-	-	-	-	-	-	-	-	-	-	-
Area Lights	-	-	-	-	-	-	-	-	-	-	-	-	-
Total	130.5	134.8	134.9	132.5	123.4	114.1	6.8	6.7	101.2	105.4	113.1	122.0	1,225.4

Figure B19. Monthly Energy Demand Profile – GM17-Baseline GSHP - Paducah

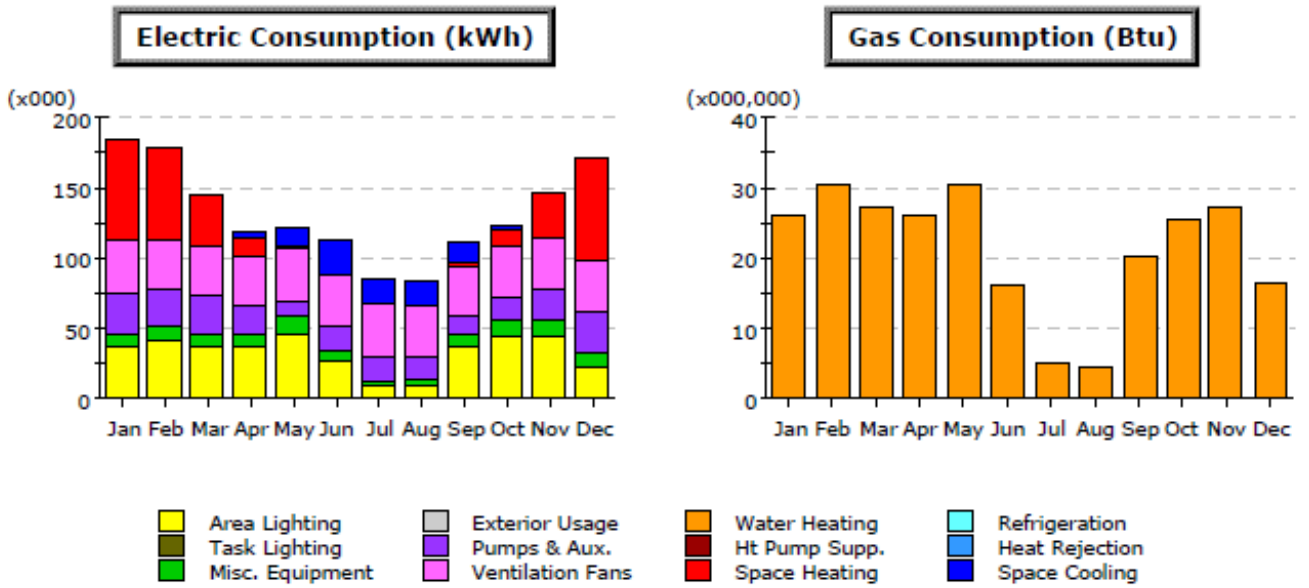

Electric Consumption (kWh x000)

	Jan	Feb	Mar	Apr	May	Jun	Jul	Aug	Sep	Oct	Nov	Dec	Total
Space Cool	-	0.0	0.0	3.3	11.8	25.9	17.4	18.0	13.7	3.4	0.4	-	94.0
Heat Reject.	-	-	-	-	-	-	-	-	-	-	-	-	-
Refrigeration	-	-	-	-	-	-	-	-	-	-	-	-	-
Space Heat	70.3	65.4	34.7	13.8	2.1	0.0	-	0.0	1.6	10.9	31.2	71.7	301.8
HP Supp.	-	-	-	-	-	-	-	-	-	-	-	-	-
Hot Water	-	-	-	-	-	-	-	-	-	-	-	-	-
Vent. Fans	36.9	33.3	36.9	35.7	36.9	35.7	36.9	36.9	35.7	36.9	35.7	36.9	434.5
Pumps & Aux.	28.9	26.9	25.6	18.9	11.7	16.7	17.6	16.4	12.0	16.2	23.2	30.7	244.7
Ext. Usage	-	-	-	-	-	-	-	-	-	-	-	-	-
Misc. Equip.	10.0	10.8	10.0	9.9	11.9	7.9	4.5	4.6	10.0	11.5	11.4	7.4	109.9
Task Lights	-	-	-	-	-	-	-	-	-	-	-	-	-
Area Lights	36.9	41.8	36.9	36.7	46.2	26.4	8.7	8.9	37.0	44.3	44.1	23.9	391.6
Total	183.1	178.1	144.2	118.3	120.6	112.6	85.1	84.7	110.0	123.2	145.9	170.6	1,576.5

Gas Consumption (Btu x000,000)

	Jan	Feb	Mar	Apr	May	Jun	Jul	Aug	Sep	Oct	Nov	Dec	Total
Space Cool	-	-	-	-	-	-	-	-	-	-	-	-	-
Heat Reject.	-	-	-	-	-	-	-	-	-	-	-	-	-
Refrigeration	-	-	-	-	-	-	-	-	-	-	-	-	-
Space Heat	-	-	-	-	-	-	-	-	-	-	-	-	-
HP Supp.	-	-	-	-	-	-	-	-	-	-	-	-	-
Hot Water	26.17	30.34	26.98	26.23	30.52	15.93	4.83	4.73	20.28	25.43	27.11	16.50	255.05
Vent. Fans	-	-	-	-	-	-	-	-	-	-	-	-	-
Pumps & Aux.	-	-	-	-	-	-	-	-	-	-	-	-	-
Ext. Usage	-	-	-	-	-	-	-	-	-	-	-	-	-
Misc. Equip.	-	-	-	-	-	-	-	-	-	-	-	-	-
Task Lights	-	-	-	-	-	-	-	-	-	-	-	-	-
Area Lights	-	-	-	-	-	-	-	-	-	-	-	-	-
Total	26.17	30.34	26.98	26.23	30.52	15.93	4.83	4.73	20.28	25.43	27.11	16.50	255.05

Figure B20. Monthly Energy Use Profile – GM17-Baseline GSHP - Paducah

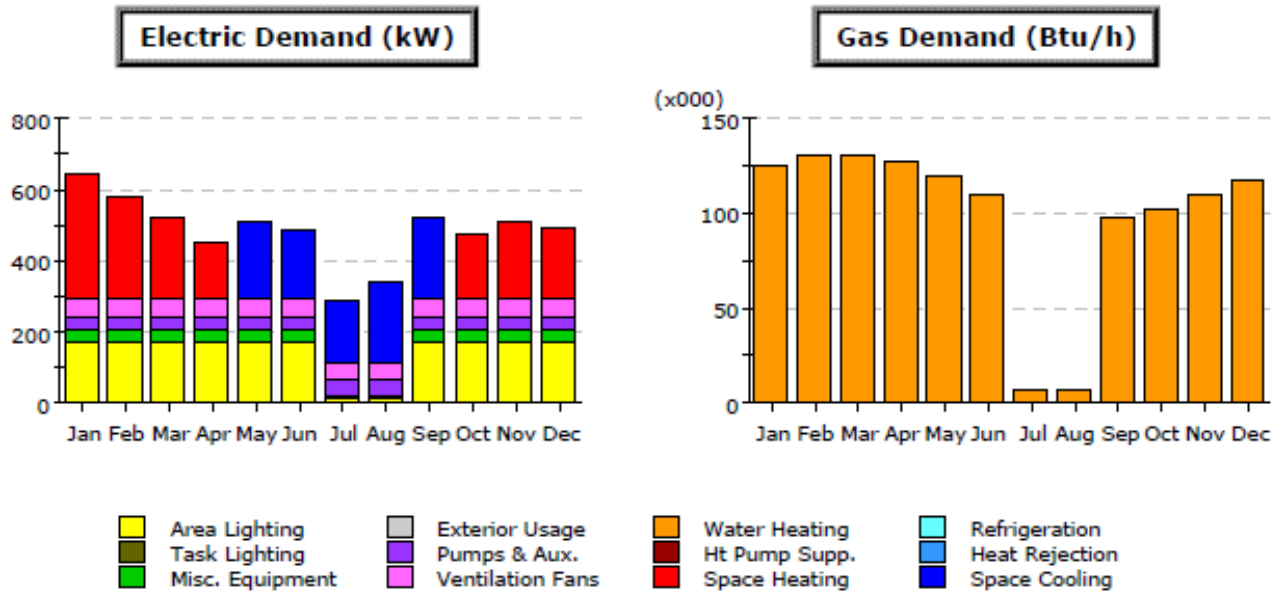

Electric Demand (kW)

	Jan	Feb	Mar	Apr	May	Jun	Jul	Aug	Sep	Oct	Nov	Dec	Total
Space Cool	-	-	-	-	215.9	193.6	171.0	232.9	230.3	-	-	-	1,043.7
Heat Reject.	-	-	-	-	-	-	-	-	-	-	-	-	-
Refrigeration	-	-	-	-	-	-	-	-	-	-	-	-	-
Space Heat	350.3	284.2	230.8	157.7	-	-	-	-	-	177.3	215.9	200.6	1,616.7
HP Supp.	-	-	-	-	-	-	-	-	-	-	-	-	-
Hot Water	-	-	-	-	-	-	-	-	-	-	-	-	-
Vent. Fans	49.4	49.4	49.4	49.4	49.4	49.4	49.4	49.4	49.4	49.4	49.4	49.4	592.2
Pumps & Aux.	38.9	38.9	38.9	38.9	38.9	38.9	38.9	38.9	38.9	38.9	38.9	38.9	467.1
Ext. Usage	-	-	-	-	-	-	-	-	-	-	-	-	-
Misc. Equip.	36.0	36.0	36.0	36.0	36.6	36.6	7.7	7.7	36.6	36.0	36.0	36.0	377.4
Task Lights	-	-	-	-	-	-	-	-	-	-	-	-	-
Area Lights	168.8	168.8	168.8	168.8	168.8	168.8	17.3	17.3	168.8	168.8	168.8	168.8	1,722.8
Total	643.4	577.3	523.9	450.8	509.6	487.3	284.3	346.2	524.0	470.5	509.1	493.7	5,820.0

Gas Demand (Btu/h x000)

	Jan	Feb	Mar	Apr	May	Jun	Jul	Aug	Sep	Oct	Nov	Dec	Total
Space Cool	-	-	-	-	-	-	-	-	-	-	-	-	-
Heat Reject.	-	-	-	-	-	-	-	-	-	-	-	-	-
Refrigeration	-	-	-	-	-	-	-	-	-	-	-	-	-
Space Heat	-	-	-	-	-	-	-	-	-	-	-	-	-
HP Supp.	-	-	-	-	-	-	-	-	-	-	-	-	-
Hot Water	125.1	129.3	129.5	127.3	118.9	110.3	6.6	6.5	98.3	102.4	109.5	117.5	1,181.4
Vent. Fans	-	-	-	-	-	-	-	-	-	-	-	-	-
Pumps & Aux.	-	-	-	-	-	-	-	-	-	-	-	-	-
Ext. Usage	-	-	-	-	-	-	-	-	-	-	-	-	-
Misc. Equip.	-	-	-	-	-	-	-	-	-	-	-	-	-
Task Lights	-	-	-	-	-	-	-	-	-	-	-	-	-
Area Lights	-	-	-	-	-	-	-	-	-	-	-	-	-
Total	125.1	129.3	129.5	127.3	118.9	110.3	6.6	6.5	98.3	102.4	109.5	117.5	1,181.4

Figure B21. Monthly Energy Demand Profile –GM20-GSHP Modified Fans-Corbin

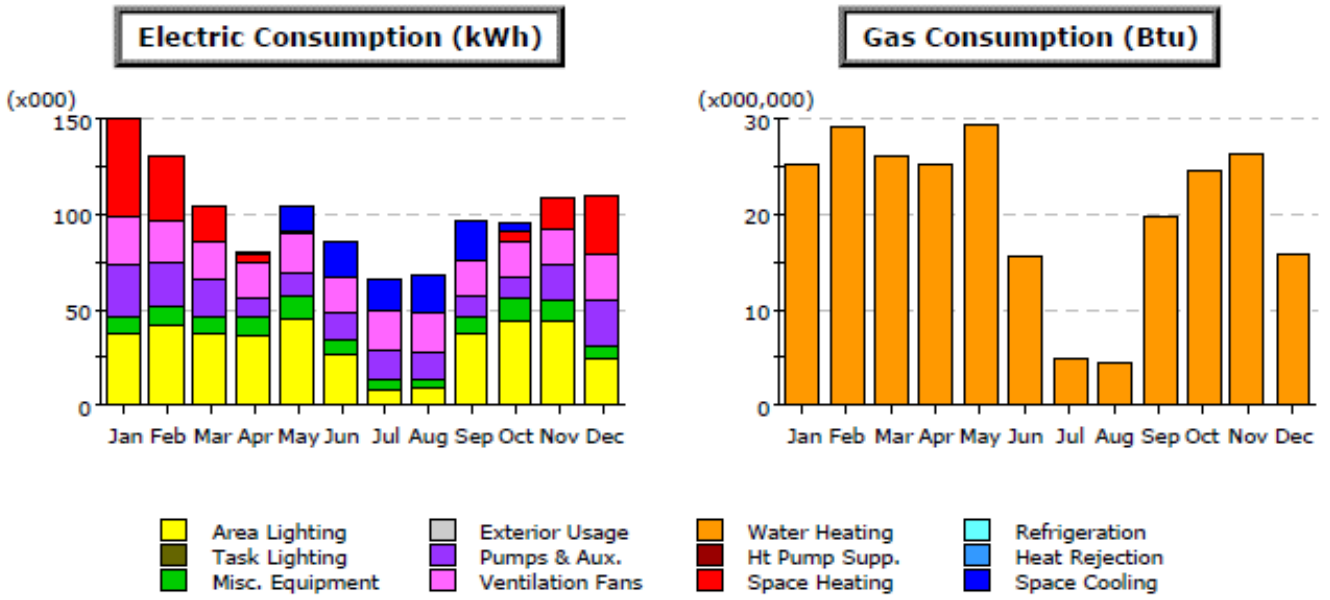

Electric Consumption (kWh x000)

	Jan	Feb	Mar	Apr	May	Jun	Jul	Aug	Sep	Oct	Nov	Dec	Total
Space Cool	0.1	-	0.0	1.6	13.3	17.8	16.5	20.0	19.8	4.4	0.8	0.3	94.5
Heat Reject.	-	-	-	-	-	-	-	-	-	-	-	-	-
Refrigeration	-	-	-	-	-	-	-	-	-	-	-	-	-
Space Heat	50.0	34.0	18.8	3.9	2.1	0.0	0.0	0.0	0.2	4.9	15.1	31.1	160.0
HP Supp.	-	-	-	-	-	-	-	-	-	-	-	-	-
Hot Water	-	-	-	-	-	-	-	-	-	-	-	-	-
Vent. Fans	25.3	20.3	20.8	19.3	19.9	19.3	19.9	19.9	19.3	20.0	19.7	24.2	247.7
Pumps & Aux.	27.2	23.1	18.6	9.2	11.7	13.7	16.2	15.3	10.1	10.6	17.9	23.5	197.1
Ext. Usage	-	-	-	-	-	-	-	-	-	-	-	-	-
Misc. Equip.	10.0	10.8	10.0	9.9	11.9	7.9	4.5	4.6	10.0	11.5	11.4	7.4	109.9
Task Lights	-	-	-	-	-	-	-	-	-	-	-	-	-
Area Lights	36.9	41.8	36.9	36.7	46.2	26.4	8.7	8.9	37.0	44.3	44.1	23.9	391.6
Total	149.5	129.8	105.1	80.5	105.0	85.1	65.7	68.7	96.4	95.7	109.0	110.4	1,200.8

Gas Consumption (Btu x000,000)

	Jan	Feb	Mar	Apr	May	Jun	Jul	Aug	Sep	Oct	Nov	Dec	Total
Space Cool	-	-	-	-	-	-	-	-	-	-	-	-	-
Heat Reject.	-	-	-	-	-	-	-	-	-	-	-	-	-
Refrigeration	-	-	-	-	-	-	-	-	-	-	-	-	-
Space Heat	-	-	-	-	-	-	-	-	-	-	-	-	-
HP Supp.	-	-	-	-	-	-	-	-	-	-	-	-	-
Hot Water	25.22	29.15	25.96	25.21	29.46	15.49	4.74	4.66	19.74	24.73	26.27	15.91	246.54
Vent. Fans	-	-	-	-	-	-	-	-	-	-	-	-	-
Pumps & Aux.	-	-	-	-	-	-	-	-	-	-	-	-	-
Ext. Usage	-	-	-	-	-	-	-	-	-	-	-	-	-
Misc. Equip.	-	-	-	-	-	-	-	-	-	-	-	-	-
Task Lights	-	-	-	-	-	-	-	-	-	-	-	-	-
Area Lights	-	-	-	-	-	-	-	-	-	-	-	-	-
Total	25.22	29.15	25.96	25.21	29.46	15.49	4.74	4.66	19.74	24.73	26.27	15.91	246.54

Figure B22. Monthly Energy Use Profile – GM20-GSHP Modified Fans- Corbin

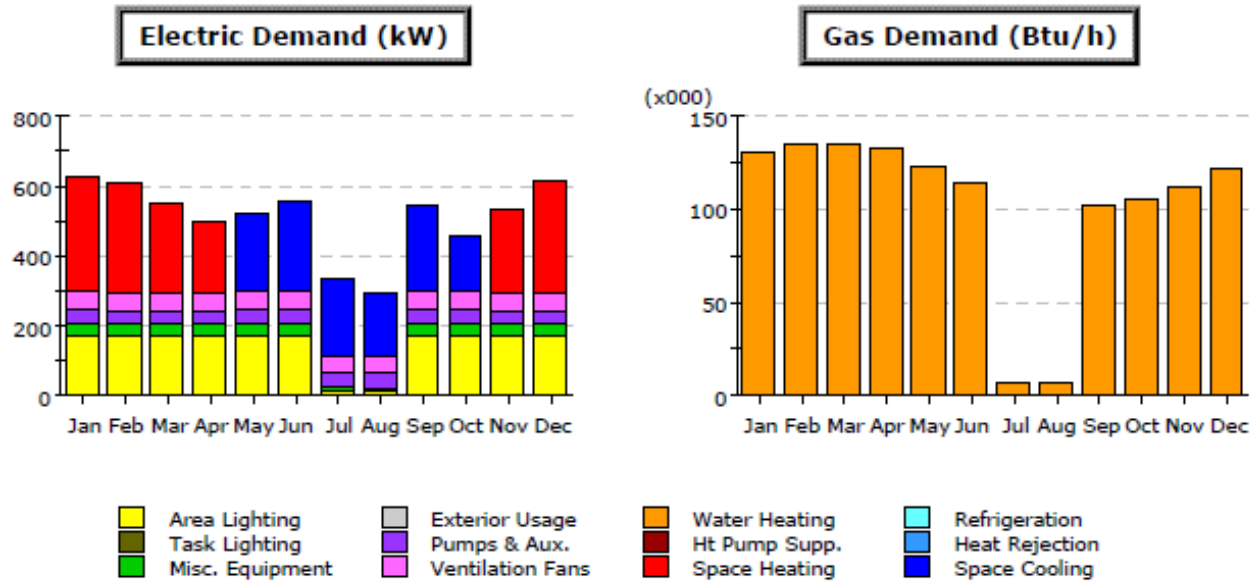

Electric Demand (kW)

	Jan	Feb	Mar	Apr	May	Jun	Jul	Aug	Sep	Oct	Nov	Dec	Total
Space Cool	-	-	-	-	224.4	259.7	217.7	178.5	247.6	155.5	-	-	1,283.4
Heat Reject.	-	-	-	-	-	-	-	-	-	-	-	-	-
Refrigeration	-	-	-	-	-	-	-	-	-	-	-	-	-
Space Heat	335.4	313.1	250.9	204.0	-	-	-	-	-	-	241.4	315.1	1,659.9
HP Supp.	-	-	-	-	-	-	-	-	-	-	-	-	-
Hot Water	-	-	-	-	-	-	-	-	-	-	-	-	-
Vent. Fans	49.6	49.6	49.6	49.6	49.6	49.6	49.6	49.6	49.6	49.6	49.6	49.6	595.2
Pumps & Aux.	41.4	41.4	41.4	41.4	41.4	41.4	41.4	41.4	41.4	41.4	41.4	41.4	497.1
Ext. Usage	-	-	-	-	-	-	-	-	-	-	-	-	-
Misc. Equip.	36.9	36.0	36.0	36.0	36.6	40.3	7.8	7.7	36.6	40.3	36.0	36.0	386.3
Task Lights	-	-	-	-	-	-	-	-	-	-	-	-	-
Area Lights	168.8	168.8	168.8	168.8	168.8	168.8	17.4	17.3	168.8	168.8	168.8	168.8	1,722.9
Total	632.1	609.0	546.8	499.9	520.9	559.8	333.9	294.5	544.0	455.6	537.2	611.0	6,144.7

Gas Demand (Btu/h x000)

	Jan	Feb	Mar	Apr	May	Jun	Jul	Aug	Sep	Oct	Nov	Dec	Total
Space Cool	-	-	-	-	-	-	-	-	-	-	-	-	-
Heat Reject.	-	-	-	-	-	-	-	-	-	-	-	-	-
Refrigeration	-	-	-	-	-	-	-	-	-	-	-	-	-
Space Heat	-	-	-	-	-	-	-	-	-	-	-	-	-
HP Supp.	-	-	-	-	-	-	-	-	-	-	-	-	-
Hot Water	130.5	134.8	134.9	132.5	123.4	114.1	6.8	6.6	101.2	105.4	113.1	122.0	1,225.2
Vent. Fans	-	-	-	-	-	-	-	-	-	-	-	-	-
Pumps & Aux.	-	-	-	-	-	-	-	-	-	-	-	-	-
Ext. Usage	-	-	-	-	-	-	-	-	-	-	-	-	-
Misc. Equip.	-	-	-	-	-	-	-	-	-	-	-	-	-
Task Lights	-	-	-	-	-	-	-	-	-	-	-	-	-
Area Lights	-	-	-	-	-	-	-	-	-	-	-	-	-
Total	130.5	134.8	134.9	132.5	123.4	114.1	6.8	6.6	101.2	105.4	113.1	122.0	1,225.2

Figure B23. Monthly Energy Demand Profile – GM20-GSHP Modified Fans-Paducah

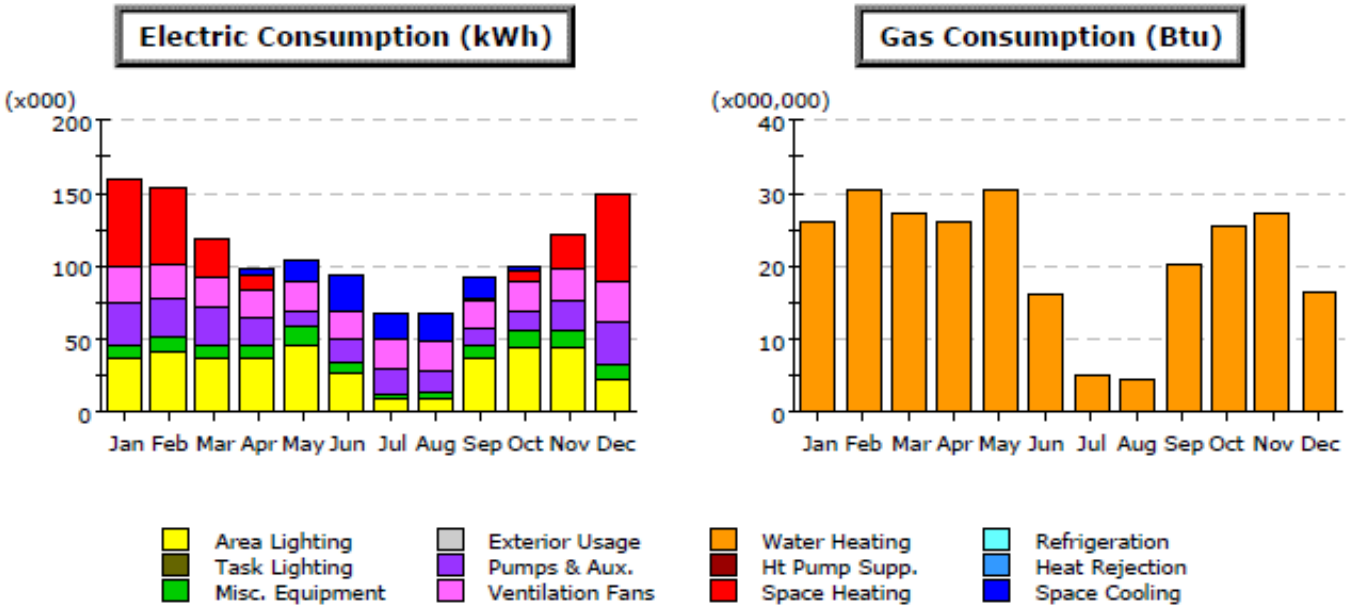

Electric Consumption (kWh x000)

	Jan	Feb	Mar	Apr	May	Jun	Jul	Aug	Sep	Oct	Nov	Dec	Total
Space Cool	-	0.0	0.0	3.8	13.3	25.9	17.3	18.0	14.7	4.0	0.5	-	97
Heat Reject.	-	-	-	-	-	-	-	-	-	-	-	-	
Refrigeration	-	-	-	-	-	-	-	-	-	-	-	-	
Space Heat	58.3	52.4	25.3	9.8	1.2	0.0	0.0	0.0	0.9	6.3	22.1	60.5	236
HP Supp.	-	-	-	-	-	-	-	-	-	-	-	-	
Hot Water	-	-	-	-	-	-	-	-	-	-	-	-	
Vent. Fans	25.5	22.6	22.5	20.2	20.0	19.4	20.0	20.0	19.4	20.2	20.8	27.7	258
Pumps & Aux.	28.2	26.8	23.8	17.4	10.9	15.9	16.8	15.6	10.7	13.4	22.1	30.6	232
Ext. Usage	-	-	-	-	-	-	-	-	-	-	-	-	
Misc. Equip.	10.0	10.8	10.0	9.9	11.9	7.9	4.5	4.6	10.0	11.5	11.4	7.4	109
Task Lights	-	-	-	-	-	-	-	-	-	-	-	-	
Area Lights	36.9	41.8	36.9	36.7	46.2	26.4	8.7	8.9	37.0	44.3	44.1	23.9	391
Total	158.9	154.3	118.6	97.8	103.4	95.5	67.3	67.0	92.7	99.7	121.0	150.2	1,326

Gas Consumption (Btu x000,000)

	Jan	Feb	Mar	Apr	May	Jun	Jul	Aug	Sep	Oct	Nov	Dec	Total
Space Cool	-	-	-	-	-	-	-	-	-	-	-	-	
Heat Reject.	-	-	-	-	-	-	-	-	-	-	-	-	
Refrigeration	-	-	-	-	-	-	-	-	-	-	-	-	
Space Heat	-	-	-	-	-	-	-	-	-	-	-	-	
HP Supp.	-	-	-	-	-	-	-	-	-	-	-	-	
Hot Water	26.17	30.34	26.98	26.23	30.51	15.93	4.83	4.74	20.28	25.42	27.11	16.50	255.
Vent. Fans	-	-	-	-	-	-	-	-	-	-	-	-	
Pumps & Aux.	-	-	-	-	-	-	-	-	-	-	-	-	
Ext. Usage	-	-	-	-	-	-	-	-	-	-	-	-	
Misc. Equip.	-	-	-	-	-	-	-	-	-	-	-	-	
Task Lights	-	-	-	-	-	-	-	-	-	-	-	-	
Area Lights	-	-	-	-	-	-	-	-	-	-	-	-	
Total	26.17	30.34	26.98	26.23	30.51	15.93	4.83	4.74	20.28	25.42	27.11	16.50	255.

Figure B24. Monthly Energy Use Profile – GM20-GSHP Modified Fans- Paducah

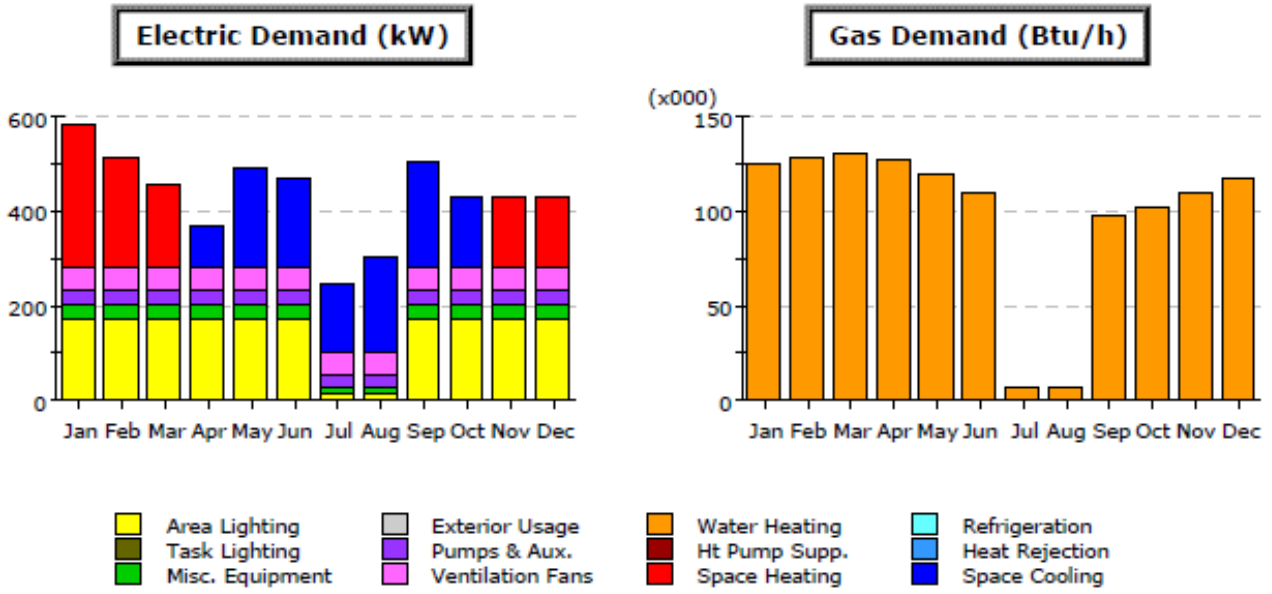

Electric Demand (kW)

	Jan	Feb	Mar	Apr	May	Jun	Jul	Aug	Sep	Oct	Nov	Dec	Total
Space Cool	-	-	-	84.7	208.3	187.3	146.1	202.0	217.6	142.8	-	-	1,188.9
Heat Reject.	-	-	-	-	-	-	-	-	-	-	-	-	-
Refrigeration	-	-	-	-	-	-	-	-	-	-	-	-	-
Space Heat	301.9	232.0	172.8	-	-	-	-	-	-	-	145.2	146.3	998.3
HP Supp.	-	-	-	-	-	-	-	-	-	-	-	-	-
Hot Water	-	-	-	-	-	-	-	-	-	-	-	-	-
Vent. Fans	49.2	49.2	49.2	49.2	49.2	49.2	49.2	49.2	49.2	49.2	49.2	49.2	590.5
Pumps & Aux.	28.8	28.8	28.8	28.8	28.8	28.8	28.8	28.8	28.8	28.8	28.8	28.8	345.6
Ext. Usage	-	-	-	-	-	-	-	-	-	-	-	-	-
Misc. Equip.	36.0	36.0	36.0	36.6	36.6	36.6	7.7	7.7	36.6	36.6	36.0	36.0	378.6
Task Lights	-	-	-	-	-	-	-	-	-	-	-	-	-
Area Lights	168.8	168.8	168.8	168.8	168.8	168.8	17.3	17.3	168.8	168.8	168.8	168.8	1,722.8
Total	584.8	514.9	455.6	368.2	491.8	470.7	249.1	305.0	501.1	426.2	428.1	429.2	5,224.5

Gas Demand (Btu/h x000)

	Jan	Feb	Mar	Apr	May	Jun	Jul	Aug	Sep	Oct	Nov	Dec	Total
Space Cool	-	-	-	-	-	-	-	-	-	-	-	-	-
Heat Reject.	-	-	-	-	-	-	-	-	-	-	-	-	-
Refrigeration	-	-	-	-	-	-	-	-	-	-	-	-	-
Space Heat	-	-	-	-	-	-	-	-	-	-	-	-	-
HP Supp.	-	-	-	-	-	-	-	-	-	-	-	-	-
Hot Water	125.0	129.2	129.5	127.2	118.8	110.3	6.6	6.5	98.3	102.4	109.5	117.5	1,180.8
Vent. Fans	-	-	-	-	-	-	-	-	-	-	-	-	-
Pumps & Aux.	-	-	-	-	-	-	-	-	-	-	-	-	-
Ext. Usage	-	-	-	-	-	-	-	-	-	-	-	-	-
Misc. Equip.	-	-	-	-	-	-	-	-	-	-	-	-	-
Task Lights	-	-	-	-	-	-	-	-	-	-	-	-	-
Area Lights	-	-	-	-	-	-	-	-	-	-	-	-	-
Total	125.0	129.2	129.5	127.2	118.8	110.3	6.6	6.5	98.3	102.4	109.5	117.5	1,180.8

Figure B25. Monthly Energy Demand Profile – GM-Option2 ECM'S and GSHP-Corbin

Project/Run: Geothermal - Corbin - 42 Run Date/Time: 04/06/11 @ 11:45

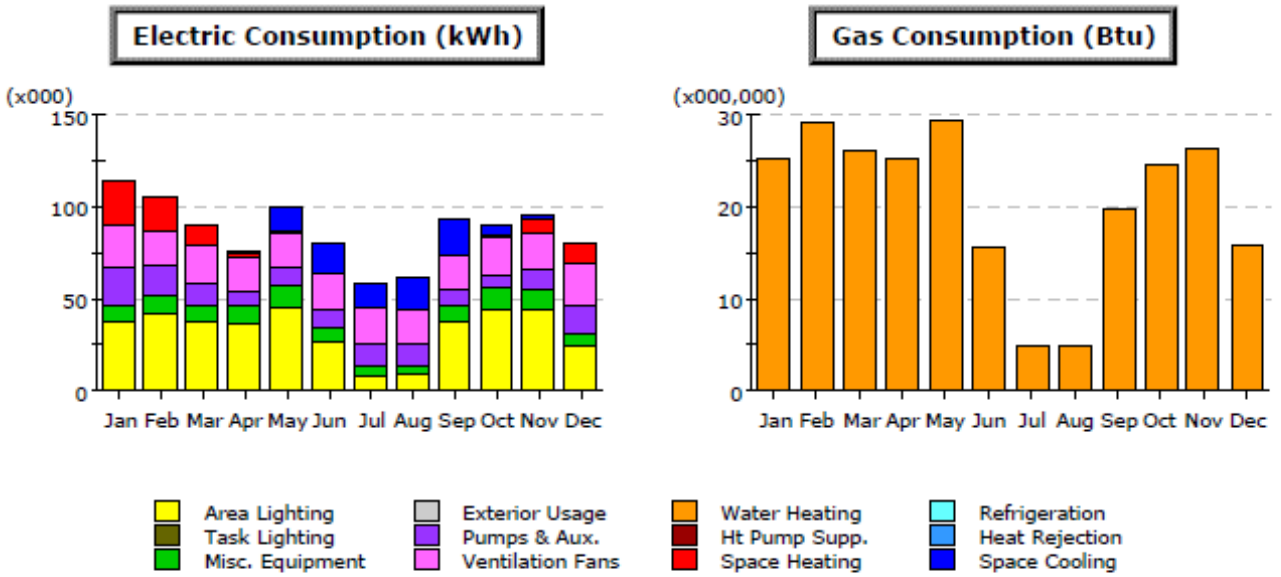

Electric Consumption (kWh x000)

	Jan	Feb	Mar	Apr	May	Jun	Jul	Aug	Sep	Oct	Nov	Dec	Total
Space Cool	0.1	-	0.1	2.0	13.4	16.6	13.9	17.2	19.4	5.0	1.0	0.4	89.1
Heat Reject.	-	-	-	-	-	-	-	-	-	-	-	-	-
Refrigeration	-	-	-	-	-	-	-	-	-	-	-	-	-
Space Heat	24.5	18.9	10.2	2.1	1.0	0.0	-	-	0.1	2.5	8.0	10.2	77.5
HP Supp.	-	-	-	-	-	-	-	-	-	-	-	-	-
Hot Water	-	-	-	-	-	-	-	-	-	-	-	-	-
Vent. Fans	23.0	18.9	20.1	19.2	19.8	19.2	19.9	19.9	19.2	19.8	19.3	22.5	240.8
Pumps & Aux.	19.5	15.6	12.0	6.6	8.4	10.3	12.2	11.4	7.8	6.8	10.8	16.0	137.6
Ext. Usage	-	-	-	-	-	-	-	-	-	-	-	-	-
Misc. Equip.	10.0	10.8	10.0	9.9	11.9	7.9	4.5	4.6	10.0	11.5	11.4	7.4	109.9
Task Lights	-	-	-	-	-	-	-	-	-	-	-	-	-
Area Lights	36.9	41.8	36.9	36.7	46.2	26.4	8.7	8.9	37.0	44.3	44.1	23.9	391.6
Total	114.1	105.9	89.4	76.5	100.8	80.5	59.1	61.9	93.5	90.0	94.6	80.4	1,046.6

Gas Consumption (Btu x000,000)

	Jan	Feb	Mar	Apr	May	Jun	Jul	Aug	Sep	Oct	Nov	Dec	Total
Space Cool	-	-	-	-	-	-	-	-	-	-	-	-	-
Heat Reject.	-	-	-	-	-	-	-	-	-	-	-	-	-
Refrigeration	-	-	-	-	-	-	-	-	-	-	-	-	-
Space Heat	-	-	-	-	-	-	-	-	-	-	-	-	-
HP Supp.	-	-	-	-	-	-	-	-	-	-	-	-	-
Hot Water	25.19	29.11	25.92	25.20	29.46	15.52	4.79	4.70	19.74	24.70	26.24	15.87	246.43
Vent. Fans	-	-	-	-	-	-	-	-	-	-	-	-	-
Pumps & Aux.	-	-	-	-	-	-	-	-	-	-	-	-	-
Ext. Usage	-	-	-	-	-	-	-	-	-	-	-	-	-
Misc. Equip.	-	-	-	-	-	-	-	-	-	-	-	-	-
Task Lights	-	-	-	-	-	-	-	-	-	-	-	-	-
Area Lights	-	-	-	-	-	-	-	-	-	-	-	-	-
Total	25.19	29.11	25.92	25.20	29.46	15.52	4.79	4.70	19.74	24.70	26.24	15.87	246.43

Figure B26. Monthly Energy Use Profile – GM-Option2 ECM'S and GSHP-Corbin

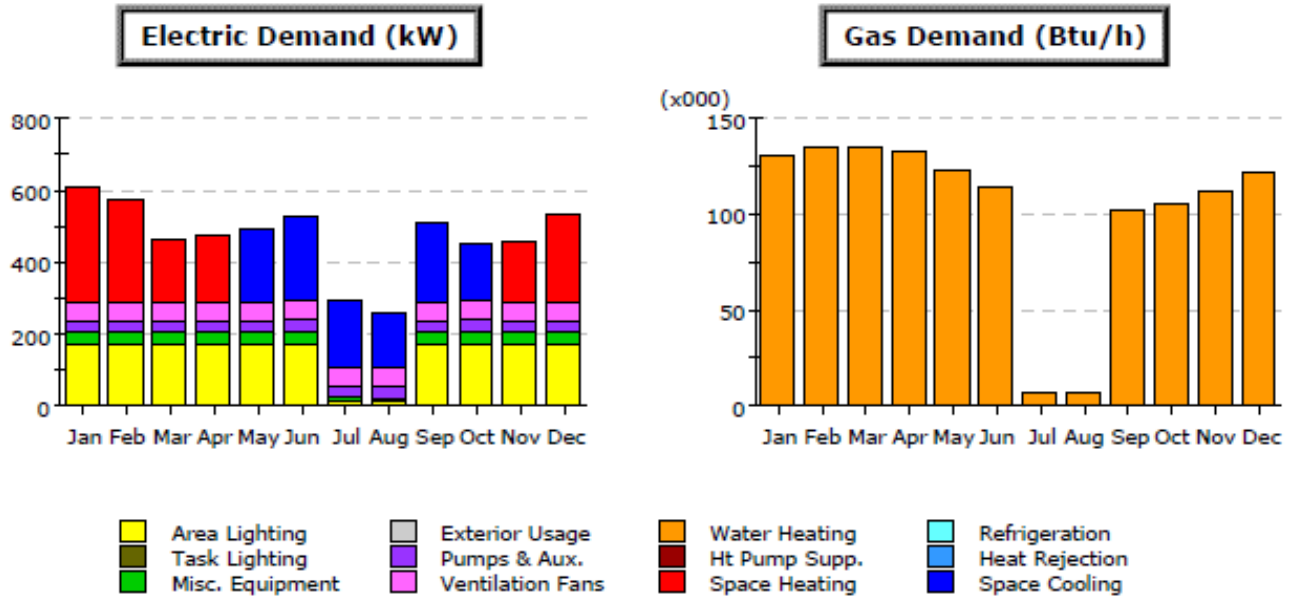

Electric Demand (kW)

	Jan	Feb	Mar	Apr	May	Jun	Jul	Aug	Sep	Oct	Nov	Dec	Total
Space Cool	-	-	-	-	210.0	241.5	184.3	153.1	222.4	157.9	-	-	1,169.1
Heat Reject.	-	-	-	-	-	-	-	-	-	-	-	-	-
Refrigeration	-	-	-	-	-	-	-	-	-	-	-	-	-
Space Heat	322.8	288.1	180.9	184.5	-	-	-	-	-	-	173.9	250.8	1,401.1
HP Supp.	-	-	-	-	-	-	-	-	-	-	-	-	-
Hot Water	-	-	-	-	-	-	-	-	-	-	-	-	-
Vent. Fans	49.4	49.4	49.4	49.4	49.4	49.4	49.4	49.4	49.4	49.4	49.4	49.4	592.6
Pumps & Aux.	31.1	31.1	31.1	31.1	31.1	31.1	31.1	31.1	31.1	31.1	31.1	31.1	373.2
Ext. Usage	-	-	-	-	-	-	-	-	-	-	-	-	-
Misc. Equip.	36.0	36.0	36.0	36.0	36.6	40.3	7.8	7.7	36.6	40.3	36.0	36.0	385.5
Task Lights	-	-	-	-	-	-	-	-	-	-	-	-	-
Area Lights	168.8	168.8	168.8	168.8	168.8	168.8	17.4	17.3	168.8	168.8	168.8	168.8	1,722.9
Total	608.2	573.5	466.2	469.8	495.9	531.0	290.0	258.6	508.3	447.4	459.3	536.1	5,644.3

Gas Demand (Btu/h x000)

	Jan	Feb	Mar	Apr	May	Jun	Jul	Aug	Sep	Oct	Nov	Dec	Total
Space Cool	-	-	-	-	-	-	-	-	-	-	-	-	-
Heat Reject.	-	-	-	-	-	-	-	-	-	-	-	-	-
Refrigeration	-	-	-	-	-	-	-	-	-	-	-	-	-
Space Heat	-	-	-	-	-	-	-	-	-	-	-	-	-
HP Supp.	-	-	-	-	-	-	-	-	-	-	-	-	-
Hot Water	130.1	134.6	134.8	132.4	123.3	114.0	6.8	6.6	101.1	105.3	113.0	121.9	1,224.1
Vent. Fans	-	-	-	-	-	-	-	-	-	-	-	-	-
Pumps & Aux.	-	-	-	-	-	-	-	-	-	-	-	-	-
Ext. Usage	-	-	-	-	-	-	-	-	-	-	-	-	-
Misc. Equip.	-	-	-	-	-	-	-	-	-	-	-	-	-
Task Lights	-	-	-	-	-	-	-	-	-	-	-	-	-
Area Lights	-	-	-	-	-	-	-	-	-	-	-	-	-
Total	130.1	134.6	134.8	132.4	123.3	114.0	6.8	6.6	101.1	105.3	113.0	121.9	1,224.1

Figure B27. Monthly Energy Demand Profile – GM-Option2 ECM'S and GSHP - Paducah

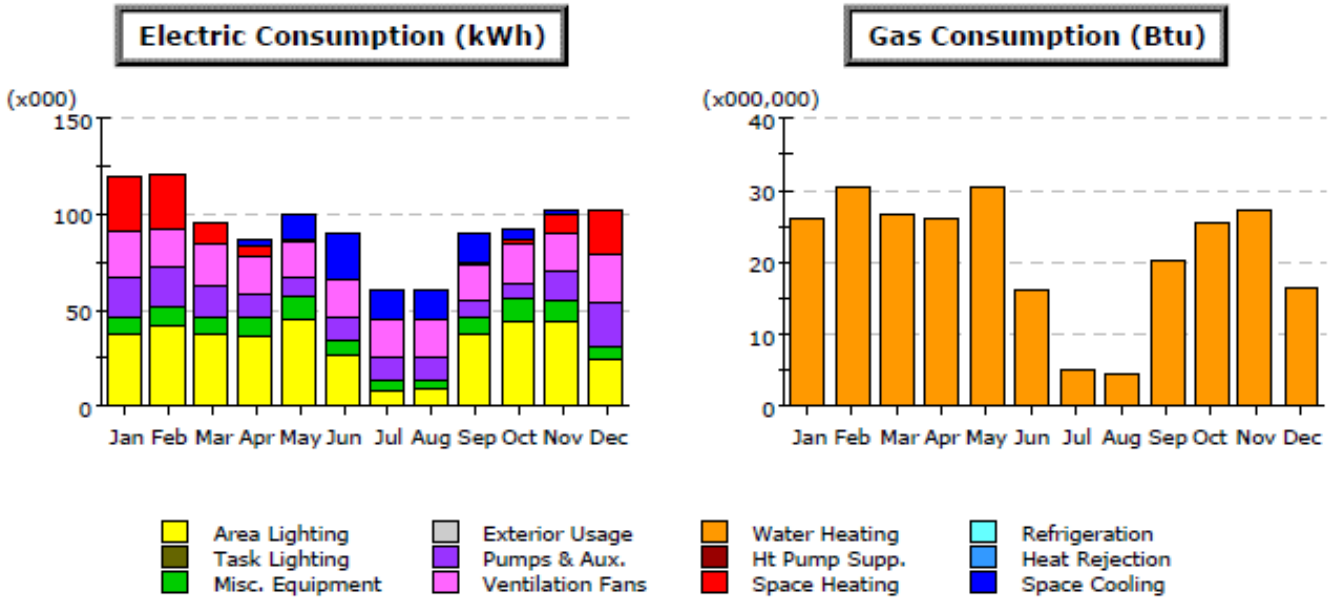

Electric Consumption (kWh x000)

	Jan	Feb	Mar	Apr	May	Jun	Jul	Aug	Sep	Oct	Nov	Dec	Total
Space Cool	-	0.0	0.1	4.4	14.1	24.0	14.6	15.4	14.5	4.7	0.8	-	92.5
Heat Reject.	-	-	-	-	-	-	-	-	-	-	-	-	-
Refrigeration	-	-	-	-	-	-	-	-	-	-	-	-	-
Space Heat	28.3	28.0	10.6	4.4	0.6	0.0	-	-	0.5	3.3	10.9	23.0	109.6
HP Supp.	-	-	-	-	-	-	-	-	-	-	-	-	-
Hot Water	-	-	-	-	-	-	-	-	-	-	-	-	-
Vent. Fans	23.2	20.1	21.3	19.7	19.9	19.3	19.9	19.9	19.3	20.0	19.8	25.1	247.3
Pumps & Aux.	20.5	19.6	16.4	11.9	8.3	12.0	12.7	11.8	7.9	8.5	14.9	22.5	167.1
Ext. Usage	-	-	-	-	-	-	-	-	-	-	-	-	-
Misc. Equip.	10.0	10.8	10.0	9.9	11.9	7.9	4.5	4.6	10.0	11.5	11.4	7.4	109.9
Task Lights	-	-	-	-	-	-	-	-	-	-	-	-	-
Area Lights	36.9	41.8	36.9	36.7	46.2	26.4	8.7	8.9	37.0	44.3	44.1	23.9	391.6
Total	118.9	120.3	95.3	87.0	100.9	89.6	60.4	60.5	89.2	92.3	101.8	101.8	1,118.1

Gas Consumption (Btu x000,000)

	Jan	Feb	Mar	Apr	May	Jun	Jul	Aug	Sep	Oct	Nov	Dec	Total
Space Cool	-	-	-	-	-	-	-	-	-	-	-	-	-
Heat Reject.	-	-	-	-	-	-	-	-	-	-	-	-	-
Refrigeration	-	-	-	-	-	-	-	-	-	-	-	-	-
Space Heat	-	-	-	-	-	-	-	-	-	-	-	-	-
HP Supp.	-	-	-	-	-	-	-	-	-	-	-	-	-
Hot Water	26.13	30.30	26.95	26.22	30.51	15.96	4.88	4.77	20.28	25.39	27.07	16.46	254.91
Vent. Fans	-	-	-	-	-	-	-	-	-	-	-	-	-
Pumps & Aux.	-	-	-	-	-	-	-	-	-	-	-	-	-
Ext. Usage	-	-	-	-	-	-	-	-	-	-	-	-	-
Misc. Equip.	-	-	-	-	-	-	-	-	-	-	-	-	-
Task Lights	-	-	-	-	-	-	-	-	-	-	-	-	-
Area Lights	-	-	-	-	-	-	-	-	-	-	-	-	-
Total	26.13	30.30	26.95	26.22	30.51	15.96	4.88	4.77	20.28	25.39	27.07	16.46	254.91

Figure B28. Monthly Energy Use Profile – GM-Option2 ECM'S and GSHP - Paducah

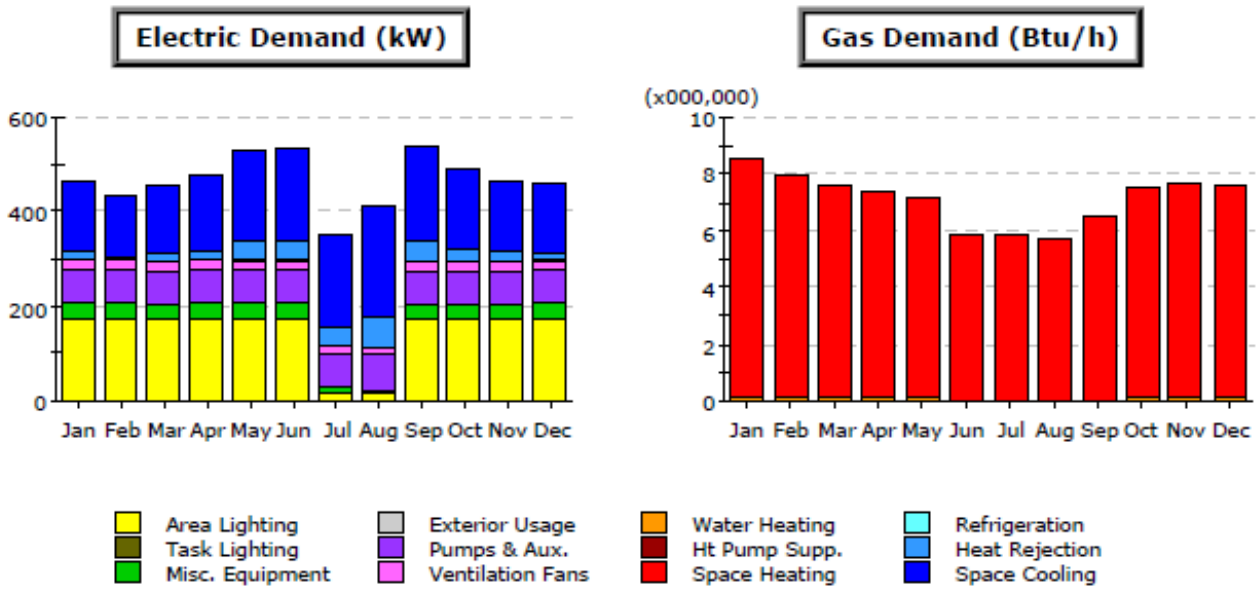

Electric Demand (kW)

	Jan	Feb	Mar	Apr	May	Jun	Jul	Aug	Sep	Oct	Nov	Dec	Total
Space Cool	149.5	125.8	144.1	160.1	197.3	197.5	196.8	236.5	205.8	169.6	154.6	148.3	2,085.7
Heat Reject.	15.0	6.0	12.5	18.3	38.0	38.2	38.9	62.4	40.8	25.7	17.6	14.7	327.9
Refrigeration	-	-	-	-	-	-	-	-	-	-	-	-	-
Space Heat	1.2	1.7	1.5	1.8	1.0	0.9	1.2	-	0.9	1.0	1.0	1.1	13.2
HP Supp.	-	-	-	-	-	-	-	-	-	-	-	-	-
Hot Water	-	-	-	-	-	-	-	-	-	-	-	-	-
Vent. Fans	20.3	20.3	20.3	20.3	20.3	20.3	20.3	20.3	20.3	20.3	20.3	20.3	243.3
Pumps & Aux.	69.8	69.8	69.8	69.8	69.8	69.8	69.8	69.8	69.8	69.8	69.8	69.8	837.1
Ext. Usage	-	-	-	-	-	-	-	-	-	-	-	-	-
Misc. Equip.	39.9	40.3	36.6	39.1	37.9	37.9	7.7	7.6	36.6	36.6	36.6	37.9	394.6
Task Lights	-	-	-	-	-	-	-	-	-	-	-	-	-
Area Lights	168.8	168.8	168.8	168.8	168.8	168.8	17.4	16.5	168.8	168.8	168.8	168.8	1,722.0
Total	464.4	432.6	453.5	478.0	533.0	533.3	352.1	412.9	542.9	491.7	468.5	460.8	5,623.8

Gas Demand (Btu/h x000,000)

	Jan	Feb	Mar	Apr	May	Jun	Jul	Aug	Sep	Oct	Nov	Dec	Total
Space Cool	-	-	-	-	-	-	-	-	-	-	-	-	-
Heat Reject.	-	-	-	-	-	-	-	-	-	-	-	-	-
Refrigeration	-	-	-	-	-	-	-	-	-	-	-	-	-
Space Heat	8.48	7.90	7.53	7.36	7.03	5.91	5.87	5.73	6.50	7.47	7.62	7.56	84.98
HP Supp.	-	-	-	-	-	-	-	-	-	-	-	-	-
Hot Water	0.07	0.07	0.07	0.07	0.07	0.01	0.01	0.01	0.01	0.06	0.06	0.07	0.58
Vent. Fans	-	-	-	-	-	-	-	-	-	-	-	-	-
Pumps & Aux.	-	-	-	-	-	-	-	-	-	-	-	-	-
Ext. Usage	-	-	-	-	-	-	-	-	-	-	-	-	-
Misc. Equip.	-	-	-	-	-	-	-	-	-	-	-	-	-
Task Lights	-	-	-	-	-	-	-	-	-	-	-	-	-
Area Lights	-	-	-	-	-	-	-	-	-	-	-	-	-
Total	8.56	7.98	7.60	7.43	7.10	5.92	5.88	5.74	6.51	7.53	7.68	7.63	85.56

Figure B29. Monthly Energy Demand Profile – M2-Large Set Back- Corbin

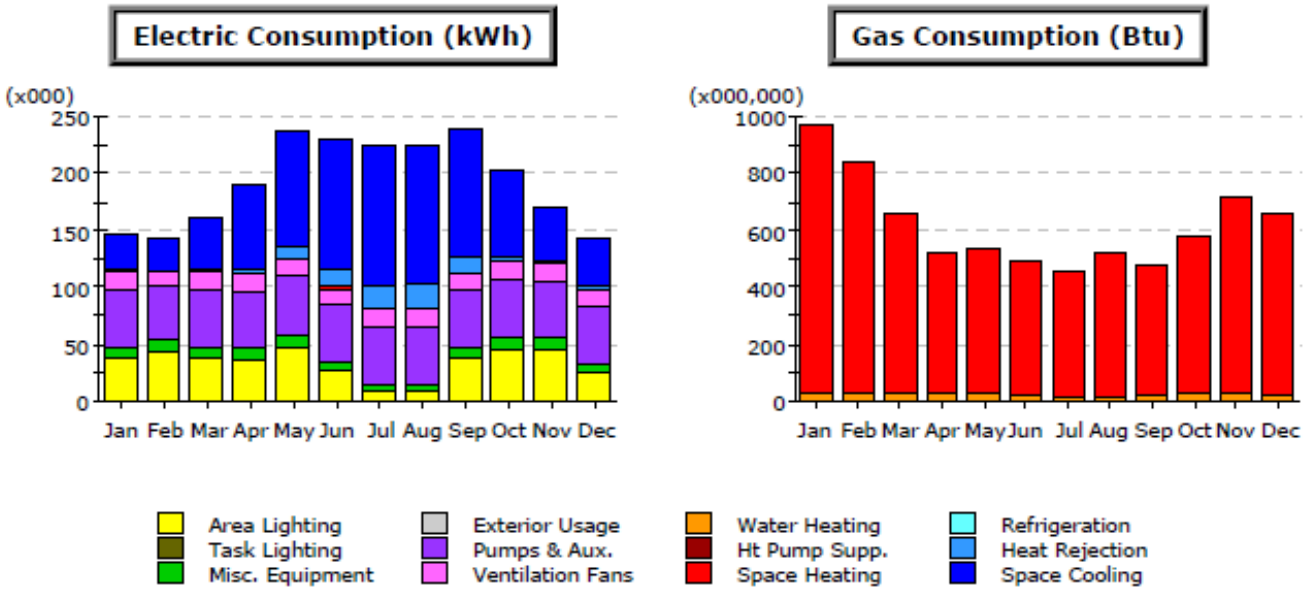

Electric Consumption (kWh x000)

	Jan	Feb	Mar	Apr	May	Jun	Jul	Aug	Sep	Oct	Nov	Dec	Total
Space Cool	32.4	28.1	46.0	73.2	99.5	113.6	124.1	124.7	111.9	75.2	46.2	42.6	917.8
Heat Reject.	0.5	0.1	1.2	4.0	11.0	15.9	20.8	20.9	14.9	5.2	1.6	1.3	97.4
Refrigeration	-	-	-	-	-	-	-	-	-	-	-	-	-
Space Heat	0.6	0.5	0.3	0.3	0.3	0.3	0.2	0.3	0.2	0.3	0.4	0.4	4.0
HP Supp.	-	-	-	-	-	-	-	-	-	-	-	-	-
Hot Water	-	-	-	-	-	-	-	-	-	-	-	-	-
Vent. Fans	15.3	13.8	15.1	14.6	15.1	14.6	15.1	15.1	14.6	15.1	14.7	15.1	178.2
Pumps & Aux.	51.9	46.9	51.9	50.2	51.9	50.2	51.9	51.9	50.2	51.9	50.2	51.9	611.1
Ext. Usage	-	-	-	-	-	-	-	-	-	-	-	-	-
Misc. Equip.	10.0	10.8	10.0	9.9	11.9	7.9	4.5	4.6	10.0	11.5	11.4	7.4	109.9
Task Lights	-	-	-	-	-	-	-	-	-	-	-	-	-
Area Lights	36.9	41.8	36.9	36.7	46.2	26.4	8.7	8.9	37.0	44.3	44.1	23.9	391.6
Total	147.6	141.9	161.6	189.0	235.9	229.0	225.3	226.3	238.9	203.6	168.5	142.7	2,310.0

Gas Consumption (Btu x000,000)

	Jan	Feb	Mar	Apr	May	Jun	Jul	Aug	Sep	Oct	Nov	Dec	Total
Space Cool	-	-	-	-	-	-	-	-	-	-	-	-	-
Heat Reject.	-	-	-	-	-	-	-	-	-	-	-	-	-
Refrigeration	-	-	-	-	-	-	-	-	-	-	-	-	-
Space Heat	946.1	811.5	630.9	489.4	505.4	476.4	448.6	512.9	449.7	556.6	686.6	646.0	7,160.1
HP Supp.	-	-	-	-	-	-	-	-	-	-	-	-	-
Hot Water	25.5	29.3	26.2	25.5	29.8	15.8	5.2	5.1	20.1	25.0	26.5	16.2	250.1
Vent. Fans	-	-	-	-	-	-	-	-	-	-	-	-	-
Pumps & Aux.	-	-	-	-	-	-	-	-	-	-	-	-	-
Ext. Usage	-	-	-	-	-	-	-	-	-	-	-	-	-
Misc. Equip.	-	-	-	-	-	-	-	-	-	-	-	-	-
Task Lights	-	-	-	-	-	-	-	-	-	-	-	-	-
Area Lights	-	-	-	-	-	-	-	-	-	-	-	-	-
Total	971.6	840.9	657.1	514.9	535.2	492.3	453.8	517.9	469.8	581.6	713.1	662.1	7,410.2

Figure B30. Monthly Energy Use Profile – M2-Large Set Back- Corbin

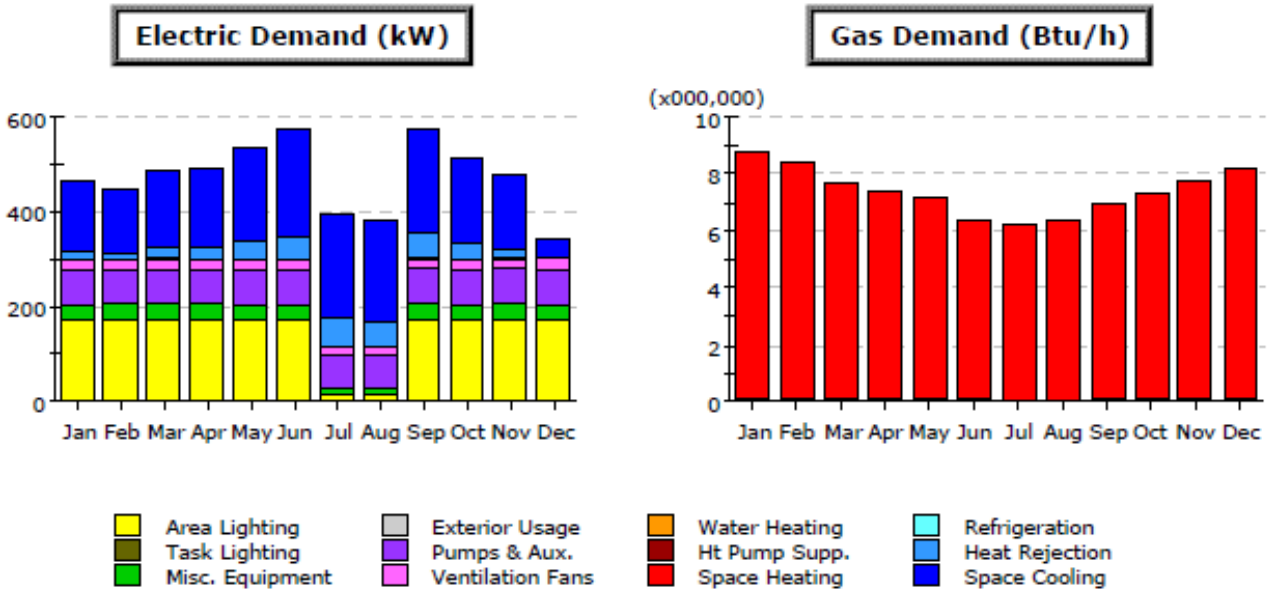

Electric Demand (kW)

	Jan	Feb	Mar	Apr	May	Jun	Jul	Aug	Sep	Oct	Nov	Dec	Total
Space Cool	152.1	139.3	163.7	165.7	198.6	225.0	222.5	212.9	220.0	184.9	155.3	36.4	2,076.3
Heat Reject.	14.0	8.5	21.7	22.2	36.9	49.5	55.2	46.8	48.4	33.0	16.0	-	352.1
Refrigeration	-	-	-	-	-	-	-	-	-	-	-	-	-
Space Heat	1.7	1.8	1.8	1.0	1.1	1.0	1.2	1.3	1.0	0.9	1.1	3.5	17.3
HP Supp.	-	-	-	-	-	-	-	-	-	-	-	-	-
Hot Water	-	-	-	-	-	-	-	-	-	-	-	-	-
Vent. Fans	20.3	20.3	20.3	20.3	20.3	20.3	20.3	20.3	20.3	20.3	20.3	26.6	249.8
Pumps & Aux.	72.5	72.5	72.5	72.5	72.5	72.5	72.5	72.5	72.5	72.5	72.5	72.5	869.7
Ext. Usage	-	-	-	-	-	-	-	-	-	-	-	-	-
Misc. Equip.	36.6	37.9	39.9	39.9	36.6	36.6	7.8	7.7	40.3	36.6	40.3	36.0	396.2
Task Lights	-	-	-	-	-	-	-	-	-	-	-	-	-
Area Lights	168.8	168.8	168.8	168.8	168.8	168.8	17.4	17.4	168.8	168.8	168.8	168.8	1,723.0
Total	466.0	449.0	488.7	490.3	534.8	573.6	396.9	378.8	571.2	516.9	474.3	343.9	5,684.5

Gas Demand (Btu/h x000,000)

	Jan	Feb	Mar	Apr	May	Jun	Jul	Aug	Sep	Oct	Nov	Dec	Total
Space Cool	-	-	-	-	-	-	-	-	-	-	-	-	-
Heat Reject.	-	-	-	-	-	-	-	-	-	-	-	-	-
Refrigeration	-	-	-	-	-	-	-	-	-	-	-	-	-
Space Heat	8.70	8.30	7.63	7.35	7.10	6.26	6.24	6.30	6.91	7.24	7.69	8.16	87.89
HP Supp.	-	-	-	-	-	-	-	-	-	-	-	-	-
Hot Water	0.07	0.08	0.08	0.08	0.07	0.07	0.01	0.01	0.06	0.06	0.07	0.07	0.71
Vent. Fans	-	-	-	-	-	-	-	-	-	-	-	-	-
Pumps & Aux.	-	-	-	-	-	-	-	-	-	-	-	-	-
Ext. Usage	-	-	-	-	-	-	-	-	-	-	-	-	-
Misc. Equip.	-	-	-	-	-	-	-	-	-	-	-	-	-
Task Lights	-	-	-	-	-	-	-	-	-	-	-	-	-
Area Lights	-	-	-	-	-	-	-	-	-	-	-	-	-
Total	8.78	8.38	7.70	7.43	7.18	6.33	6.25	6.31	6.97	7.30	7.76	8.23	88.60

Figure B31. Monthly Energy Demand Profile – M2-Large Set Back - Paducah

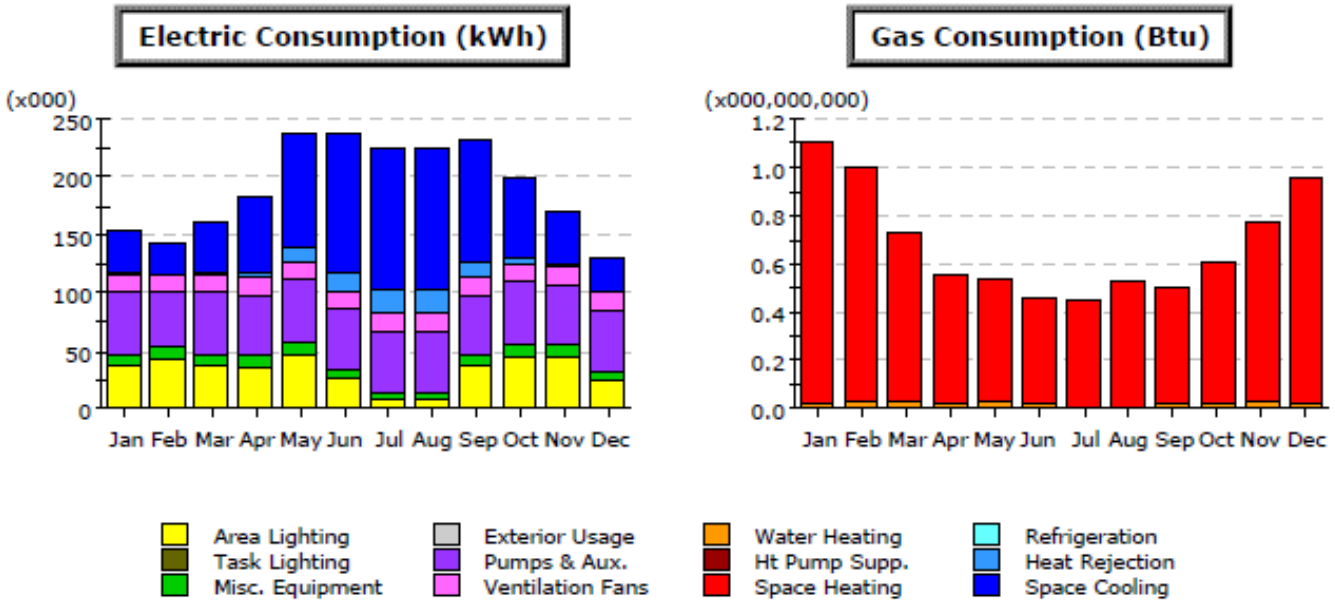

Electric Consumption (kWh x000)

	Jan	Feb	Mar	Apr	May	Jun	Jul	Aug	Sep	Oct	Nov	Dec	Total
Space Cool	37.3	26.6	44.2	66.5	99.4	118.0	124.2	124.7	105.6	69.3	44.5	28.9	889.
Heat Reject.	0.8	0.1	1.2	3.5	9.9	17.7	19.4	19.1	13.6	4.9	1.4	0.0	91.
Refrigeration	-	-	-	-	-	-	-	-	-	-	-	-	
Space Heat	0.6	0.6	0.4	0.3	0.3	0.2	0.2	0.3	0.3	0.3	0.4	0.6	4.
HP Supp.	-	-	-	-	-	-	-	-	-	-	-	-	
Hot Water	-	-	-	-	-	-	-	-	-	-	-	-	
Vent. Fans	15.3	13.8	15.1	14.6	15.1	14.6	15.1	15.1	14.6	15.1	14.7	15.2	178.
Pumps & Aux.	53.9	48.7	53.9	52.2	53.9	52.2	53.9	53.9	52.2	53.9	52.2	53.9	634.
Ext. Usage	-	-	-	-	-	-	-	-	-	-	-	-	
Misc. Equip.	10.0	10.8	10.0	9.9	11.9	7.9	4.5	4.6	10.0	11.5	11.4	7.4	109.
Task Lights	-	-	-	-	-	-	-	-	-	-	-	-	
Area Lights	36.9	41.8	36.9	36.7	46.2	26.4	8.7	8.9	37.0	44.3	44.1	23.9	391.
Total	154.9	142.3	161.8	183.7	236.7	237.0	225.9	226.6	233.2	199.4	168.7	129.9	2,300.

Gas Consumption (Btu x000,000,000)

	Jan	Feb	Mar	Apr	May	Jun	Jul	Aug	Sep	Oct	Nov	Dec	Total
Space Cool	-	-	-	-	-	-	-	-	-	-	-	-	
Heat Reject.	-	-	-	-	-	-	-	-	-	-	-	-	
Refrigeration	-	-	-	-	-	-	-	-	-	-	-	-	
Space Heat	1.08	0.96	0.70	0.53	0.50	0.45	0.45	0.52	0.48	0.59	0.74	0.93	7.9
HP Supp.	-	-	-	-	-	-	-	-	-	-	-	-	
Hot Water	0.03	0.03	0.03	0.03	0.03	0.02	0.01	0.01	0.02	0.03	0.03	0.02	0.2
Vent. Fans	-	-	-	-	-	-	-	-	-	-	-	-	
Pumps & Aux.	-	-	-	-	-	-	-	-	-	-	-	-	
Ext. Usage	-	-	-	-	-	-	-	-	-	-	-	-	
Misc. Equip.	-	-	-	-	-	-	-	-	-	-	-	-	
Task Lights	-	-	-	-	-	-	-	-	-	-	-	-	
Area Lights	-	-	-	-	-	-	-	-	-	-	-	-	
Total	1.11	0.99	0.73	0.56	0.53	0.46	0.45	0.53	0.50	0.61	0.77	0.95	8.2

Figure B32. Monthly Energy Use Profile – M2-Large Set Back - Paducah

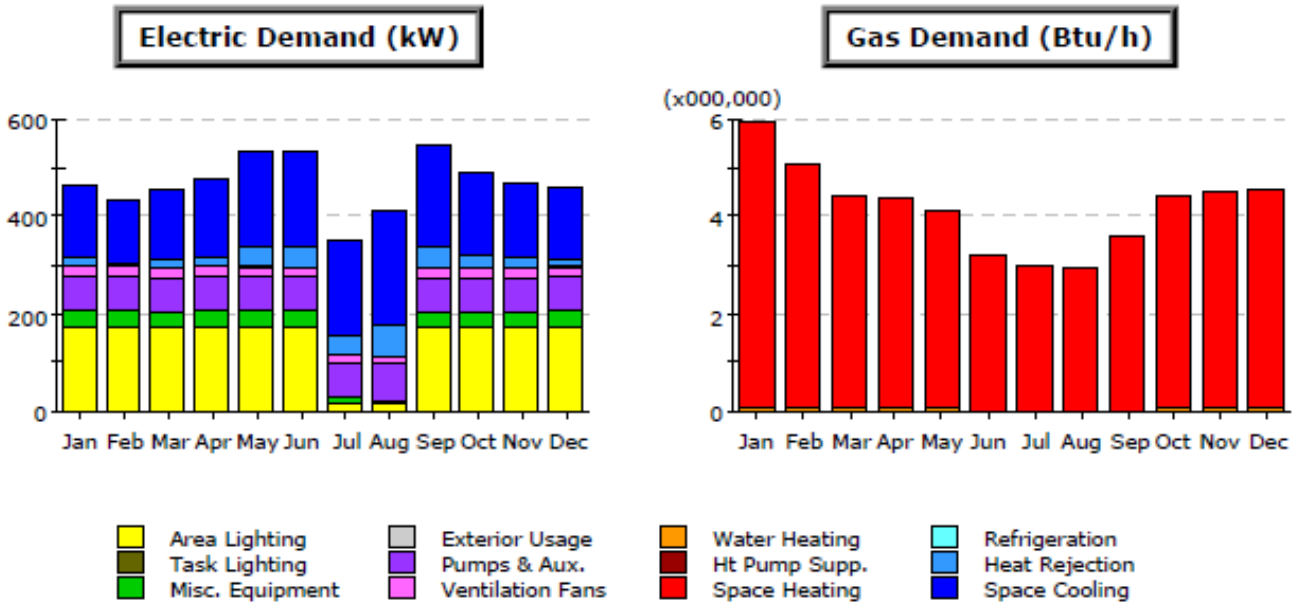

Electric Demand (kW)

	Jan	Feb	Mar	Apr	May	Jun	Jul	Aug	Sep	Oct	Nov	Dec	Total
Space Cool	150.5	125.7	145.5	160.1	198.5	198.6	198.1	238.5	207.0	170.8	155.6	149.1	2,097.8
Heat Reject.	15.2	6.0	12.8	18.3	38.2	38.4	39.1	62.4	41.0	26.0	17.8	14.9	330.1
Refrigeration	-	-	-	-	-	-	-	-	-	-	-	-	-
Space Heat	1.0	1.2	1.0	1.1	0.6	0.5	1.0	0.1	0.4	0.7	0.7	1.0	9.2
HP Supp.	-	-	-	-	-	-	-	-	-	-	-	-	-
Hot Water	-	-	-	-	-	-	-	-	-	-	-	-	-
Vent. Fans	20.3	20.3	20.3	20.3	20.3	20.3	20.3	20.3	20.3	20.3	20.3	20.3	243.3
Pumps & Aux.	69.8	69.8	69.8	69.8	69.8	69.8	69.8	69.8	69.8	69.8	69.8	69.8	837.1
Ext. Usage	-	-	-	-	-	-	-	-	-	-	-	-	-
Misc. Equip.	39.9	40.3	36.6	39.1	37.9	37.9	7.7	7.6	36.6	36.6	36.6	37.9	394.6
Task Lights	-	-	-	-	-	-	-	-	-	-	-	-	-
Area Lights	168.8	168.8	168.8	168.8	168.8	168.8	17.4	16.5	168.8	168.8	168.8	168.8	1,722.0
Total	465.5	432.0	454.7	477.3	534.1	534.2	353.4	415.1	543.9	492.9	469.5	461.6	5,634.2

Gas Demand (Btu/h x000,000)

	Jan	Feb	Mar	Apr	May	Jun	Jul	Aug	Sep	Oct	Nov	Dec	Total
Space Cool	-	-	-	-	-	-	-	-	-	-	-	-	-
Heat Reject.	-	-	-	-	-	-	-	-	-	-	-	-	-
Refrigeration	-	-	-	-	-	-	-	-	-	-	-	-	-
Space Heat	5.88	5.03	4.39	4.30	4.06	3.18	2.97	2.96	3.59	4.41	4.46	4.48	49.72
HP Supp.	-	-	-	-	-	-	-	-	-	-	-	-	-
Hot Water	0.07	0.07	0.07	0.07	0.07	0.01	0.01	0.01	0.01	0.06	0.06	0.07	0.58
Vent. Fans	-	-	-	-	-	-	-	-	-	-	-	-	-
Pumps & Aux.	-	-	-	-	-	-	-	-	-	-	-	-	-
Ext. Usage	-	-	-	-	-	-	-	-	-	-	-	-	-
Misc. Equip.	-	-	-	-	-	-	-	-	-	-	-	-	-
Task Lights	-	-	-	-	-	-	-	-	-	-	-	-	-
Area Lights	-	-	-	-	-	-	-	-	-	-	-	-	-
Total	5.95	5.11	4.47	4.37	4.13	3.19	2.98	2.96	3.60	4.47	4.52	4.54	50.30

Figure B33. Monthly Energy Demand Profile – M6-Modified Fans- Corbin

Project/Run: Corbin - 31 Run Date/Time: 04/07/11 @ 13:57

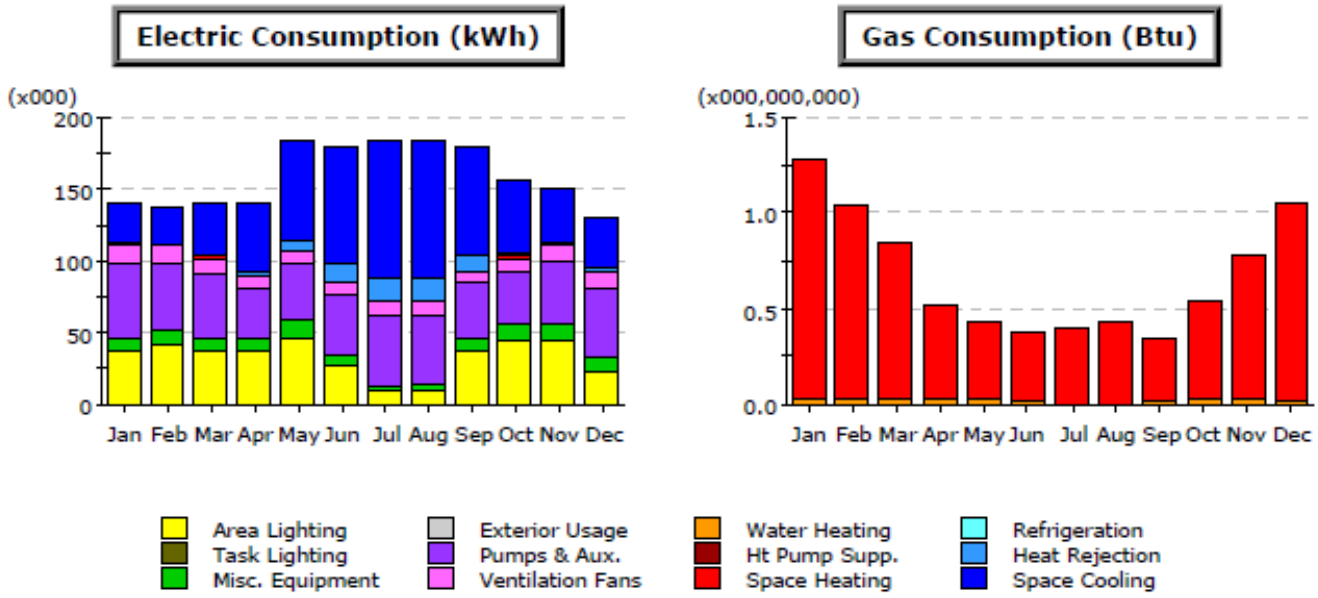

Electric Consumption (kWh x000)

	Jan	Feb	Mar	Apr	May	Jun	Jul	Aug	Sep	Oct	Nov	Dec	Total
Space Cool	29.6	27.4	37.2	48.6	69.5	83.3	97.4	97.1	76.6	50.7	38.3	36.4	692.3
Heat Reject.	0.3	0.1	1.0	2.8	7.7	11.2	15.1	15.3	10.1	3.3	1.2	0.9	68.9
Refrigeration	-	-	-	-	-	-	-	-	-	-	-	-	-
Space Heat	0.7	0.6	0.5	0.3	0.3	0.2	0.2	0.2	0.2	0.3	0.5	0.6	4.7
HP Supp.	-	-	-	-	-	-	-	-	-	-	-	-	-
Hot Water	-	-	-	-	-	-	-	-	-	-	-	-	-
Vent. Fans	13.6	11.6	10.8	8.6	8.9	8.9	9.5	9.4	8.6	9.1	10.3	12.6	121.8
Pumps & Aux.	50.6	45.8	44.6	34.4	39.6	42.9	49.3	48.5	37.9	37.5	44.3	48.8	524.1
Ext. Usage	-	-	-	-	-	-	-	-	-	-	-	-	-
Misc. Equip.	10.0	10.8	10.0	9.9	11.9	7.9	4.5	4.6	10.0	11.5	11.4	7.4	109.9
Task Lights	-	-	-	-	-	-	-	-	-	-	-	-	-
Area Lights	36.9	41.8	36.9	36.7	46.2	26.4	8.7	8.9	37.0	44.3	44.1	23.9	391.6
Total	141.7	138.1	141.1	141.2	184.0	180.8	184.7	184.0	180.4	156.8	150.0	130.7	1,913.4

Gas Consumption (Btu x000,000,000)

	Jan	Feb	Mar	Apr	May	Jun	Jul	Aug	Sep	Oct	Nov	Dec	Total
Space Cool	-	-	-	-	-	-	-	-	-	-	-	-	-
Heat Reject.	-	-	-	-	-	-	-	-	-	-	-	-	-
Refrigeration	-	-	-	-	-	-	-	-	-	-	-	-	-
Space Heat	1.26	1.01	0.82	0.50	0.39	0.36	0.39	0.42	0.32	0.51	0.75	1.04	7.78
HP Supp.	-	-	-	-	-	-	-	-	-	-	-	-	-
Hot Water	0.03	0.03	0.03	0.03	0.03	0.02	0.01	0.00	0.02	0.02	0.03	0.02	0.25
Vent. Fans	-	-	-	-	-	-	-	-	-	-	-	-	-
Pumps & Aux.	-	-	-	-	-	-	-	-	-	-	-	-	-
Ext. Usage	-	-	-	-	-	-	-	-	-	-	-	-	-
Misc. Equip.	-	-	-	-	-	-	-	-	-	-	-	-	-
Task Lights	-	-	-	-	-	-	-	-	-	-	-	-	-
Area Lights	-	-	-	-	-	-	-	-	-	-	-	-	-
Total	1.29	1.04	0.85	0.52	0.42	0.37	0.40	0.43	0.34	0.53	0.78	1.05	8.03

Figure B34. Monthly Energy Use Profile – M6-Modified Fans- Corbin

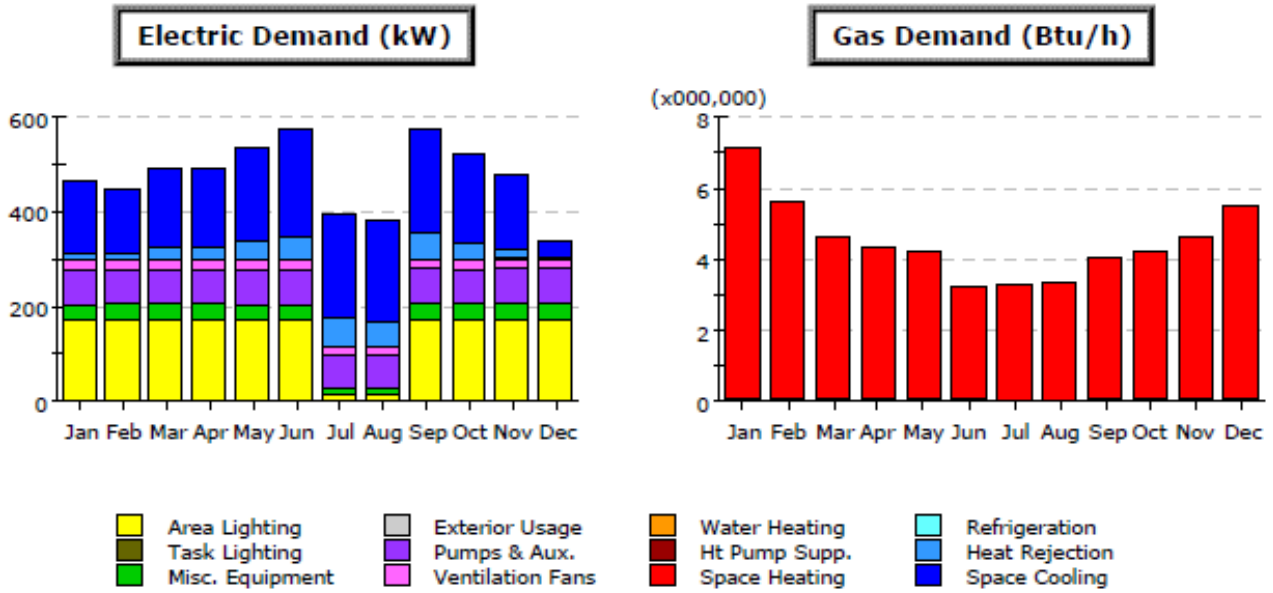

Electric Demand (kW)

	Jan	Feb	Mar	Apr	May	Jun	Jul	Aug	Sep	Oct	Nov	Dec	Total
Space Cool	152.1	140.7	165.5	166.8	200.1	226.2	224.0	214.4	221.4	183.3	156.6	36.4	2,087.7
Heat Reject.	14.0	8.8	22.2	22.5	37.2	49.8	55.6	47.2	48.7	32.6	16.3	-	354.8
Refrigeration	-	-	-	-	-	-	-	-	-	-	-	-	-
Space Heat	1.1	1.1	1.1	0.7	0.9	0.6	1.0	1.0	0.7	0.6	0.9	1.7	11.3
HP Supp.	-	-	-	-	-	-	-	-	-	-	-	-	-
Hot Water	-	-	-	-	-	-	-	-	-	-	-	-	-
Vent. Fans	20.3	20.3	20.3	20.3	20.3	20.3	20.3	20.3	20.3	20.3	20.3	20.3	243.4
Pumps & Aux.	72.5	72.5	72.5	72.5	72.5	72.5	72.5	72.5	72.5	72.5	72.5	72.5	869.7
Ext. Usage	-	-	-	-	-	-	-	-	-	-	-	-	-
Misc. Equip.	36.6	37.9	39.9	39.9	36.6	36.6	7.8	7.7	40.3	39.9	40.3	40.3	403.7
Task Lights	-	-	-	-	-	-	-	-	-	-	-	-	-
Area Lights	168.8	168.8	168.8	168.8	168.8	168.8	17.4	17.4	168.8	168.8	168.8	168.8	1,723.0
Total	465.3	450.1	490.2	491.5	536.4	574.8	398.5	380.5	572.7	517.9	475.6	340.0	5,693.5

Gas Demand (Btu/h x000,000)

	Jan	Feb	Mar	Apr	May	Jun	Jul	Aug	Sep	Oct	Nov	Dec	Total
Space Cool	-	-	-	-	-	-	-	-	-	-	-	-	-
Heat Reject.	-	-	-	-	-	-	-	-	-	-	-	-	-
Refrigeration	-	-	-	-	-	-	-	-	-	-	-	-	-
Space Heat	7.05	5.54	4.54	4.29	4.14	3.14	3.30	3.36	3.98	4.16	4.55	5.44	53.50
HP Supp.	-	-	-	-	-	-	-	-	-	-	-	-	-
Hot Water	0.07	0.08	0.08	0.08	0.07	0.07	0.01	0.01	0.06	0.06	0.06	0.07	0.71
Vent. Fans	-	-	-	-	-	-	-	-	-	-	-	-	-
Pumps & Aux.	-	-	-	-	-	-	-	-	-	-	-	-	-
Ext. Usage	-	-	-	-	-	-	-	-	-	-	-	-	-
Misc. Equip.	-	-	-	-	-	-	-	-	-	-	-	-	-
Task Lights	-	-	-	-	-	-	-	-	-	-	-	-	-
Area Lights	-	-	-	-	-	-	-	-	-	-	-	-	-
Total	7.13	5.61	4.62	4.36	4.21	3.21	3.31	3.37	4.04	4.22	4.61	5.51	54.20

Figure B35. Monthly Energy Demand Profile – M6-Modified Fans - Paducah

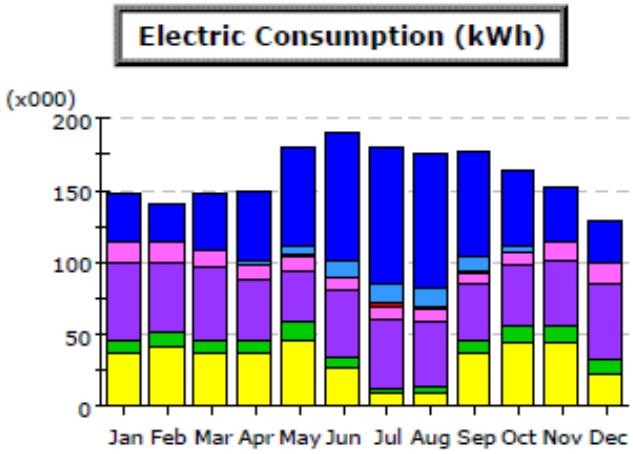

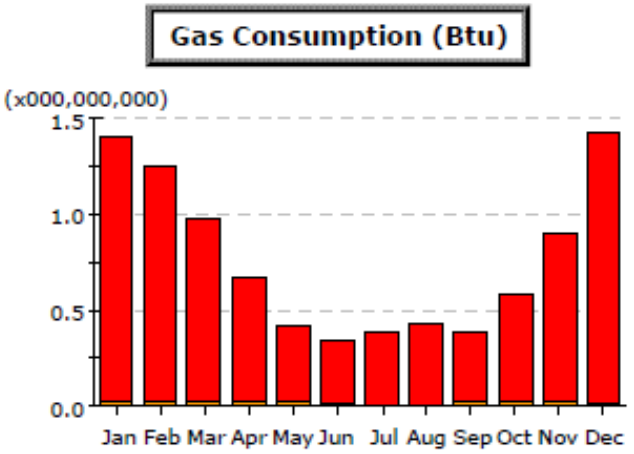

Electric Consumption (kWh x000)

	Jan	Feb	Mar	Apr	May	Jun	Jul	Aug	Sep	Oct	Nov	Dec	Total
Space Cool	33.9	26.3	38.7	49.5	68.3	88.4	94.6	91.8	72.8	52.6	36.4	28.7	682.
Heat Reject.	0.6	0.1	1.0	2.7	7.1	12.9	14.3	13.7	9.5	3.7	0.9	0.0	66.
Refrigeration	-	-	-	-	-	-	-	-	-	-	-	-	-
Space Heat	0.8	0.7	0.6	0.4	0.3	0.2	0.2	0.2	0.2	0.4	0.5	0.8	5.
HP Supp.	-	-	-	-	-	-	-	-	-	-	-	-	-
Hot Water	-	-	-	-	-	-	-	-	-	-	-	-	-
Vent. Fans	13.6	12.7	11.9	9.9	8.8	8.9	9.3	9.2	8.5	9.5	11.2	14.3	127.
Pumps & Aux.	52.8	48.3	49.3	41.4	37.4	45.2	47.9	45.9	38.1	42.0	46.9	53.9	549.
Ext. Usage	-	-	-	-	-	-	-	-	-	-	-	-	-
Misc. Equip.	10.0	10.8	10.0	9.9	11.9	7.9	4.5	4.6	10.0	11.5	11.4	7.4	109.
Task Lights	-	-	-	-	-	-	-	-	-	-	-	-	-
Area Lights	36.9	41.8	36.9	36.7	46.2	26.4	8.7	8.9	37.0	44.3	44.1	23.9	391.
Total	148.7	140.7	148.4	150.5	179.9	190.0	179.5	174.3	176.2	164.1	151.4	129.1	1,932.

Gas Consumption (Btu x000,000,000)

	Jan	Feb	Mar	Apr	May	Jun	Jul	Aug	Sep	Oct	Nov	Dec	Total
Space Cool	-	-	-	-	-	-	-	-	-	-	-	-	-
Heat Reject.	-	-	-	-	-	-	-	-	-	-	-	-	-
Refrigeration	-	-	-	-	-	-	-	-	-	-	-	-	-
Space Heat	1.38	1.22	0.96	0.64	0.39	0.33	0.39	0.42	0.37	0.57	0.87	1.40	8.9
HP Supp.	-	-	-	-	-	-	-	-	-	-	-	-	-
Hot Water	0.03	0.03	0.03	0.03	0.03	0.02	0.01	0.00	0.02	0.03	0.03	0.02	0.2
Vent. Fans	-	-	-	-	-	-	-	-	-	-	-	-	-
Pumps & Aux.	-	-	-	-	-	-	-	-	-	-	-	-	-
Ext. Usage	-	-	-	-	-	-	-	-	-	-	-	-	-
Misc. Equip.	-	-	-	-	-	-	-	-	-	-	-	-	-
Task Lights	-	-	-	-	-	-	-	-	-	-	-	-	-
Area Lights	-	-	-	-	-	-	-	-	-	-	-	-	-
Total	1.41	1.25	0.98	0.67	0.42	0.35	0.39	0.43	0.39	0.59	0.90	1.41	9.1

Figure B36. Monthly Energy Use Profile – M6-Modified Fans - Paducah

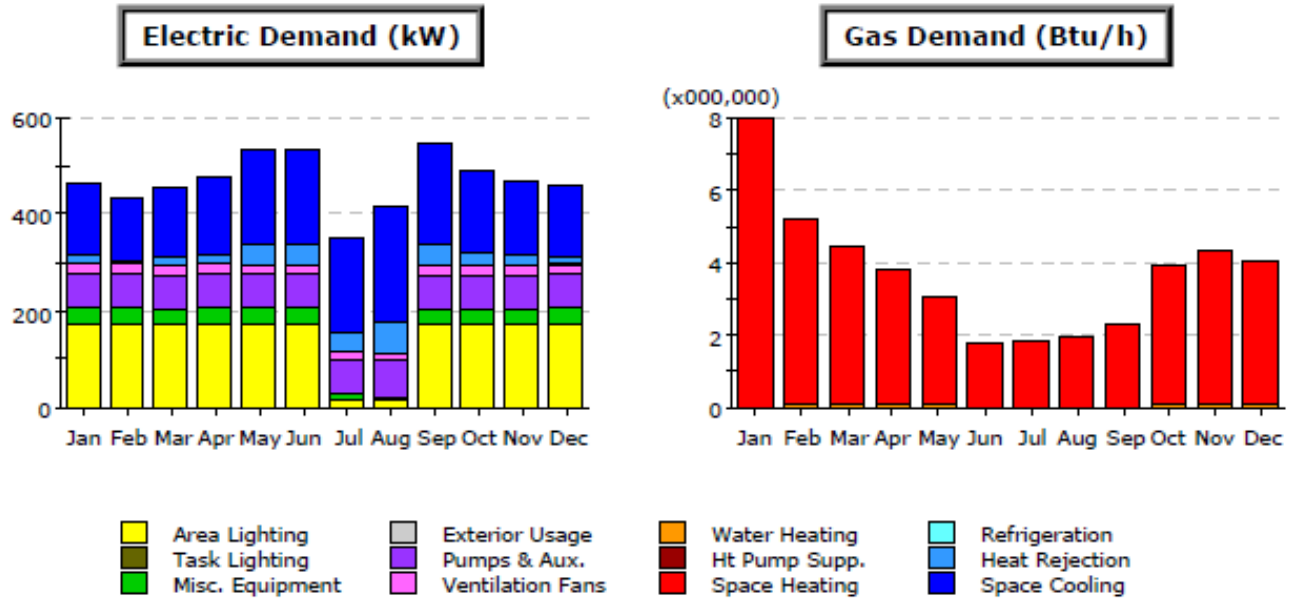

Electric Demand (kW)

	Jan	Feb	Mar	Apr	May	Jun	Jul	Aug	Sep	Oct	Nov	Dec	Total
Space Cool	150.8	125.7	145.7	160.1	199.3	199.5	199.0	240.8	208.0	171.3	155.8	149.3	2,105.5
Heat Reject.	15.3	6.0	12.9	18.3	38.4	38.6	39.3	62.4	41.2	26.1	17.9	14.9	331.3
Refrigeration	-	-	-	-	-	-	-	-	-	-	-	-	-
Space Heat	0.9	1.1	1.0	0.8	0.3	0.3	0.9	0.1	0.3	0.4	0.5	0.9	7.5
HP Supp.	-	-	-	-	-	-	-	-	-	-	-	-	-
Hot Water	-	-	-	-	-	-	-	-	-	-	-	-	-
Vent. Fans	20.3	20.3	20.3	20.3	20.3	20.3	20.3	20.3	20.4	20.3	20.3	20.3	243.4
Pumps & Aux.	69.8	69.8	69.8	69.8	69.8	69.8	69.8	69.8	69.8	69.8	69.8	69.8	837.1
Ext. Usage	-	-	-	-	-	-	-	-	-	-	-	-	-
Misc. Equip.	39.9	40.3	36.6	39.1	37.9	37.9	7.7	7.6	36.6	36.6	36.6	37.9	394.6
Task Lights	-	-	-	-	-	-	-	-	-	-	-	-	-
Area Lights	168.8	168.8	168.8	168.8	168.8	168.8	17.4	16.5	168.8	168.8	168.8	168.8	1,722.0
Total	465.8	431.9	455.1	477.0	534.8	535.1	354.5	417.4	545.0	493.3	469.7	461.9	5,641.5

Gas Demand (Btu/h x000,000)

	Jan	Feb	Mar	Apr	May	Jun	Jul	Aug	Sep	Oct	Nov	Dec	Total
Space Cool	-	-	-	-	-	-	-	-	-	-	-	-	-
Heat Reject.	-	-	-	-	-	-	-	-	-	-	-	-	-
Refrigeration	-	-	-	-	-	-	-	-	-	-	-	-	-
Space Heat	7.95	5.13	4.33	3.73	3.00	1.80	1.84	1.94	2.27	3.86	4.29	4.02	44.17
HP Supp.	-	-	-	-	-	-	-	-	-	-	-	-	-
Hot Water	0.01	0.07	0.07	0.07	0.07	0.01	0.01	0.01	0.01	0.06	0.06	0.07	0.52
Vent. Fans	-	-	-	-	-	-	-	-	-	-	-	-	-
Pumps & Aux.	-	-	-	-	-	-	-	-	-	-	-	-	-
Ext. Usage	-	-	-	-	-	-	-	-	-	-	-	-	-
Misc. Equip.	-	-	-	-	-	-	-	-	-	-	-	-	-
Task Lights	-	-	-	-	-	-	-	-	-	-	-	-	-
Area Lights	-	-	-	-	-	-	-	-	-	-	-	-	-
Total	7.96	5.21	4.40	3.80	3.07	1.81	1.85	1.94	2.28	3.92	4.35	4.09	44.68

Figure B37. Monthly Energy Demand Profile – M10- Minimum Air Flow-Corbin

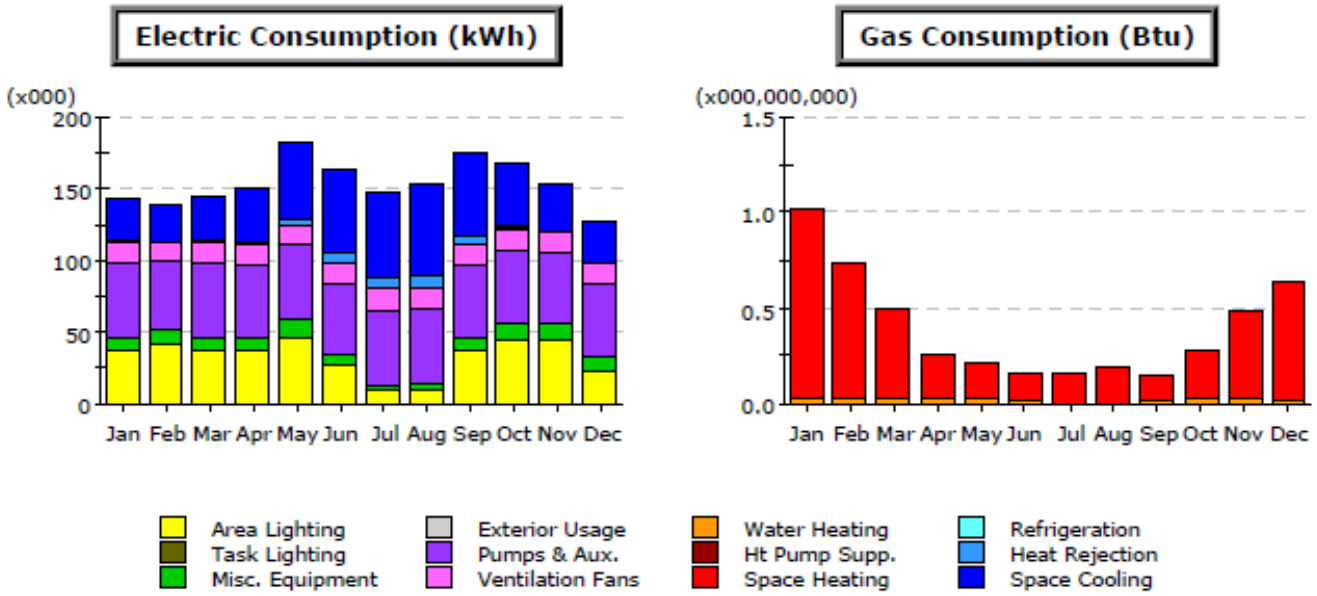

Electric Consumption (kWh x000)

	Jan	Feb	Mar	Apr	May	Jun	Jul	Aug	Sep	Oct	Nov	Dec	Total
Space Cool	28.5	25.7	30.2	38.7	53.7	58.9	61.1	65.2	57.6	43.4	33.4	29.4	525.9
Heat Reject.	0.2	0.1	0.2	1.0	4.2	6.1	7.8	8.8	5.7	1.8	0.5	0.2	36.6
Refrigeration	-	-	-	-	-	-	-	-	-	-	-	-	-
Space Heat	0.6	0.4	0.3	0.2	0.1	0.1	0.1	0.1	0.1	0.2	0.3	0.4	2.8
HP Supp.	-	-	-	-	-	-	-	-	-	-	-	-	-
Hot Water	-	-	-	-	-	-	-	-	-	-	-	-	-
Vent. Fans	14.5	13.1	14.4	14.0	14.5	14.0	14.5	14.5	14.0	14.5	14.0	14.4	170.5
Pumps & Aux.	51.9	46.9	51.9	50.2	51.9	50.2	51.9	51.9	50.2	51.9	50.2	51.9	611.1
Ext. Usage	-	-	-	-	-	-	-	-	-	-	-	-	-
Misc. Equip.	10.0	10.8	10.0	9.9	11.9	7.9	4.5	4.6	10.0	11.5	11.4	7.4	109.9
Task Lights	-	-	-	-	-	-	-	-	-	-	-	-	-
Area Lights	36.9	41.8	36.9	36.7	46.2	26.4	8.7	8.9	37.0	44.3	44.1	23.9	391.6
Total	142.6	138.7	144.0	150.7	182.5	163.7	148.5	153.9	174.7	167.5	154.0	127.6	1,848.5

Gas Consumption (Btu x000,000,000)

	Jan	Feb	Mar	Apr	May	Jun	Jul	Aug	Sep	Oct	Nov	Dec	Total
Space Cool	-	-	-	-	-	-	-	-	-	-	-	-	-
Heat Reject.	-	-	-	-	-	-	-	-	-	-	-	-	-
Refrigeration	-	-	-	-	-	-	-	-	-	-	-	-	-
Space Heat	0.99	0.70	0.47	0.23	0.18	0.15	0.16	0.18	0.13	0.26	0.45	0.63	4.52
HP Supp.	-	-	-	-	-	-	-	-	-	-	-	-	-
Hot Water	0.03	0.03	0.03	0.03	0.03	0.02	0.00	0.00	0.02	0.02	0.03	0.02	0.25
Vent. Fans	-	-	-	-	-	-	-	-	-	-	-	-	-
Pumps & Aux.	-	-	-	-	-	-	-	-	-	-	-	-	-
Ext. Usage	-	-	-	-	-	-	-	-	-	-	-	-	-
Misc. Equip.	-	-	-	-	-	-	-	-	-	-	-	-	-
Task Lights	-	-	-	-	-	-	-	-	-	-	-	-	-
Area Lights	-	-	-	-	-	-	-	-	-	-	-	-	-
Total	1.01	0.73	0.49	0.26	0.21	0.16	0.16	0.19	0.15	0.28	0.48	0.64	4.77

Figure B38. Monthly Energy Use Profile – M10- Minimum Air Flow-Corbin

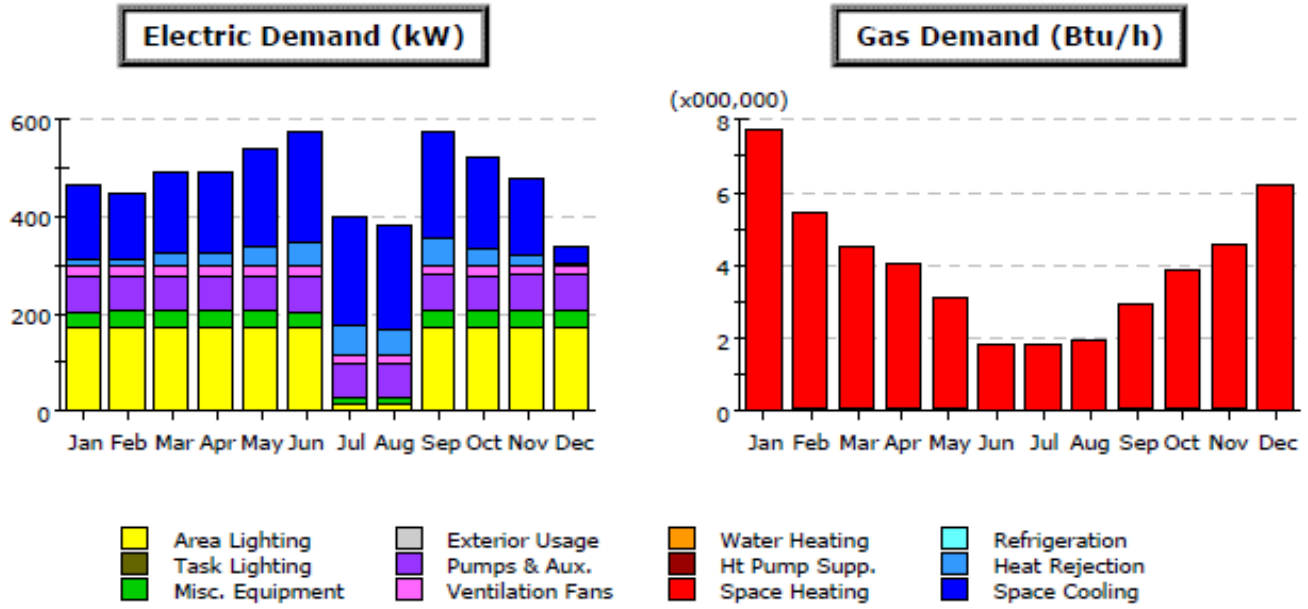

Electric Demand (kW)

	Jan	Feb	Mar	Apr	May	Jun	Jul	Aug	Sep	Oct	Nov	Dec	Total
Space Cool	152.1	140.7	165.7	167.3	202.1	226.9	225.8	215.6	223.0	183.8	156.9	36.4	2,096.4
Heat Reject.	14.0	8.8	22.2	22.6	37.4	49.9	56.0	47.5	49.1	32.7	16.4	-	356.6
Refrigeration	-	-	-	-	-	-	-	-	-	-	-	-	-
Space Heat	1.1	1.1	1.0	0.5	0.2	0.3	0.6	0.8	0.3	0.4	0.8	1.7	8.9
HP Supp.	-	-	-	-	-	-	-	-	-	-	-	-	-
Hot Water	-	-	-	-	-	-	-	-	-	-	-	-	-
Vent. Fans	20.3	20.3	20.3	20.3	20.6	20.3	20.4	20.3	20.4	20.3	20.3	20.4	244.1
Pumps & Aux.	72.5	72.5	72.5	72.5	72.5	72.5	72.5	72.5	72.5	72.5	72.5	72.5	869.7
Ext. Usage	-	-	-	-	-	-	-	-	-	-	-	-	-
Misc. Equip.	36.6	37.9	39.9	39.9	39.1	36.6	7.8	7.7	40.3	39.9	40.3	40.3	406.2
Task Lights	-	-	-	-	-	-	-	-	-	-	-	-	-
Area Lights	168.8	168.8	168.8	168.8	168.8	168.8	17.4	17.4	168.8	168.8	168.8	168.8	1,723.0
Total	465.3	450.0	490.4	491.9	540.8	575.3	400.4	381.8	574.5	518.4	475.9	340.0	5,704.7

Gas Demand (Btu/h x000,000)

	Jan	Feb	Mar	Apr	May	Jun	Jul	Aug	Sep	Oct	Nov	Dec	Total
Space Cool	-	-	-	-	-	-	-	-	-	-	-	-	-
Heat Reject.	-	-	-	-	-	-	-	-	-	-	-	-	-
Refrigeration	-	-	-	-	-	-	-	-	-	-	-	-	-
Space Heat	7.73	5.36	4.44	3.98	3.09	1.85	1.87	1.91	2.88	3.83	4.52	6.22	47.68
HP Supp.	-	-	-	-	-	-	-	-	-	-	-	-	-
Hot Water	0.01	0.08	0.08	0.08	0.07	0.01	0.01	0.01	0.06	0.06	0.06	0.01	0.52
Vent. Fans	-	-	-	-	-	-	-	-	-	-	-	-	-
Pumps & Aux.	-	-	-	-	-	-	-	-	-	-	-	-	-
Ext. Usage	-	-	-	-	-	-	-	-	-	-	-	-	-
Misc. Equip.	-	-	-	-	-	-	-	-	-	-	-	-	-
Task Lights	-	-	-	-	-	-	-	-	-	-	-	-	-
Area Lights	-	-	-	-	-	-	-	-	-	-	-	-	-
Total	7.74	5.44	4.52	4.05	3.17	1.85	1.88	1.92	2.94	3.89	4.59	6.23	48.21

Figure B39. Monthly Energy Demand Profile – M10- Minimum Air Flow - Paducah

Project/Run: Paducah - 35 Run Date/Time: 04/08/11 @ 12:50

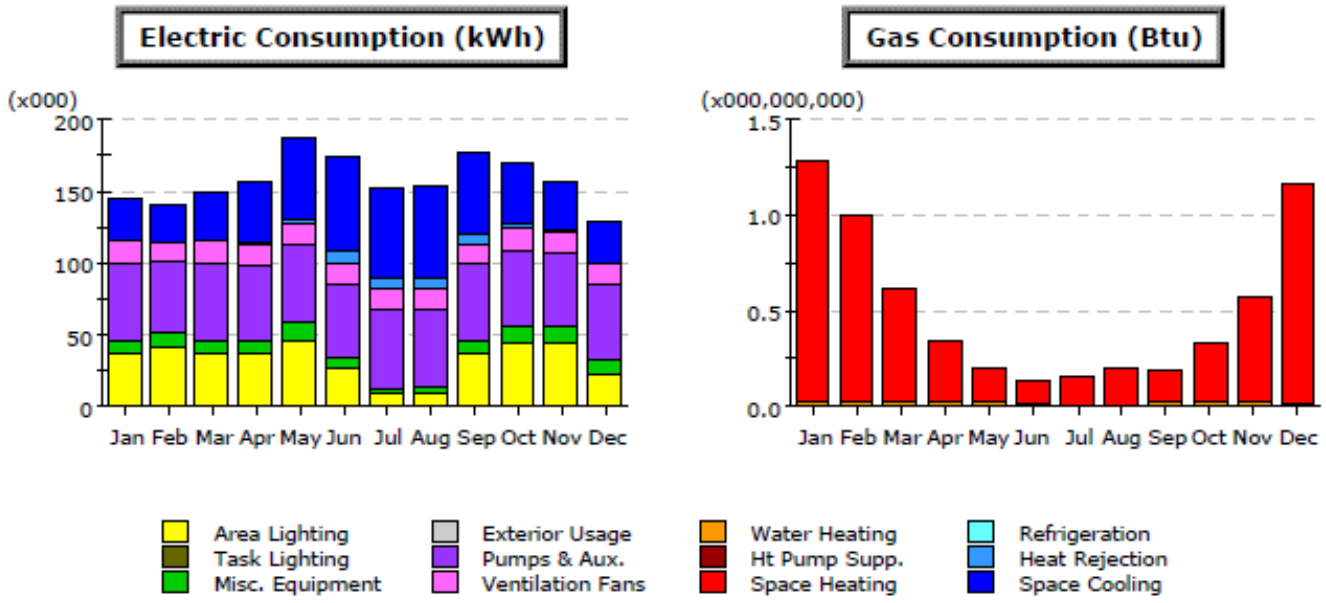

Electric Consumption (kWh x000)

	Jan	Feb	Mar	Apr	May	Jun	Jul	Aug	Sep	Oct	Nov	Dec	Total
Space Cool	28.9	25.6	34.1	42.3	55.9	64.2	62.1	64.4	57.4	43.7	34.4	27.3	540.4
Heat Reject.	0.1	0.1	0.4	1.5	4.2	8.2	7.6	7.8	5.7	1.8	0.6	-	38.1
Refrigeration	-	-	-	-	-	-	-	-	-	-	-	-	-
Space Heat	0.7	0.6	0.4	0.2	0.1	0.1	0.1	0.1	0.1	0.2	0.3	0.7	3.7
HP Supp.	-	-	-	-	-	-	-	-	-	-	-	-	-
Hot Water	-	-	-	-	-	-	-	-	-	-	-	-	-
Vent. Fans	14.7	13.1	14.4	14.0	14.5	14.1	14.5	14.5	14.0	14.5	14.0	14.4	170.8
Pumps & Aux.	53.9	48.7	53.9	52.2	53.9	52.2	53.9	53.9	52.2	53.9	52.2	53.9	634.9
Ext. Usage	-	-	-	-	-	-	-	-	-	-	-	-	-
Misc. Equip.	10.0	10.8	10.0	9.9	11.9	7.9	4.5	4.6	10.0	11.5	11.4	7.4	109.9
Task Lights	-	-	-	-	-	-	-	-	-	-	-	-	-
Area Lights	36.9	41.8	36.9	36.7	46.2	26.4	8.7	8.9	37.0	44.3	44.1	23.9	391.6
Total	145.2	140.6	150.3	156.8	186.7	173.1	151.4	154.2	176.4	170.0	157.0	127.7	1,889.4

Gas Consumption (Btu x000,000,000)

	Jan	Feb	Mar	Apr	May	Jun	Jul	Aug	Sep	Oct	Nov	Dec	Total
Space Cool	-	-	-	-	-	-	-	-	-	-	-	-	-
Heat Reject.	-	-	-	-	-	-	-	-	-	-	-	-	-
Refrigeration	-	-	-	-	-	-	-	-	-	-	-	-	-
Space Heat	1.25	0.97	0.59	0.32	0.17	0.12	0.16	0.20	0.17	0.31	0.55	1.15	5.96
HP Supp.	-	-	-	-	-	-	-	-	-	-	-	-	-
Hot Water	0.03	0.03	0.03	0.03	0.03	0.02	0.00	0.00	0.02	0.03	0.03	0.02	0.26
Vent. Fans	-	-	-	-	-	-	-	-	-	-	-	-	-
Pumps & Aux.	-	-	-	-	-	-	-	-	-	-	-	-	-
Ext. Usage	-	-	-	-	-	-	-	-	-	-	-	-	-
Misc. Equip.	-	-	-	-	-	-	-	-	-	-	-	-	-
Task Lights	-	-	-	-	-	-	-	-	-	-	-	-	-
Area Lights	-	-	-	-	-	-	-	-	-	-	-	-	-
Total	1.28	1.00	0.61	0.35	0.20	0.14	0.17	0.20	0.19	0.33	0.58	1.16	6.22

Figure B40. Monthly Energy Use Profile – M10- Minimum Air Flow - Paducah

Project/Run: OD Corbin - Baseline Design Run Date/Time: 04/15/11 @ 10:43

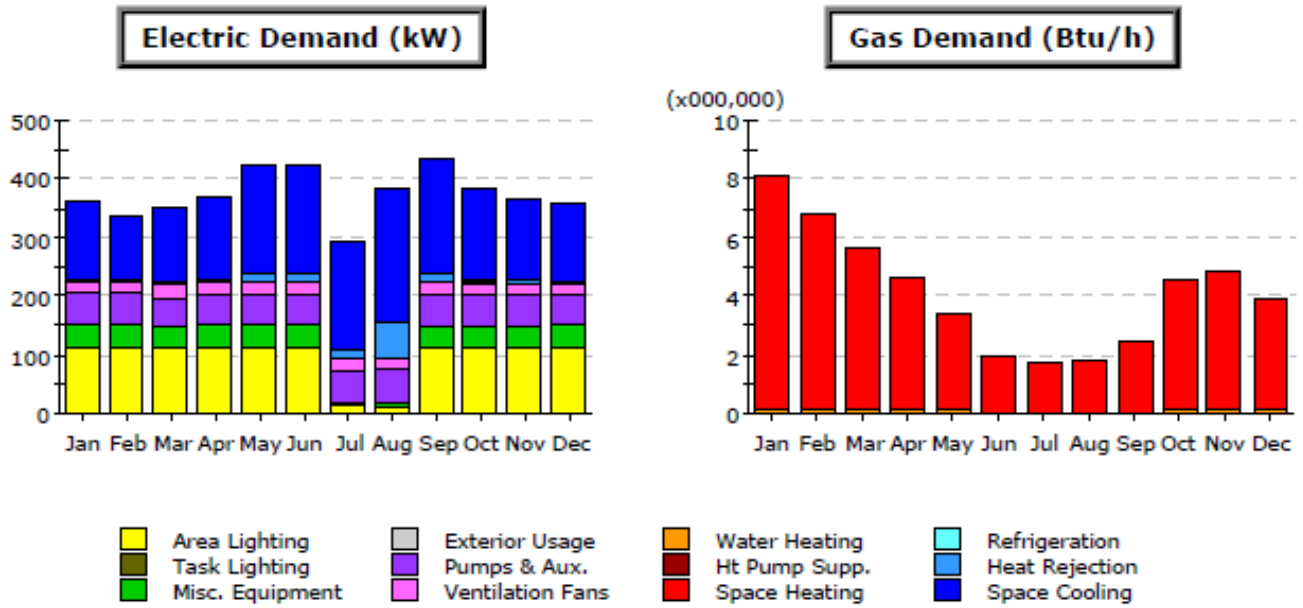

Electric Demand (kW)

	Jan	Feb	Mar	Apr	May	Jun	Jul	Aug	Sep	Oct	Nov	Dec	Total
Space Cool	131.7	106.2	129.4	143.3	187.2	186.8	187.1	228.6	196.2	156.3	138.7	131.8	1,923.3
Heat Reject.	4.1	1.5	3.8	5.2	11.8	11.9	12.7	62.3	13.7	8.2	5.2	4.3	144.8
Refrigeration	-	-	-	-	-	-	-	-	-	-	-	-	-
Space Heat	1.0	1.2	1.0	0.9	0.5	0.4	0.9	-	0.4	0.5	0.7	1.0	8.5
HP Supp.	-	-	-	-	-	-	-	-	-	-	-	-	-
Hot Water	-	-	-	-	-	-	-	-	-	-	-	-	-
Vent. Fans	20.3	20.3	20.3	20.3	20.3	20.3	20.3	20.3	20.3	20.3	20.3	20.3	243.4
Pumps & Aux.	52.7	50.6	49.9	52.7	52.9	52.8	52.7	56.1	52.8	52.4	51.3	50.0	626.8
Ext. Usage	-	-	-	-	-	-	-	-	-	-	-	-	-
Misc. Equip.	39.1	40.3	36.6	39.1	37.9	37.9	7.7	7.6	36.6	36.6	36.6	37.9	393.8
Task Lights	-	-	-	-	-	-	-	-	-	-	-	-	-
Area Lights	112.7	112.5	111.1	111.3	112.2	112.3	11.5	10.9	111.4	111.6	111.9	111.8	1,141.1
Total	361.6	332.7	352.0	372.7	422.7	422.4	292.9	385.7	431.4	386.0	364.6	357.1	4,481.8

Gas Demand (Btu/h x000,000)

	Jan	Feb	Mar	Apr	May	Jun	Jul	Aug	Sep	Oct	Nov	Dec	Total
Space Cool	-	-	-	-	-	-	-	-	-	-	-	-	-
Heat Reject.	-	-	-	-	-	-	-	-	-	-	-	-	-
Refrigeration	-	-	-	-	-	-	-	-	-	-	-	-	-
Space Heat	8.08	6.71	5.54	4.61	3.29	1.98	1.73	1.81	2.36	4.51	4.79	3.87	49.30
HP Supp.	-	-	-	-	-	-	-	-	-	-	-	-	-
Hot Water	0.07	0.07	0.07	0.07	0.07	0.01	0.01	0.01	0.01	0.06	0.06	0.07	0.58
Vent. Fans	-	-	-	-	-	-	-	-	-	-	-	-	-
Pumps & Aux.	-	-	-	-	-	-	-	-	-	-	-	-	-
Ext. Usage	-	-	-	-	-	-	-	-	-	-	-	-	-
Misc. Equip.	-	-	-	-	-	-	-	-	-	-	-	-	-
Task Lights	-	-	-	-	-	-	-	-	-	-	-	-	-
Area Lights	-	-	-	-	-	-	-	-	-	-	-	-	-
Total	8.15	6.79	5.61	4.68	3.36	1.98	1.74	1.82	2.37	4.57	4.85	3.94	49.88

Figure B41. Monthly Energy Demand Profile –Combo ECM's VAV- Corbin

Project/Run: OD Corbin - Baseline Design Run Date/Time: 04/15/11 @ 10:43

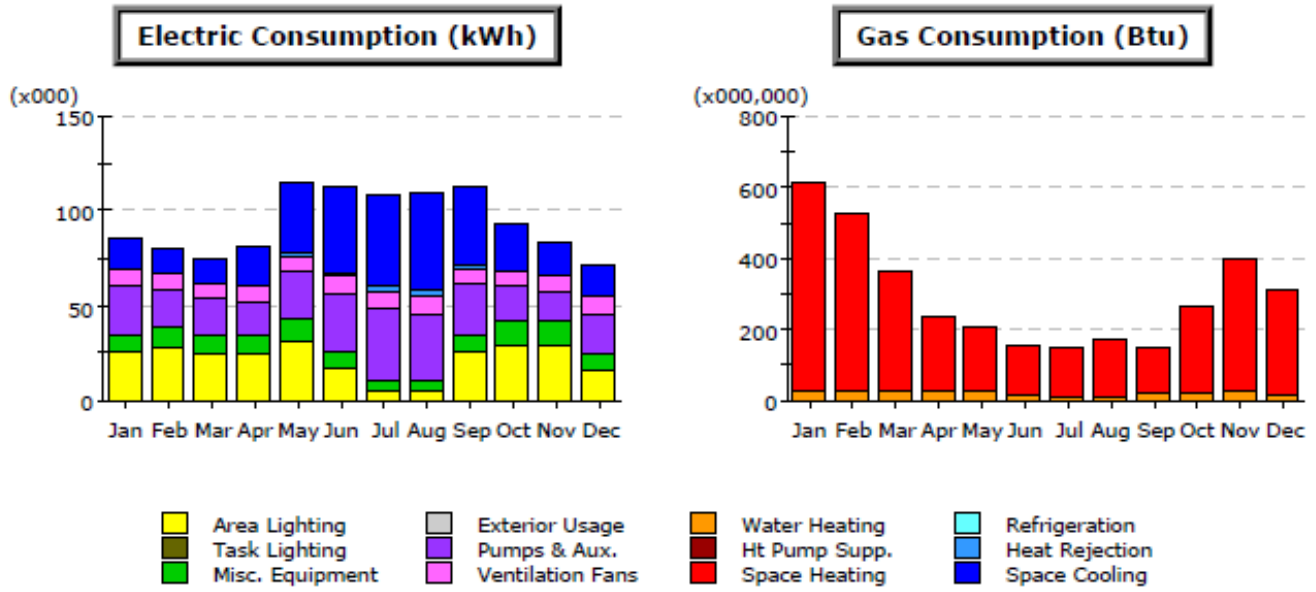

Electric Consumption (kWh x000)

	Jan	Feb	Mar	Apr	May	Jun	Jul	Aug	Sep	Oct	Nov	Dec	Total
Space Cool	16.3	13.6	14.0	20.9	37.1	44.6	47.6	51.2	41.2	24.9	16.8	15.4	343.4
Heat Reject.	0.1	0.0	0.1	0.3	1.3	2.0	3.2	3.4	1.8	0.5	0.1	0.1	12.9
Refrigeration	-	-	-	-	-	-	-	-	-	-	-	-	-
Space Heat	0.4	0.3	0.2	0.1	0.1	0.1	0.1	0.1	0.1	0.2	0.2	0.2	2.2
HP Supp.	-	-	-	-	-	-	-	-	-	-	-	-	-
Hot Water	-	-	-	-	-	-	-	-	-	-	-	-	-
Vent. Fans	9.7	7.7	8.0	7.7	8.4	8.6	9.2	9.1	8.2	8.0	7.8	9.1	101.5
Pumps & Aux.	24.8	19.9	18.6	17.9	25.5	31.2	37.5	35.7	26.2	18.8	17.1	22.5	295.6
Ext. Usage	-	-	-	-	-	-	-	-	-	-	-	-	-
Misc. Equip.	10.0	10.8	10.0	9.9	11.9	7.9	4.5	4.6	10.0	11.5	11.4	7.4	109.9
Task Lights	-	-	-	-	-	-	-	-	-	-	-	-	-
Area Lights	24.9	28.1	24.7	24.5	30.8	17.6	5.8	6.0	24.8	29.8	29.7	16.1	262.8
Total	86.1	80.4	75.6	81.3	115.1	112.0	107.9	110.0	112.4	93.6	83.0	70.9	1,128.2

Gas Consumption (Btu x000,000)

	Jan	Feb	Mar	Apr	May	Jun	Jul	Aug	Sep	Oct	Nov	Dec	Total
Space Cool	-	-	-	-	-	-	-	-	-	-	-	-	-
Heat Reject.	-	-	-	-	-	-	-	-	-	-	-	-	-
Refrigeration	-	-	-	-	-	-	-	-	-	-	-	-	-
Space Heat	589.0	501.8	340.2	212.3	181.2	141.5	144.6	165.8	128.2	236.8	371.6	300.0	3,312.8
HP Supp.	-	-	-	-	-	-	-	-	-	-	-	-	-
Hot Water	25.4	29.3	26.1	25.3	29.6	15.6	4.9	4.8	19.8	24.8	26.4	16.1	248.1
Vent. Fans	-	-	-	-	-	-	-	-	-	-	-	-	-
Pumps & Aux.	-	-	-	-	-	-	-	-	-	-	-	-	-
Ext. Usage	-	-	-	-	-	-	-	-	-	-	-	-	-
Misc. Equip.	-	-	-	-	-	-	-	-	-	-	-	-	-
Task Lights	-	-	-	-	-	-	-	-	-	-	-	-	-
Area Lights	-	-	-	-	-	-	-	-	-	-	-	-	-
Total	614.4	531.0	366.3	237.6	210.7	157.1	149.5	170.6	148.0	261.6	398.0	316.0	3,560.8

Figure B42. Monthly Energy Use Profile – Combo ECM's VAV - Corbin

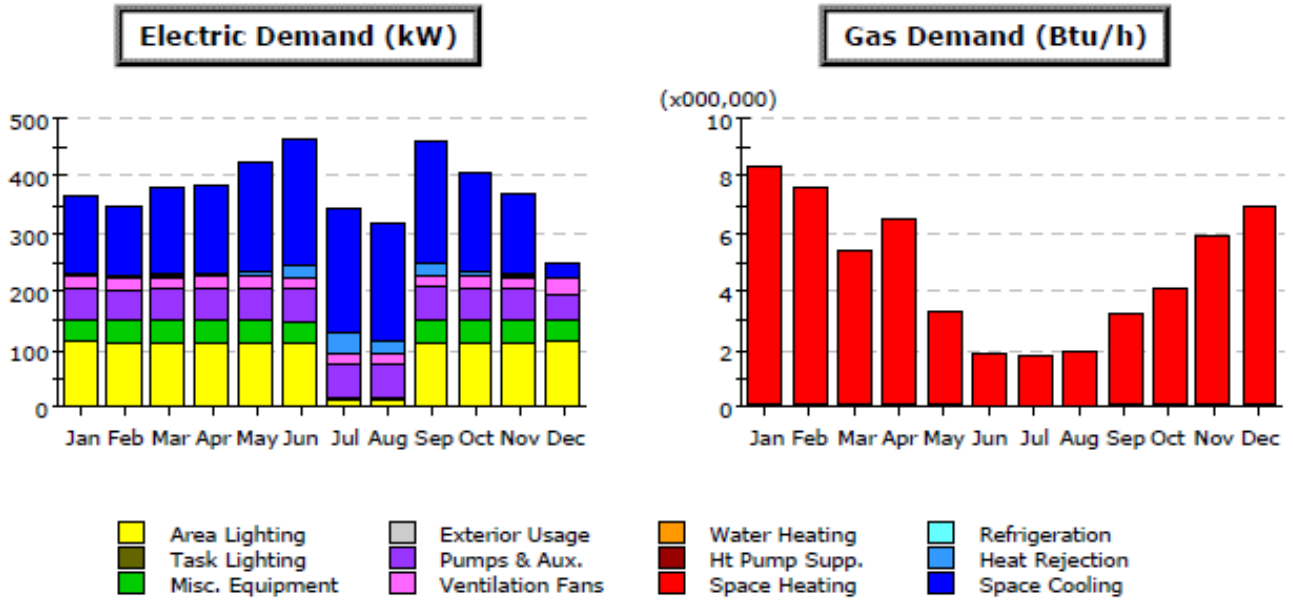

Electric Demand (kW)

	Jan	Feb	Mar	Apr	May	Jun	Jul	Aug	Sep	Oct	Nov	Dec	Total
Space Cool	133.1	120.0	148.2	150.0	188.2	215.3	214.5	203.6	211.1	169.0	137.6	24.8	1,915.4
Heat Reject.	4.1	2.3	6.7	6.8	11.2	22.9	34.9	20.2	21.9	9.5	4.7	-	145.1
Refrigeration	-	-	-	-	-	-	-	-	-	-	-	-	-
Space Heat	1.8	1.5	1.1	0.6	0.3	0.4	0.6	0.9	0.4	0.6	0.9	3.1	12.4
HP Supp.	-	-	-	-	-	-	-	-	-	-	-	-	-
Hot Water	-	-	-	-	-	-	-	-	-	-	-	-	-
Vent. Fans	20.3	20.3	20.3	20.3	20.5	20.3	20.4	20.3	20.4	20.3	20.3	25.0	248.7
Pumps & Aux.	54.8	51.0	53.2	53.9	54.9	55.6	55.1	54.8	55.2	55.0	52.7	46.1	642.4
Ext. Usage	-	-	-	-	-	-	-	-	-	-	-	-	-
Misc. Equip.	36.6	39.9	39.9	39.9	39.1	36.6	7.8	7.7	40.3	39.9	39.9	36.0	403.6
Task Lights	-	-	-	-	-	-	-	-	-	-	-	-	-
Area Lights	114.0	111.7	111.1	111.7	111.2	111.2	11.5	11.6	112.2	111.3	112.4	114.5	1,144.4
Total	364.7	346.8	380.6	383.2	425.4	462.3	344.8	319.1	461.5	405.6	368.5	249.4	4,512.0

Gas Demand (Btu/h x000,000)

	Jan	Feb	Mar	Apr	May	Jun	Jul	Aug	Sep	Oct	Nov	Dec	Total
Space Cool	-	-	-	-	-	-	-	-	-	-	-	-	-
Heat Reject.	-	-	-	-	-	-	-	-	-	-	-	-	-
Refrigeration	-	-	-	-	-	-	-	-	-	-	-	-	-
Space Heat	8.27	7.48	5.35	6.47	3.25	1.91	1.77	1.95	3.12	4.06	5.87	6.86	56.34
HP Supp.	-	-	-	-	-	-	-	-	-	-	-	-	-
Hot Water	0.07	0.08	0.08	0.08	0.07	0.01	0.01	0.01	0.06	0.06	0.07	0.07	0.65
Vent. Fans	-	-	-	-	-	-	-	-	-	-	-	-	-
Pumps & Aux.	-	-	-	-	-	-	-	-	-	-	-	-	-
Ext. Usage	-	-	-	-	-	-	-	-	-	-	-	-	-
Misc. Equip.	-	-	-	-	-	-	-	-	-	-	-	-	-
Task Lights	-	-	-	-	-	-	-	-	-	-	-	-	-
Area Lights	-	-	-	-	-	-	-	-	-	-	-	-	-
Total	8.34	7.55	5.43	6.55	3.32	1.92	1.77	1.95	3.17	4.12	5.94	6.93	56.99

Figure B43. Monthly Energy Demand Profile – Combo ECM's VAV - Paducah

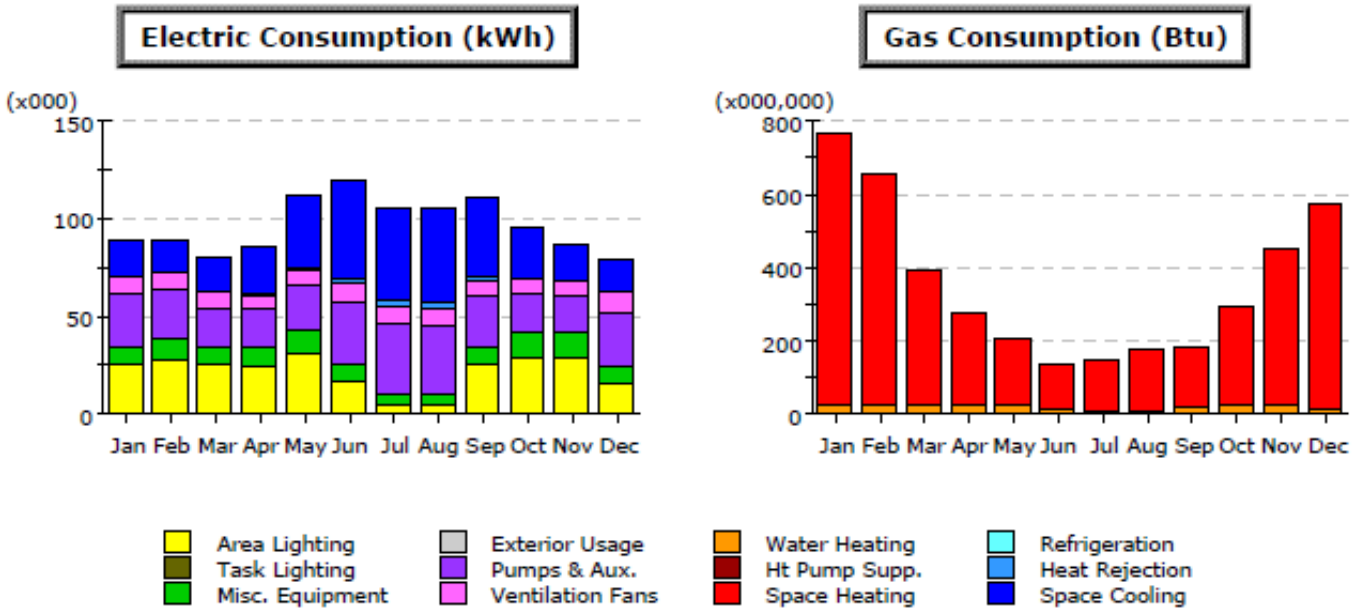

Electric Consumption (kWh x000)

	Jan	Feb	Mar	Apr	May	Jun	Jul	Aug	Sep	Oct	Nov	Dec	Tota
Space Cool	16.2	15.2	16.9	23.9	37.3	49.5	47.4	49.1	40.5	25.5	18.1	16.4	35
Heat Reject.	0.0	0.0	0.1	0.4	1.3	3.2	3.1	3.2	2.0	0.5	0.2	-	1
Refrigeration	-	-	-	-	-	-	-	-	-	-	-	-	
Space Heat	0.5	0.4	0.2	0.2	0.1	0.1	0.1	0.1	0.1	0.2	0.3	0.4	
HP Supp.	-	-	-	-	-	-	-	-	-	-	-	-	
Hot Water	-	-	-	-	-	-	-	-	-	-	-	-	
Vent. Fans	10.0	8.6	8.5	7.8	8.2	8.7	9.1	9.0	8.1	8.0	8.0	10.6	10
Pumps & Aux.	26.2	24.8	19.4	18.7	23.2	32.2	36.0	34.5	25.9	20.1	19.3	28.6	30
Ext. Usage	-	-	-	-	-	-	-	-	-	-	-	-	
Misc. Equip.	10.0	10.8	10.0	9.9	11.9	7.9	4.5	4.6	10.0	11.5	11.4	7.4	10
Task Lights	-	-	-	-	-	-	-	-	-	-	-	-	
Area Lights	24.9	28.1	24.8	24.5	30.8	17.6	5.8	6.0	24.8	29.7	29.7	16.2	26
Total	87.8	87.9	80.0	85.3	112.8	119.1	106.0	106.5	111.4	95.6	86.9	79.6	1,15

Gas Consumption (Btu x000,000)

	Jan	Feb	Mar	Apr	May	Jun	Jul	Aug	Sep	Oct	Nov	Dec	Tota
Space Cool	-	-	-	-	-	-	-	-	-	-	-	-	
Heat Reject.	-	-	-	-	-	-	-	-	-	-	-	-	
Refrigeration	-	-	-	-	-	-	-	-	-	-	-	-	
Space Heat	739.5	627.0	367.8	251.9	177.5	122.1	146.0	176.6	164.3	266.8	421.6	557.7	4,01
HP Supp.	-	-	-	-	-	-	-	-	-	-	-	-	
Hot Water	26.3	30.5	27.1	26.4	30.6	16.1	5.0	4.9	20.4	25.5	27.2	16.7	25
Vent. Fans	-	-	-	-	-	-	-	-	-	-	-	-	
Pumps & Aux.	-	-	-	-	-	-	-	-	-	-	-	-	
Ext. Usage	-	-	-	-	-	-	-	-	-	-	-	-	
Misc. Equip.	-	-	-	-	-	-	-	-	-	-	-	-	
Task Lights	-	-	-	-	-	-	-	-	-	-	-	-	
Area Lights	-	-	-	-	-	-	-	-	-	-	-	-	
Total	765.8	657.5	394.9	278.3	208.1	138.2	151.0	181.5	184.6	292.3	448.8	574.4	4,27

Figure B44. Monthly Energy Use Profile – Combo ECM's VAV – Paducah

Appendix C Project Personnel

Principal Investigator: W. Mark McGinley, Ph.D. PE

Graduate Research Assistants: Robert Shaw – CEE
Graduate Research Assistants: Shawn Mueller – ME
Graduate Research Assistants: Chad Riggs – ME
Graduate Research Assistants: Kevin Muldoon– ME

Research Associate (for Survey Preparation) – Joshua Revard - CIR

Construction Estimator – Patrick Fini – F&R Construction Services

Quarterly Progress Report

(Field Office Project Template)

Project Title: Nano **Final Report**
(Field Office Project Template)

Project Title: Nanostructured Device Designs for Enhancing the Performance of Thin Film CdTe/CdS and CIS/CdS Solar Cell Devices

Award Number: DE-FG36-05G085013 / ULRF 05-1231G

Recipient: University of Kentucky Research Foundation

P.I: Vijay Singh; Co-P.I s: Suresh Rajaputra, Janet Lumpp and Dali Qian

Project Location: 651 F. Paul Anderson Tower (FPAT), University of Kentucky, Lexington, KY 40506-0046

Reporting Period: October 1, 2009 to May 15, 2011

Date of Report: June 20, 2011

Written by: Vijay Singh/Suresh Rajaputra

The increasing demand for energy (from 14 terawatts in year 2000 and projected to grow to 50 terawatts in year 2050) and its environmental impact requires a

renewed effort and novel approaches to developing clean and efficient energy sources. Within this context nanoscience and nanotechnology offers exciting and requisite approaches to addressing these challenges. At the root of the opportunities provided by the nanotechnology is the fact that, all the elementary steps of energy conversion (such as charge transfer, molecular rearrangement, chemical reactions etc) take place at the nanoscale. Thus the development of new materials, device structures as well as methods to characterize, manipulate and assemble them, creates an entirely new paradigm for developing new and revolutionary energy technologies. For the realization of the possibilities offered by nanoscale science and technology, development of novel techniques for fabricating large area, uniform, self-ordered films, is indispensable. Thus, there is a need for a process to economically fabricate large periodic arrays of semiconductor nanostructures that will allow (a) the size and composition to be varied, (b) encapsulation in a rugged host material, (c) flexibility to use a variety of substrate materials. Furthermore, to make practical devices, one must study and understand the electrical and optical properties of Nanostructured materials and their interfaces with other materials, so that new devices can be engineered. A clear understanding of charge transport in nanoscale hetero-junctions is essential for the development of a host of opto-electronic devices.

This project involves the fabrication, characterization and analysis of Nanoscale hetero-junctions inside an insulating Alumina (Al_2O_3) matrix and applying this understanding to increase the short circuit currents and efficiencies of solar cells based on above semiconductors. The potential applications of this research include energy conversion, display devices and sensors. The existing cadmium sulfide (CdS)/cadmium telluride (CdTe) thin film hetero junction solar cells have reached an efficiency level of 16.5%. The existing challenges for achieving still better performance are, (i) light absorption in the CdS window layer, (ii) interface states at the CdTe-CdS hetero junction and, (iii) less than optimal contact to CdTe. Our proposed solutions are, (i) use of nanowire design to reduce light absorption in the CdS window layer, and, (ii) carbon nanotubes (CNTs) based electrode to p-CdTe, instead of the traditional graphite paste electrode. These improvements are expected to yield not only stable electrode, but also efficiencies as high as 21%.

Copper indium gallium diselenide (CIGS)/cadmium sulfide (CdS) solar cells have reached a power conversion efficiency of 19.6%. The path to higher efficiency is through higher open circuit voltage. In this proposal, a size dependent quantum confinement of the band gap energy is proposed as a route to achieve higher open circuit voltage in CIS/CdS solar cells. With our nanowire technology, the CIS

energy band gap will be increased from 1.04 eV to 1.5 eV, and efficiency will increase from 19.6% to 25%.

Objectives: (1) Fabricating controlled diameter nanowire heterojunctions and, understanding the physics of electron transport in them, (2) Using nanowires as ideal absorbers in photovoltaic device structures and, performing a scientific study of the effect of size (wire diameter) on the electro-optical and material characteristics of films and junctions at nanoscale. (3) Applying this knowledge toward achieving higher efficiencies of power conversion in Nanostructured single junction CIS/CdS and CdTe/CdS solar cells.

Methodology: Nanotemplates, consisting of a pattern able uniform array with anodized aluminum oxide (AAO) pores of controllable size (pore diameters ranging from 4 nm to 40 nm and pore lengths of a few micrometers) and spacing will be prepared. Next, pores will be filled sequentially with nanowires of various semiconductors, like CdS, CdTe, CIS, and conducting electrodes (Au, Mo, carbon nanotubes embedded in a polymer, graphite paste, for example). Vertical nanowire junctions and devices, thus obtained, will be characterized and analyzed to develop theoretical models. Theoretical models developed above will be applied toward enhancing the performance (conversion efficiency, lack of degradation with use and time, etc) of these devices.

Anticipated Benefits: Our technology establishes a clear path for increasing the CdS/CIS cell efficiencies to 25% from the current value of 19.6%, and the CdS/CdTe cell efficiencies to 21% from the current value of 16.5%. These thin film solar cells are already a multi-billion industry, which is growing at a fast pace.

DOE Challenges Addressed: This project addresses Kentucky's as well as the National 25X25 Roadmap, specifically the *Solar Photovoltaics* under the Renewable Energy Production theme. This project will also address two (second and forth) of the DOE-BESAC Grand Challenges. Also, from the list of the 10 "Basic Research Needs" workshop reports of the DOE-BES, this proposal will address the needs listed in Report No. 12, "Basic Research Needs for Solar Energy Utilization". Thirdly, this work will address the research targets numbered (iii) and (iv) and employ crosscutting themes, (ii), (iii), (iv), (v) and (vi) listed in Report No. 15 of the DOE-BES Subcommittee, titled, Nanoscience Research for Energy Needs. Also, our work ties in with the DOE's ongoing research efforts http://www1.eere.energy.gov/solar/pv_research_development.html under the Solar Energy Technologies Program (SETP).

Towards this end the following tasks were executed for achieving the listed proposed goals were achieved.

Status:

Task number: 1. *Preparation of sets of anodized porous alumina and titania on molybdenum (Mo) and ITO substrates (1-6 months).*

Planned Activities:

(i) Fabrication of nanoporous alumina on ITO and Mo substrates

(ii) Fabrication of free-standing nanoporous titania

Actual Accomplishments:

Nanoporous anodic aluminum oxide (AAO) was successfully formed on glass-ITO substrates.

In the initial experiments, a residual thin aluminum oxide barrier layer between ITO and the AAO pores remained. Also, there were non-uniformities in the thickness of residual aluminum oxide barrier layer. It was observed that in many templates, even the pores closest to each other could have their barrier layer thicknesses differ by as much as from 10 nm to 20 nm. Residual barrier layer is a serious problem encountered in porous alumina technology because it can cause serious problems in the quality of nanowires deposited later in these pores. Also, this problem is quite common; there are numerous reports on it in the literature.

In our research over the last several months, causes and remedies for this non-uniform residual barrier layer were investigated, including the effects of a thin Ti interlayer inserted between ITO and AAO. Templates with different Ti layer thickness and annealing conditions were compared. Mechanisms for the formation of voids beneath the barrier layer were analyzed and studied experimentally. Reactive ion etch (RIE) was successfully employed as a method to mitigate process non-uniformities. Using above methods, barrier-free AAO templates on ITO substrate were obtained; their thicknesses ranged from 200 nm to 1000 nm. Characteristics of CdS nanowires electrodeposited into the initial templates with non-uniform barrier layer thicknesses and into the processed, barrier-free templates were evaluated and compared. A Manuscript describing this technological advance was published in the IOP Journal *Nanotechnology*. [Piao Liu , Vijay Singh, Suresh Rajaputra "Barrier layer non-uniformity effects in anodized aluminum oxide nanopores on ITO substrates" Nanotechnology, 21 (2010) 115303].

Barrier layer free alumina was also fabricated from Al films deposited using sputtering, e-beam evaporation and thermal evaporation, by optimizing the process parameters (film thickness, buffer layer thickness, anodization conditions, RIE etch conditions).

On the Titania project, high quality films of nanoporous Titania films were prepared by anodization of titanium foils. Techniques developed for free standing films would, next, be extended to the glass-ITO substrates.

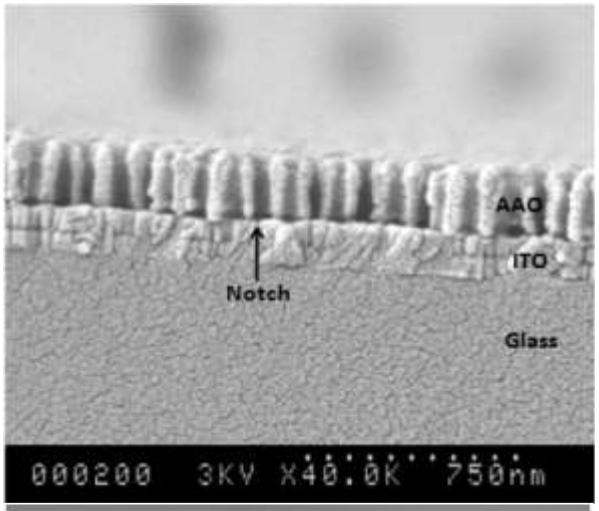

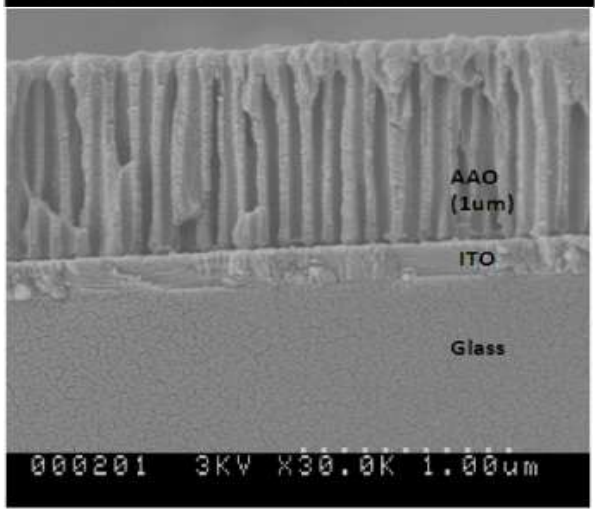

200nm thick AAO on ITO

1micron thick AAO on ITO

Nanoporous AAO on Molybdenum Substrates:

Nanoporous AAO templates have been successfully used to grow semiconductor nanowires using electrochemical and CVD based techniques. In the work related to the fabrication of nanostructured photovoltaic devices, the control of various aspects of the templates are paramount to realizing the theoretical advantages of nanostructured materials. These include the pore diameter, aspect ratio and the pore density. As with any PV technology, the contact formation between the active material and the current collecting contact is crucial for the fabrication of efficient nanostructured PV devices. The use of commercially available AAO templates poses significant limitations in

one's ability to study and conduct research on nanowire based PV devices. Of specific interest to the group's work is the fabrication of $CuInSe_2$ nanowire arrays.

Prior work has established the fact that the chalcogenide nanowires can indeed be electrochemically grown using AAO templates. This was demonstrated using Aluminum (Al) foil as the starting substrate. Such a method however restricts the use of Al as the metal forming a contact with $CuInSe_2$. Due to its innate ability to easily form a protective oxide layer, such an oxide at the bottom of the pore could form easily despite taking steps to etch the barrier layer. This would add to the impedance of the overall device. Also, due to its low work function, Al presents a Schottky barrier to the active p-type $CuInSe_2$ and this is an undesirable trait for a contact to exhibit in a solar cell. An alternative to this would be the growth of the same nanowires in commercially available Whatman templates. This would however limit the growth of nanowires of only one particular diameter. It has hence become imperative to pursue the fabrication AAO templates with metals like Molybdenum (Mo), Nickel (Ni) or Gold (Au) at the bottom of the pores.

AAO templates on rigid ITO substrates have already been successfully fabricated on ITO substrates. This requires the use of a thin Titanium (Ti) interlayer between the substrate and Al. The purpose of this interlayer is primarily to promote adhesion between the substrate and the subsequently formed AAO template. This barrier layer at the bottom of the pores is later removed using a combination of wet and dry etching methods to facilitate a low-resistance electrical path between the semiconductor wire and ITO. To form an ohmic contact, the ITO film is replaced with a thin Mo film. The results however are not identical. It results in templates with pores of unequal depths.

A brief discussion elaborating the observed results is given below. Corrective steps to achieve barrier layer free AAO templates on Mo substrates are also discussed. Similar experimental conditions have thus far led to a spike in the current during the late stages of the third phase of anodization. A typical current transient of the anodization process pertaining to Al on Mo with a thin Ti interlayer is shown in Fig.1. The spike is associated with the rapid removal of all the conducting layers on the insulating glass substrate at the electrolyte-air interface. This essentially causes an open circuit obstructing any further anodization processes. Similar results had been observed on AAO on ITO substrates when the Ti layers weren't thick enough. In the absence of the Mo film, but a thick layer of Ti, neither the spike in current nor the removal of the interface region is observed. In this case, the current gradually drops after the third phase of anodization. Barrier layer template on thick Ti films is shown in Fig.2. This is due to the gradual decrease in the amount of Al available. Once the barrier layer is reached there

is no more Al left to oxidize. Since Ti has a much lower electrical conductivity than Al, the drop in current is not significantly affected. Mo however has a significantly higher electrical conductivity than that of Ti. As a result, once the Al is depleted, the electrolyte comes in close proximity to Mo causing the potential to drastically increase across the film. At the interface between air and the solution however, this change is more pronounced causing the rapid anodization along the length of the air-solution interface. This eventually leads to the complete dissolution of all the conductive layers and thus resulting in the removal of a conducting path between the electrode and the porous membrane. This is characterized by a sudden drop in current. An attempt to circumvent the problem using a thin SiO_2 film (100 nm) on top of the Al film bridging the air and solution resulted in significantly lower rate of dissolution at the interface. Experiments are now being conducted to study this phenomenon while trying to improve the quality of the AAO templates. Shown in Fig.-3 below is an SEM micrograph illustrating the proper formation of AAO pores on thin Mo and Ti layers. Notice the presence of the oxide barrier layer at the bottom of these pores.

Nanoporous Titania Membranes: With our success in making high quality nanoporous alumina membranes all our template needs for device research were met and the task of pursuing nanoporous titania membranes was abandoned.

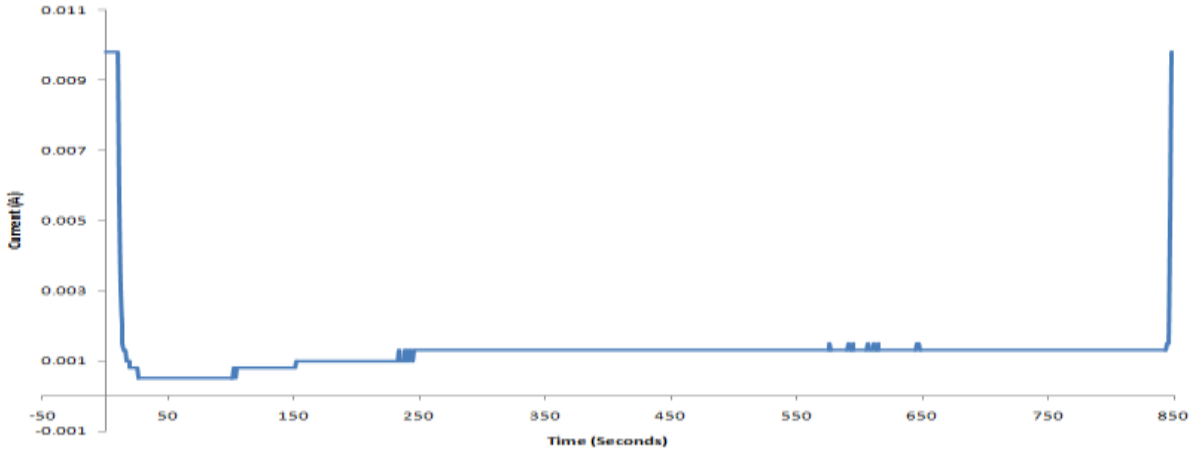

Figure 1: Typical Current Transient for AAO corresponding to AAO templates on Glass with Mo and Ti interlayers

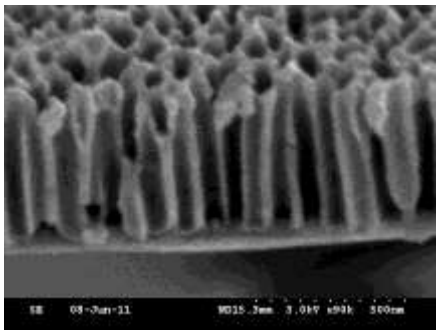

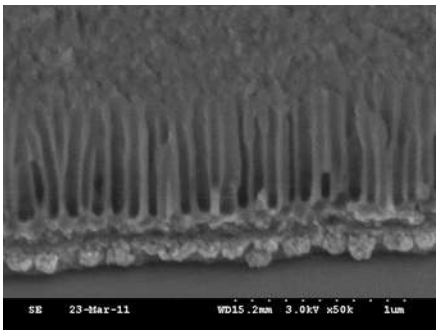

Figure 2: Barrier layer free AAO template on glass with thick Ti interlayer; Figure 3: AAO template on Glass with Mo and Ti interlayers

Task Number 2: ***Electrodeposition of CdS and CIS in nanopores:***

Planned Activities:

Electrodeposition of CdS and CIS in nanopores

Actual accomplishments:

Nanowires of CdS and CIS were electrodeposited into AAO templates. These nanowires were characterized by XRD, SEM and UV-Vis absorption spectroscopy. Lengths of CdS nanowires were in the 100–500 nm range, while the diameter was 30 nm. Also, Au/CdS Schottky diodes were formed on CdS nanowires and analyzed for their electrical and optical characteristics. Transmission electron microscopy observations revealed the single crystalline nature of annealed CdS nanowires. Au/CdS Schottky diodes were formed and their current-voltage characteristics measured to estimate the carrier concentration in the n-type CdS nanowires.

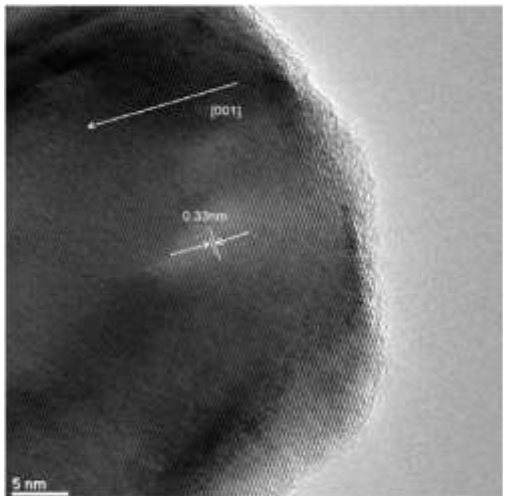

Advantages of a CdS NW window layer in a heterojunction Solar cell:

(a) Cadmium Sulfide (CdS) nanowires on ITO/AAO substrates:

We continued to use the already well established process for the deposition of n-CdS nanowires in the pores of alumina membranes to produce the feedstock for the subsequent deposition of planar CdTe for the CdS-CdTe solar cell devices (described under Task 3 below).

In our nanowire solar cell design, the AAO template is built directly on top of transparent electrode; thus the sunlight can be shined from the CdS side without any substantial loss in transmission. This is operationally close to the traditional front wall CdS/CdTe solar cell device structure, which has the desirable feature that most of sunlight gets absorbed near the p-n heterojunction.

The nanowire CdS layer has higher transmittivity than the traditional planar CdS window layer. It has been observed by us and by several other research groups17-18 that the absorption peak of CdS nanowires is shifted towards the blue region, compared with bulk CdS. For our CdS nanowires, the optical absorption edge lies at a wavelength of 480 nm instead of the 512 nm for the traditional thin film CdS case. This enhances the number of sunlight photons incident on the CdTe absorption layer, and increases the light-generated current and the overall efficiency of solar cell. Furthermore, because aluminum oxide is an insulator with much higher optical transmittivity and CdS nanowires only occupy a portion (depending on the porosity of AAO template) of the window layer, the overall transparency is further increased and more photons can be absorbed in the CdTe layer.

A simulation of photocurrent generated in the CdTe layer is shown below. The x-axis is the photon energy indicated in wavelength (nm), and the *y*-axis is the corresponding current density that is generated by photons at different wavelength (proportional to the number of incident photons). Here we can see that the light generated current density is larger at < 500 nm due to the absorption edge shift in CdS nanowires, especially in the range of 480 ~ 500 nm.

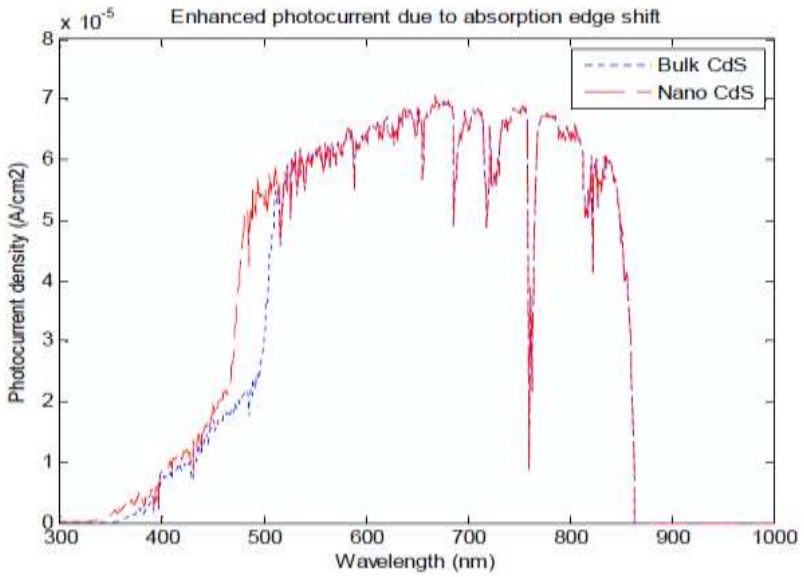

Calculation results reveal that for a CdS layer thickness of 200 nm (both for planar and nano structure), the light generated current gain is about 17%, from 22.4 mA/cm2 to 26.1 mA/cm2. In other words, the number of useful photons reaching the depletion region in CdTe absorption layer will be 17% higher for the AAO embedded NW-CdS window layer (with an absorption edge at a wavelength of 480 nm) than for the traditional CdS window layer (with an absorption edge at a wavelength of 512 nm and same thickness). Thus a 17% improvement in short-circuit current density (Jsc) can be expected.

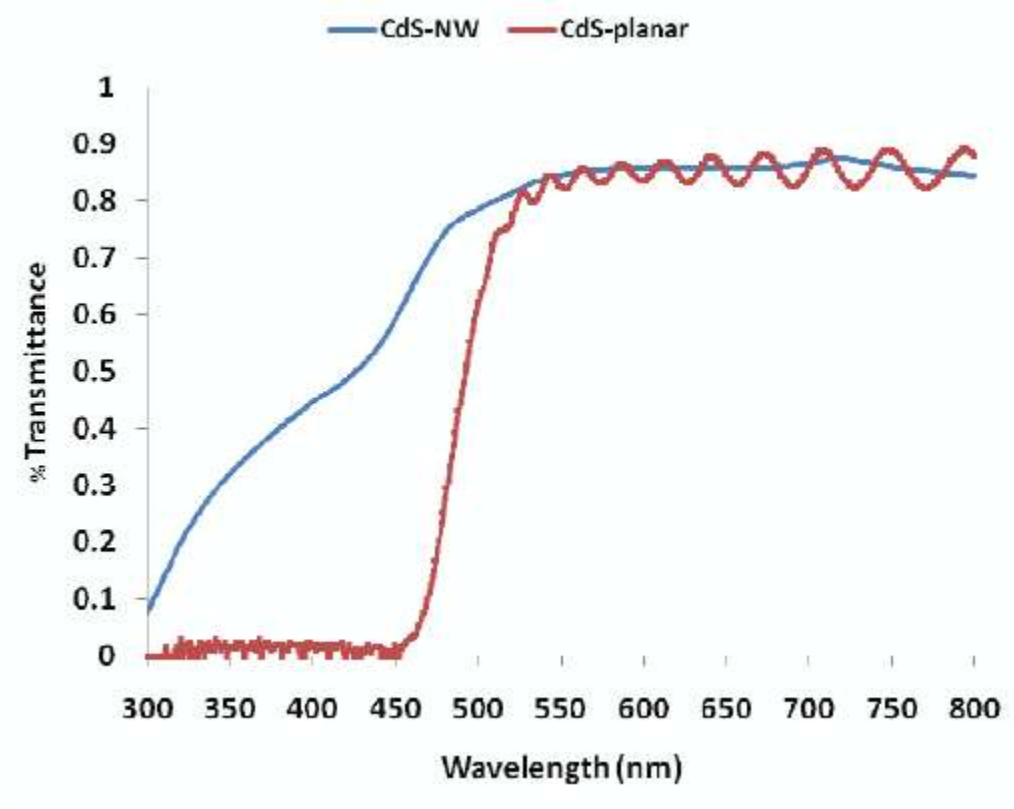

Figure shown above compares the transmittance of a planar CdS film and the CdS nanopillars embedded in a porous alumina template, of 200 nm thickness each. An improvement of light transmission in the wavelength range of 300 - 510 nm for the nanowire matrix can be observed. This is attributed to: (i) higher transmittivity of the aluminum oxide component of the nanowire matrix, and (ii) a reduction in the absorption edge wavelength for the embedded CdS nanowires, as observed experimentally by several research groups in the past. In apparent contrast, a few researchers have reported recently that silicon nanowire arrays have higher absorption than a planar silicon film of equal thickness. This was attributed to the suppressed surface reflection and effectively longer optical path caused by light scattering and the multi-tube of nanostructures in the nanowire matrix. It should be noted, however, that in our case, CdS is a direct bandgap material exhibiting efficient absorption in the wavelength range of 300 - 510 nm. On the other hand, silicon is an indirect bandgap material with less efficient absorption. Therefore, in CdS, enhanced absorption caused by increased optical scattering from nanostructure may not be as important a factor as in the case of silicon. Thus, in our case, higher transmittivity of aluminum oxide and the reduction in absorption edge dominates the optical scattering effect.

Fabrication of Copper Indium Diselenide (CIS) Nanowires by Electrodeposition

CIS nanowires were fabricated using three-electrode deposition in an electrolytic solution consisting of Copper sulfate hydrate, Indium sulfate hydrate, Seleneous acid, Lithium chloride and Potassium hydrogen phthalate of varying quantities. The pH of the solution was adjusted by adding a small amount of HCl to the electrolyte. A one micron thick AAO template on ITO substrate with 50-60 nm pore diameter was used for electro-deposition of CIS nanowires. In the present work, electrochemical deposition was carried out using a simple three-electrode cell with AAO template as the working electrode, a Pt foil as the counter electrode and a saturated calomel electrode (SCE) as the reference electrode. The electrodeposition was performed at a constant voltage of -0.8V. Growth of CIS nanowires in AAO was verified by the Scanning electron microscopy. Cross sectional image of a broken CIS NW/AAO template, UV-Vis absorption spectra of the AAO template, as deposited CIS and annealed CIS are shown below.

CIS nanowires were formed for the first time ever on an ITO/AAO substrate. Previously, we were the first group to fabricate CIS nanowires in an Al/AAO substrate.

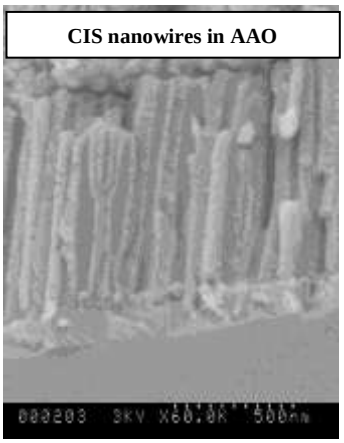

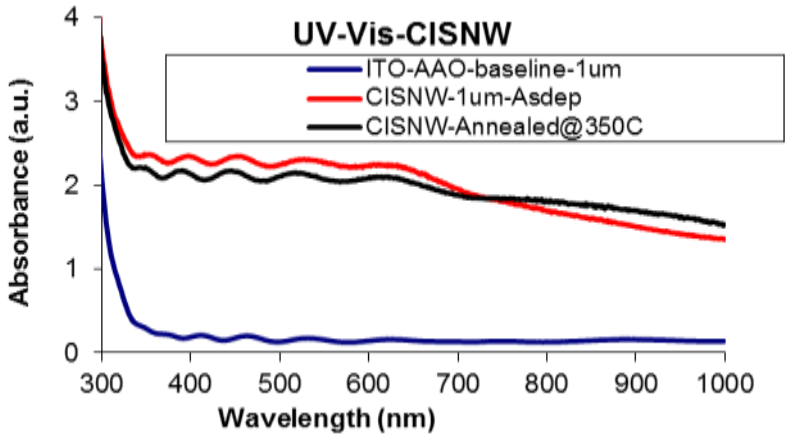

……

CdTe deposition in AAO Templates: We have also carried out CdTe deposition in AAO templates. The electrolyte for CdTe deposition was a mixture of

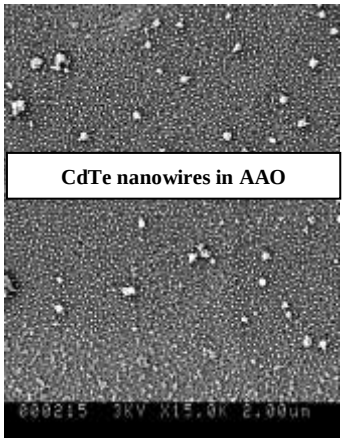

Cadmium Sulfate ($3CdSO_4.8H_2O$) and Tellurium (IV) oxide (TeO_2). For the electrodeposition of CdTe, a 1"x1" platinum electrode was used as the counter electrode, AAO/ITO substrate served as the working electrode and Saturated Calomel Electrode acted as the reference electrode. Electrodeposition was carried out at 600 mV against the reference electrode. The temperature of the electrolyte was maintained at 70° C during the process of electro deposition. The deposited CdTe nanowires were then annealed in N_2 environment to increase the crystallinity of nanowires. Further characterization of these nanowires through EDXA and I-V, C-V measurements is under progress. One of the major problems encountered is the dissolution of the AAO template during CdTe electro-deposition, due to the very acidic (low pH) nature of the bath. We have found ways to mitigate this.

II-VI compound semiconductor materials are being extensively used in the solar cell industry to bring down the cost/Watt of the solar cells. Out of all the metal chalcogenides, Cadmium Telluride (CdTe) is quintessential to the fabrication of low cost solar cells. This is primarily due to its optimal bandgap of ~1.5eV, which matches well with the AM 1.5 solar spectrum; and its high absorption co-efficient (a), which is of the order of 10^5 cm^{-1}. Typically, Cadmium Sufide (CdS) is used as a window layer, and CdTe plays the role of an absorber layer in the thin-film CdS-CdTe heterojunction solar cells. A thin window layer of n-type cadmium telluride nanowires is an interesting alternative to the thin-film CdS window layer used commonly in the present-day CdS-CdTe heterojunction solar cells. We have formed n-CdTe nanowires inside the pores of anodized aluminum oxide (AAO) membranes by electro-deposition and studied their material and electro-optical characteristics. The driving force behind the research was that the efficiency of CdS-CdTe thin-film heterojunction solar cells is stalled at 16.5% for about a decade. The efficiencies of the modules are even less, which stands at about 10-12%. In an attempt to increase the efficiency of the thin-film CdS-CdTe photovoltaics, we have perceived a nanowire homojunction path. The advantage of homojuction is that one could replace the use of Cadmium Sulfide (CdS) as a window layer with CdTe, by confining the CdTe in a 1D or a 0D geometry. This is possible with the realization of CdTe nanowires and quantum dots. Several groups have already reported the quantum confinement phenomenon observed in CdTe nanowires and quantum dots. The main idea here is to tune the bandgap of CdTe nanowire close to the bandgap of CdS. One could also reap benefits by doping CdTe n-type, which could serve as an effective homojunction with bulk p-CdTe with non-existent lattice mismatch. Conventional way of fabricating n-type CdTe is, either by doping CdTe with elements such as phosphorous, Arsenic, Indium etc. as reported previously in the literature. These dopants act as shallow donors, as substitutional sites, in the CdTe crystal lattice by

donating excess electrons to the conduction band at room temperature, which type converts CdTe into an electron rich semiconductor. CdTe could also be made n-type by enhancing the Cd/Te ratio. In electrochemistry, this is done by depositing CdTe at less negative potentials, which favors the underpotential deposition of Cadmium. Furthermore, there were reports indicating the formation of n-CdTe at higher current densities in a galvanostatic deposition.

As a first step towards the formation of CdTe homojunction solar cells, we have chosen the cheapest available route, which is the bottom-up fabrication of n-CdTe nanowires by employing glavanostatic pulse electro-deposition. Here, anodic aluminum oxide (AAO) matrix served as the base template. The AAO matrix is the chosen template because of its excellent periodicity and chemical inertness. Also, AAO matrices have the pore density values ranging from 10^{10}-10^{12} cm^{-2}, which is important for the realization of highly dense nanostructured devices. Two types of AAO matrices were used for the deposition of n-CdTe nanowires. Firstly, for the control, a commercially available Whatman disk with average pore diameters of 160nm, was used with Nickel as a back contact. Secondly, a 50nm diameter and 100nm-500nm length AAO matrix, fabricated in our lab, on ITO-glass substrate was used for the fabrication of low aspect ratio n-CdTe nanowires. Low aspect ratios are crucial for the formation of CdTe homojunctions; this is because of the improved spectral transmittance of the nanowires. The advantage of this is that more carriers are generated in the junction between the n-CdTe nanowire/bulk p-CdTe interface, which could be easily swept by the electric field. Another advantage of using nanowire embedded AAO structure is that the effective optical area of the junction remains the same, because of the high spectral transmittance of AAO template. However, the effective electrical area is going to be reduced by two to four times, depending on the porosity of AAO; which significantly reduces the reverse saturation current density.

For the electro-deposition, a 1"X1" area Platinum plate was used as the anode, and the substrate with AAO pores served as the cathode. The electrolyte consists of 1M $CdCl_2$, 0.01M $TeCl_4$ and 0.3M KI dissolved in Ethylene Glycol. The electro-deposition was carried at a temperature of 163^{o}C. The duty cycle was fixed at 25%, and the current density at 5mA/cm^2. The nanowires obtained were next annealed in a reducing gas (Ar) ambient at 360^{o}C for 30 minutes, to improve the crystallinity of the nanowires. X-ray diffraction of the nanowires confirmed that the CdTe nanowires grow in a cubic phase with a preferential orientation along the [111] direction. Transmission measurements performed on the CdTe nanowires suggested the band edge at ~550nm, which corresponds to an effective absorption band gap of 2.25eV. SEM and TEM analysis was performed to find the filling ratio, wire diameter, length, and crystallite size

of the n-CdTe nanowires. EDAX analysis also suggested that the nanowires were Cd rich, indicating n-type behavior of the CdTe nanowires.
Current-voltage analysis was performed to verify that the CdTe nanowires were n-type. First, indium electrodes of area 0.07cm2 were deposited by thermal evaporation, on top of the CdTe nanowires standing on top of the ITO substrate. J-V curves of this In-CdTe nanowires-ITO sandwich were linear indicating an ohmic contact between CdTe and indium and also between CdTe and ITO. A typical value of CdTe resistivity (ρ) value, calculated from this data, was 2.4*103 Ω-cm. Next, graphite paste electrodes, instead of indium, were applied to the top of the CdTe nanowires. This time, the current-voltage measurements indicated Schottky diodes instead of resistors. Analysis of Schottky diode characteristics in the dark and under 1-sun illumination yielded diode ideality factor (n) values of 3.9 and 6.1 respectively. The corresponding values for the effective reverse saturation current densities (Jo) were 0.41μA/cm^2 in the dark, and 2.86μA/cm^2 under 1-sun illumination.

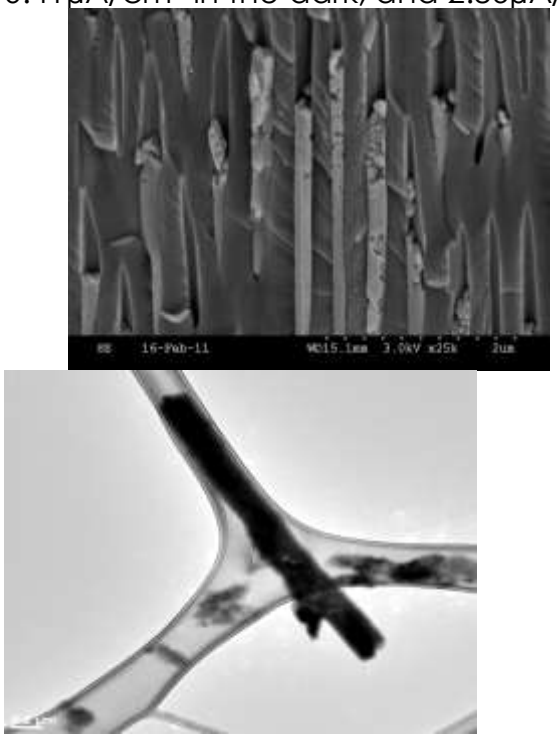

(a) **(b)**

Fig. (a): SEM image of n-CdTe nanowires embedded in AAO; Fig. 1 (b): Low magnification TEM image of n-CdTe nanowire dispersed on a Cu grid

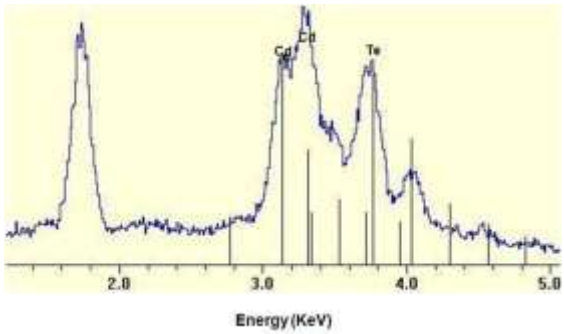

Fig : EDAX profile of CdTe nanowires embedded in alumina membrane

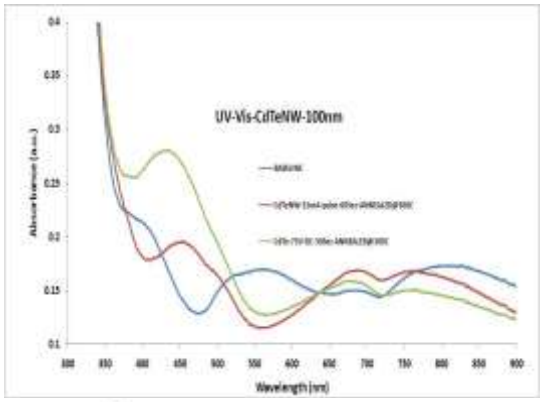

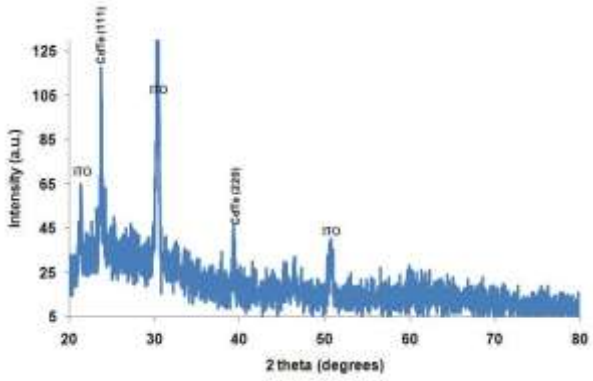

(a) (b)

Fig (a): Spectral transmittance of n-CdTe nanowires in AAO matrix; Fig (b) Diffraction pattern of n-CdTe nanowires showing c-axis oriented in longitudinal direction along the (111) plane

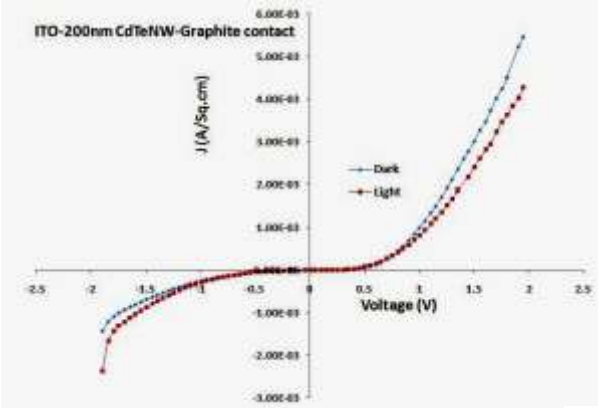

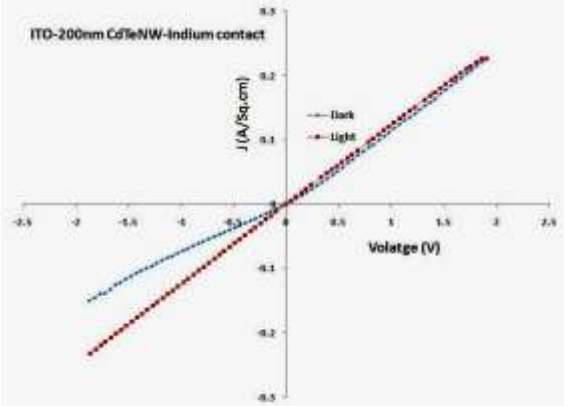

(a) **(b)**

Fig (a): JV curve of an ITO-n-CdTe nanowires-Graphite structure embedded in alumina matrix; Fig (b) JV curve of an ITO-n-CdTe nanowires-Indium structure embedded in alumina matrix

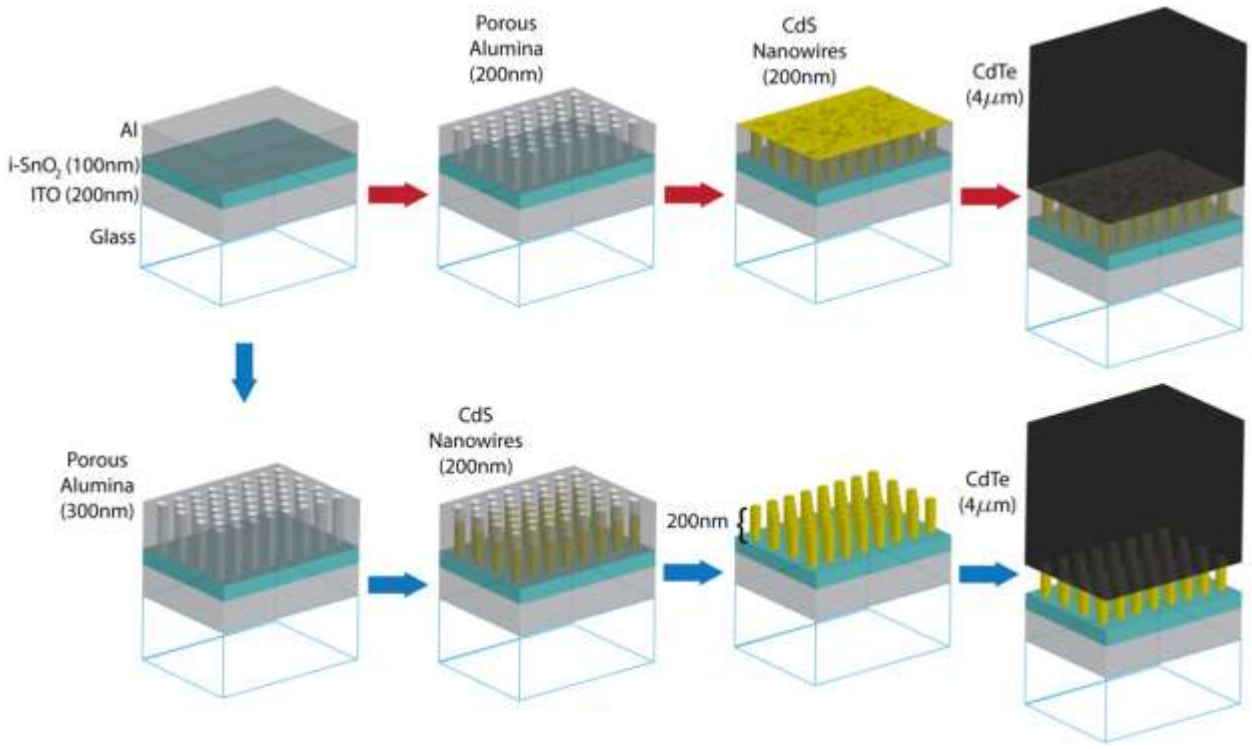

Figure . Flowchart of the newly designed fabrication process of CdS-nanowire-based CdTe–CdS solar cells. Top row—design A: CdS nanowires remained embedded in nanoporous alumina (AAO) templates; Bottom row—design B: CdS nanowires were free-standing.

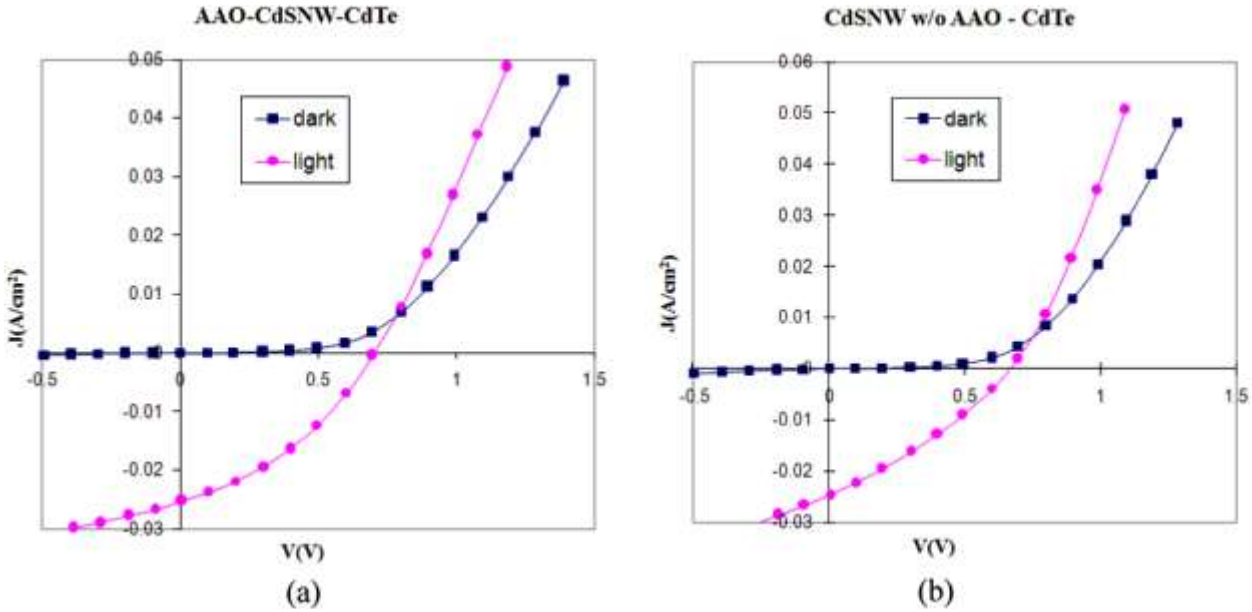

Figure . Solar cell *I–V* characteristics of (a) design A: CdTe on CdS nanowires embedded in AAO and (b) design B: CdTe on free-standing CdS nanowires

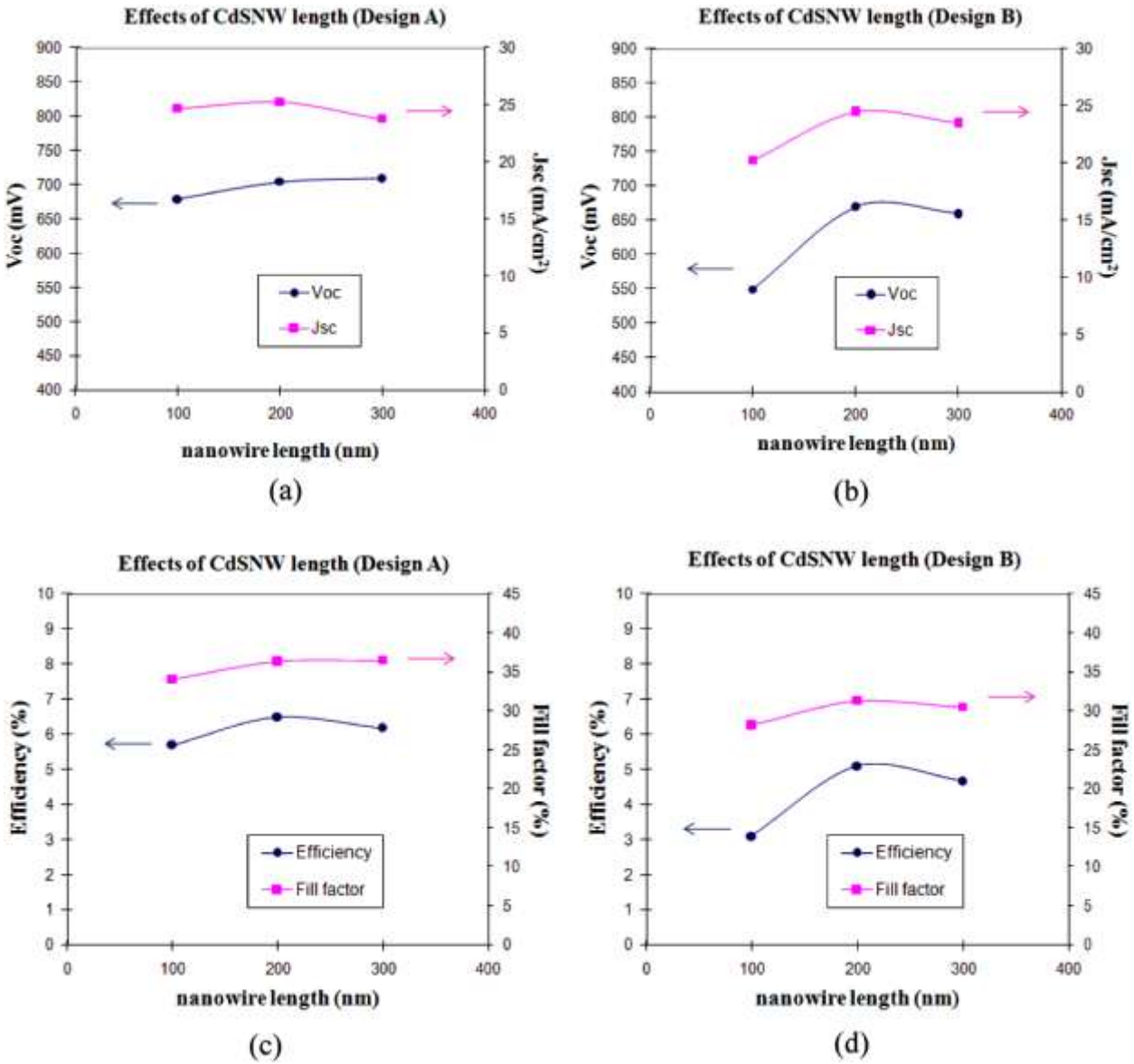

Figure. Top: open circuit voltage and short circuit current density of solar cell, (a) Design A and (b) design B. Bottom: fill factor and efficiency of (c) design A and (d) design B.

Materials and electro-optical characterization of semiconductor nanowire heterojunctions:

Actual accomplishments: Structural, electronic and optical characterizations including XRD, SEM, TEM, current-voltage (I-V), capacitance-voltage (C-V), and spectral absorption, were performed on the NW, n-CdS/Bulk, p-CdTe solar cell device above. Interestingly, higher performance was observed in the devices of Case I (CdS NWs embedded in AAO matrix) than the devices of Case II (freestanding CdS nanopillars on ITO; AAO matrix dissolved).

CdS, CIS and CdTe nanowires (NWs) were characterized with SEM, XRD, EDX, spectral transmission in the UV-Vis and near infra-red wavelength range, and current-voltage and capacitance-voltage characteristics of Schottky diodes formed on the nanowires. CIS nanowires were found to have p-type conductivity while the CdTe nanowires were n-type.

In addition we also designed and built vapor deposition systems (chemical vapor deposition (CVD), and close space sublimation (CSS) to serve as alternate methods for the growth of semiconductor layers.

Close Spaced Sublimation of CdTe films

A deposition system capable of independently controlling the source and substrate temperatures up to 650^0C, operating down to a pressure of 48 mTorr, utilizing 4 quartz lamps (1000W each), SCR power control was setup. The system can be used to deposit films in Vacuum, Ar or He ambient. The system is capable of reaching up to 100^0C/min ramping rate. Several CdTe films were deposited through modification of chamber pressure, varying δT (source-substrate temperature), in situ annealing. The films were characterized by X-ray diffraction, Scanning Electron Microscopy and UV-Vis Absorption spectra. The X-ray diffractogram of as grown CdTe film shows a cubic phase.

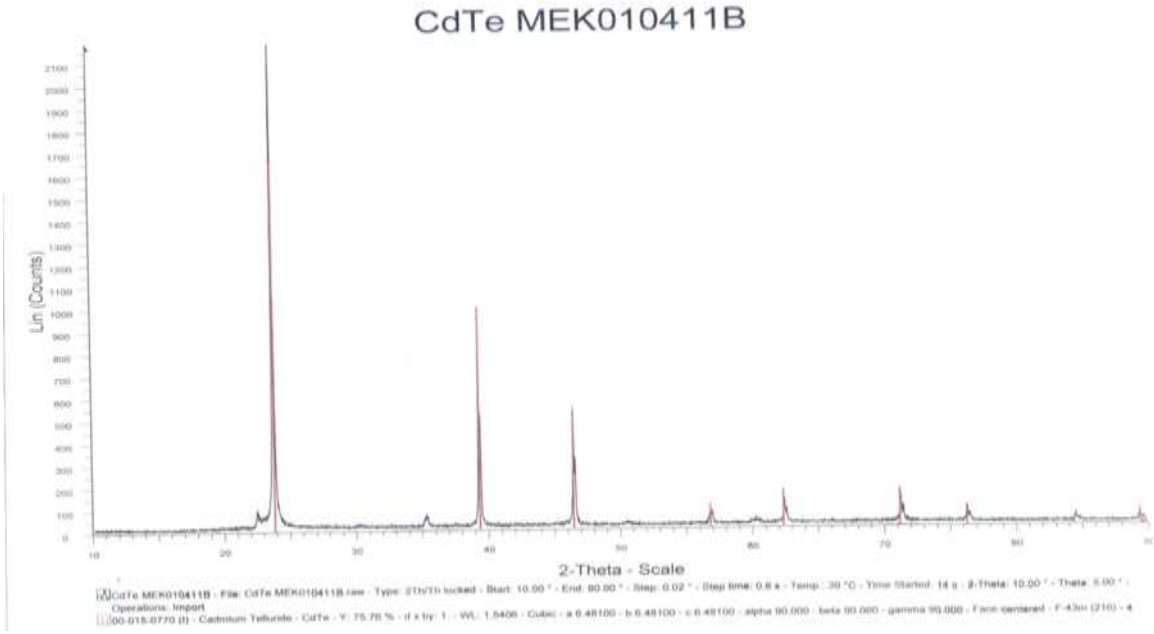

UV-Vis absorption measurements of CdTe film showed an absorption edge around 850nm.

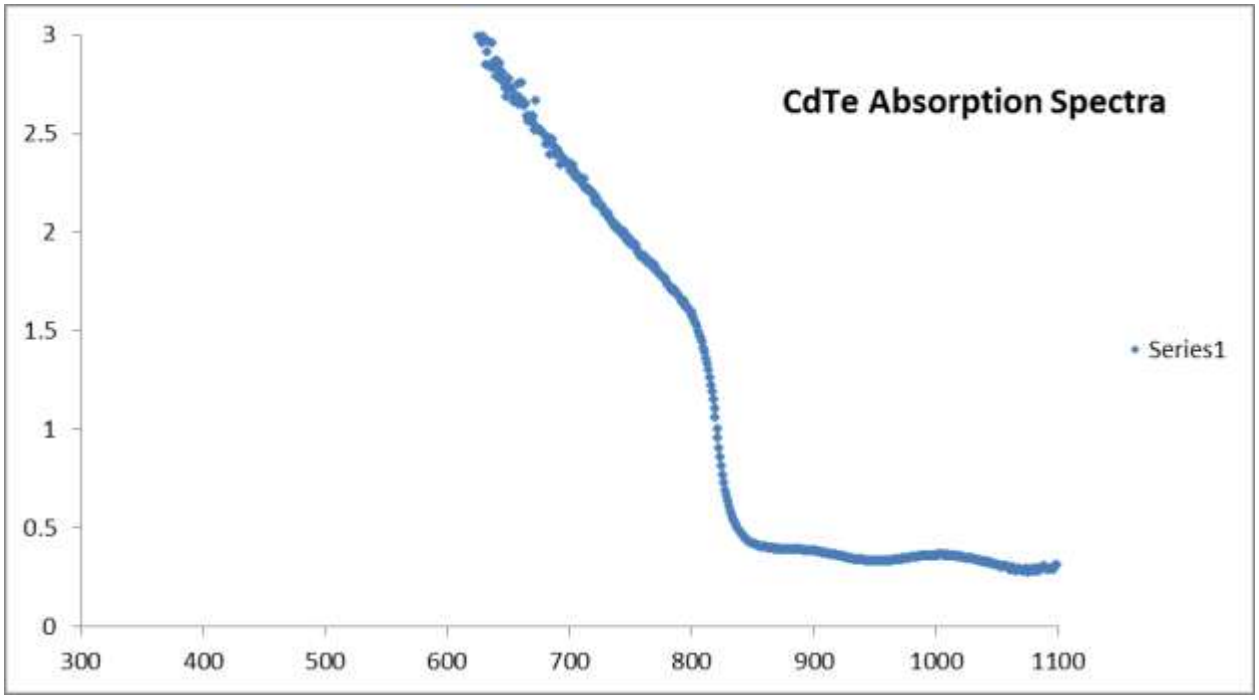

Electron microscopy observations revealed that the CdTe grain size is a sensitive function of chamber pressure.

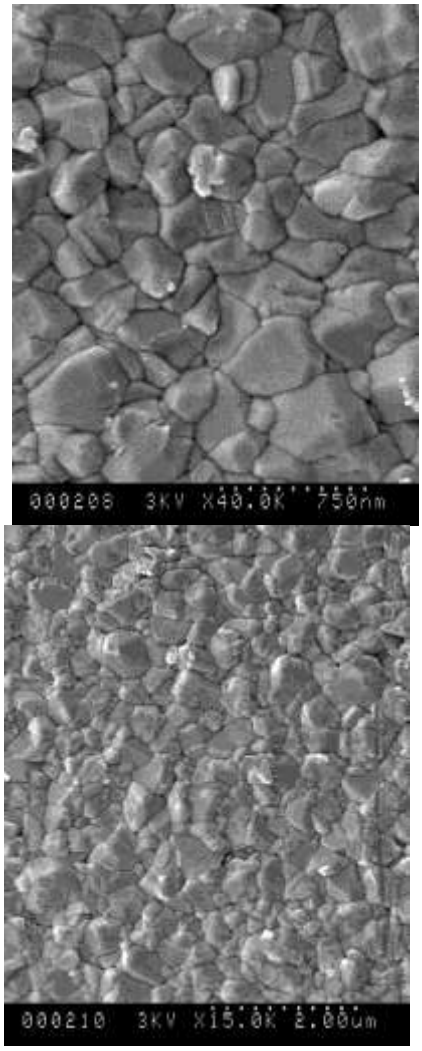

CdTe films deposited by CSS at 150 mTorr (□T=200^{0}C)

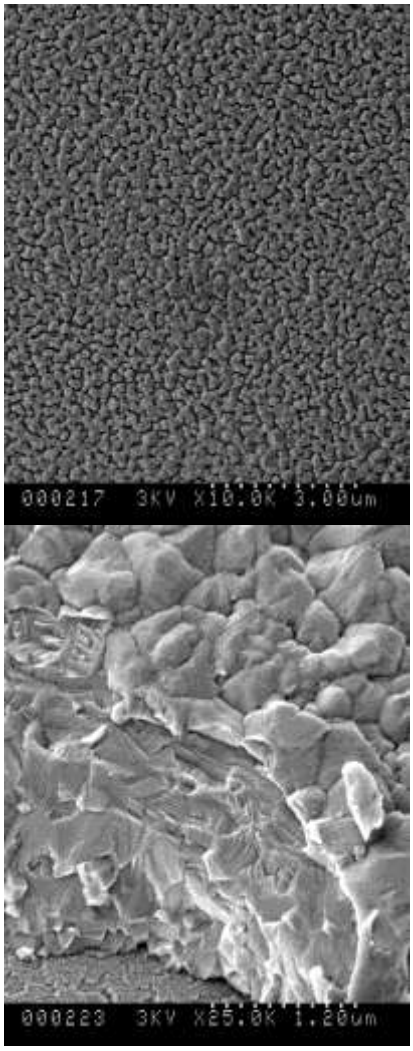

CdTe films deposited by CSS at 100 mTorr (□T=200^{0}C)

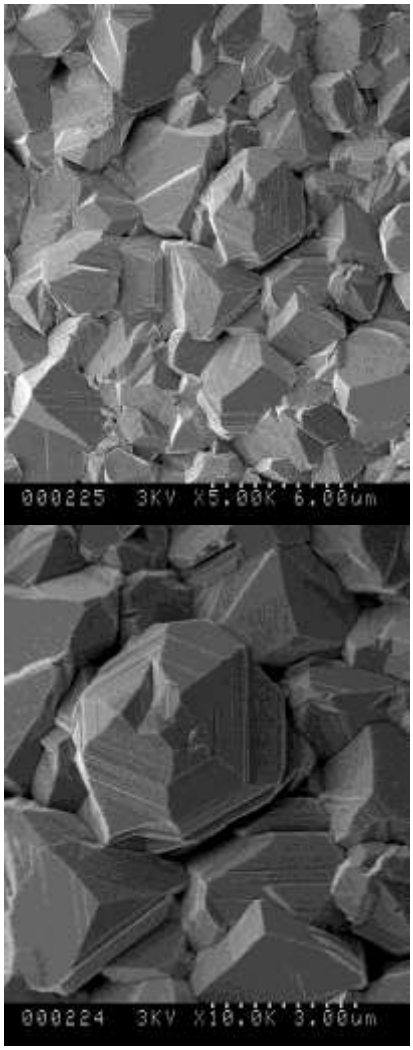

CdTe films deposited by CSS at 100 mTorr (□T=100^{0}C)

The CdTe grain size can be controlled from about 200nm – 6μm by varying the process parameters. Currently we are fabricating CdS/CdTe heterojunction devices using the CSS process for the CdTe layer deposition. The devices are being characterized for their material, optical and optoelectronic properties.

Publications:

1. "Nanostructured Solar Cells Based on Cadmium Sulfide and Copper Pthalocyanine", Presented at 19 th International Materials Research Congress, Cancun, Mexico, August 18, 2010.

2. "Schottky Diodes on Nanowires of CIS and CdTe Embedded in Porous Alumina Templates", Invited Talk at TMS- 2010, 139th Annual Meeting, Seattle, Washington, USA, February 15, 2010.

3. Piao Liu, Vijay P. Singh, Suresh Rajaputra "Barrier layer non-uniformity effects in anodized aluminum oxide nanopores on ITO substrates" Nanotechnology, 21 (2010) 115303

4. Piao Liu, Vijay P. Singh, Suresh Rajaputra, Sovannary Phok and Zhi Chen "Characteristics of copper indium diselenide nanowires embedded in porous alumina templates", *J. Mater. Res., Vol. 25, No. 2, Feb 2010*

5. Sai Guduru, Vijay P. Singh, Suresh Rajaputra, Shounak Mishra and Ingrid St. Omer "Characteristics of gold/cadmium sulfide nanowire Schottky diodes" *Thin Solid Films 518 (2010) 1809–1814*

6. Piao Liu, Vijay P. Singh, Carlos A. Jarro, Suresh Rajaputra "Cadmium sulfide nanowires for the window semiconductor layer in thin film CdS-CdTe solar cells", 2011 *Nanotechnology* **22** 145304

Our publication on nanowire solar cells has received lot of attention in the PV and nanotech community. Our article has been downloaded more than 250 times within the first 4 weeks of publication, as per the email from the editor.
www.nanotechweb.org, the premier website for advances in nanotechnology featured a blog about our article. http://nanotechweb.org/cws/article/lab/45726

New Grant:

Project Title: Power and Energy Institute of Kentucky (PEIK)
Award Amount: $2.5 Million; Funding Agency: Department of Energy
Award Period: 04/01/2010 to 03/31/2013 ;
PI: Larry Holloway; Co-PIs: Vijay Singh, Yuan Liao, Aaron Cramer, Joe Sottille, Paul Dolloff, Y.T. Cheng, Steve Lipka, Donld Colliver, et al

Grants Pending:

- **Funding Agency:** National Science Foundation; Grant/Contract Number: Decision Pending; **Project/Proposal Title**: Nanowire Heterojunctions for Enhancing the Performance of Thin Film Solar Cell Devices; ***P.I:*** *Vijay P Singh,* **Co-PIs**: Suresh Rajaputra and Charles E May ; **Total Award Period Covered:** 09/01/2011 to 08/31/2014; **Total Requested Amount**: $398,771

Final Report

Project Title: Li ion batteries for electric vehicle applications

Award Number:

Recipient: Prof. Mahendra Sunkara and Prof. Gamini U. Sumanasekera, University of Louisville
Project Location: Conn Center for Renewable Energy Research, Ernst Hall, University of Louisville, Louisville, KY 40292

Reporting Period: 10/15/2009 – 6/20/2011 (including no cost extension)
Date of Report: 6-26-2011
Written by: Prof. M. Sunkara (PI) and Prof. Gamini U. Sumanasekera, Co PI
Status:

Task number 1: Scale up production of tin oxide nanowires

Planned Activities: Batch scale production on gram scale and scale-up production to hundred-gram scale

Actual Accomplishments

- We assembled a version of atmospheric plasma reactor using a smart match power supply for continuous operation over several hours. Prior version of the reactor experienced interruptions of plasma due to problems with power supply and manual matching.
- Performed continuous production runs using zinc oxide as model system. Made tens of grams of nanowire powders (with high quality).
- Examined various options such as cyclone separator, filter bags, charged plate collection, and bubbling gas through solvents, etc. It is determined that filter bag is the best possible option for collecting nanowire powders in our reactor configuration.
- This task has been successful in terms of achieving hundred gram capacity production using our atmospheric plasma discharge reactor. The process chemistry for producing tin oxide nanowires is similar to that of zinc oxide (i.e., direct oxidation of metal powders during down pour inside atmospheric plasma system).
- A manuscript is currently being written up for a journal publication (the reactor design and optimization studies).

Task number 2: Coin cell assembly and testing

Planned Activities: Make coin cells using tin oxide nanowire materials.
Actual Accomplishments:

- Basic and fundamental studies were conducted using tin cluster covered tin oxide nanowire powders for understanding their lithiation and de-lithiation behavior.
- Studied MoO_3 NW array films for capacity and lithium ion intercalation/de-intercalation properties. The MoO_{3-x} nanowire arrays are shown to retain a capacity of ~630 $mAhg^{-1}$ for up to 20 cycles at a current density of 50 mAg^{-1}. These nanowire arrays undergo a 2 stage lithiation/de-lithiation mechanism which occurs above 1.5 V and below 0.7 V leading to retention of 3.4 Li ions per Mo. In addition, nanowire arrays show good capacity retention of ~500 $mAhg^{-1}$ below 0.7 V indicating viable practical applicability of the material. In addition, Si/MoO_{3-x} hybrid nanowires synthesized by the direct deposition of Si on MoO_{3-x} nanowire arrays have shown higher capacity retentions of ~780 $mAhg^{-1}$ paving ways for high capacity stable anode materials.
- The student (Praveen Meduri) graduated and joined PNNL. So, we have trained new graduate students with fabrication and testing of coin cells, pouch cells and flooded cells.
- Ordered necessary supplies for fabricating coin cells and pouch cells and fresh electrolyte. Several students have been trained on assembling coin cells, flooded cells, and pouch cells and also in testing them using both charge-discharge procedures, cyclic voltammetry and electrochemical impedance spectroscopy.
- Coin cells were made using tin oxide powders and standard materials.

Task number 3: Synthesis of hundreds of grams of the material and fabrication of bigger 18650 cells.

Planned Activities: Make pouch cells using tin oxide nanowires and perform initial testing.

Actual Accomplishments:

- In the present scenario, pouch cells are attractive than the 18650 cells for automotive applications due to the simplicity involved in their fabrication, their flexibility and are lightweight compared to other types of batteries.
- Several students were trained on the assembly of pouch cells using standard materials. Students produced pouch cells (single stack) and demonstrated their performance with lighting up small LED lights. Dr. E. Dayalan provided initial training for students.
- Assembled pouch cells using molybdenum oxide nanowire array coated substrates.
- Assembled pouch cells using tin oxide powders (paste and producing films using doctor blading technique and thermal annealing).

Task number 4: Report writing

Final report is submitted on June 26, 2011.

Contributed to the on-going Patent applications:

1. M.K. Sunkara, P. Meduri and G.U. Sumanasekera, “High capacity anode materials for Li Ion batteries”, US Provisional Patent Application 61/141,502, December 2008.

2. M.K. Sunkara, J.H. Kim and V. Kumar, "Reactor and Method for Production of Nanowires", US Provisional Patent Application Filed, 60/978,673, October (2007).

Publications in refereed journals.

1. M K Sunkara, C Pendyala, D Cummins, P Meduri, J. Jasinski, V Kumar, H B Russell, E L Clark, and J H Kim, “Inorganic nanowires: a perspective about their role in energy conversion and storage applications”, *J. Phys. D.,* (2010).

2. P. Meduri, E.L. Clark, E. Dayalan, G.U. Sumanasekera, and M.K. Sunkara, “Kinetically limited de-lithiation behavior of nanoscale tin covered tin oxide nanowires”, *Energy and Environmental Science*, 4, 1695-1699 (2011)

3. P. Meduri, J.H. Kim, H.B. Russell, J. Jasinksi, G.U. Sumanasekera and M.K. Sunkara, "Thin Walled Carbon Microtubes as High Capacity and High Rate Anodes in Lithium Ion Batteries", *J. Phys. Chem. C.*, 114, 10621 (2010)

4. P. Meduri, E.L. Clark, E. Dayalan, G.U. Sumanasekera, and M.K. Sunkara, “Durability and high capacity retention of pure and silicon coated MoO3-x nanowire arrays for Lithium Ion batteries”, Manuscript in submission stages (2011). (A draft of this manuscript is attached at the end of this report).

Durability and high capacity retention of pure and silicon coated MoO_{3-x} nanowire arrays for Lithium-Ion Batteries

*Praveen Meduri,[1] Ezra Clark,[1] Ethirajulu Dayalan,[2] Gamini U. Sumanasekera,[3] and Mahendra K. Sunkara[1,] **

[1]Department of Chemical Engineering, [3]Department of Physics

University of Louisville, Louisville, KY 40292

[2]ENSER Corporation, Orlando, FL 32817

*Corresponding author: mahendra@louisville.edu

Abstract

In this study, the electrochemical properties of vertical nanowire arrays of MoO_{3-x} grown on metallic substrates are presented. The MoO_{3-x} nanowires with diameters of ~90 nm show high capacity retention of ~650 $mAhg^{-1}$ for up to 20 cycles at 50 mAg^{-1} current density. In addition, these materials exhibit a capacity retention of ~500 $mAhg^{-1}$ in the voltage window of 0.7 – 0.1 V, higher than the theoretical capacity of graphite and better performance than their nanoparticle counterparts. The enhanced capacity retention is attributed to high surface area, 1-dimensional electronic conductivity and shorter Li ion diffusion lengths inside the material. In addition, 10 nm Si coated MoO_{3-x} nanowire arrays have shown a capacity retention of ~780 $mAhg^{-1}$ indicating that high capacity hybrid materials are the next generation materials forg lithium ion batteries.

Introduction

Lithium ion batteries have gained tremendous interest for portable devices because of their superior energy capacity, long shelf life and longer lifespan.[1] Safe, non-toxic and high rate capable materials present significant interest for use in hybrid electric vehicles.[2] The most widely used graphite anode has a theoretical capacity of 372 $mAhg^{-1}$ at ~0.1 V w.r.t Li/Li^{+}. In operation, graphite anodes have even lower reversible capacities. Other forms of carbon including carbon fibers,[3] carbon nanosprings[4] and carbon microtubes[5] have shown to yield higher capacities but still have significant problems at low potential operation (<0.1 V). Metal oxides are possible choices for anode materials but suffer from capacity fading with cycling due to enormous volume expansions on lithium intercalation and de-intercalation and poor kinetics. Recently, cobalt oxide,[6] Sn/SnO_2 hybrid architectures[7] and iron oxide[8] have shown high capacity retention with low capacity fading.

MoO_3 is a well known anode material for lithium insertion.[9] However, bulk MoO_3 has shown high initial capacity followed by significant capacity fading with cycling. MoO_3 doped with sodium and tin have shown high initial capacity but suffer from capacity degradation as well.[10, 11] Recently, chemical vapor deposited MoO_3 nanoparticles exhibited a capacity of 630 $mAhg^{-1}$ for up to 150 cycles when cycled between 3.5 V and 0.005 V.[12] Ball milled MoO_{3-x} samples have also been shown to exhibit a high initial discharge capacity of 1100 $mAhg^{-1}$ but the material undergoes

capacity degradation with cycling with a capacity retention ~620 $mAhg^{-1}$ after 35 cycles.[13] In addition, the capacity in these electrodes is obtained over the entire potential which hinders their use as an ideal electrode material. To our knowledge, one-dimensional MoO_3 nanowires have not been investigated as electrode materials. One-dimensional nanowires can provide good conduction pathways for electronic conductivity along with smaller length dimensions (diameter) for lithium interaction. Here, single crystalline MoO_3 nanowire arrays have been synthesized directly on conducting substrates and studied for electrochemical and lithium intercalation properties.

Experimental Details

MoO_3 nanowires were synthesized in a hot-filament chemical vapor deposition reactor under low oxygen partial pressure over molybdenum hot filaments. Molybdenum filaments were resistively heated to 775 ^oC using 10 sccm of oxygen at a pressure of 1.1 Torr. Under these conditions, the oxygen flow over Mo filaments resulted in molybdenum oxide vapor. Stainless steel substrates were placed 1.5 cm apart from the hot-filament. MoO_3 NW arrays were also grown on various substrates beyond stainless steel such as copper, platinum mesh, fluorinated tin oxide coated quartz and quartz. The synthesis was carried out for duration of 30 minutes. Nanowire arrays were characterized for their morphology and using scanning electron microscopy (FEI Nova 600). The nanowire was also characterized using X-ray diffraction (XRD) (Bruker D8 Discover, Cu Kα radiation) and Raman spectroscopy (in-Via Renishaw micro-Raman system with a

cooled CCD detector) with a HeNe laser (632.8 nm) as an excitation source to obtain the crystal structure.

The as synthesized nanowires on conducting substrates were used as electrodes for electrochemical measurements. A three electrode cell was employed consisting of working electrode (nanowire sample) and lithium as both the reference and the auxiliary electrode. The electrolyte is a 1M lithium hexaflourophosphate ($LiPF_6$) mixed with 1:1 volume ratio of ethylene carbonate (EC) and diethyl carbonate (DEC). The cell assembly and testing was carried out in glove box filled with argon using an eDAQ potentiostat and e-corder for all the electrochemical measurements.

Results and Discussion

MoO_3 nanowires were synthesized using chemical vapor transport of molybdenum vapors using oxygen/air flow over hot filaments made of Molybdenum. The condensation of molybdenum oxide vapors on stainless steel substrates resulted in MoO3 NW arrays. Figure 1a shows that nanowires have average diameters of ~90 nm. The XRD spectrum presented in Figure1b indicates an oxygen deficient $Mo_{17}O_{47}$ phase.[14] Oxygen deficiency renders the dark blue color to the resulting films. Raman spectrum for these arrays is shown in Figure 1c. The peaks at higher wavenumbers (905 and 984 cm^{-1}) are as a result of the Mo-O vibrations whereas the peaks at 830 cm^{-1} is due to the vibrations of Mo-O_2 bonds. In addition, Mo-O_3 vibrations result in the 799 cm^{-1} peak.[14] The presence of multiple peaks indicates complex interactions of Mo an O atoms further indicating that the nanowire arrays are oxygen deficient.

MoO_{3-x} nanowires were cycled between 100 mV and 3.5 V. The data in Figure 2a shows that the specific capacity retention of the nanowires is ~630 $mAhg^{-1}$ for up to 25 cycles. The initial discharge capacity is ~770 $mAhg^{-1}$ at a current density of 25 mAg^{-1} corresponding to 4.1 Li^+ ions per MoO_{3-x}. The second discharge capacity is ~635 $mAhg^{-1}$ which remains constant until 20 cycles, at a current density of 50 $mAhg^{-1}$. MoO_{3-x} electrodes in the present study are cycled until 100 mV, which prevents the lithium plating at the expense of capacity. The first cycle irreversible capacity loss is 176 $mAhg^{-1}$ corresponding to a columbic efficiency of 70% which is quite low in transition metal oxide systems. The columbic efficiency as indicated in Figure 2a is over 90% for the subsequent cycles. The lithiation in MoO_3 is believed to take place in two stages:[15] Stage I occurs up to a potential of 1.5 V. During this stage, Li intercalates with MoO_3 as follows:[10, 16]

$$MoO_3 + xLi^+ + xe^- \rightarrow Li_xMoO_3 \quad (1)$$

The lithium content in this solid solution ranges between 1 – 1.5 up to a potential of 1.5 V. The high lithium content is accommodated in the interlayer spacing between octahedron Mo-O layers and intralayers. Most of the Li ions intercalated at these potentials can subsequently be extracted from the material leading to reversibility of the reaction.

Lithium ion intercalation during stage II corresponds to potentials below 0.7 V and occurs by the following mechanism:[17]

$$Li_xMoO_3 + yLi^+ + ye^- \rightarrow Mo + 3Li_2O \quad (2)$$

In the lower voltage range, lithium reacts with the solid solution to consequently form metal and Li_2O. The metal particles help in reversibly decomposing Li_2O and form MoO_{3-x}. Discharge curves presented in Figure 2b indicate a curve which is continuous and smooth until 0.7 V followed by a plateau unlike the bulk material performance devoid of plateaus. MoO_3 nanoparticles have been known to show similar two-stage behavior; however, the curves in that particular case are continuous and have much lower capacity retention below 0.7 V. This reversibility of Li_2O is a primary reason for the material to exhibit good columbic efficiency.

The differential capacity curves shown in Figures 2c and 2d support the two stage mechanism. The first cycle differential capacity (DC) curve shows a small peak in the higher potential region above 1.5 V and multiple peaks in the low potential region below 0.5 V. These peaks indicate the Li intercalation by a mechanism shown in Equations 1 and 2. DC curves for the next few cycles also indicate peaks above 1.5 V and below 0.5 V, further confirming the mechanism. These peaks appear until the 10^{th} cycle as indicated in Figure 2c showing excellent reversibility of the electrode.[18] Figure 2d is the DC curves for the charge cycle of these arrays. The charge cycles clearly indicate peaks around 0.5 V, 1.2 V, 1.8 V and 2.6 V indicating that the de-lithiation occurs in two stages. In addition, the peak occurrence suggests that MoO_{3-x} is reversible formed with low loss in the capacity with cycling.

A complete reduction of MoO_3 requires 6 Li^+ ions per Mo. The first cycle capacity of ~770 $mAhg^{-1}$ corresponds to 4.1 Li^+ ions per one Mo atom, of which 1.1 Li^+ ions are intercalated as indicated in Equation 1. The remaining 3 Li^+ ions intercalate with the solid solution by the mechanism indicated in Equation 2. This indicates an incomplete

conversion to Li_2O + Mo. Further cycles indicate capacities close to ~650 $mAhg^{-1}$ corresponding to 3.4 Li^+/Mo. However, the data over next few cycles shows interesting behavior, i.e., the addition of lithium (Equation 1) accounts to less than 100 $mAhg^{-1}$ that corresponds to only ~0.6 Li^+/Mo. The alloying reaction (Equation 2) accounts for ~500 $mAhg^{-1}$ capacity equivalent to 2.8 Li^+/Mo, indicating a good reversibility of the alloying reaction. The data pertaining to capacity retention between 0.7 V and 0.1 V is presented in Figure 3a which makes the materials practically usable. Nanowire arrays have shown capacity retentions of 632 $mAhg^{-1}$ and 590 $mAhg^{-1}$ at current densities of 50 $mAhg^{-1}$ and 100 mAg^{-1} respectively (Figure 3b). It is to be noted that a capacity of 685 $mAhg^{-1}$ at 25 mAg^{-1} is obtained on switching from the high rate back to low rate. These nanowire arrays can hence, be used as base materials to develop hybrid architectures with high capacity materials. Si is particularly interesting as the intercalation potentials of Si and MoO_3 match well at around 0.7 V making them ideal hybrid materials.

In order to prove the hybrid architecture proposition, MoO_{3-x} nanowire arrays were coated with silicon. The TEM image presented in Figure 4a shows a 10 nm Si deposition on the surface. However, line scan of the image shows the presence of low oxygen amounts in silicon. In theory, ~10% silicon is present in these samples (by weight) which corresponds to a theoretical capacity of ~1370 $mAhg^{-1}$ for the sample, compared to 1116 $mAhg^{-1}$ for pure MoO_{3-x} nanowire arrays. The specific capacity data in Figure 4b shows that the hybrid material shows an initial capacity of 1065 $mAhg^{-1}$ with capacity retention of ~780$mAhg^{-1}$ until 15 cycles. Most importantly, the cycling data over 15 cycles shows stable performance of hybrid material. The capacity of these can be significantly improved by thicker Si deposition. In a typical MoO_3 nanowire array

sample, there is about $10^9/cm^2$ density of MoO_{3-x} nanowires which leaves about 50% volume for including silicon to obtain a 50-50 mixture of Si and MoO_{3-x} hybrid material with a theoretical capacity of ~2650 $mAhg^{-1}$. The rate performance presented in Figure 4c shows a stable performance of ~580 $mAhg^{-1}$ at 200 mAg^{-1}. This study shows illustrates that Si based hybrid architectures are ideal high capacity and high rate capable anode materials.

Conclusions

In this study, MoO_{3-x} nanowire arrays are shown to retain a capacity of ~630 $mAhg^{-1}$ for up to 20 cycles at a current density of 50 mAg^{-1}. These nanowire arrays undergo a 2 stage lithiation/de-lithiation mechanism which occurs above 1.5 V and below 0.7 V leading to retention of 3.4 Li ions per Mo. In addition, nanowire arrays show good capacity retention of ~500 $mAhg^{-1}$ below 0.7 V indicating viable practical applicability of the material. In addition, Si/MoO_{3-x} hybrid nanowires synthesized by the direct deposition of Si on MoO_{3-x} nanowire arrays have shown higher capacity retentions of ~780 $mAhg^{-1}$ paving ways for high capacity stable anode materials.

Acknowledgements

The authors gratefully acknowledge the financial support from Kentucky Renewable Energy Consortium (DE-FG36-05GO85013) and the US Department of Energy (DE-FG02-07ER46375).

References

1. Scrosati, B. *Nature* **1995**, *373*, 557-558.

2. Tarascon, J. M.; Armand, M. *Nature* **2001**, *414*, 359-367.
3. Subramanian, V.; Zhu, H.; Wei, B., *Journal of Physical Chemistry B* **2006**, 110, 7178.
4. Wu, X. –L.; Liu, Q.; Guo, Y. –G.; Song, W. –G., *Electrochemistry Communications* **2009**, 11, 1468.
5. Meduri, P.; Kim, J. H.; Benjamin, H. R.; Jasinksi, J.; Sumanasekera, G. U.; Sunkara, M. K., *Journal of Physical Chemistry C* 2010, 114, 10621.
6. Li, Y.; Tan, B.; Wu, Y. J., *Nano Letters* **2008**, 8, 265.
7. Meduri, P.; Pendyala, C.; Kumar, V.; Sumanasekera, G. U.; Sunkara, M. K., *Nano Letters* **2009**, 9, 612.
8. Taberna, P. L.; Mitra, S.; Poizot, P.; Simon, P.; Tarascon, J. –M., *Nature Materials* **2006**, 5, 567.
9. Whittingham, *J. Electrochem. Soc.* **1976**, 123, 315.
10. Besenhard, J. O.; Heydecke, J.; Wudy, E.; Fritz, H. P.; Foag, W., *Solid State Ionics* **1983**, 8, 61.
11. Bonino, F.; Bicelli, L. P.; Rivolta, B.; Lazzari, M.; Festorazzi, F., *Solid State Ionics* **1985**, 17, 21.
12. Lee, S. –H.; Kim, Y. –H.; Deshpande, R.; Parilla, P. A.; Whitney, E.; Gillaspie, D. T.; Jones, K. M.; Mahan, A. H.; Zhang, S.; Dillon, A. C., *Advanced Materials* **2008**, 20, 1.
13. Jung, Y. S.; Lee, S.; Ahn, D.; Dillon, A. C.; Lee, S. –H., *Journal of Power Sources* **2009**, 188, 286.
14. Dieterle, M.; Mestl, G., *Physical Chemistry Chemical Physics* **2002**, 4, 822.

15. Światowska-Mrowiecka, J.; de Diesbach, S.; Maurice, V.; Zanna, S.; Klein, L.; Briand, E.; Vickridge, I.; Marcus, P., *Journal of Physical Chemistry C* **2008**, 112, 11050.
16. Yu, A.; Kumagai, N.; Liu, Z. L.; Lee, J. Y., *Solid State Ionics* **1998**, 106, 11.
17. Dickens, P. G.; Reynolds, G. J., *Solid State Ionics* **1981**, 5, 331.
18. Mariotti, D.; Lindström, H.; Bose, A. C.; Ostrikov, K., *Nanotechnology* **2008**, 19, 495302.

(a)

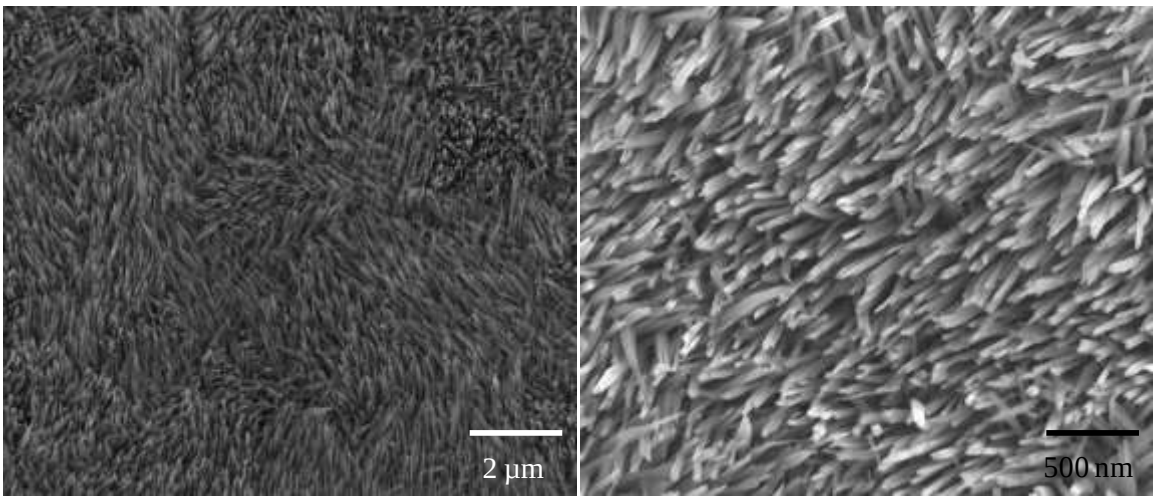

(b)

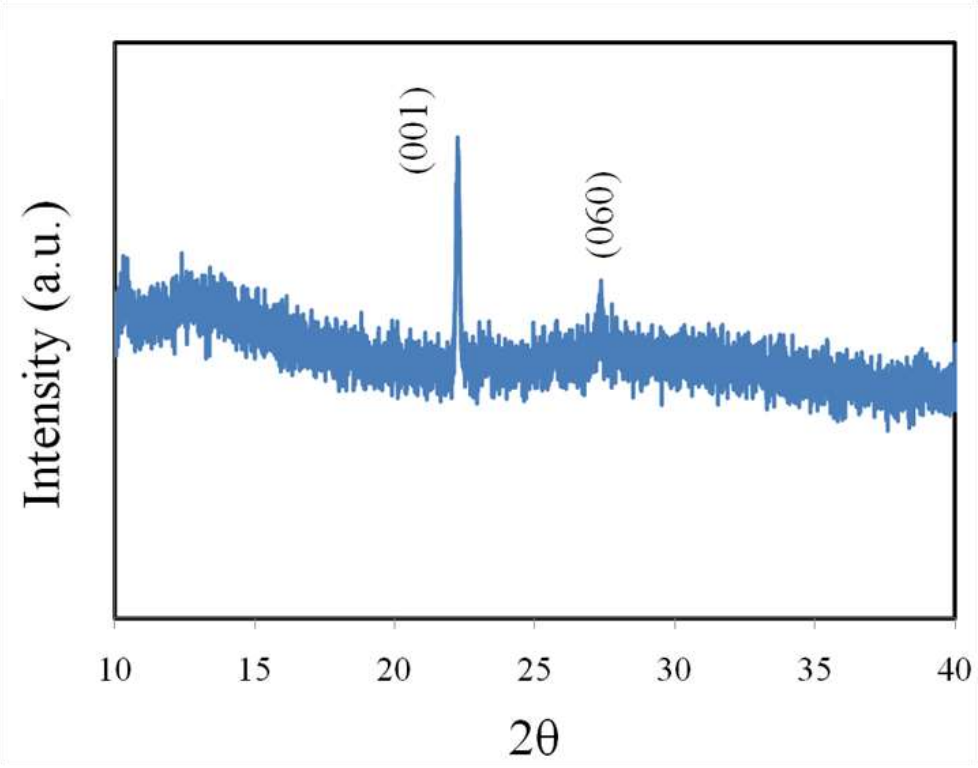

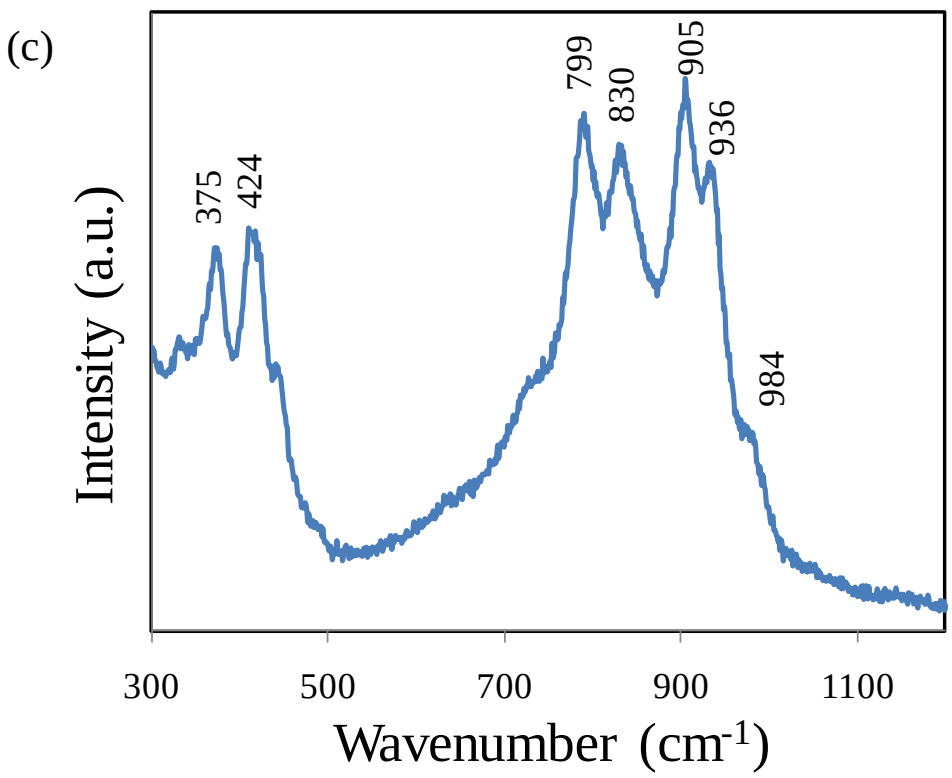

Figure 1: Characterization of as synthesized $Mo_{17}O_{47}$ nanowires (a) SEM images showing the array architecture. (b) XRD spectrum indicating peaks corresponding to the phase $M_{17}O_{47}$. (c) Raman spectrum indicating various Mo-O interactions in the material.

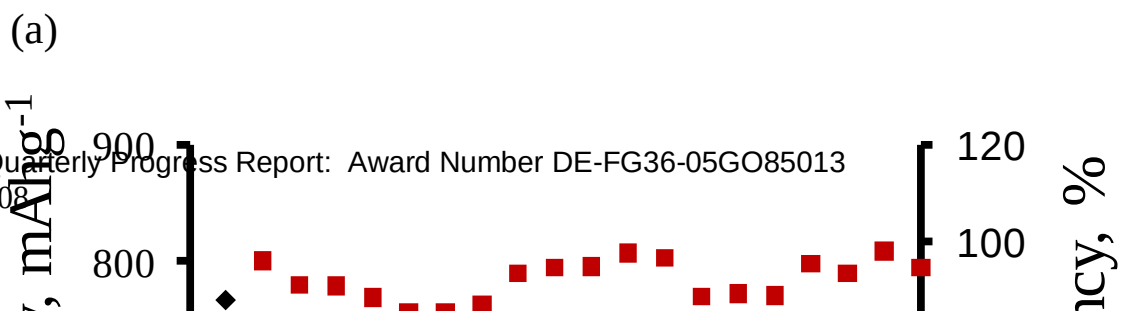

(b)

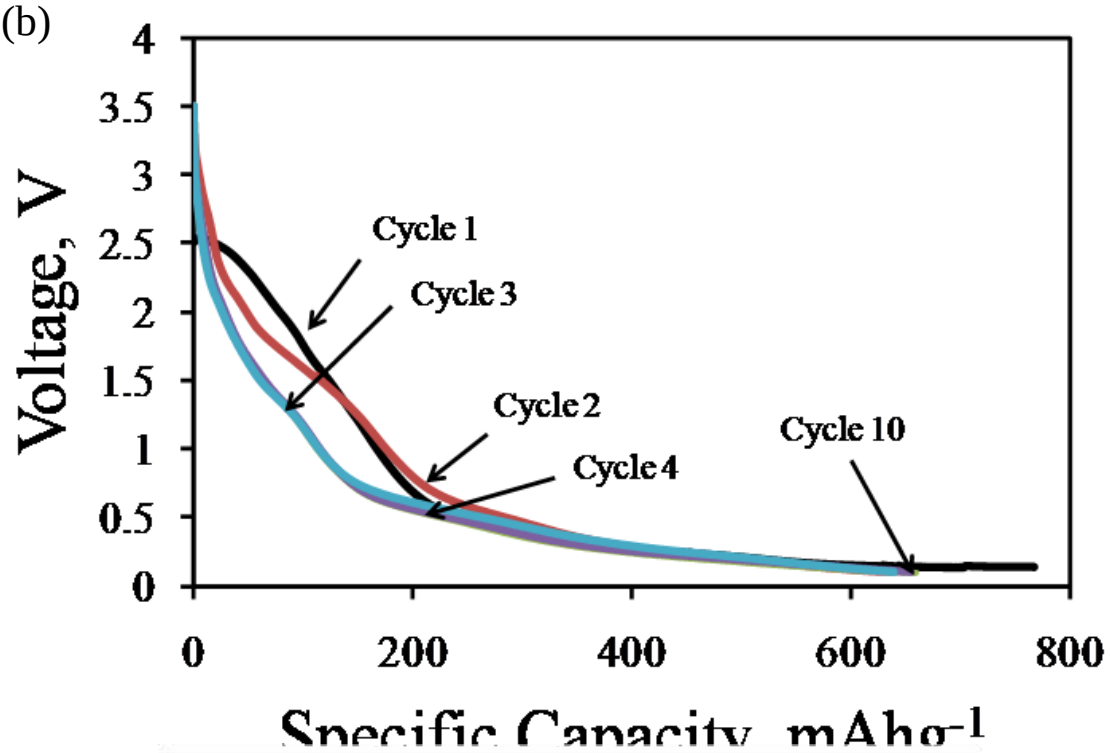
Voltage, V
4
3.5
3
2.5
2
1.5
1
0.5
0
Cycle 1
Cycle 3
Cycle 2
Cycle 4
Cycle 10
0
200
400
600
800
Specific Capacity, mAhg-1

(c)

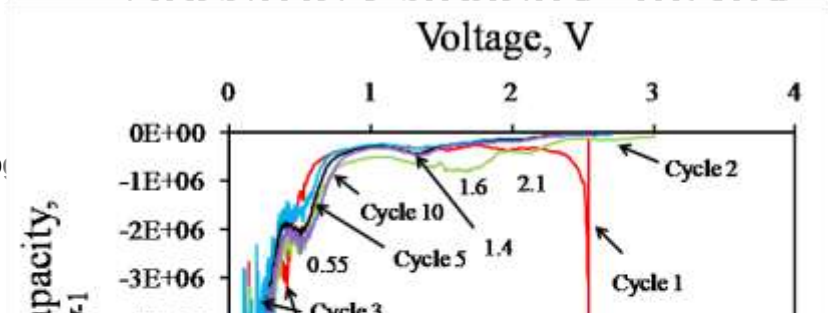
Voltage, V
0
1
2
3
4
0E+00
-1E+06
-2E+06
-3E+06
Cycle 2
1.6
2.1
Cycle 10
Cycle 5
1.4
0.55
Cycle 1
Cycle 3

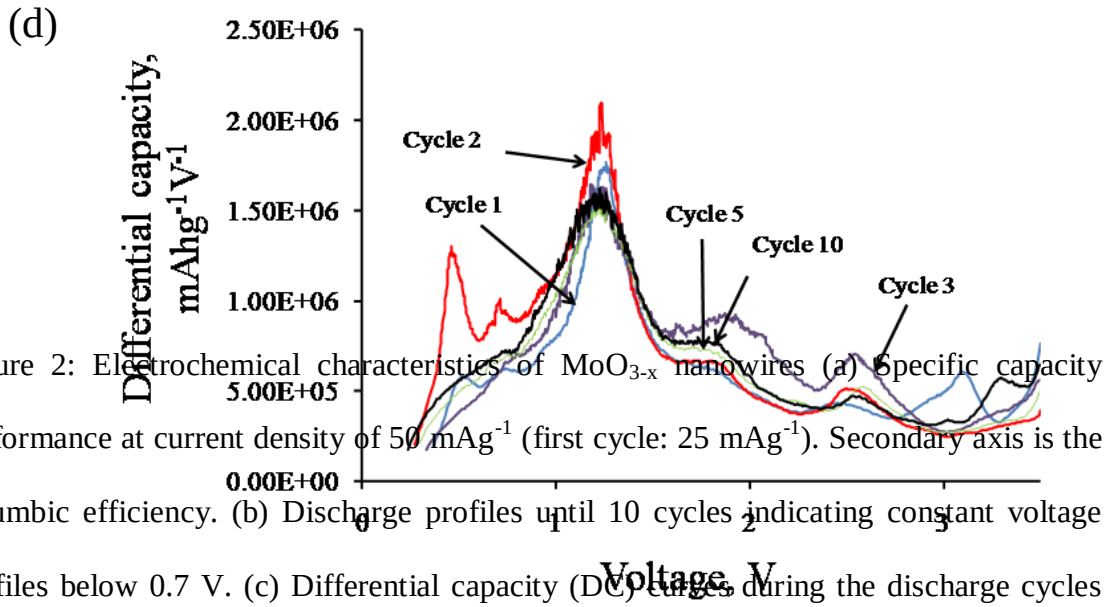

Figure 2: Electrochemical characteristics of MoO_{3-x} nanowires (a) Specific capacity performance at current density of 50 mAg^{-1} (first cycle: 25 mAg^{-1}). Secondary axis is the columbic efficiency. (b) Discharge profiles until 10 cycles indicating constant voltage profiles below 0.7 V. (c) Differential capacity (DC) curves during the discharge cycles indicating lithiation. (d) DC curves during the charge cycles indicating de-lithiation characteristics.

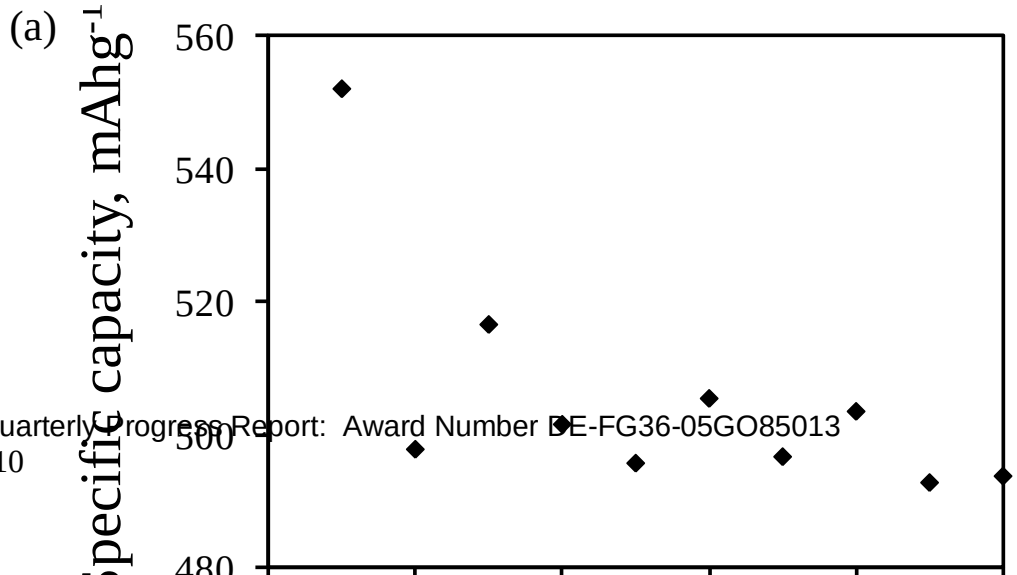

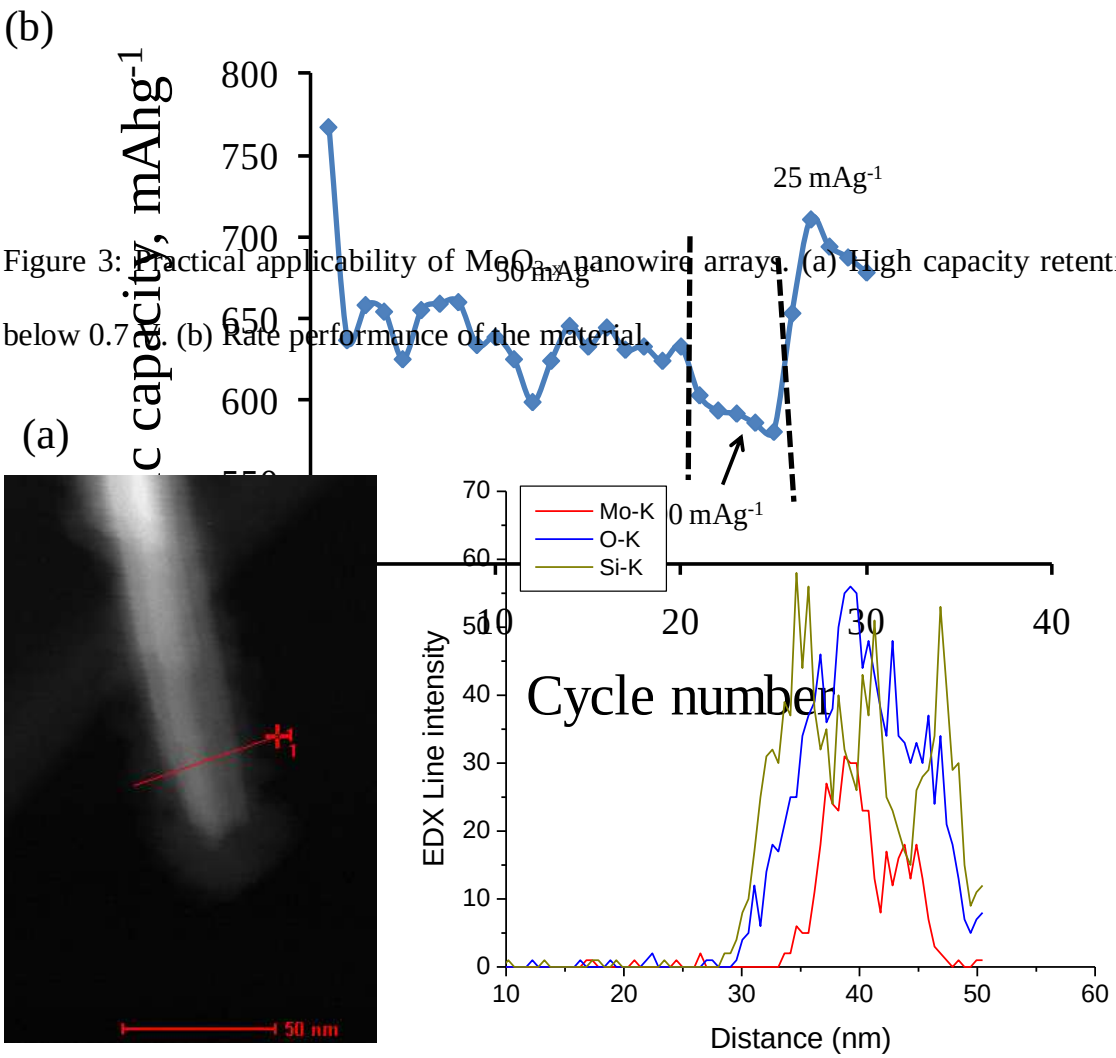

Figure 3: Practical applicability of MoO_{3-x} nanowire arrays. (a) High capacity retention below 0.7 V. (b) Rate performance of the material.

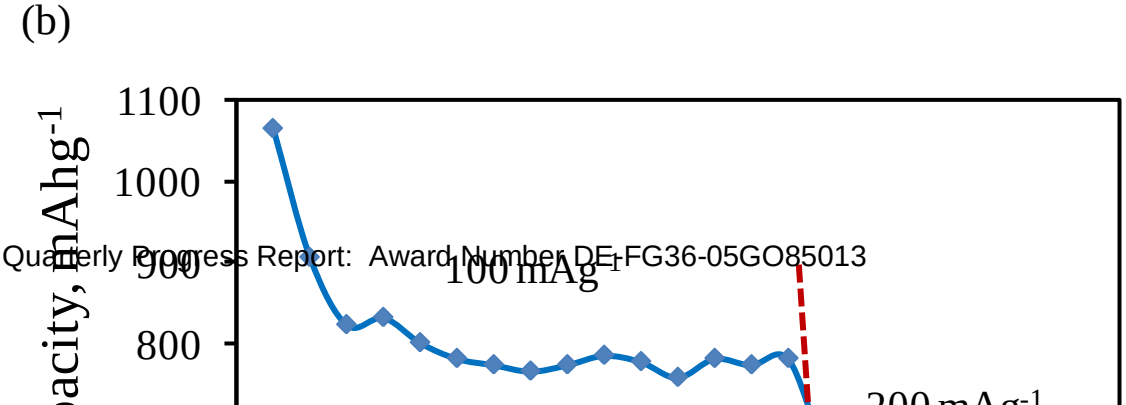

Figure 4: Si/MoO_{3-x} hybrid architectures (a) Line scan in a TEM showing 10 nm silicon coating on MoO_{3-x} nanowires. (b) Specific capacity of hybrid materials with capacity retentions of 780 and ~580 $mAhg^{-1}$ at rates of 100 and 200 mAg^{-1}, respectively.

Final KREC Report
(Field Office Project Template)

Project Title: Investigation of Cooling Season Performance of a Solar Heat Pipe System

Award Number: [Official Award Number per the agreement]

Recipient: M. Keith Sharp
Project Location: [Location of project activities; if multiple locations, please list all in use.] Shumaker Research Building

Reporting Period: [e.g., January 1, 2006 to March 31, 2006] 1 Oct 2009 – 31 Mar 2011
Date of Report: [e.g., April 30, 2006] 11 Jul 2011
Written by: [Name] M. Keith Sharp, Brian S. Robinson

> **IMPORTANT NOTE:** If any part of your quarterly report contains **proprietary/confidential information**, or details that should not be released to the general public, the specific sections of the report should be marked as such, by clearly marking the beginning and end of the confidential information. The marked sections will not be released to the general public or any unauthorized parties.

Status: [In this section each task, as defined by the Project Management Plan (PMP), should be discussed by following the outline given below. The discussion for each task should include subtasks. Milestones, deliverables, and go/no go decision points covered in Table C of the accompanying excel quarterly report and the PMP may be discussed in more detail in this section; however, please ensure Table C is completely and accurately filled in.]

Task number: [(e.g., A)]

1. **Planned Activities**: [This section should include the planned activities that were stated in the previous quarterly report for the task being discussed, including subtasks, milestones, deliverables, and go/no go decision points.]

Planned deliverables:

Task 1: Computer simulation of system performance during cooling season – An evaluation of absorber, heat pipe and storage parameters will be performed to predict the solar conditions and design that optimizes performance. Parameters to be evaluated include the effects of several shading conditions on the unit and mechanisms that change the system operating conditions during the cooling season. Simulated shading conditions on the unit will consist of direct sunlight, indirect (diffuse) radiation, and a "cover" condition in which the unit is exposed to no sunlight at all. Mechanisms to be evaluated include the implementation of on/off valves to stop latent heat transfer along the heat pipe, so that the system neither heats nor cools during the summer, and slope changes to make the heat pipe a cooling device during the summer. To implement cooling, the evaporator must be raised above the condenser, effectively exchanging the functions of these two components. To make this change more practical, the evaporator, along with its attached absorber, and the condenser should be level, while the adiabatic section is switched from positive to negative slope. These new variables will be tested with the existing simulation model, which was used previously to evaluate heating season performance only. A comparison of cooling season performance to that of conventional direct gain and indirect gain systems will be conducted. Simulations will be performed for the moderate temperature, moderately sunny climate of Louisville, as well as for sunny and mild Albuquerque, NM, sunny and cold Rock Springs, WY, and cloudy and cold Madison, WI.

2. **Actual Accomplishments**: [The discussion should include all significant work completed in the past quarter to support the project and accomplish the specific task being discussed, including subtasks, milestones, deliverables, or go/no go decision points. When a task-level milestone has been completed, please include a brief explanation of how completion of the task achieves/supports/furthers completion of the C-level milestone as indicated in the PMP (cell X48). Actual work completed should conform to the "Planned Activities" described in the above section. If it does not, an explanation of the variance is required and should be discussed below in section **3. Explanation of Variances**.]

Task 1: Computer simulation of system performance during cooling season – **Background**

The heat pipe augmented solar wall is a passive solar space heating system that greatly improves upon performance relative to conventional passive space heating systems. Previous research conducted at the University of Louisville (UofL) confirms this. Using MATLAB software, a set of programmed thermal networks were used to simulate the performance of several conventional passive solar heating systems, including direct gain, concrete wall and water wall indirect gain, and that of the heat pipe system (Fig. 1). Four locations (Louisville, KY, Albuquerque, NM, Madison, WI, and Rock Springs, WY), were chosen to represent a wide range of winter temperatures and solar resource.

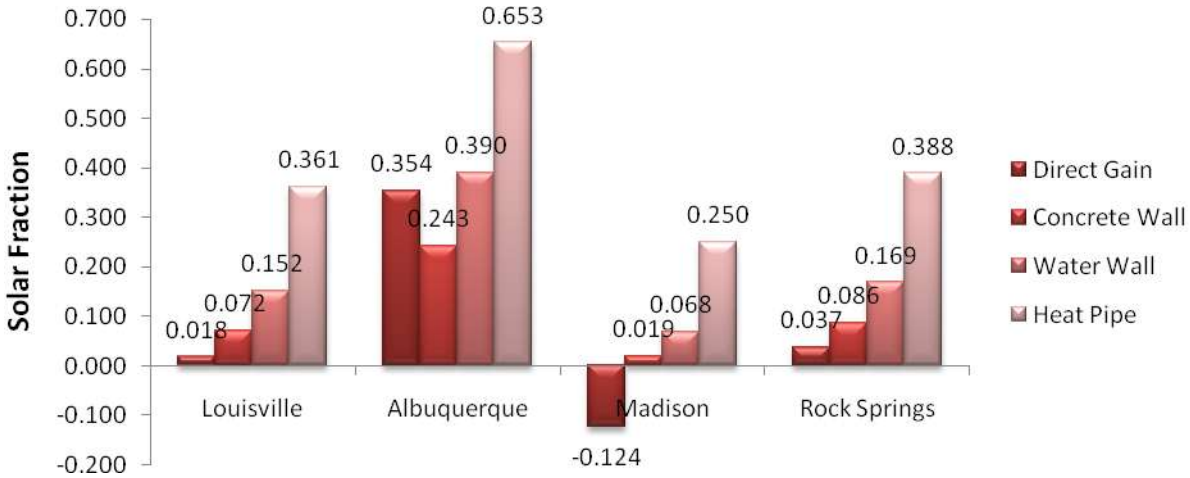

Figure 1. Annual solar fraction for conventional passive solar space heating systems and heat pipe wall for four locations.

Furthermore, a bench-scale experiment was constructed & tested to confirm system performance and test a range of component variations. Under ideal conditions, the bench-scale system obtained an average thermal efficiency of 89.1%. Additionally, a full-scale prototype was constructed and installed in a classroom on the UofL campus. The prototype consisted of 5 heat pipe units and resulted in an average thermal efficiency of 61.4%. The primary reasons that the prototype efficiency wasn't as great as the bench-scale is that aluminum absorbers were used in place of copper, the external face of the prototype faced 10^{o} east of south instead of due south, and an existing overhang and side protrusion caused shading on the unit at several times during the year.

Objective

While the solar heat pipe wall provides beneficial heat gains during the heating season, unwanted thermal gains during the cooling season may increase the cooling load. Annual heating and cooling loads for each of the four selected locations, for an average sized living space *without the heat pipe wall* are shown in Figure 2. It is evident that the heating load dominates in all locations.

Annual heating and cooling loads for each of the four locations, for the same living space *with the heat pipe wall* are shown in Figure 3. The heat pipe wall alleviates a large portion of the heating load, but the cooling load is considerably increased due to unwanted gains from the system at times when the room needs to be cooled. In fact, the

unwanted gains increase the total annual load in Louisville by 6.3%. The objective of this study was to investigate additional features and control strategies that can be employed during the cooling season to reduce unwanted gains.

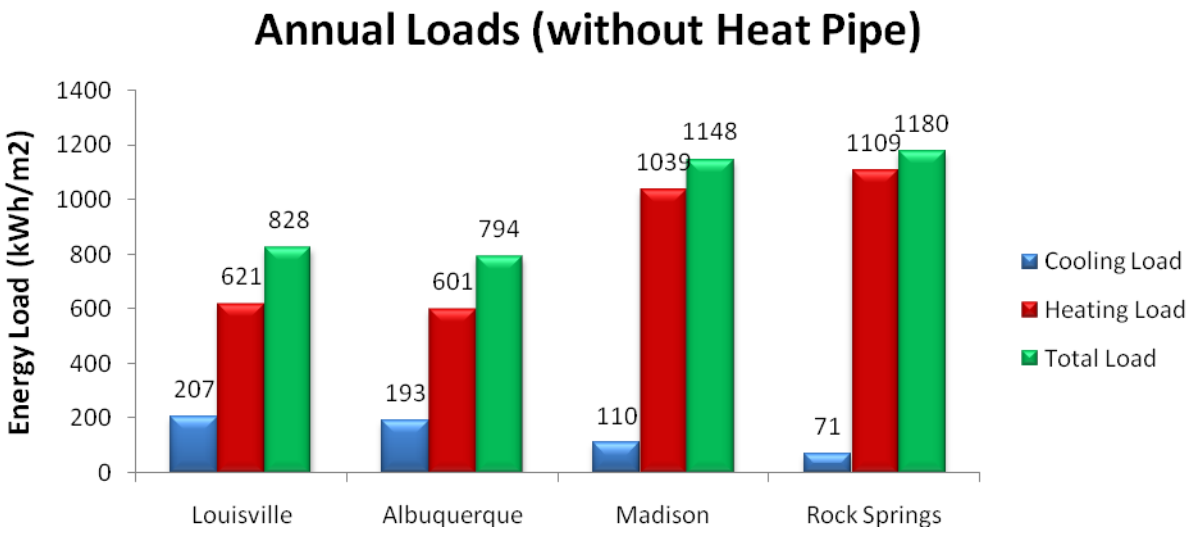

Figure 2. Annual loads for four selected locations without the heat pipe wall.

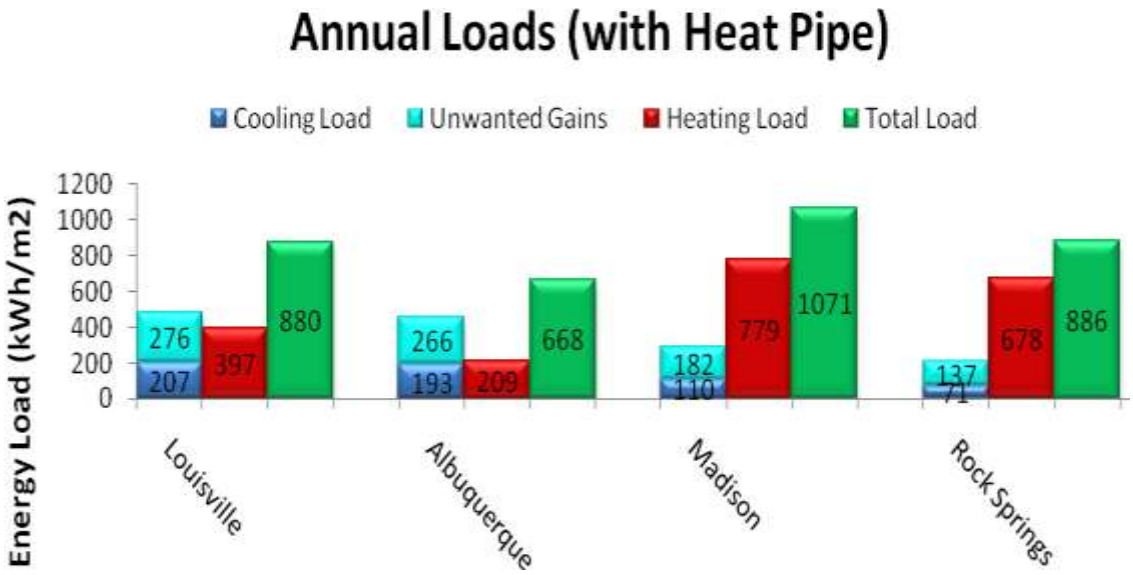

Figure 3. Annual loads for four selected locations with the heat pipe wall.

Methods

This study was conducted via modification of the computer simulations used to assess passive system performances (discussed in the 'Background' section of this

report). Four different unwanted gains reduction mechanisms (Figures 4-7) were investigated:

- Shading – an overhang above the heating unit is installed to shade the unit, effectively eliminating beam insolation, but allowing diffuse and ground reflected insolation to be received by the collector.
- Cover – an opaque cover is installed over the collector, effectively eliminating any solar insolation to be received by the collector.
- Mechanical Valve – a valve installed in the adiabatic section of the heat pipe, effectively turning the system 'on' or 'off'.
- Switching – switching the elevations of the evaporator and condenser sections of the heat pipe to provide heat transfer *out* of the room during the cooling season.

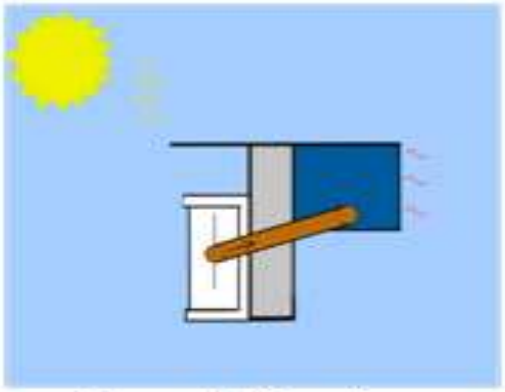

Figure 4: Shading.

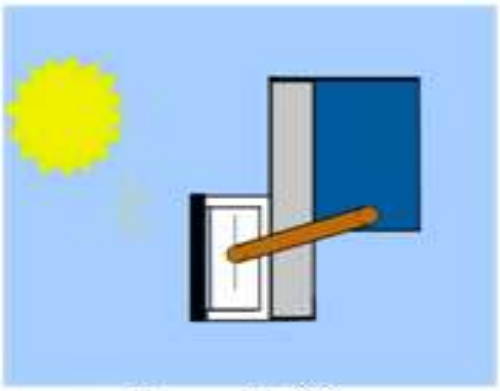

Figure 5: Cover.

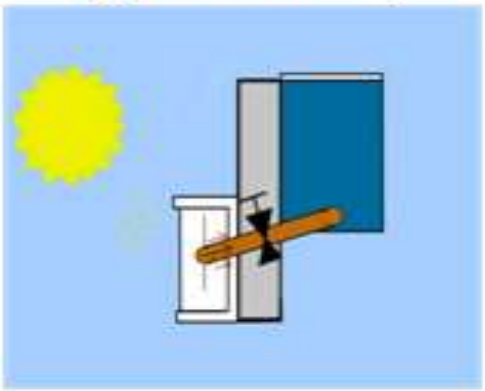

Figure 6: Valve.

Figure 7: Switching.

For each mechanism, three different control strategies were used:

- Twice-Yearly – for which the prescribed mechanism is employed at the beginning of the cooling season and removed at the end of the cooling season.
- Ambient Temperature-Based Control – for which the prescribed mechanism is employed if the forecast for the *next* hour (based on TMY3 weather data) is greater than 65^{o}F.

- Room Temperature-Based Control – similar to a typical thermostat, in which the prescribed mechanism is employed if the room temperature for the *previous* hour is greater than the upper limit of the defined room comfort temperature range.

A means to define the cooling season, needed for the twice-yearly strategy, was developed. First, for each of four locations, simulations were conducted with an opaque cover on the heat pipe system for every feasible monthly combination that could represent the cooling season. The most desirable scenario is that which minimizes total auxiliary energy use: $(1\text{-}SF)Q_{hl} + Q_{cl} + Q_{uwg}$, where SF is the solar fraction, Q_{hl} is the heating load, Q_{cl} is the cooling load and Q_{uwg} is the unwanted gains. The optimal definition for the cooling season is that which minimized this sum.

The selected cooling season was then compared to a newly defined parameter, the Season Determination (SD) ratio, calculated as

$$SD = \frac{Q_{uwg}}{Q_{hl}} \tag{1}$$

The SD ratio, resulting from normal (unshaded) operation, was calculated for each month of the year for each location. The monthly SD values was compared to assess the usefulness of SD for identifying the optimal cooling season months. Four additional locations, chosen to represent each U.S. time zone and a typical four-season climate, were also simulated to ensure repeatability and validity of the SD ratio. These additional locations were Boston, MA, Chicago, IL, Denver, CO, and Seattle, WA.

Another bench-scale experiment was also constructed to determine the change in system performance when the evaporator and condenser sections were leveled (which would be required to accommodate the switching mechanism).

Results

The defined room comfort temperature range had a large impact on the annual load. The annual unwanted gains, auxiliary heating and total energy load for Louisville utilizing the heat pipe wall (without any reduction strategies employed) for three defined comfort temperature ranges are shown in Figure 8. Unless otherwise noted, all other results in this report are for a defined room comfort temperature range of 68-72^{o}F.

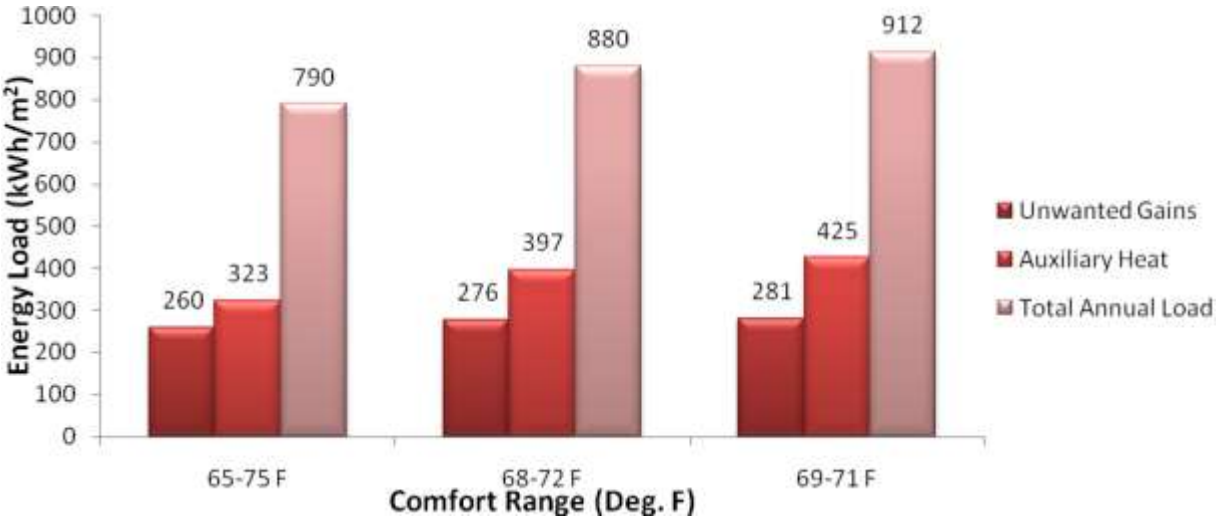

Figure 8. Annual unwanted gains, auxiliary heating and total energy load for Louisville utilizing the heat pipe wall (without any reduction strategies employed) for defined room comfort ranges of 65-75°F, 68-72°F & 69-71°F.

Results for the eight locations showed that any month with SD ≥ 0.8 should be included as part of the cooling season to minimize auxiliary energy use. For 0.7 < SD < 0.8, and if Q_{hl} is less than ($3*Q_{cl}$), then that month should also be included in the cooling season.

Annual unwanted gains and load in Louisville for the heat pipe under normal operation and with each mechanism, and practical combinations of each, are shown in Figure 9 for annual control based on ambient temperature. Not included in the simulation of the switching mechanism was a decrease in average system thermal efficiency of 6.9%, which was measured in the bench-scale experiment when the evaporator and condenser sections were leveled.

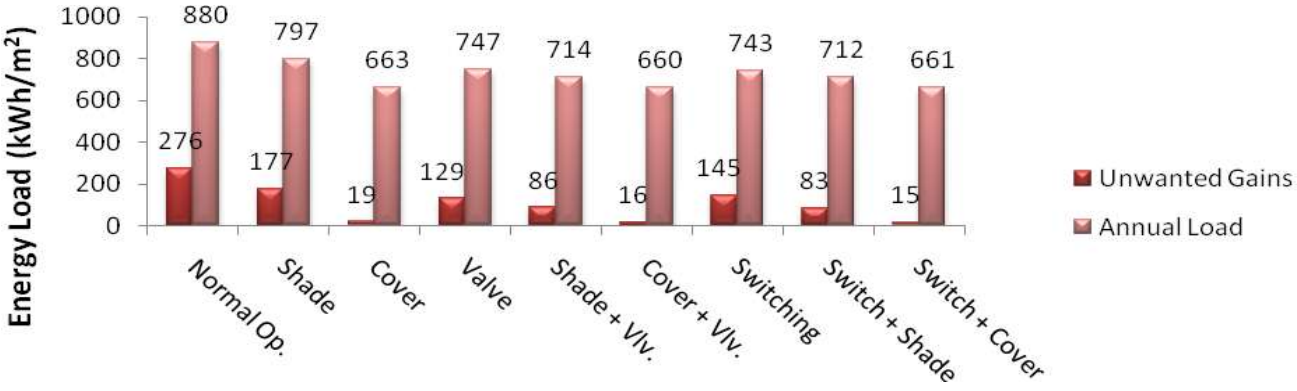

Figure 9. Annual unwanted gains and load in Louisville for the heat pipe under normal operation and with each mechanism, and practical combinations of each.

Discussion

The results for all locations suggested that the SD ratio may be a 'universal' parameter that can be applied to any location for quick assessment of its optimal cooling season.

The control strategy based on ambient temperature, used for the results shown in Figure 9, proved to be the best strategy for all locations and mechanisms. Surprisingly, the twice-yearly strategy yielded better annual performance than that of control based on room temperature. The best overall combination of mechanisms was the cover and valve; and the best single mechanism was the cover. The switching mechanism proved relatively ineffective, primarily because the heat pipe system was designed for heating and was, therefore, a poor cooling device. In addition, leveling the evaporator and condenser sections of the heat pipe to accommodate switching would reduce performance in both the heating and cooling modes (this is *not* included in the simulation results in Figure 9). Together, these effects render the switching mechanism a poor choice in all locations.

The mechanical valve mechanism did not alleviate unwanted gains as much as expected. It was found from these simulations that even with the valve closed, significant heat transfer still conducted along the copper pipe wall of the adiabatic section. Conduction along the pipe wall also contributed to undesirable thermal losses back out of the system during heating season operation. Thermal conduction through the fiberglass insulated wall of the heat pipe system was 1.4718 W/m^2*k. Conduction through the pipe walls of a unit consisting of five heat pipes was 0.5732 W/m^2*k, which adds an additional 39% in losses. To improve performance, the heat pipe system design was modified with an adiabatic section constructed of rubber, and the fiberglass insulation was replaced with significantly higher thermally resistive polyurethane.

Results for the modified design, otherwise utilizing the same parameters as for Figure 9, are shown in Figure 10. Whereas the previous annual load in Louisville was 880 kWh/m^2, the modified design alone reduced it to 848 kWh/m^2. The combination of the cover and valve again yielded the lowest overall load, but, this time, the best single strategy was the mechanical valve. Performance using the cover was close to that of the mechanical valve, but opening and closing a valve is more convenient than placing and removing a cover. Even though it forced the value of unwanted gains to zero, the switching mechanism remained an unattractive option.

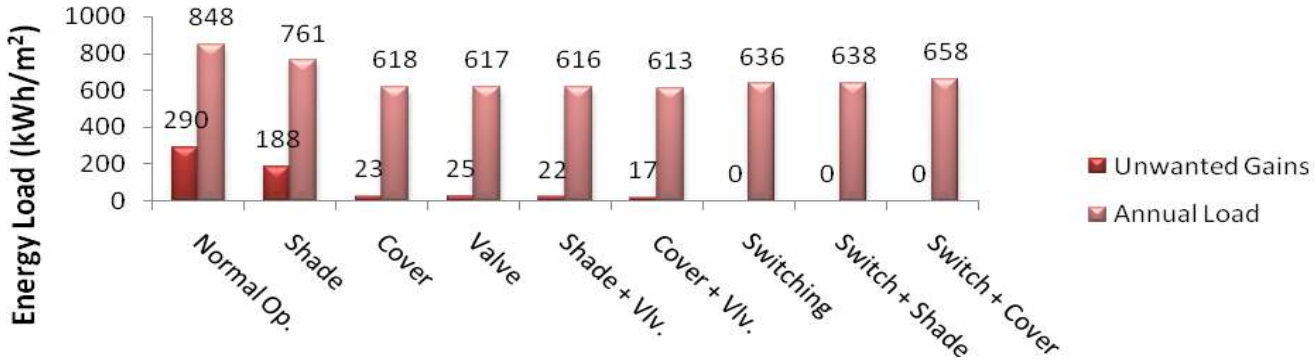

Figure 10. Modified design results, using the same parameters as Figure 9 results.

In summary, the heat pipe augmented solar wall performed best with the modified design and a control strategy based on ambient temperature utilizing the mechanical valve mechanism. While in many cases the combination of the valve with a cover produced slightly better performance than that of the mechanical valve alone, these additional reductions are insignificant when weighed against the additional design requirements and associated costs needed to accommodate the extra mechanism.

The results reflected in this report were for a Load to Collector Ratio, LCR (the ratio of the UA value for the space to the collector area) equal to 10 W/m^2 K. This value represents an approximate lower limit for improving performance due to increasing unwanted gains as collector area is increased. However, by applying the mechanisms identified during this study, larger collectors can be used without increasing unwanted gains to unacceptable levels. Larger LCR also offsets a greater portion of the annual heating load. Loads for decreasing LCR are shown in Figure 11.

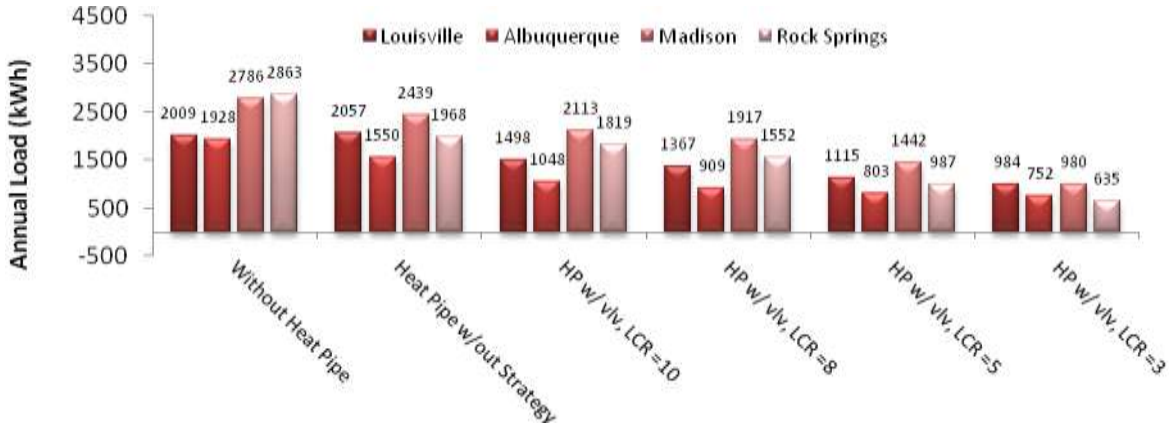

Figure 11. Annual energy load for four locations with decreasing LCR.

Revisiting the effect of defined room comfort temperature range (Fig. 8), the loads for Louisville, utilizing the optimum control strategy and mechanism, are shown in Figure 12.

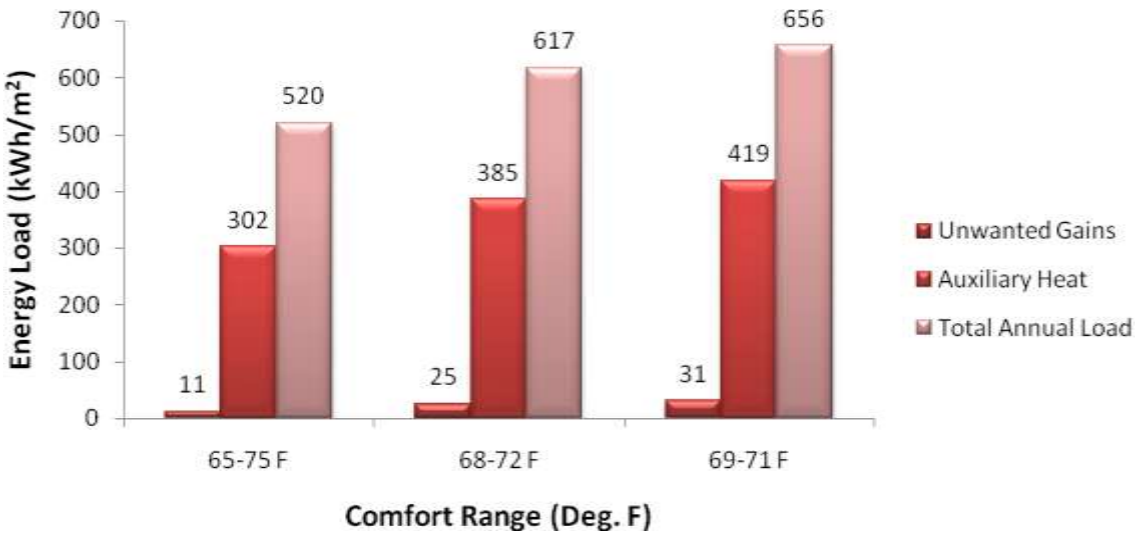

Figure 12. Annual unwanted gains, auxiliary heating and total energy load for Louisville utilizing the heat pipe wall (with ambient temperature-based control and valve) for three room comfort ranges.

The increase in annual load from 65-75°F to 68-72°F and 69-71°F is 18.7% and 26.2%, respectively. While the 65-75 range may be too large for many households, any range greater than the 68-72 used for most of the results shown here would reduce the annual load.

3. **Explanation of Variance**: [This section should discuss any differences between the planned activities (section 1) and the actual accomplishments (section 2). These differences should be included even if the setback was out of the control of the recipient, such as a change in the availability of equipment and/or facilities. Issues, concerns, successes or requested changes and the resulting impact to the Statement of Project Objectives, budget and/or schedule should be discussed. If progress (Section C, column V of the accompanying excel file) is Y or R, please explain the corrective actions that will be taken to mitigate scope, schedule, and budget changes or shortfalls.]

Task 1: Computer simulation of system performance during cooling season – N/A

4. **Plans for Next Quarter**: [Planned activities for this task, to be conducted during the next quarter should be discussed here.]

[REPEAT these discussions for each task in the Project Management Plan (e.g. A, B, C, etc…)]

Task 1: Computer simulation of system performance during cooling season – N/A

Patents: [A **cumulative** list of patents applied for or resulting from the award, including date of application and receipt of patent(s) and date and status of DOE notification.]

none

Publications / Presentations: [Identify and briefly summarize, in a few sentences, all publications and presentations made for industry or government groups resulting from the project during this quarter and, if possible, include a URL link or other method of accessing the publication or presentation. In addition, please upload the electronic file to the PMC if required (see your "Federal Assistance Reporting Checklist," form 4600.2, for required uploads).]

KREC final presentation.

KREC Final Report

A. Project Title: Development of a solid catalyst-based technology for production of biodiesel from waste vegetable oils
B. Recipient: Professors. Mahendra Sunkara and Paul Ratnasamy, University of Louisville
C. Project Location: Conn Center for Renewable Energy Research, Ernst Hall, University of Louisville, Louisville, KY 40292
D. Project Period: 10-15-2009 to 9/30/2010 (extended to 6-30-2011 without additional funds).
E. Date of Report: 6-24-2011
Total Project Funding: $ 199941-.
Project Participants: Prof. Paul Ratnasamy and Prof. Moises A. Carreon.
F. Written by: Professor. Paul Ratnasamy
G. Project current Status: Project will be terminated on 6-30-2011
H. Project Objectives:
The major objective of the project is the development of a technically and economically viable process for the conversion of waste vegetable oils to biodiesel by process routes using solid catalysts.
I. Project strategy: Two process routes were investigated to achieve the project objective:
a. Catalytic skeletal Isomerisation of the commercially available biodiesel (linear fatty acid methyl esters) to branched isomers with lower pour points and better cold flow properties; and
b. Conversion of the waste vegetable oils into diesel hydrocarbons boiling in the diesel range("drop-in " or " green" diesel fuels) in 3 stages: (1) Hydrolysis of the triglycerides in waste vegetable oils to free fatty acids ,(2) decarboxylation of the free fatty acids to linear paraffins and (3) hydroisomerisation of the linear paraffins into branched paraffins boiling in the diesel range. The latter constitutes "green" diesel or jet fuel depending, mainly, on the boiling point range and freezing point of the material from the third stage.

J.Summary Of Project Achievements : The results of the research carried out in this project have been already published in detail in journal publications, patents, research disclosures and symposia presentations. The total "visible" outputs during October 2009 to June 2011 are:

1. **Publications in refereed Journals (Three);**

    1. Hydrolysis of vegetable oils and fats to fatty acids over solid acid catalysts.

Applied Catalysis, General, 379(2010)125

2. Synthesis and catalytic properties of mesoporous, bifunctional, gallium-niobium mixed oxides. **Chemical Communications**, 47(2010)6347.

3. Catalytic Transformations of methyl oleate and biodiesel over mesoporous Gallium-niobium oxides, **Catalysis Communications**, 12(2011) 644-650.

2. Patents already Filed (Three):

1. Catalytic Isomerisation of fatty acid esters. U.S. patent, **U.S. 61/ 350238**; patent filed

on June1, 2010.

2. Process for the production of paraffinic hydrocarbons. ULRF- 10070;U.S. patent,

U.S.61/439112, patent filed on February,3, 2011.

3. Process for the production of fatty acid alkyl esters(ULRF-11013; U.S. Patent :

US61/485267, patent filed on 12,may,2011.)

3. Research Disclosures filed with the Office of Technology Transfer, University of Louisville(Six):

1. Filed Nov. 9, 2009.: **ULRF- 10031**:Catalyst and process for the isomerisation of unsaturated linear fatty acids and esters.
2. Filed Feb 5, 2010; **ULRF-10063**: Process for conversion of triglycerides to jet fuels.

   Filed April 14,2010;

   3. **ULRF- 10070**: Process for the production of paraffinic hydrocarbons.

4. Filed August 17, 2010: **ULRF- 11013**: Process for the production of fatty acid alkyl esters.

5. Filed , September 30, 2010: **ULRF- 11024**: Process for the manufacture of fatty acid alkyl esters.

6. Filed 25 , January,2011:**ULRF- 11060**: Process for the production of branched chain olefinic hydrocarbons.

4. Papers presented at National Symposia(four) :

1. Catalytic Transformations of Methyl oleate and Biodiesel over mesoporous gallium- niobium oxides : Paper presented at the **North American Catalysis Society Meeting,** Detroit, June,2011.

2. Zeolitic Imidazolate Framework- 8: A novel catalyst for biodiesel synthesis : Paper presented at the **North American Catalysis Society Meeting**, Detroit, June,2011.

3. Synthesis and characterization of zeolitic Imidazolate Framework-8 by Evaporation Induced Self Assembly : Paper presented at the **North American Catalysis Society Meeting**, Detroit, June,2011.

4. Catalytic Activity of mixed mesoporous Gallium – Niobium oxides : **AIChE Symposium,** Salt Lake City, Utah, November, 2010.

5. Creation of *new* Infrastructure / Facilities for R & D in the production of biofuels by *non- enzymatic* technologies:

- **Design, Fabrication and Installation of new heterogeneous catalytic reactors** : A new state-of-art continuous, fixed bed reactor system for studying heterogeneous catalytic reactions using solids has been designed, fabricated, installed and commissioned at the Conn Center. It is, currently, being used in the production of biodiesel, green diesels and jet fuels. A photograph of this new facility is shown below. A high pressure autoclave reactor for lignocellulose conversions to fuels has also been fabricated and commissioned. These are *new* equipment facilities which can be utilized for carrying out reactions using solid catalysts and, thereby, expand the potential of the Conn Center to carry out research in the area of heterogeneous catalysis.

Figure 1. Reactor Unit for heterogeneous catalytic reactions: Designed, fabricated and commissioned at Conn Center.

- **Installation of new analytical facilities** : Installation and commissioning of gas chromatographic(Hewlett Packard) and HPLC (Waters) instruments for analysis of lipids – derived biofuels.

6. Human Resource Development :

-Trained two grad students and one temporary worker in the operation of fixed bed and semi-batch catalytic reactors and analysis of lipids and biodiesel products.

- Delivered two lectures," Solid catalysts in the production of biofuels" to the faculty and graduate students of the chemical engineering dept.

K. Project Narrative

As mentioned earlier, we adopted a two-pronged approach in the preparation of biodiesels with superior cold flow qualities: The first was the skeletal isomerization of

linear fatty acid methyl esters(FAME) to branched isomers using solid acid catalysts and the second approach was the conversion of the vegetable oils into *hydrocarbon mixtures* (green diesels) with composition, structure and functional properties similar to those of diesels derived from petroleum fractions. The background and salient features of these two research activities are described below.

1. *Preparation of biodiesels with superior cold flow properties by catalytic skeletal Isomerisation of fatty acid methyl esters over solid acid catalysts*:

The major components of biodiesels are unsaturated, linear fatty acid methyl esters (FAME). Biodiesel is produced to ASTM D 6751 specifications, or the European Union standard, EN14214. Transesterification of the triglycerides in vegetable oils like soy, canola, corn, etc. with methanol yields glycerol and FAME biodiesel(1). Biodiesels have higher pour and cloud points than petro diesels and are, hence, less suitable than the latter in cold climates. The cold flow properties of biodiesels can be improved by (i) blending it with conventional petrodiesel, (ii) introducing additional double bonds, (iii) introducing alkyl or aromatic side chains in the FAME molecule by alkylation /arylation at the double bond, (iv) catalytic skeletal isomerisation of the linear to branched FAME chains over acidic catalysts, (v) deoxygenating the fatty acid methyl esters to hydrocarbon "green" diesels, and (vi) adding pour point depressants . Alternative (iv) is described in this section. Alternative (v) is described thereafter.

Although it is a known practice in the petrochemical industry to isomerise linear to branched olefins, the task of converting straight chain fatty *acids* or their *esters* to branched analogs is more challenging and is not in commercial practice. Lee et al. [2] have reported the reduction in the crystallization temperature of biodiesel by 7–14 °C using branched alcohols in the transesterification reaction. The currently available branched monomeric fatty acids and esters are limited to byproducts of the dimer acid production process starting from unsaturated fatty acids [3]. Christy [4] reported the thermal, non-catalytic isomerisation of 9t12t methyl linoelaidate to the conjugated ester at 250 °C. Lewis acid catalysts, such as aluminium and indium chlorides [5] lead to extensive cracking. In addition to double bond isomerisation, cis-trans isomerisations have been also observed [6–8]. In the past few years, isomerisation over solid acid catalysts at 250°–300 °C has been attempted for the skeletal branching of fatty acids and FAMEs for reducing their pour points [9,10]. Yori et al. [11] had observed a decrease of ~5 °C in the cloud point on isomerising the linear to branched chain oleic acid molecules over sulfated zirconia and H-mordenite catalysts. Best results were observed with sulfated zirconia at 125 °C. However, extensive cracking, coking and leaching of the sulfonic acid groups during the catalytic reaction and, the consequent catalytic deactivation, were major problems. The influence of isomerisation on the cold flowproperties of oleic acid was not mentioned. Zhang and Zhang [12] reported the skeletal isomerisation of oleic acid to branched isomers on a series of beta zeolites. The activities of these beta zeolites under identical conditions were found to vary in a wide range, even with similar silica to alumina ratios, crystallinity and particle size. Dalley Jr. and Prevost [13,14] brominated methyl oleate in the allylic positions. Subsequent

reaction of the allylic bromides with lithium dimethyl cuprate gave the branched chain derivatives.

Recently, we had reported the synthesis of novel, nanocrystalline, mesoporous gallium oxides by a novel self-assembly, hydrothermalassisted (SAHA) method [15]. Gallium and niobium oxides are active catalyst in both acid and redox reactions [16–18]. Herein, we report the catalytic transformations of methyl oleate, a model FAME molecule, and a commercial sample of biodiesel over novel mesoporous gallium–niobium oxides. The results are compared with those obtained over conventional acidic molecular sieve catalysts like H–ZSM-5, H–Beta, H–Y, SAPO-11 and H–MCM-22. Even though reactions of methyloleate and oleic acid over aluminosilicate zeolites had been studied [10–12], to the best of our knowledge, this is the first report of the catalytic transformations of a commercial sample of biodiesel over
solid acids and bifunctional catalysts with both acidic and redox properties.

The catalytic activity was determined by reacting 0.5 g of the catalyst (activated in air overnight at 220 °C) with 5 ml of the reactant (methyl oleate or biodiesel) in a 20 ml, Teflon-lined autoclave at 180 – 400 °C and autogeneous pressures for 6 h. No solvents or carrier gases were used. At the end of the period, the reactor was cooled to room temperature. The catalyst was removed by filtration and the reaction products were analyzed by a combination of different techniques.

Mesoporous gallium–niobium oxides had surface areas as high as 360 m2/g with unimodal average pore sizes in the 3–7 nm range . The average pore size decreased as the niobium content was increased in the mixed oxides. In general, as the amount of niobium increased, the average size of the particles also increased. All these samples displayed type-IV adsorption–desorption isotherms typical of mesoporous material. The samples containing lower amounts of niobium (GaNb1 and GaNb2) exhibit a two-step, N_2 adsorption–desorption isotherm, with one step at P/P0 between 0.5 and 0.8 due to the filling of framework mesopores and the second step at P/P0 = 0.9 due to filling of interparticle textural pores [20]. The mixed oxide samples containing higher amounts of niobium (GaNb3 to GaNb5) and pure niobium oxide displayed type IV isotherms with H2 hysteresis loops, again confirming the mesoporous nature of these materials [21]. The mixed oxides containing higher amounts of niobium displayed surface areas in the range of 230 to 270 m^2/g with the average pore sizes in the 3–4 nm range (Table 2). The surface area of the niobium oxide was ~196 m^2/g. A control sample, GaNb4A, synthesized in the absence of the SDA displayed microporous structure with average pore size of ~1 nm. The average size of the crystallites for the mixed oxides as well as niobium oxide was in the range of 3–5 nm resulting in the broadening of the peaks. The XRD pattern for gallium oxide revealed strong reflections at dspacing= 4.7, 2.5, 2.02, 1.6 and 1.5 Å corresponding to the (111), (311), (400), (333) and (440) planes of the cubic spinel lattice, respectively, in agreement with previous reports [22].To obtain more structural information, the niobium oxide sample was calcined at (182) planes,

respectively, of pure Nb_2O_5 [18,22]. For the pure Nb_2O_5 sample calcined at 600 °C, much larger grain sizes and well-defined diffraction patterns are observed confirming that these large well crystalline Nb_2O_5 have grown from the smaller crystallites of Nb2O5 present after calcination at 350 °C. Measurements of several intense rings provide interplanar spacing values of 0.396, 0.325 and 0.246 nm, in good agreement with the d-spacings of (001), (180) and (181) planes, respectively, in Nb_2O_5. The electron diffraction results are, thus, consistent with those from X-Ray diffraction.

The products from the reaction of fatty acid methyl esters (oleic, linoleic and linolenic) over our

catalysts consisted of isomers (both double bond and skeletal),dehydrogenation products (of both the saturated and mono olefinic fatty acid esters in the feed) and dimers of the mono olefinic FAME esters. Significant amo unts of cracked products (C14 and C16) were also observed especially over the aluminosilicate molecular sieve catalysts. The high resolving power of 13C NMR spectroscopy has allowed many of the isomers of long chain fatty acid esters to be differentiated (see Supplementary content). In the case of methyl oleate, for example, the shifts of the olefinic carbon atoms appear at δc 129.8 and 130.0 for the C-9 and C-10 carbon atoms, respectively [25]. The terminal methyl carbon shift (C-18) is found at δc 14.1. The carbonyl carbon of the ester fraction (C-1) is observed at δc=174.3. The methyl carbon of the ester appears at δc=51.5. A typical composition of the product for GaNb4 was as follows (in wt.%):methyl oleate=26.0%; methyl elaidate=3.2%; methyl linoleate= 26.9%; methyl linolenate=5.1%; methyl stearate=0%; methyl palmitate=4.1%; methyl palmitoate = 4.0; skeletal isomers=27.6%; dimers=2.3% and oleic acid=0.8%. The presence of dehydrogenated, diolefinic products (mainly linoleates) was deduced from 13C NMR, gas chromatography and iodine number measurements. The decrease in the concentration of the saturated FAMEs, methyl stearate and palmitate also supports this conclusion. When traces of water were present (N10 ppm) in the biodiesel, hydrolysis of the FAME to fatty acids over the acid sites occurred as could be inferred from the increase in the acid number of the product. The dimerisation of the FAME molecules was observed over certain catalysts (H–Y, H–MCM-22, GaNb2 and GaNb3, for example). Above 220 °C, cracked products (C16, C14 and C12 hydrocarbons) were observed over both the zeolite and mesoporous Ga–Nb oxide catalysts. Selectivity for skeletal isomerization was obtained from the increase in the intensity of the 13C NMR peaks at 30.91 ppm (characteristic of the −CH–carbon) and 18.36 ppm (characteristic of the −CH3 group) relative to those in the reactants. The side products consisted, mainly, of dimers of methyl oleate.

Both the acidity and catalytic activity for methyl oleate conversion of the catalysts increased with increasing niobia content, reach a maximum for GaNb3–GaNb4 samples and decrease thereafter .The lower activity of pure Nb2O5 may be, partly due to its lower surface area and pore volume as compared to the Ga–Nb mixedoxides. In addition to the skeletal and double bond isomerization products formed over the acid sites, the products over Ga–Nb oxides included significant amounts of dehydrogenated products. This latter conclusion is supported by the higher iodine number values of the products . The iodine number of the methyl oleate feed was 83. We could not identify all the individual diolefinic isomers by gas chromatography-cum-mass spectrometry. The iodine

number is indicative of unsaturation (number of double bonds) in the product molecules. Dehydrogenation reactions increase the iodine value while dimerisation of the mono olefinic esters (also catalyzed by acidic sites) leads to a decrease in their iodine values. Skeletal isomerisation does not alter the iodine values. The net increase in iodine number observed over all the Ga–Nb catalysts confirm the bifunctional acidic and dehydrogenative) catalytic activity of these mixed Ga–Nb oxides. While the pour points of the commercial methyl oleate sample was −14 °C, there was a slight decrease (−2 to−6 °C) in the pour points of the products of the reactions. The catalytic stability of GaNb4 in the reaction of methyl oleate was evaluated. After reaction at 220 °C for 12 h, this catalyst was washed in acetone at room temperature, dried at 120 °C and reused in the conversion of methyl oleate at 220 °C. This procedure was repeated twice. The observed conversion of methyl oleate was 92, 90 and 87% for the three experiments, respectively. There was no significant change in product selectivity. The observed slight deactivation was due to the deposition of carbonaceous matter on the catalyst surface since regeneration in air at 400 °C restored the original catalytic activity.

Methyl oleate and biodiesel undergo a complex series of reactions in the presence of aluminosilicate and silicoaluminophosphatemolecular sieves and mesoporous Ga–Nb oxides. Acid catalyzed reactions, like double bond and skeletal isomerisations, and dimerisation as well as redox reactions like the dehydrogenation of the methyl oleates to methyl linoleates, methyl palmitates to palmitoates were observed over the mesoporous Ga–Nb oxides.Hydrolysis of the FAMEs to free fatty acids occurs when water was present, as an impurity, in the feedstock. While skeletal isomerization and dehydrogenation decreases the pour point of biodiesel, the formation of dimers and free fatty acids increases it and degrades its cold flow properties. Among the mesoporous Ga–Nb oxides both catalyst acidity and catalytic activity in the conversion of methyl oleate reach a maximum at a Ga/Nb molar ratio of about 0.08–0.14. While conversions of methyl ocbleate or biodiesel are low over catalysts of low acidity or at low temperatures, cracking reactions are observed above 220 °C. Among the solid catalysts that we have testedin this study, GaNb4 and SAPO-11 have the highest selectivities for skeletal isomerisation. While the superior performance of SAPO-11 and Pt-SAPO-11 in the skeletal isomerisation of long chain olefins and paraffins, respectively, is well known, this is the first report of the high selectivity of mesoporous, Ga–Nb mixed oxides and SAPO-11 in the skeletal isomerisation of unsaturated, linear fatty acid alkyl esters. The selectivity for skeletal isomerisation of the linear FAMEs over the mesoporous Ga–Nb oxides is comparable, if not better, than those observed over the aluminosilicate and silicoaluminophosphate molecular sieves. The ability of mesoporous Ga–Nb oxides to dehydrogenate the fatty acid esters in the same temperature range (150–220 °C) wherein significant skeletal isomerisation is also observed over the same catalysts is an interesting finding with many potential applications in the manufacture of biodiesels with superior cold flow properties.

One of the significant achievements of this project was the discovery of novel mesoporous mixed oxides of germanium and niobium as catalysts for the preparation of superior quality biodiesel by the skeletal isomerization of conventional linear biodiesel molecules to their branched isomers. Fig 1 illustrates the shape and sizes of our novel

materials. The catalytic activity of these mesoporous phases in the skeletal isomerization of typical biodiesel molecules like fatty acid methyl esters such as methyl oleate, was evaluated by reacting the catalyst with methyl oleate in a batch autoclave at 220C and under autogenous pressure. Methyl oleate is a fatty acid methyl ester (FAME) and is a major component of biodiesel obtained from triglyceride oils, like soy beans oil, by transesterification with methanol. One of the major drawbacks of such FAME biodiesels, compared to petro diesels, is their high freezing points due to which they cannot be used in very cold climates. Skeletal isomerisation, over acid sites, of the linear, unsaturated esters to branched esters or dehydrogenation (over redox sites) of the mono-olefinic esters to the diolefinic esters can reduce their freezing points. The branched iso-stearic acid, for example, has a lower freezing point compared to the linear isomer stearic acid (_30 vs. +70 1C). Similarly, the freezing point of diolefinic linoleic acid is lower than that of the mono-olefinic oleic acid (_5 vs. +16 1C). Yori et al.(11) reported the skeletal isomerisation and cracking of methyl oleate over mordenite and sulfated zirconia. Leaching of the sulfonic acid groups and deactivation were major problems observed in these catalysts. Zhang and Zhang (12) reported the skeletal isomerisation of methyl oleate over beta -zeolites. The presence of mesoporosity in their samples was identified as an important parameter enhancing catalytic activity. The gallium–niobium oxides possess both acidic and redox sites and may be expected to catalyze isomerisation as well as dehydrogenation reactions. Mesoporosity is an added advantage in the reactions of these long chain molecules to avoid transport and diffusional limitations.Product identification was done by a combination of gas chromatography, mass spectrometry and 1H/13C NMR spectroscopies. The gas chromatographic peaks corresponding to M+296 and M+294 peaks in the mass spectra were used to identify and quantify the concentrations of methyl oleate and linoleate, respectively. The concentration of the skeletal isomers was obtained from gas chromatography/mass spectrometry and also from the ratio of the intensities of the 1H NMR peaks at 5.3–5.5 ppm (characteristic of internal olefinic C–H protons) and those at 1.92–2.08 ppm (characteristic of allylic protons), respectively.16 The presence of oleic acid was inferred from gas chromatography-cum-mass spectrometry and acid–base titration as well as changes in the 13C NMR peaks of the carbonyl carbon (of the ester) at 174.3 ppm and the methyl carbon of the ester at 51.5 ppm. The quantification of the oleic acid concentration was done using peaks in the 2.37–2.41 ppm region in the 1H NMR spectra by procedures published elsewhere.17 The products consisted of branched methyl and ethyl isomers of methyl oleate, dehydrogenated diolefinic product from methyl oleate (methyl linoleate), methyl palmitoleate (C16:1 from the dehydrogenation of methyl palmitate, C16:0 an impurity in the methyl oleate)Oleic acid (also found for pure niobia and samples rich inNb2O5) was probably formed by the hydrolysis of methyl oleate by the residual water or surface hydroxyl groups. It is important to mention that hydroxyl groups on pure niobia are completely removed only above 350 1C. As shown in Table 2 both the acidity and catalytic activity of the catalysts increase with increasing niobia content, reach a maximum for GaNb3–GaNb4 samples and decrease thereafter. Even though a linear correlation between acidity and catalytic activity is not observed a clear dependence of activity on acidity may be discerned in these data. The superior

catalytic performance of GaNb4 sample can also be partly attributed to its higher crystallinity as compared to the other samples . For comparison purposes, we evaluated the catalytic activity of a control sample which was prepared in the absence of the SDA (sample GaNb4A). The catalytic performance of the control sample was poor as compared to the mesoporous sample of the same composition.

The acidity reaches a maximum for the mixed oxide, GaNb3-GaNb4. Product identification was done by a combination of gas chromatography, mass spectrometry and ^{1}H / ^{13}C NMR and IR spectroscopies.[8] The gas chromatographic peaks corresponding to $M^{+}296$ and $M^{+}294$ peaks in the mass spectra were used to identify and quantify the concentrations of methyl oleate and linoleate, respectively. The concentration of the skeletal isomers was obtained from gas chromatography/mass spectrometry and also from the ratio of the intensities of the ^{1}H NMR peaks at 5.3-5.5 ppm (characteristic of internal olefinic C-H protons) and those at 1.92-2.08 ppm (characteristic of allylic protons), respectively. The presence of oleic acid was inferred from gas chromatography-cum-mass spectrometry and acid-base titration as well as changes in the ^{13}C NMR peaks of the carbonyl carbon (of the ester) at 174.3 ppm and the methyl carbon of the ester at 51.5 ppm. The quantification of the oleic acid concentration was done using peaks in the 2.37-2.41 ppm region in the 1H NMR spectra was done by published procedures. The products included branched(methyl and ethyl) isomers of methyl oleate, the dehydrogenated, dilolefinic product from methyl oleate (methyl linoleate), methyl palmitate(C16:1)(from the dehydrogenation of methyl palmates(C16:0),an impurity in the methyl oleate). Oleic acid (also found for pure niobia and samples rich in Nb_2O_5) was probably formed by the hydrolysis of methyl oleate by the residual water or surface hydroxyl groups. It may be mentioned that hydroxyl groups on pure niobia are completely removed only above 350˚C. Both the acidity and catalytic activity of the catalysts increae with increasing niobia content, reach a maximum for GaNb3-GaNb4 samples and decrease thereafter. Even though a linear correlation between acidity and catalytic activity is not observed a dependence of activity on acidity may be diiscerned. Catalytic activity depends on other factors in addition to acidity like surface area , mesoporisity, pore diameter etc.

The acidity reaches a maximum for the mixed oxide, GaNb3-GaNb4. Product identification was done by a combination of gas chromatography, mass spectrometry and ^{1}H / ^{13}C NMR and IR spectroscopies. The gas chromatographic peaks corresponding to $M^{+}296$ and $M^{+}294$ peaks in the mass spectra were used to identify and quantify the concentrations of methyl oleate and linoleate, respectively. The concentration of the skeletal isomers was obtained from gas chromatography/mass spectrometry and also from the ratio of the intensities of the ^{1}H NMR peaks at 5.3-5.5 ppm (characteristic of internal olefinic C-H protons) and those at 1.92-2.08 ppm (characteristic of allylic protons), respectively. The presence of oleic acid was inferred from gas chromatography-cum-mass spectrometry and acid-base titration as well as changes in the ^{13}C NMR peaks of the carbonyl carbon (of the ester) at 174.3 ppm and the methyl carbon of the ester at 51.5 ppm. The quantification of the oleic acid concentration was done using peaks in the 2.37-2.41 ppm region in the 1H NMR spectra by procedures published elsewhere[12]. The products included branched(methyl and ethyl) isomers of methyl oleate, the dehydrogenated, dilolefinic product from methyl oleate (methyl linoleate), methyl palmitate(C16:1)(from the dehydrogenation of methyl palmates(C16:0),an impurity in the methyl oleate). Oleic acid (also found for pure niobia and samples rich in Nb_2O_5) was probably formed by the hydrolysis of methyl oleate by the residual water or surface hydroxyl groups. It may be mentioned that hydroxyl groups on pure niobia

are completely removed only above 350˚C. Both the acidity and catalytic activity of the catalysts increae with increasing niobia content, reach a maximum for GaNb3-GaNb4 samples and decrease thereafter. Even though a linear correlation between acidity and catalytic activity is not observed a dependence of activity on acidity may be diiscerned[8]. Catalytic activity depends on factors in addition to acidity like surface area , mesoporisity, pore diameter etc.

In summary, novel mesoporous, bifunctional, Ga–Nb mixed oxides active in acid-catalyzed as well as redox reactions have been synthesized and structurally/texturally characterized. These material isomerise the long-chain, linear, mono-olefinic ester, methyl oleate, a major constituent of FAME biodiesel, into its branched isomers and dehydrogenate it to the diolefinic ester, methyl linoleate. The branched isomers as well as the diolefinic esters have lower pour points and superior cold flow properties compared to the conventional FAME biodiesels.

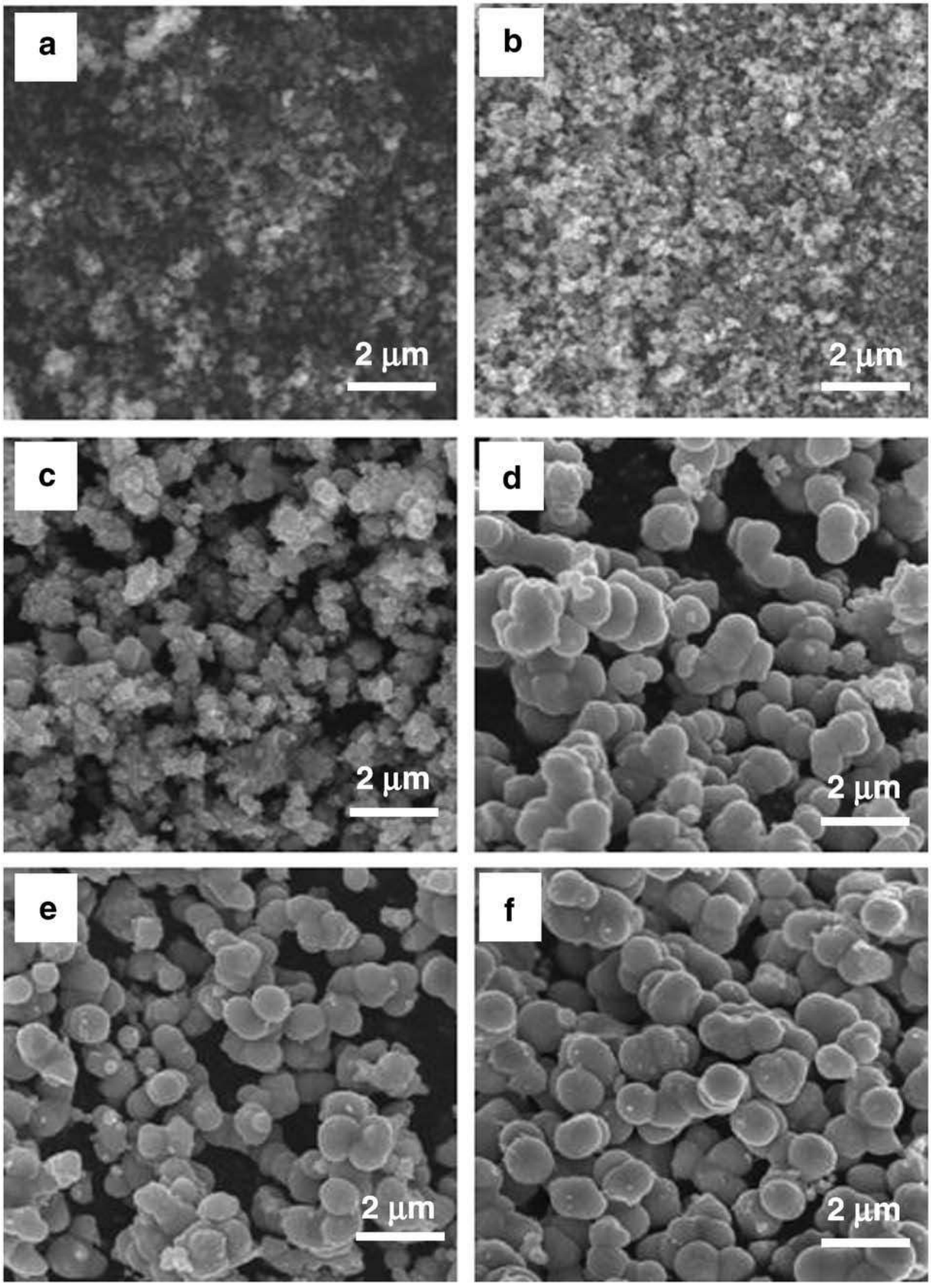
a
2 μm
b
2 μm
c
2 μm
d
2 μm
e
2 μm
f
2 μm

Fig. 2. SEM images of (a–e) mesoporous mixed Ga–Nb oxides (1–5) and (f) mesoporous Nb_2O_5 synthesized by SAHA employing F127 as SDA and calcined at 350 °C.

Table 1: General synthesis conditions, textural properties and average particle size of mesoporous gallium oxide, gallim-niobium mixd oxide and niobium oxide phases synthesized by SAHA.

Sample ID	Composition Ga/Nb molar ratio	S. S. A. m^2/g	Average Pore Size (nm)	Pore Volume (cm^3/g)	Average Particle size (μm)
Ga_2O_3	-	175	7.3	0.32	0.3
GaNb1	6.0	210	6.1	0.38	0.5
GaNb2	2.5	366	4.4	0.42	0.8
GaNb3	1.1	270	4.1	0.33	0.8
GaNb4	0.5	231	3.7	0.25	1.0
GaNb5	0.2	242	3.4	0.23	1.3
Nb_2O_5	-	196	3.2	0.17	1.8

Figure 3. The adsorption-Desorption isotherms of Nitrogen on the mesoporous Ga-Nb oxide catalysts.

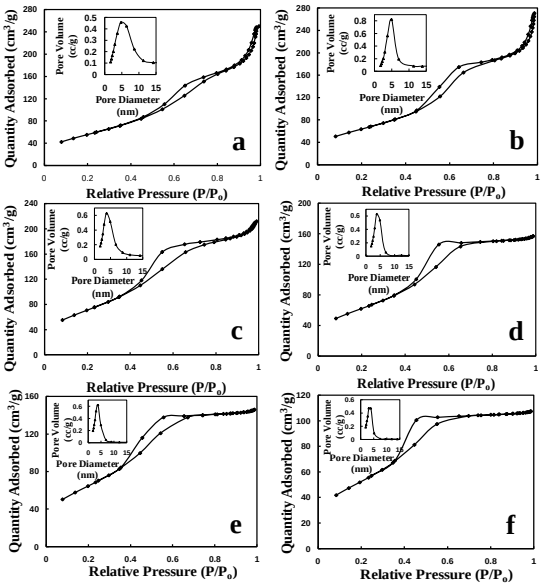

Figure 4. X-Ray diffraction patterns of the Ga-Nb oxide catalysts for Isomerisation of FAME.

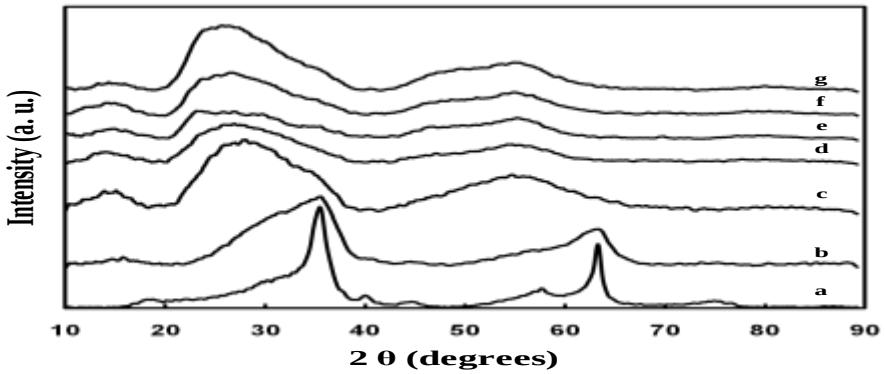

Table 2: Catalytic transformations of methyl oleate over mesoporous gallium oxide, Ga-Nb mixed oxides, and niobium oxide.

Sample ID	Acidity Moles of DPA/g of Catalysts ($\times 10^{-6}$)	MO conversion %wt	Selectivity for isomerisation %wt	Selectivity for (C14 + C16)	Others ‡ %wt
Ga_2O_3	0.28	9.7	46.4	55.5	0.0
GaNb1	0.64	10.8	43.8	50.0	7.0
GaNb2	0.70	19.5	53.4	20.7	25.9
GaNb3	0.96	22.4	48.3	24.6	27.1
GaNb4	0.74	56.5	86.0	0.0	14.0
GaNb5	0.67	13.3	38.0	53.6	8.4
Nb_2O_5	0.61	18.0	70.0	26.3	3.7

2*. Preparation of Green diesel and Jet fuels from waste oils*

This is our second approach to the preparation of superior quality biodiesels. Our research efforts in this project to develop the chemistry and technology for the preparation of green diesel and jet fuels from waste vegetable oils are described in this section.

Background : In 2008, the global aviation industry consumed about 1.6 billion barrels of Jet fuel and emitted 700 million tons of CO_2 . The aviation industry has identified the development of aviation biofuels as one of the major ways it can reduce its CO_2 emissions. The aviation biofuel must be a direct replacement for traditional kerosene fuel (Jet A1) so that manufacturers do not have to redesign the engines and airlines / airports do not have to develop new fuel delivery systems. At present, the industry is focused on producing aviation biofuel from *sustainable* , non-food sources that will enable the fuel to be a "drop-in" either as a blend or as a replacement for the Jet A1 fuel.

Technical specifications for jet fuels are very stringent (Flash point: 38^{o}C min; Freezing point: -47^{o}C max; combustion heat: 42.8 MJ/kg min; viscosity: 8.0 mm^2/s max; sulphur content: 0.3 ppm max; Density: 775-840 kg/m^3)(27,28). First generation biofuels like ethanol and conventional FAME biodiesels are not suitable. Hydrocarbon fuel is the only option for aviation. Currently, there is no foreseeable new technology to power flight beyond hydrocarbon fuels. A major constraint is that, to minimize their CO_2 footprint, these hydrocarbon fuels have to be produced from non-petroleum / coal / natural gas resources. Similarly, agricultural raw material of food-products are also not suitable. Lipids (like non-food oils / fats / greases of agri, animal and industrial origin, algae oil, tall oil) and cellulosic residues(forestry /municipal etc) are the two potential raw material. In view of its global spread, it is unlikely, however, that the aviation industry will rely on just one type of feedstock. It is more likely that aircraft will be powered by blends of jet fuel made from different types of feedstocks (depending on the location) with the petroleum-based jet fuel. *The major technology challenge is the production of an uniform grade of jet fuel from such a diverse variety of raw material in an environmentally and economically viable manner*. It is likely that a portfolio of technologies will be developed to process the different feedstocks available in different parts of the world(28,29). Jet fuel is a mixture of hydrocarbons (mainly paraffins, cyclo paraffins and aromatics) containing 10 to 15 carbon atoms and boiling in the range 150-

300^{o}C with the physical features mentioned above. The potential routes from biomass to jet fuel are :

(a) *Raw Materials are carbohydrates from cellulosicbiomass(wood, switchgrass etc.)*: a feasible process route is: (a) Gasification to syngas followed by Fischer-Tropsch synthesis (to linear paraffins) and hydro isomerisation to branched paraffins(30); (b) Liquefaction to heavy bio oil followed by mild hydrocracking and hydroisomerisation to jet fuel(31); Since around 6 tons of cellulosic solids are required to produce 1 ton of liquid hydrocarbons,600 tons of wood must be processed *per day* even in a relatively small sized plant producing 10 MGPY of jet fuel.

(b) *Raw materials are triglycerides from lipid sources(32-36)*; Examples are crude and acid palm oils, cotton / rubber seed, jatropha and karanja oils, animal rendering wastes, algae oils and black liquor from paper mills: The conventional process route(32) is the hydrogenation of the lipid triglyceride followed by reforming of the resultant linear, C_{14} to C_{18} hydrocarbons to jet fuel(C_{10} to C_{15} hydrocarbons). About 13MGPY of lipid fats/oils will be needed for the production of 10 MGPY of jet fuel.

The cellulose route is highly capital intensive, poses enormous logistic problems and the integrated technology has not yet been commercially demonstrated. The lipids-based technology has been already proven in the production of *conventional* FAME biodiesel. Conversion of triglycerides to jet fuels, however, has not been , so far, demonstrated at the commercial level.

The major *technical* requirements in the conversion of triglycerides to jet fuel hydrocarbons are(9): (1)the removal of the oxygen atoms in the triglycerides with a minimum consumption of hydrogen from outside sources,(2) conversion of the straight chain structure of the fatty acids in the triglycerides to branched chains and (3) restricting the end - boiling points of the heavy hydrocarbons (resulting from the deoxygenation and molecular rearrangements mentioned above) to 300 C. The first requirement (oxygen removal) is obvious from the stoichiometric differences between the trioglyceride and jet fuels : the molecules of the latter do not contain oxygen while those of the former do. The straight chain structures present in the fatty acids portion of the triglycerides give rise to freezing and pour points in the hydrocarbons formed on deoxygenation of the triglycerides which are higher than those specified for jet fuels, Jet A-1 (ASTM D 1655) or JP-8 (MIL-83133E). If these straight chain hydrocarbons can be rearranged to branched chain structures, then, the freezing points of the resulting molecules will be substantially lower thereby satisfying the very low freezing/ pour point requirements of jet fuels mentioned earlier. The third requirement (restriction of the end-boiling point to below 300 C) arises because the C18 and C20 hydrocarbons formed by deoxygenation have boiling points above 300 C; C18 and C20 normal hydrocarbons , for example, boil at 316 and 344 C , respectively. Selective catalytic reforming / cracking to reduce their molecular weight is, hence, necessary. A technically and commercially proven process for the conversion of triglycerides to jet fuels wherein all the above three challenges have been fully and economically resolved has not, so far, been developed.

Our Solution (references 27-37): In any conversion of biomass to hydrocarbons, the cost of hydrogen is a crucial one. We minimized the use of hydrogen in all the process

stages. In addition, we also generate the *entire* hydrogen requirement from the byproducts formed during the production of the jet fuel from lipid triglycerides. Our novel process consists of the following stages:

Stage 1. Hydrolysis of the triglycerides to glycerine and fatty acids. This is a non-catalytic reaction known in the prior art. In this process steam and the vegetable oils are passed in counter current mode through a reactor at around 270 C and 50 -70 bar pressure. The triglycerides are hydrolysed to glycerol and fatty acids in near-quantitative yields.

Stage 2,: For the removal of the oxygen atoms, instead of hydrogenation using hydrogen, which eliminates the (-COOH) groups of the fatty acids, as CH_4 and H_2O consuming a large quantity of hydrogen in the process, we decarboxylate them (as CO_2) over a novel, hydrophobic catalyst containing palladium metal *with a minimum consumption of hydrogen necessary only to saturate the double bonds of the unsaturated fatty acid molecule*.

Stage 3: Reforming- cum-Isomerisation; In this stage, the straight chain hydrocarbons from Stage 2 are skeletally isomerised to branched chain hydrocarbons (to reduce the freeze / pour points) and selectively cracked (to reduce the molecular weight and end-boiling point of the products). ;The straight chain hydrocarbon effluent from Stage -2 are passed, after removal of unconverted fatty acids, through a CO_2- tolerant, acidic catalyst containing , in addition to the acidic function, metallic components dispersed on the surface of the acidic component. One of the metals, for example, platinum functions as a hydrogenation – dehydrogenation catalyst while the other component, for example, iridium , functions as a hydrogenolysis catalyst. While the former, along with the acidic support, carries out the skeletal isomerization, the second component selectively cracks the hydrocarbon chain and reduces the molecular weight / end-boiling point of the product molecules.

The main chemical reactions that occur in the above 3 stages are illustrated below:

Hydrolysis : $C_{57}O_6H_{104} + 3H_2O \Rightarrow 3C_{18}H_{34}O_2$(Octadecanoic acid) $+ C_3H_8O_3$(glycerine) ……(1)

Deoxygenation: $3C_{18}H_{34}O_2$(Octadecanoic acid) $+ 3H_2 \Rightarrow 3CO_2 + 3C_{17}H_{36}$ (heptadecane) (2)

Reforming-cum- Isomerisation : $C_{17}H_{36} \Rightarrow$ jet fuel (3)

The hydrogen needed in Stage 2 will be fully provided by steam reforming of the glycerine byproduct from Stage-1.

Steam reforming of glycerine: $C_3H_8O_3$(glycerine)$+ 6H_2O \Rightarrow 10H_2 + 3CO_2$

We have not carried out the hydrolysis reaction (1) as this technology is already well-known and in commercial practice. Some representative results of our decarboxylation and hydroisomerization are given in the Tables below:

Table 3. Hydroisomerisation of n- hexadecene $C_{16}H_{32}$ over Pt- Sapo-11.
Reaction Conditions: 250 C; 20 bar H_2; 3hr

Catalyst	Feed	Feed	Analysis			Product	Analysis	
Sapo-11	C16H32	Ret	compound	%		Ret time	Compound	%

(2 gm)	(40 ml)	time Min	i.d.			Min	i.d.	
		13-15	C14-C15	2.1		14.5-14.7	C15	24.7
		15-16	Iso C16	41.8		15-16	Iso C16	62.8
		16.4	n-C16	44.7		16.4	n-C16	12.5
		>16.4	$C17^+$	11.3		-	$C17^+$	0
		SUM	3.86				SUM	3.1
		Iodine No:	109.1				Iodine No C16 Conv	105.872

Table 4. Hydroisomerisation of n-hexadecane ,$C_{16}H_{34}$ on Pt-Sapo-11
Reaction Conditions : 250C; 15 bar H_2; 2 hrs

Catalyst	Feed					Product	Analysis	
Sapo-11 (2 gm)	C16H34 (40 ml) Iodine no =1.0					Ret time Min	Compound i.d.	%
						<15	C15	0.6
						15-16	Iso C16	83.4
						16.4	n-C16	3.9
						>16.4	$C17^+$	12.4
							SUM	10.21
							Iodine No	0

Table 5. DeCOOH + HISOM of a mixture of (n-hexadecane($C_{16}H_{34}$) + oleic acid + Dodecanoic acid,$CH_3(CH_2)_{10}$ COOH) on Pt-Sapo-11 .

Catalyst(g)	Feed(ml)	T(C)	Press(bar)	Reaction Time,hr	Product I.d.	Product, %	Remarks
Pt-Sapo-11 (2gm)	C16H34+Oleic acid+Dodecanoic acid(40 ml	300	15	2	C9H20	0.87	FA Conv = 95.4%
	Acid No:115.1 Iodine no=27.7				C10H22	1.17	Jet Fuel yield=93.1 %
					C11H24	3.76	Product Iodine no=42.3 Acid no= 5.3

					C12H26	3.5	SUM=7.1
					C13H28	10.1	
					C14H30	27.6	
					(C15+Iso C16) n-C16 C17+	19.7 27.1 6.9	

Table 6. DeCOOH + HISOM of a mixture of (n-hexadecane($C_{16}H_{34}$) + oleic acid + Dodecanoic acid,$CH_3(CH_2)_{10}$ COOH) on(Pt-Sapo-11 + Pd-Hydrotalcite) .

Catalyst(g)	Feed(ml)	T(C)	Press(bar)	Reaction Time,hr	Product I.d.	Product, %	Remarks
Pt-Sapo-11 (2gm) + Pd-Hydrotalcite (2gm)	C16H34+Oleic acid+Dodecanoic acid(40 ml	250	11	3	C7-C8 C9H20	15.9 10.6	FA Conv = 94.2%
	Acid No:115.1 Iodine no=27.7				C10H22	10.5	Jet Fuel yield=80.9 %
					C11H24	10.6	Product Iodine no=2.8 Acid no=6.7
					C12H26	10.3	SUM=9.7
					C13H28	3.0	
					C14H30	0.65	
					(C15+C16) C17+	34.2 3.3	

A comparison of catalysts based on Pd and Pt are given in Table 5. In this Table, catalysts 1312 and 1334 are Pd (5% wt) supported on hydrotalcite. They differ in the method of preparation. The runs were carried out in a Parr autoclave of 300 mml capacity.

Table 7. Decarboxylation Studies- Comparison of Pd- and Pt - based catalysts

Catalyst	Feed		Temp C	H2 Press bar	time,hr	FA conv,%
1312,	OA+C16		330	20	TOS=5	94
do	do		330	20	TOS=13	91
do	do		330	20	TOS=29	96
do	OA+C16		330	20	4	94
1312	do		330	33	4	100
Pd-Al2O3		do	330	30	4	100
Pd-C	OA+C16		330	20	6	100
Pd-CZO	PA+C16		330	28	4	90
1312	OA+C16		350	20	2	88
1312	OA		350	20	2	90
1334	OA		350	20	2	95
1312	do		250	20	2	92
1334	do		250	20	2	90.5
1334	do		250	20	2	36.9
5%PtAl2O3	do		250	20	2	97.5
1312	OA		250	20	2	

The quality of our product after hydrolysis, decarboxylation and hydroisomerisation of the waste vegetable oils was analysed, independently, by the prestigious SWRI (South West Research Institute). **Their report, given below, confirms that our product meets all the specifications of JP-8, for a jet fuel, JP-8.**

Petroleum Products Research Department
Office of Automotive Engineering

Data Analysis

	Sample B SwRI Lab# oddb 523-501
ASTM D5291 Carbon, Hydrogen Determination	
Carbon, wt%	84.97
Hydrogen, wt%	15.05
ASTM D5773 Cloud Point of Petroleum Products (Constant Cooling Rate Method)	
Cloud Point, °C	-48.5
ASTM D5949 Pour Point of Petroleum Products (Automatic Pressure Pulsing Method)	
Pour Point, °C	-60
ASTM D1322 Smoke Point of Kerosene and Aviation Turbine Fuel	
Smoke Point, mm	*Insufficient Sample*
ASTM D240 Heat of Combustion	
GROSS BTU / lb	20184
MJ/kg	46.948
NET BTU/lb	18811
MJ/kg	43.755
ASTM D5453 Sulfur by UV *(data used to calculate D240)*	
Sulfur, ppm	17
GCMS Fingerprint	Attachment

References:

[1] R.O. Dunn, M.W. Shockley, M.O. Bagby, J.Am.Oil Chem.Soc. 73 (1996) 1719.
[2] I. Lee, L.A. Johnson, E.G. Hammond, J.Am. Oil Chem.Soc. 72 (1995) 1155.
[3] L.U. Berman, M.L. Loeb, The dimer acids, in: E.C. Leonard (Ed.), Humko Sheffield Chemicals, 1975.
[4] A.A. Christy, Chemistry and Physics of Lipids 161 (2009) 86.
[5] G. Roberts, C.M. Lok, C.J. Adams, K.R. Seddon, M.J. Earle, J.T. Hamill, Process for preparation of branched fatty acids, US Patent 6,255,504 2001.
[6] W. Tsuzuki, R. Nagata, R. Yunoki, M. Nakajima, T. Nagata, Food Chemicals 108(2008) 75.
[7] K. De Oliveira, H. Khiem, Y. Pouilloux, J. Barrault, Oleagineaux Corps Gras Lipids 10(2003) 374.
[8] C.S. Narasimhan, K. Ramnarayan, V.M. Deshpande, J. Mol. Catal. 52 (1989) 305.
[9] W.R. Hodgson, W.T. Koetsier, C.M. Lok, G. Roberts, Fatty acid isomerisation, US Patent 5,856,539 1999.
[10] S. Zhang; Z. Zhang; D. Steichen; Skeletal isomerization of alkyl esters and derivatives prepared therefrom US Patent 6, 946, 567 2003.
[11] J.C. Yori, M.A. D'Amato, J.M. Grau, C.L. Pieck, C.R. Vera, Energy & Fuels 20 (2006) 2721.
[12] S. Zhang, Z.C. Zhang, Catal. Lett. 115 (2007) 114.
[13] O.D. Dailey, J.,.N. Prevost, J.Am.Oil Chem Soc. 84 (2007) 565.
[14] O.D. Dailey Jr., N.T. Prevost, G.D. Strahan, J. Am. Oil Chem Soc. 85 (2008) 647.
[15] C.A. Deshmane, J.B. Jasinski, M.A. Carreon, Eur. J. Inorg. Chem. 22 (2009) 3275.

[16] K. Nakagawa, M. Okamura, N. Ikenaga, T. Suzuki, T. Kobayashi, Chem. Comm(1998) 1025.

[17] T. Onfroy, G. Clet, M. Houalla, J. Phys. Chem., B 109 (2005) 14588.
[18] I. Novak, M. Misiewicz, M. Ziolek, A. Kubacka, V.C. Corberan, B. Sulikowski, Appl.Catal. A: General 325 (2007) 328.
[19] R. Szostak, Handbook of molecular sieves, Van Nostrand Reinhold, New York, 1992.
[20] E. Prouzet, C. Boissiere, S.S. Kim, T.J. Pinnavaia, Micro. Meso. Mater. 119 (2009) 9.

[21] K.S.W. Sing, D.H. Everett, R.A.W. Haul, L. Moscou, R.A. Pierroti, J. Rouquerol, T.

Siemieniewska, Pure Appl. Chem. 57 (1995) 603.
[22] M. Yada, M. Ohya, M. Machida, T. Kijima, Langmuir 16 (2000) 4752.
[23] X. Chen, Y. Yu, X. Fan, H. Zhang, Z. Li, J. Ye, Z. Zou, Appl. Surf Sci. 253 (2007) 850.
[24] C.A. Deshmane, J.B. Jasinski, M.A. Carreon, Micro. Meso. Mater. 130 (2010) 97.
[25] J.K. Satyarthi, D. Srinivas, P. Ratnasamy, Energy Fuels 23 (2009) 2273.
[26] D.Y.C. Leung, X. Wu, M.K.H. Leung, Applied Energy 87 (2010) 1083

[27] Process for co-producing Jet fuels and LPG from renewable sources,U.S. 2008/0244962 A1

[28] Process for producing branched hydrocarbons, U.S. 2008/0302001 A1
[29] Process for conversion of biomass to fuel, U.S. 2009/0069610 A1
[30] Fuel,87(2008)3543-3549.
[31] Applied Catalysis A. General., 355(2009)100-108.
[32] Catalysis today, 144(2009) 362-366.
[33] Catalysis Letters, 130(2009) 48-51.
[34] Ind. Eng. Chem. Res., 45(2006)5708-5715.
[35] Catalysis today, 106(2005) 197-200.
[36] Applied Catalysis A. General., 361(2009) 99-105.
[37] Chem. Ber. 1982,115, 808

PREDICTING SOLAR RADIATION FROM SHORT-TERM WEATHER FORECAST CLOUD COVER PREDICTIONS AND ITS APPLICATIONS IN CONTROL OF ACTIVE SOLAR THERMAL SYSTEMS

FINAL REPORT

KREC II

University of Kentucky

May 12, 2011

Donald Colliver, PI

Jeffery Kellow, Graduate Research Assistant

PREDICTING SOALR RADIATION FROM SHORT-TERM WEATHER FORECAST CLOUD COVER PREDICTIONS AND ITS APPLICATIONS IN CONTROL OF ACTIVE SOLAR THERMAL SYSTEMS

SECTION 1 – Introduction

Commercial solar water heaters have been available since the 1890's (Lane, 2004). Solar thermal systems have a wide range of applications including "hydronic space heating, service water heating, industrial process water heating, energizing absorption air conditioning, pool heating," and providing a heat source for series coupled heat pumps (ASHRAE, 2004). Active solar thermal systems pump water or an antifreeze solution through collectors, which are heated by solar radiation and transfer heat to the fluid. Closed-loop solar thermal collectors run an antifreeze solution through the collectors and use heat exchangers to transfer the collected heat into potable water or other process fluids. Closed-loop systems are prevalent in areas that experience freezing conditions.

Common active solar thermal systems are driven by thermostatic control and heat a single domestic hot water tank. If a specified temperature differential between the fluid in the collectors and the fluid in the storage tank is reached, the pump circulates the fluid through the collector and moves energy into the storage tank via the heat exchanger. When the temperature differential becomes too small to efficiently transfer heat into the storage tank the pump stops circulating the fluid. An alternate method of control utilizes a variable speed DC pump powered and controlled by a dedicated photovoltaic module

(Lane, 2005). When the pump and dedicated photovoltaic module are sized properly, the flow rate of the circulating fluid is optimized by the amount of incident solar insolation (Lane, 2005).

Among the main technical points of research interest for active solar technologies stated by Papadopoulos (2003) were "development of combined solar water and space heating systems, advanced controls and design and analysis tools to integrate solar technologies more efficiently into buildings, and advanced solar thermal storage techniques to reduce the necessary installed capacities and achieve better weighted load factors."

Efforts to efficiently combine solar thermal space and water heating rely on effective energy storage. In addition to its potential for reducing equipment size and utilizing equipment more effectively, "thermal energy storage appears to be an important solution to correcting the mismatch between the supply and demand of energy" (Dinçer and Rosen, 2002). The mismatch in the time of energy supply and demand in domestic solar thermal applications calls for effective energy management and thus, improvements in energy storage strategies. Water is the most frequently used liquid storage medium and is commonly stored in a tank for service hot water applications and most space heating applications that use liquid storage (ASHRAE, 2004).

Anticipatory control is a valuable strategy for energy storage management; the availability of accurate weather forecasts online provides a new opportunity for the use of anticipatory control strategies (Candanedo and Athienitis, 2010). Combined with computer energy modeling, short-term forward forecasts could be used to predict energy harvests and optimize the collection and storage process of active solar thermal systems.

The primary objectives of this investigation of the solar thermal system installed in the S.KYBLUE House are as follows:

1. To determine the variability associated with short-term forward weather forecasting;
2. To identify and describe the factors that influence the energy collected by the solar thermal collector;
3. To model the operation of the solar thermal system;
4. To simulate system operation from short-term forward weather forecasting data and determine the impact of implementing different energy collection methods for various weather conditions; and
5. To determine the impact of control optimizations performed using short-term forward weather forecast data and the system model.

SECTION 2 – Literature Review

Solar Angles

Because of the earth's tilt and motion as it rotates around the sun and revolves around its own axis, the irradiance a surface encounters varies throughout the year and the day. The trajectory of solar rays can be determined from location on earth's surface, time of day in local solar time (LST), and day of the year (McQuiston et al, 2005).

McQuiston et al (2005) presents a method of calculating LST from clock time for any location based on its standard time zone, longitude, and the equation of time (EOT)

$$EOT = 229.2\left(0.000075 + 0.001868\cos(N) - 0.032077\sin(N) - 0.014615\cos(2N) - 0.04089\sin(2N)\right) \quad (2.8)$$

where; N = (n-1)(360/365) (Degrees),

n = day of the year between 1 and 365.

If daylight savings time is in effect, Local Standard Time is determined by subtracting an hour from clock time. From local standard time, local solar time is calculated

$$LST = (\text{Local Standard Time}) - (L_L - L_S)\ (4\ \text{min/deg}) + EOT \qquad (2.9)$$

where; L_L = longitude of location (Degrees),

L_S = standard meridian for time zone of location (Degrees).

The standard meridian for the Eastern Standard Time zone is 75°.

The trajectory of solar rays to a point on the earth's surface can be defined by three quantities used to calculate solar angles: latitude, hour angle, and declination. The latitude utilized to calculate solar angles is the same latitude used on maps and globes to relate locations to the equator. The hour angle can be calculated

$$h = \frac{(LST - 720)}{4} \qquad (2.10)$$

where; h = hour angle (Degrees),

LST = local solar time (Minutes).

When calculated by equation 2.10, the hour angle is negative before solar noon, zero at solar noon, and its absolute value is the same at sunrise and sunset. The sun's declination can be approximated

$$\begin{aligned}\delta = {} & 0.3963723 - 22.9132745\cos(N) + 4.0254304\sin(N) \\ & -0.3872050\cos(2N) + 0.05196728\sin(2N) \\ & -0.1545267\cos(3N) + 0.08479777\sin(3N)\end{aligned} \qquad (2.11)$$

where; δ = declination (Degrees),

N = (n-1)(360/365) (Degrees),

n = day of the year between 1 and 365.

(McQuiston et al, 2005)

Two important angles relate the sun's position in the sky to a horizontal surface on the surface of earth, the solar altitude angle (β) and the solar azimuth angle (ϕ). Figure 2.1 illustrates these angles.

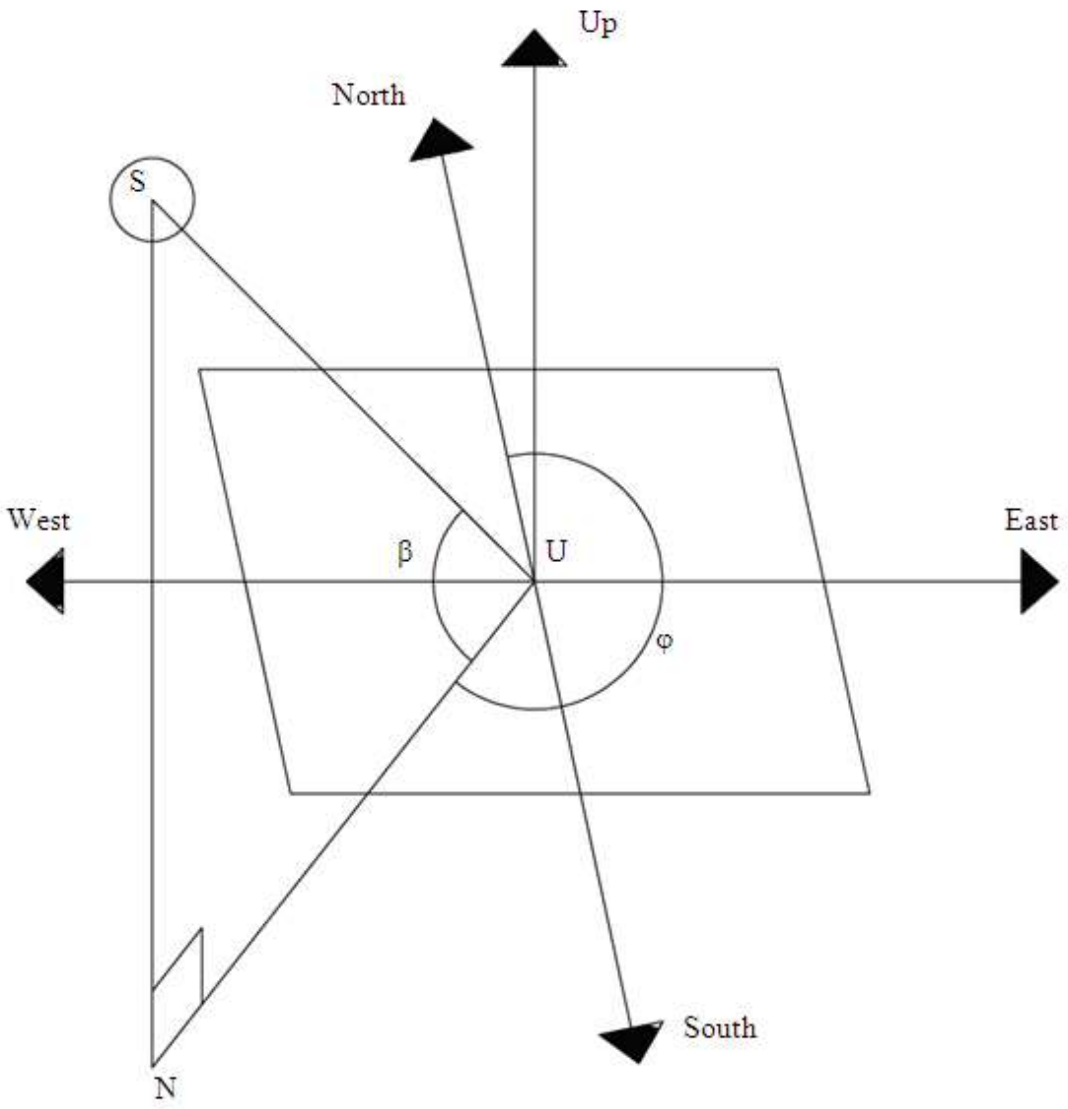

Figure 2.1 Solar altitude angle and solar azimuth angle for beam radiation on a horizontal surface with normal "Up".

The right triangle SUN describes the orientation of a point of interest on a horizontal plane, U, to the sun, S. The SU line is the path of beam solar radiation and forms the hypotenuse of SUN. The projection of the sun's rays onto the surface is the line UN. The solar altitude angle, β or SUN in Figure 2.1, describes the sun's height above the horizon and is the angle between the sun's rays and their projection on the horizontal surface. The solar azimuth angle relates the sun's position to the cardinal directions. It is the angle between the projection of the sun's rays on the horizontal surface and North and is measured clockwise from North. The following relationships from McQuiston et al. (2005) can be used to determine β and ϕ:

$$\sin(\beta) = \cos(l)\cos(h)\cos(\delta) + \sin(l)\sin(\delta) \qquad (2.12)$$

$$\cos(\phi) = \frac{\sin(\delta)\cos(l) - \cos(\delta)\sin(l)\cos(h)}{\cos(\beta)} \qquad (2.13)$$

When equation 2.13 is implemented to calculate ϕ, the quadrant it falls in must be verified. The solar azimuth angle should be less than 180° in the morning and greater than 180° in the afternoon.

When the surface of interest is tilted, two additional angles are necessary to associate it with the sun's rays, the surface solar azimuth (γ) and the angle of incidence (θ). In figure 2.2, a vertical wall is added to the diagram of Figure 2.1.

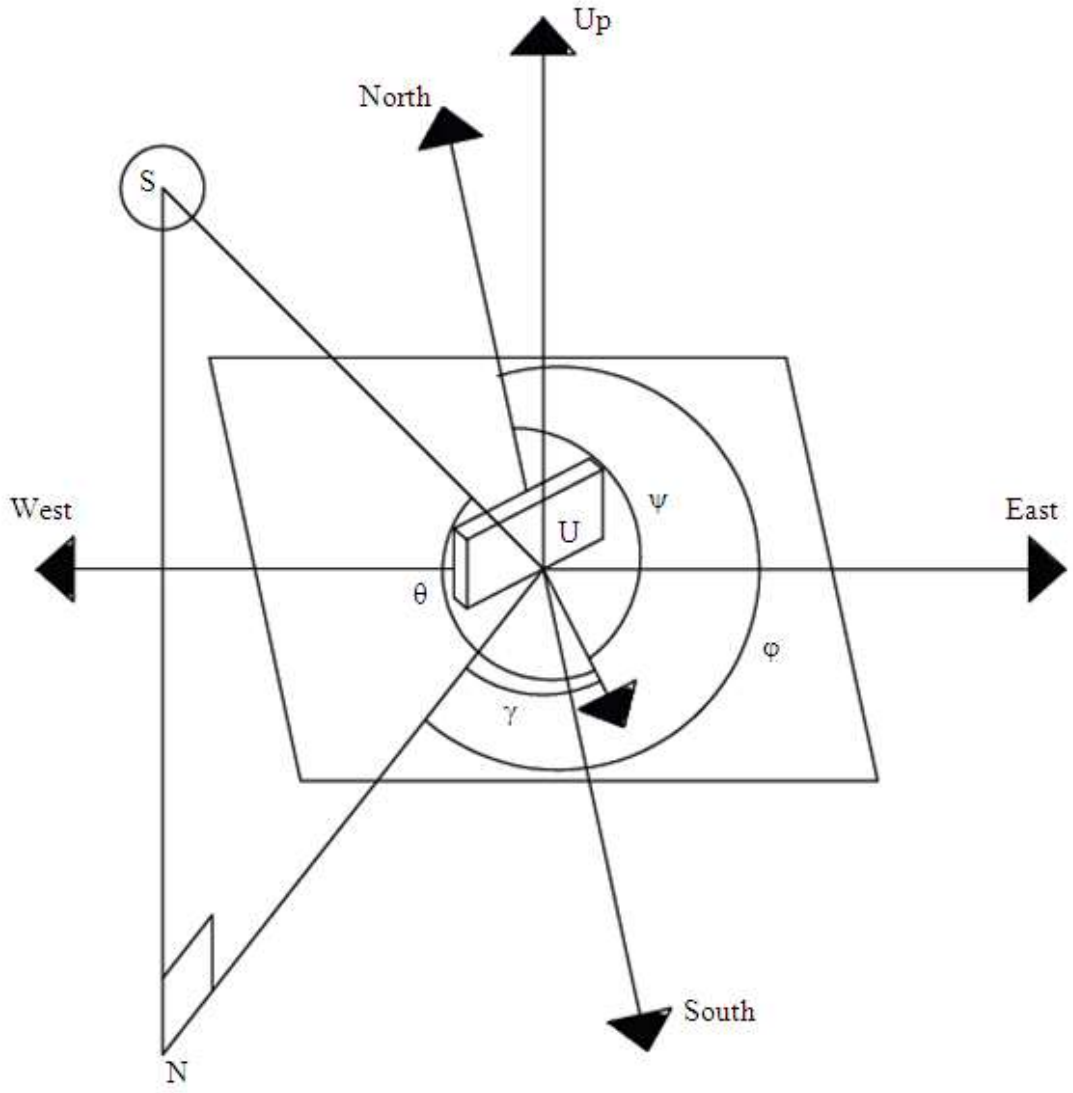

Figure 2.2 Surface solar azimuth and angle of incidence for a vertical wall. "Up" is normal to the horizontal surface.

The surface solar azimuth (γ) relates the sun's position to the facing direction of the wall, the surface azimuth (ψ). The surface azimuth is measured clockwise from North. The angle of incidence is the angle between the sun's rays and the normal to the surface. The following relationships from McQuiston et al (2005) can be used to determine γ and θ:

$$\gamma = |\phi - \psi| \qquad (2.14)$$

$$\cos(\theta) = \cos(\beta)\cos(\gamma) \qquad (2.15)$$

Equation 2.15 to determine θ is a simplified version of a general relationship that can be used to calculate θ for a surface with any tilt and orientation. The general formula is readily available in the literature and appears in McQuiston et al. (2005).

Solar Radiation

As solar radiation travels through earth's atmosphere, some of it is scattered and absorbed. Therefore, a surface within earth's atmosphere can receive solar radiation in three different forms: direct solar radiation that has not been scattered or absorbed (commonly called "beam radiation"), diffuse solar radiation from the sky due to the scattered and absorbed radiation, and radiation reflected from other surfaces. The total radiation on a terrestrial surface normal to the sun's rays is summarized by the following summation from McQuiston (2005):

$$G_t = G_{ND} + G_d + G_R \qquad (2.16)$$

where; G_t = total irradiation on a surface normal to the suns rays $\left(\frac{Btu}{hr \times ft^2}\right)$,

G_{ND} = direct normal irradiation $\left(\frac{Btu}{hr \times ft^2}\right)$,

G_d = diffuse irradiation $\left(\frac{Btu}{hr \times ft^2}\right)$,

G_R = reflected irradiation $\left(\frac{Btu}{hr \times ft^2}\right)$.

Estimation of the total radiation available for collection on terrestrial surfaces of various orientations is important to solar energy collection and utilization. Analysis of

historical radiation and meteorological data is the source for solar irradiance models of varying complexity.

Cloud cover records exist for many regions for which radiation or daylight data do not; a model linking solar radiation and cloud cover is desirable to provide irradiance knowledge for such regions (Muneer, 2004). Kasten and Czeplak (1980) model cloudless sky solar radiation in Hamburg based on the solar altitude angle and local constants and relate it to radiation on an actual day based on cloud amount

$$I_{Gc} = \left(A\sin(\beta) - B\right) \tag{2.17}$$

$$\frac{I_G}{I_{Gc}} = 1 - C(N/8)^D \tag{2.18}$$

where; I_{Gc} = solar radiation under a cloudless sky $\left(\frac{Btu}{hr \times ft^2}\right)$,

I_G = global irradiation $\left(\frac{Btu}{hr \times ft^2}\right)$,

N = cloud amount (octa),

A, B, C, and D = coefficients for Hamburg

(Muneer, 2004). Gul and Muneer (1998) extend the work of Kasten and Czeplak (1980) by determining coefficients for other locations (Muneer, 2004). Perez et al. (2007) modified the format of the Kasten Czeplak (1980) model for solar radiation based on clear sky radiation to determine hourly global irradiance from sky cover forecasting and obtained the relationship

$$\frac{GHI}{GHI_{clear}} = \left(1 - A \times SK^B\right) \tag{2.19}$$

where; GHI = hourly global irradiance $\left(\frac{Btu}{hr \times ft^2}\right)$,

GHI_{clear} = clear sky hourly global irradiance $\left(\frac{Btu}{hr \times ft^2}\right)$,

SK = forecasted sky cover (fractional units),

A = 0.87,

B = 1.9,

for Albany, New York.

Threlkeld and Jordan (1958) investigate the amount of direct solar radiation a surface can receive on a clear day. They relate direct normal irradiation to solar angles, atmospheric conditions, surface elevation, the outer limit of the earth's atmosphere at the time the radiation is received, and the solar constant. The solar constant is the solar radiation flux in the direction of the sun's rays at the outer limit of the earth's atmosphere at the mean distance between the earth and the sun. A solar constant of 442.4 Btu/hr x ft^2 is used in Threlkeld and Jordan's work. To handle the variance in atmospheric conditions, Threlkeld and Jordan (1958) define a standard atmosphere at sea level with 2.5 mm of ozone, 200 dust particles per cc, and monthly varying precipitable water depth between 0.3 inches in winter around December and January and 1.1 inches in summer around July and August. A clearness number relates the actual atmospheric conditions of regions in the United States to the standard atmospheric condition. Charts relay the direct normal radiation for each month of the year at different times of day for four Northern Latitudes calculated with a clearness number of 1. Multiplying the direct normal radiation values from the charts by clearness numbers provide the direct normal radiation for different regions. Threlkeld and Jordan (1958) develop relationships based on solar angles to relate the direct normal radiation for a location to the direct radiation on surfaces of other orientations. Threlkeld (1963) relates direct normal radiation to the

calculation of diffuse and reflected radiation. The work of Threlkeld and Jordan (1958) and Threlkeld (1963) form the basis for the ASHRAE clear sky model.

According to the 1999 *ASHRAE Handbook of Fundamentals*, Stephenson (1967) generates the relationship

$$I_{DN} = Ae^{-B/\sin\beta} \qquad (2.20)$$

where; I_{DN} = direct normal irradiation $\left(\frac{Btu}{hr \times ft^2}\right)$,

A = apparent solar radiation just outside earth's atmosphere $\left(\frac{Btu}{hr \times ft^2}\right)$,

B = atmospheric extinction coefficient (dimensionless).

Stephenson builds off of the work of Threlkeld and Jordan (1958) to define the coefficients A and B to account for radiation variance with date, the earth-sun distance, and seasonal changes in relative humidity. The original values of A and B and the diffuse radiation factor (C) are presented in the 1972 *ASHRAE Handbook of Fundamentals* for the 21st day of each month. Machler and Iqbal (1985) updated the coefficients for the model presented in ASHRAE (1972) to improve the model's winter performance and account for a change in the accepted solar constant to 433 Btu/hr x ft^2. The modified coefficients are presented in Table 2.1. Al-Sanea et al. (2004) implement linear interpolation to approximate the coefficients A, B, and C for days other than the 21st of the month in their work to define adjustment factors for the ASHRAE clear sky model for Riyadh Saudi Arabia where clearness numbers are not defined.

Table 2.1 Clear sky model constants (McQuiston et al., 2005)

	A	B	C

	Btu/hr x ft^2	Dimensionless	Dimensionless
Jan 21	381	0.141	0.103
Feb 21	376.2	0.142	0.104
Mar 21	368.9	0.149	0.109
Apr 21	358.2	0.164	0.12
May 21	350.6	0.177	0.13
June 21	346.1	0.185	0.137
July 21	346.4	0.186	0.138
Aug 21	350.9	0.182	0.134
Sep 21	360.1	0.165	0.121
Oct 21	369.6	0.152	0.111
Nov 21	377.2	0.142	0.106
Dec 21	381.6	0.141	0.103

McQuiston et al. (2005) organizes the components of the ASHRAE clear sky model into a calculation process for the total solar irradiation on a surface of any tilt and orientation as follows from Equation 2.21 to Equation 2.28. The total solar radiation incident on a vertical surface is the combination of direct, diffuse, and reflected solar radiation. The basis for estimating all three quantities is the calculation of normal direct irradiation from the constants in Table 2.1 and the solar angles

$$G_{ND} = \frac{A}{e^{(B/\sin\beta)}} C_N \qquad (2.21)$$

where; G_{ND} = normal direct irradiation $\left(\frac{Btu}{hr \times ft^2}\right)$,

C_N = clearness number (Dimensionless).

The clearness number is 0.95 in summer and winter for Kentucky. The direct radiation for a surface of any orientation is

$$G_D = G_{ND} \cos\theta \qquad (2.22)$$

where; G_D = direct radiation $\left(\frac{Btu}{hr \times ft^2}\right)$.

The direct radiation is zero when θ is greater than or equal to 90 degrees so that the surface is shaded from direct radiation. If the sky is assumed to have uniform brightness (an isotropic sky), the normal direct radiation is multiplied by C from Table 2.1 and a view factor to obtain the diffuse radiation on a surface. For vertical surfaces, the brighter regions of the sky surrounding the sun are accounted for by replacing the view factor with a ratio of the diffuse sky radiation on a vertical surface to the diffuse sky radiation on a horizontal surface, approximated

$$\frac{G_{dV}}{G_{dH}} = 0.55 + 0.437\cos\theta + 0.313\cos^2\theta \qquad (2.23)$$

where $\frac{G_{dV}}{G_{dH}}$ = ratio of vertical to horizontal diffuse sky radiation (Dimensionless).

When $\cos\theta \le -0.2$, $\frac{G_{dV}}{G_{dH}} = 0.45$. Thus, the diffuse sky radiation for vertical surfaces is

$$G_d = \frac{G_{dV}}{G_{dH}} C G_{ND} \qquad (2.24)$$

where G_d = diffuse sky radiation $\left(\frac{Btu}{hr \times ft^2}\right)$.

To calculate the solar radiation reflected from the ground onto a vertical surface, the total radiation incident on the horizontal surface must be calculated

$$G_{tH} = G_{ND}(\sin\beta + C) \qquad (2.25)$$

where G_{tH} = total irradiation on the horizontal surface $\left(\frac{Btu}{hr \times ft^2}\right)$. Then, the radiation reflected onto the vertical surface from the ground is

$$G_R = G_{tH}\rho_g F_{wg} \qquad (2.26)$$

where; G_R = radiation reflected on the vertical surface by the ground $\left(\frac{Btu}{hr \times ft^2}\right)$,

ρ_g = reflectance of the ground (dimensionless),

F_{wg} = view factor from the wall to the ground (dimensionless).

The view factor for a surface of any orientation to the ground, or the fraction of radiation leaving the surface that strikes the ground, is given by

$$F_{wg} = \frac{1 - \cos\alpha}{2} \qquad (2.27)$$

where α = the angle between the normal to the surface and the normal of a horizontal surface (dimensionless).

The total solar radiation on a vertical surface can be calculated

$$G_t = G_D + G_d + G_R \qquad (2.28)$$

where G_t = total solar radiation $\left(\frac{Btu}{hr \times ft^2}\right)$.

Muneer (2004) provides ground reflectance constants of 0.23 to 0.25 for a lawn, 0.10 for weathered blacktop, and 0.27 for dark building surfaces.

The Solar Thermal Collector

Evacuated tube solar thermal collectors consist of rows of transparent glass tubes which encase absorbers covered with a selective coating which maximizes radiation absorption and minimizes reflection (Papadopoulos, 2003; Apricus, 2006). A common method for creating evacuated tubes is to fuse two glass tubes together and create a vacuum between the tubes (Apricus, 2006). The vacuum eliminates the heat losses by convection at the absorber surface (Ng et al, 2000). In evacuated tube heat pipe collectors, each evacuated tube contains a heat pipe with an internal phase change

material. The evaporator of the heat pipe is placed in the tube so that the solar energy vaporizes the phase change material. The condenser is inserted into a manifold at the top of the tubes to transfer the heat into the circulating fluid as the phase change material condenses. 'Dry' condensers are inserted into a secondary exchanger inside the manifold of the collector; 'wet' condensers are inserted directly into the circulating fluid in the manifold with sealing gaskets to prevent the release of the transfer fluid (Ng et al., 2000). Because they do not directly contact the transfer fluid, 'dry' condenser evacuated tube heat pipes do not require gasket maintenance and can be removed for service without draining the system. With near isothermal operation, heat pipes can collect solar energy from a large area and transfer it to a small area where it can be transferred to a circulating fluid (Chi, 1976). Heat pipes act as thermal diodes, preventing thermal losses from the collecting fluid when the collector cools (Chi, 1976).

The important components of flat plate collectors are the energy-absorbing surface with the capability to transfer the absorbed energy into the fluid, the transparent cover for the absorber to reduce thermal losses to the environment from radiation and conduction, and back insulation to reduce conductive losses. An energy balance approach is used to relate the characteristics of the collectors that describe the important components to collector performance analytically. The useful energy gain of the collector is the incident solar energy less thermal and optical losses. This relationship is defined by

$$\dot{Q}_u = A_c\left[S - U_L\left(T_{pm} - T_a\right)\right] \qquad (2.29)$$

where; $\dot{Q}_u$= useful energy gain $\left(\frac{Btu}{hr}\right)$,

A_c = collector area (ft^2),

S = incident solar radiation less the optical losses $\left(\frac{Btu}{hr \times ft^2}\right)$,

U_L = heat transfer coefficient $\left(\frac{Btu}{hr \times ft^2 \times {}^\circ F}\right)$,

T_{pm} = mean absorber plate temperature (°F),

T_a = ambient temperature (°F).

The heat transfer coefficient relates the difference between the mean absorber plate temperature and the ambient temperature to thermal losses from conduction, convection, and infrared radiation. Because the mean absorber plate temperature is difficult to measure, it is related to the inlet fluid temperature of the collector by a parameter called the collector heat removal factor, which can be analytically or empirically determined. (Duffie and Beckman, 2006)

Ng et al (2000) performs an analytical energy balance for evacuated tube heat pipe collectors. The incident solar radiation that reaches the absorber is the product of the incident solar radiation and the effective transmittance-absorptance product of the absorber, which represents the optical loss when the radiation passes through the collector cover. Most of the energy that reaches the absorber is transferred to the heat pipe evaporator, which conveys it to the condenser located in the collector manifold. In the manifold, the energy is transferred to the circulating fluid producing the useful heating effect and some is lost to the environment through thermal leaks. The useful energy gain equals (collector area)(collector heat removal factor)(energy absorbed – energy lost). Equation 2.1 is modified to

$$\dot{Q}_u = A_c F_R \left[I(\tau\alpha) - U_L (T_i - T_a) \right] \quad (2.30)$$

where; F_R = collector heat removal factor (dimensionless),

I = incident solar radiation $\left(\frac{Btu}{hr \times ft^2} \right)$,

$\tau\alpha$ = effective transmittance-absorptance product of absorber (dimensionless),

T_i = fluid temperature at collector inlet (°F),

T_a = ambient temperature (°F).

The collector heat removal factor (F_R) is a modified version of the collector efficiency factor (F'), which accounts for the temperature difference between the inlet fluid temperature and the absorber plate temperature through relationships based on the flow rate and specific heat of the transfer fluid. F' is related to the thermal resistance of the heat pipe evaporator, the thermal resistance of the heat pipe condenser, and the heat loss between the absorber and the environment from radiation (assuming negligible convective losses). The heat transfer coefficient (U_L) is related to the thermal resistance of the manifold, the heat loss between the absorber and the environment from radiation (assuming negligible convective losses), and F'. Thus, the instantaneous steady state collector efficiency is given by

$$\eta_i = \frac{\dot{Q}_u}{A_c I} = \frac{F_R \left[I(\tau\alpha) - U_L (T_i - T_a) \right]}{I} \quad (2.31)$$

where; η_i = steady state instantaneous collector efficiency (dimensionless).

The heat transfer coefficient and collector heat removal factor are assumed to be independent of solar radiation. (Ng et al, 2000)

In their work in 1981, Cooper and Dunkle propose a linear relationship between the overall loss coefficient and the temperature difference between the collector and the ambient air,

$$U_L F' = a + b(T - T_a) \tag{2.32}$$

where; T = measure of collector temperature (°F),

a = constant $\left(\frac{Btu}{hr \times ft^2 \times {}^\circ F}\right)$,

b = constant $\left(\frac{Btu}{hr \times ft^2 \times {}^\circ F^2}\right)$.

According to the methods of Cooper and Dunkle, the instantaneous efficiency becomes

$$\eta_i = F'(\tau\alpha) - a\frac{\Delta T_m}{I} - b\frac{\Delta T_m^2}{I} \tag{2.33}$$

where; ΔT_m = the true mean fluid temperature difference (°F).

Cooper and Dunkle determined the true mean fluid temperature difference could be accurately approximated

$$\Delta T_m = \frac{(T_i + T_o)}{2} - T_a \tag{2.34}$$

where; T_o = fluid temperature at collector outlet (°F).

In the United States, the collector efficiency factor is often replaced with the collector heat removal factor and the true mean fluid temperature difference is approximated by $(T_i - T_a)$. Thus, the instantaneous efficiency becomes

$$\eta_i = F_R(\tau\alpha) - a\frac{(T_i - T_a)}{I} - b\frac{(T_i - T_a)^2}{I}. \tag{2.35}$$

(Duffie and Beckman, 2006)

Duffie and Beckman (2006) propose an approximate transformation ratio to modify $F_R(\tau\alpha)$ and F_RU_L to adjust performance equations when the flow rate through the collector is different from the one utilized to determine the equation. The modification is applicable when the change in the convection coefficient between the transfer fluid and the pipes in the manifold is relatively small for the change in flow rate. For liquid collectors operating at "normal flow rates," it is reasonable to assume the change in the convection coefficient between the manifold pipes and the transfer fluid is relatively small when the flow rate of the transfer fluid is adjusted and $F'U_L$ for the collector is approximately the same at both flow rates (Duffie and Beckman, 2006). With test conditions referring to the flow rate for which the performance equation was developed and use conditions referring to the alternated desired operation conditions, the transformation ratio (r) can be calculated as follows:

$$r = \frac{\left.\frac{\dot{m}c_p}{A}\left[1-\exp\left(-\frac{AF'U_L}{\dot{m}c_p}\right)\right]\right|_{use}}{F_RU_L\big|_{test}} \qquad (2.36)$$

where; A = the measure of collector area used for the performance equation (ft^2),

$$F'U_L = -\frac{\dot{m}c_p}{A}\ln\left(1-\frac{F_RU_LA}{\dot{m}c_p}\right)\Bigg|_{test} \qquad (2.37)$$

Solar thermal collector performance is evaluated empirically by testing and rating groups such as the Solar Rating & Certification Corporation (SRCC) in Cocoa, Florida and the Solartechnik Prüfung Forschung (SPF) in Switzerland. The SRCC performs its tests according to ASHRAE Standard 93-77 or 96-1980 (SRCC, 1994). The SPF conducts its testing in accordance with EN 12975 (SPF, 2010). The SRCC and SPF

create equations relating collector performance to incident solar radiation, ambient temperature, and a measure of the fluid temperature in the collector; inlet fluid temperature for the SRCC and the average of the inlet and outlet temperature for the SPF (ANSI/ASHRAE, 1986; SPF, 2010; SRCC 1994). The experimental measurements used to determine the performance of the collectors by the SRCC and the SPF are collected at steady-state or quasi-steady state conditions (ANSI/ASHRAE, 1986; SPF, 2010). According to *ANSI/ASHRAE Standard 93* (1986), "quasi-steady state describes solar collector test conditions when the flow rate, fluid inlet temperature, collector temperature, solar irradiance, and ambient environment have stabilized to such an extent that these conditions may be considered essentially constant." The conditions must remain steady-state or quasi-steady state for 10 minutes or two time constants, whichever value is greater, before and during the period in which data is collected (ANSI/ASHRAE, 1986). The average wind velocity surrounding the testing period is 5 to 10 miles per hour according to *ANSI/ASHRAE Standard 93* (1986) and the flow rate of the heat transfer fluid through the collector is to be standardized at one level for all data points. Tests are preformed on clear days when G_t, which is used for I, is dominated by G_D (Duffie and Beckman, 2006; ANSI/ASHRAE, 1986).

The angle of incidence has an impact on collector performance; therefore, rating groups determine incidence angle modifiers (IAM) to describe the relationship between the sun's position relative to the collector and collector performance. In equations 2.33 and 2.35, I is replaced by $I K_{\tau\alpha}$ where $K_{\tau\alpha}$, the IAM, is the ratio of the experimental effective transmittance-absorptance product of absorber to the effective transmittance-absorptance product when normal incidence occurs (Duffie and Beckman, 2006;

ANSI/ASHRAE, 1986). Because direct radiation dominates the total radiation when testing is performed, the empirical IAM is a function of the incidence angle, which describes the path of beam radiation (Duffie and Beckman, 2006). For optically nonsymmetrical collectors, like tubular collectors, the IAM depends on both the longitudinal and transversal angles of incidence (Duffie and Beckman, 2006; ANSI/ASHRAE, 1986; Apricus, 2006; SPF, 2010; SRCC, 1994). The longitudinal IAM is related to the sun's height in the sky. For a collector with a fixed orientation; the longitudinal IAM changes most dramatically with the seasons. Figure 2.3 displays the longitudinal component of the angle of incidence θ_L for a tubular collector, which is 0 when the beam radiation is normal to the collector's longitudinal axis and 90 when the beam radiation is parallel to the collector's longitudinal axis.

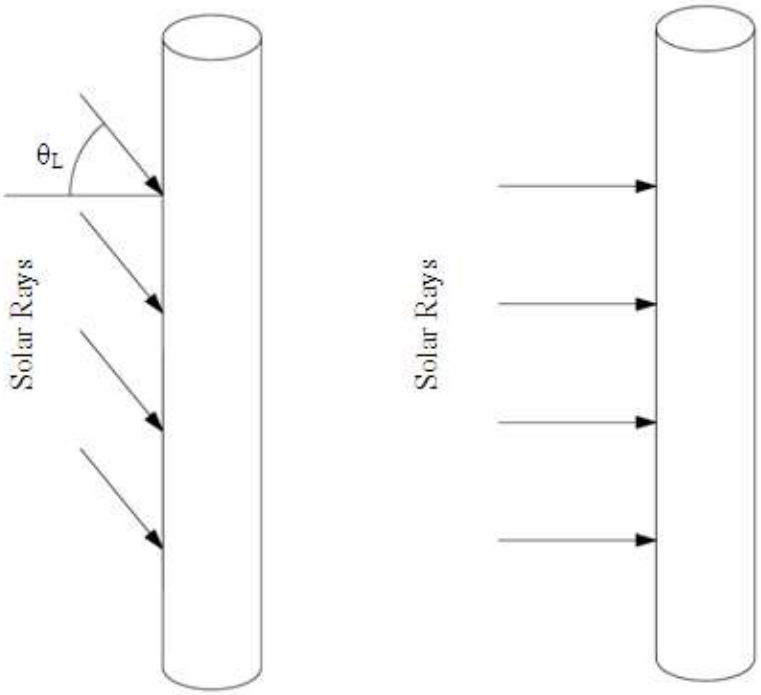

Figure 2.3 Longitudinal component of incidence angle for tubular collectors; θ_L when the solar rays strike from above the collector as they do the tube on the left and 0 when the solar rays are perpendicular to the longitudinal axis of the collector as they are for the tube on the right.

The transversal IAM changes most drastically with time of day for a collector with a fixed orientation. For tubular collectors separated by spaces, a larger collector area is exposed to beam radiation when the transversal component θ_T of the angle of incidence is greater than 0 (Apricus, 2006). Figures 2.4 and 2.5 illustrate the change in incident surface area for tubular collectors with changes in θ_T. The overall IAM for optically nonsymmetrical collectors is the product of the transversal and longitudinal IAMs

$$K_{\tau\alpha} = K(\theta_L)K(\theta_T). \qquad (2.36)$$

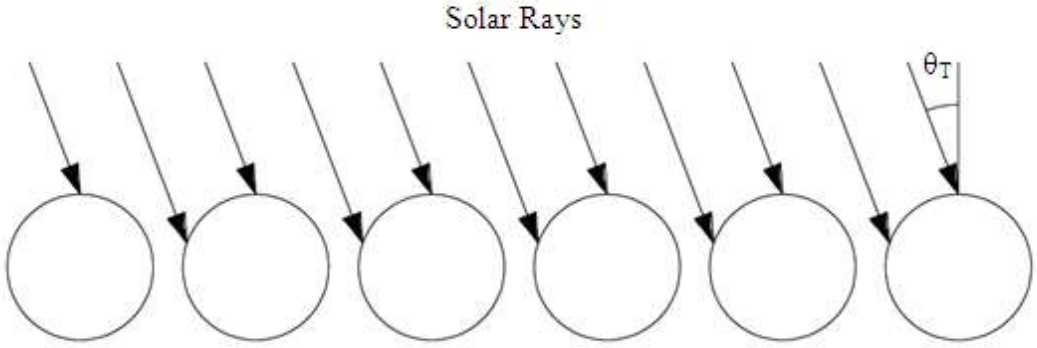

Figure 2.4 Top view of bank of tubular collectors indicating θ_T.

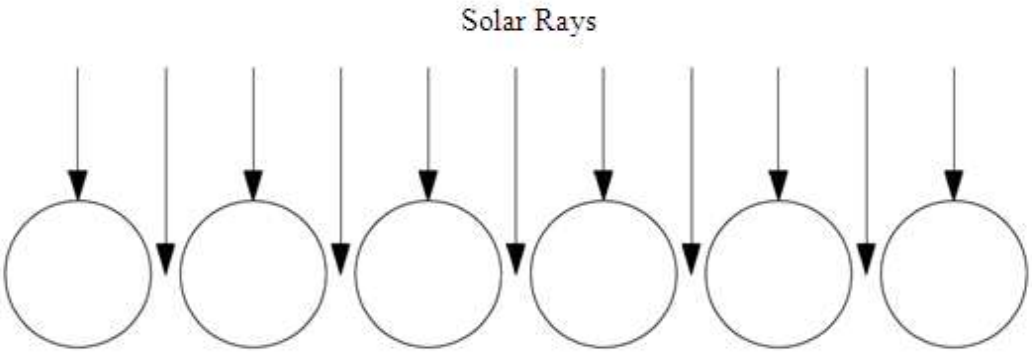

Figure 2.5 Top view of bank of tubular collectors when θ_T is 0.

Figure 2.6 illustrates the location of the angle of incidence with its longitudinal and transversal components for a tubular collector mounted on the vertical surface of Figure 2.2.

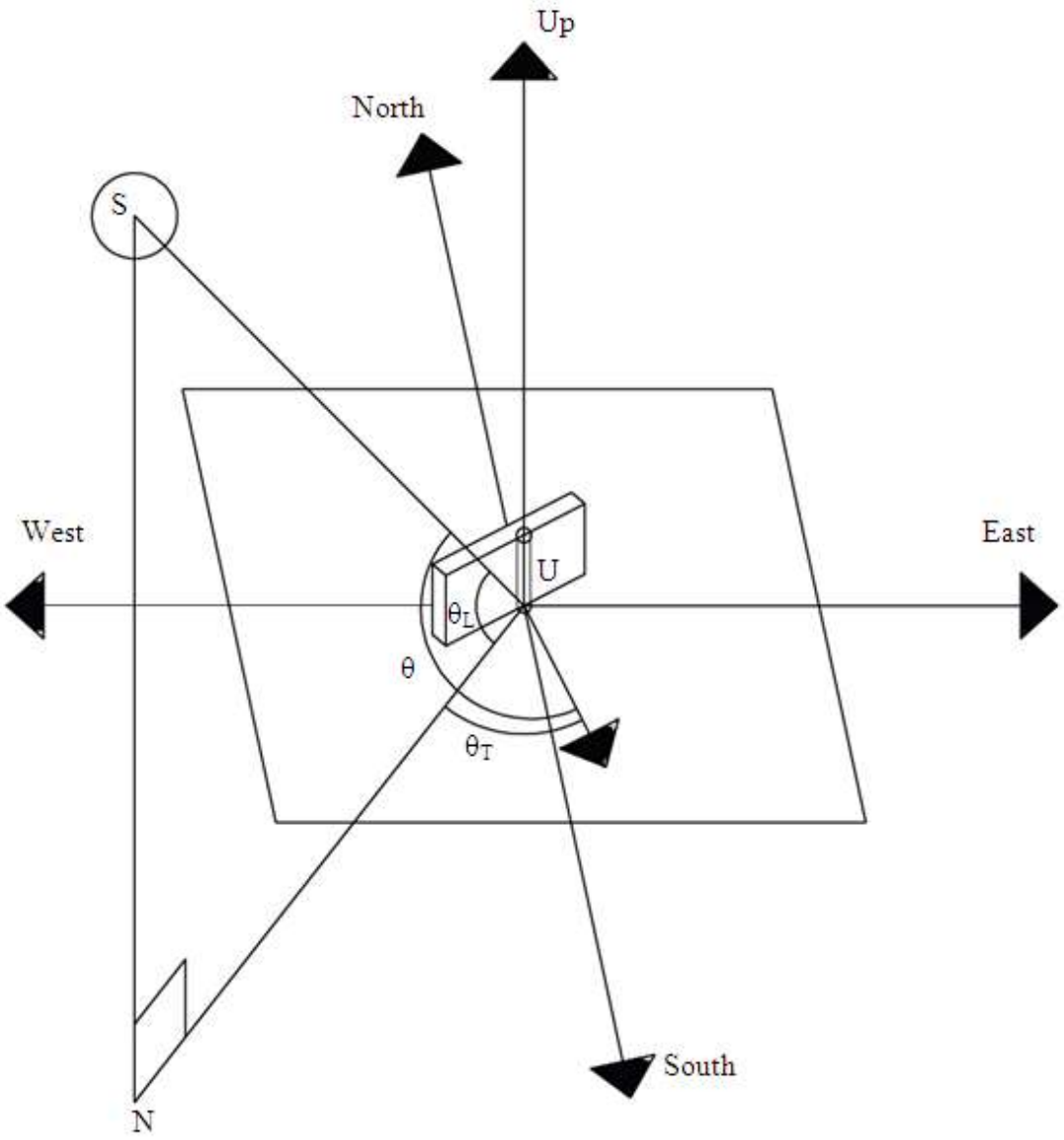

Figure 2.6 Angle of Incidence (θ) with its longitudinal component (θ_L) and transversal component (θ_T).

Comparison of Figures 2.1, 2.2, and 2.6 reveals that θ_L is equivalent to β and θ_T is equivalent to γ for a tubular collector mounted on a vertical surface. The IAMs for Apricus AP-30 evacuated tube heat pipe solar thermal collectors are reported in Table 2.2.

Table 2.2 Incidence Angle Modifiers for Apricus AP-30 solar thermal collectors (Apricus, 2006; Bohren and Gobler, 2004).

θ_L or θ_T (Degrees)	0	10	20	30	40	50	60	70	80	90
$K(\theta_L)$	1	1	0.99	0.98	0.96	0.93	0.87	0.74	0.38	0
$K(\theta_T)$	1	1.02	1.08	1.18	1.37	1.4	1.34	1.24	0.95	0

Operating an Apricus AP-30 evacuated tube solar thermal collector at 1.32 GPM with water as the test fluid, the SRCC obtained

$$\eta_i = 0.456 - 0.23796\frac{(T_i - T_a)}{I} - 0.00037\frac{(T_i - T_a)^2}{I} \qquad (2.37)$$

based on gross collector area and a linear relationship between the overall loss coefficient and the temperature difference between the collector and the ambient air (SRCC, 2010). The gross collector area for the Apricus AP-30 is 44.76 ft^2 (SRCC, 2010). The performance equation presented by Apricus (2006) was determined by the SPF based on absorber area and 33.3% ethylene glycol transfer fluid flowing at 120 l/h (0.53 GPM) to be

$$\eta_i = 0.717 - 1.52\frac{\Delta T_m}{I} - 0.0085\frac{\Delta T_m{}^2}{I} \qquad (2.38)$$

where; I = incident solar radiation $\left(\frac{W}{m^2}\right)$,

ΔT_m = mean fluid temperature difference (Kelvin)

(Bohren and Gubler, 2004).

When based on gross area and converted to English units, equation 2.38 becomes

$$\eta_i = 0.399 - 0.1497\frac{\Delta T_m}{I} - 0.00046\frac{\Delta T_m{}^2}{I} \qquad (2.39)$$

where; I = incident solar radiation $\left(\frac{Btu}{hr \times ft^2}\right)$,

ΔT_m = mean fluid temperature difference (ºF).

Bohren and Gubler (2004) report a time constant of 1160 seconds (19.3 minutes) for the Apricus evacuated tube heat pipe solar thermal collector in their report.

Comparing the accuracy of different dynamic models with stationary models such as those determined by the SRCC and the SPF, Schnieders (1997) indicates the error of stationary models reduces from around 15 percent with one-minute average input data to a few percent with hourly input data.

The Heat Exchanger

Incropera et al. (2007) present the method to predict the performance of a heat exchanger. The total heat transfer rate of the heat exchanger is related to the inlet and outlet fluid temperatures, the total heat transfer surface area, and the overall heat transfer coefficient. The overall heat transfer coefficient accounts for the conduction and convections resistances between the hot and cold fluids separated by the heat transfer surface and the resistance due to fouling of the heat exchanger surfaces. Assuming negligible heat transfer between the heat exchanger and its surroundings, negligible kinetic and potential energy changes in the heat exchanger, no phase change, and constant specific heats,

$$q_{HE} = \dot{m}_h c_{p,h}\left(T_{h,i} - T_{h,o}\right), \qquad (2.40)$$

and

$$q_{HE} = \dot{m}_c c_{p,c}\left(T_{c,o} - T_{c,i}\right) \qquad (2.41)$$

where; q_{HE} = total rate of heat transfer $\left(\frac{Btu}{\min}\right)$,

$\dot{m}_h$ = mass flow rate of the hot fluid $\left(\frac{lbm}{\min}\right)$,

$\dot{m}_c$ = mass flow rate of the cold fluid $\left(\frac{lbm}{\min}\right)$,

$c_{p,h}$ = specific heat of the hot fluid $\left(\frac{Btu}{lbm \times °F}\right)$,

$c_{p,c}$ = specific heat of the cold fluid $\left(\frac{Btu}{lbm \times °F}\right)$,

$T_{h,i}$ = mean inlet fluid temperature of the hot fluid (ºF),

$T_{h,o}$ = mean outlet fluid temperature of the hot fluid (ºF),

$T_{c,i}$ = mean inlet fluid temperature of the cold fluid (ºF),

$T_{h,o}$ = mean outlet fluid temperature of the cold fluid (ºF).

An extension of Newton's law of cooling relates q_{HE} to the temperatures of the hot and cold fluids with the overall heat transfer coefficient and the heat transfer surface area. Because the temperatures of the hot and cold fluids differ with position in the heat exchanger, a log mean temperature difference is used to describe the difference between the temperatures of the hot and cold fluids such that

$$q_{HE} = UA_{HE}\Delta T_{lm} \qquad (2.42)$$

where; U = overall heat transfer coefficient $\left(\frac{Btu}{\min \times ft^2 \times °F}\right)$,

A_{HE} = heat transfer surface area (ft^2),

ΔT_{lm} = log mean temperature difference (ºF).

Use of equation (2.?) relies on the additional assumptions of negligible axial conduction along the channels and a constant overall heat transfer coefficient. Though specific heats

may change with changes in temperature and the overall heat transfer coefficient may change with variations in fluid properties and flow conditions, the assumptions are often reasonable. For a counter flow heat exchanger,

$$\Delta T_{lm} = \frac{T_{h,o} - T_{c,i} - \left(T_{h,i} - T_{c,o}\right)}{\ln\left(\frac{T_{h,o} - T_{c,i}}{T_{h,i} - T_{c,o}}\right)}. \qquad (2.43)$$

Thermal Energy Storage

Solar thermal energy is intermittent and is often out of phase with residential heating and hot water demands. However, thermal energy storage provides a means through which solar thermal systems can meet demands, operate with greater flexibility, and implement equipment more efficiently (Dinçer and Rosen, 2002). For domestic hot water systems, water can serve as the energy storage medium and the final product. Because of its low cost and the high value of the product of its density and specific heat, water is also a feasible storage medium for space conditioning; though, it is harder to contain than solid storage mediums (Dincer and Rosen, 2002). Water is also an attractive storage medium because it is simple to transfer energy into and out of it (Duffie and Beckman, 2006). Water storage systems are easily interfaced with hydronic heating systems and can be comprised from one or more commercial hot water heaters (ASHRAE, 2004).

Stratification in water storage tanks enhances the performance of the solar thermal system by feeding the collectors with cooler water from the bottom of the tank, which allows them to operate with the lowest possible surface temperature (ASHRAE, 2004). The heated water returning from the collector is supplied to the top of the tank where it

can be fed to the load. Vertical storage tanks encourage stratification (ASHRAE, 2004); therefore, they are preferable to horizontal storage tanks for solar thermal systems.

Duffie and Beckman (2006) describe two approaches for modeling stratified tanks: the multimode approach and the plug flow approach. Both approaches divide stratified tanks into smaller sub-sections with different temperatures. The multimode approach performs an energy balance on each sub-section, node, and implements differential equations to describe their temperature-time relationship. The plug flow approach is algebraic in nature. The tank is sub-divided into volumes of fluid with a common temperature. When warmer fluid from a collector or cooler fluid from a load moves into the system, its volume displaces the other volumes of fluid in the tank. The new temperature distribution in the tank is determined from volumetric relationships based on the relative sizes of entering volumes and the volumes in the tank. Plug flow models are only appropriate for computer modeling.

SECTION 3 – Experimental Facility and Instrumentation

The Experimental Facility

The University of Kentucky participated in the 2009 Solar Decathlon Competition in Washington, D.C., www.solardecathlon.gov. The grid-tied, net-zero-energy S.KY BLUE House was constructed for the competition with integrated, cutting edge solar thermal and photovoltaic collection technology. Grid-tied, net-zero-energy buildings are designed to produce as much or more energy than they consume over the period of a year. They are connected to the electrical power grid and purchase energy from it in times of poor production, at night or on cloudy days. When the buildings produce more

energy than they use, the buildings sell energy back to the grid to offset the energy they purchased.

The Solar Decathlon was successfully completed with a top ten finish and the S.KYBLUE House with its cutting edge systems provides and invaluable research facility. The house has a 13-kilowatt photovoltaic collection array to generate electricity, 60 evacuated tube heat pipe solar thermal collectors to heat hot water, an air to water heat pump to augment the solar thermal collection system, and a versatile computer control system built with off the shelf data acquisition devices, relays, and software.

Data for this investigation was collected after the competition of the Solar Decathlon at two sites in Lexington, KY. From July 8, 2010 to July 27, 2010, data was collected at the University of Kentucky (38.04N, 84.51W) (iTouchMap.com, 2010). While located at the University of Kentucky, the south wall of the house containing the solar thermal collectors faced due South. From August 18, 2010 to October 10, 2010, data was collected at the Kentucky Horse Park (38.15N, 84.52W) (iTouchMap.com, 2010). While located at the Kentucky Horse Park, the wall containing the solar thermal collectors faced 9 degrees East of due South.

The solar thermal system and the transducers, data acquisition devices, and control equipment and software associated with it were used to conduct this research. The active, closed-loop solar thermal system contains two Apricus AP-30 evacuated tube heat pipe solar thermal collectors with ‘dry’ condensers, a variable speed pump, and high and low temperature heat tanks designed for domestic hot water and radiant floor heating respectively. The two solar thermal collectors can operate with series or parallel flow.

The solar thermal system has multiple operation modes, which can be determined and implemented by the control system.

Control algorithms were used to investigate the effect of short-term forward weather forecast integrated control on the performance of active solar thermal systems. Control algorithms simulated the performance of the solar thermal system operating in different modes under the conditions predicted by the short-term forward weather forecasts to determine the optimum operation mode. Flow rate and storage tank destination were the factors considered for this investigation, and each combination of flow rate and storage tank destination was simulated by the control system for the predicted weather conditions to determine the collection potential of each possible mode of operation. The control algorithm implemented the mode of operation capable of collecting the most energy.

Equipment and Sensor Locations

The S.KYBLUE house contains integrated transducers to measure temperatures, flow rates, and solar radiation incident on the wall containing the solar thermal collectors. The system diagram for the house is displayed in Figure 3.1; it also indicates the locations of the transducers in the systems. The reverse cycle chiller is an air-to-water heat pump used to meet the HVAC needs of the home. It is designed to draw heat from HT-2 when it is available. Pump 2 is the variable speed pump in the solar thermal system. The solenoid valves and three way valves are used to direct the fluid through the two collector headers in series or parallel and to select the heat tank where the collected energy is stored. All the equipment, valves, and transducers interface with the control computer. The notation used in Figure 3.1 is summarized in Table 3.1.

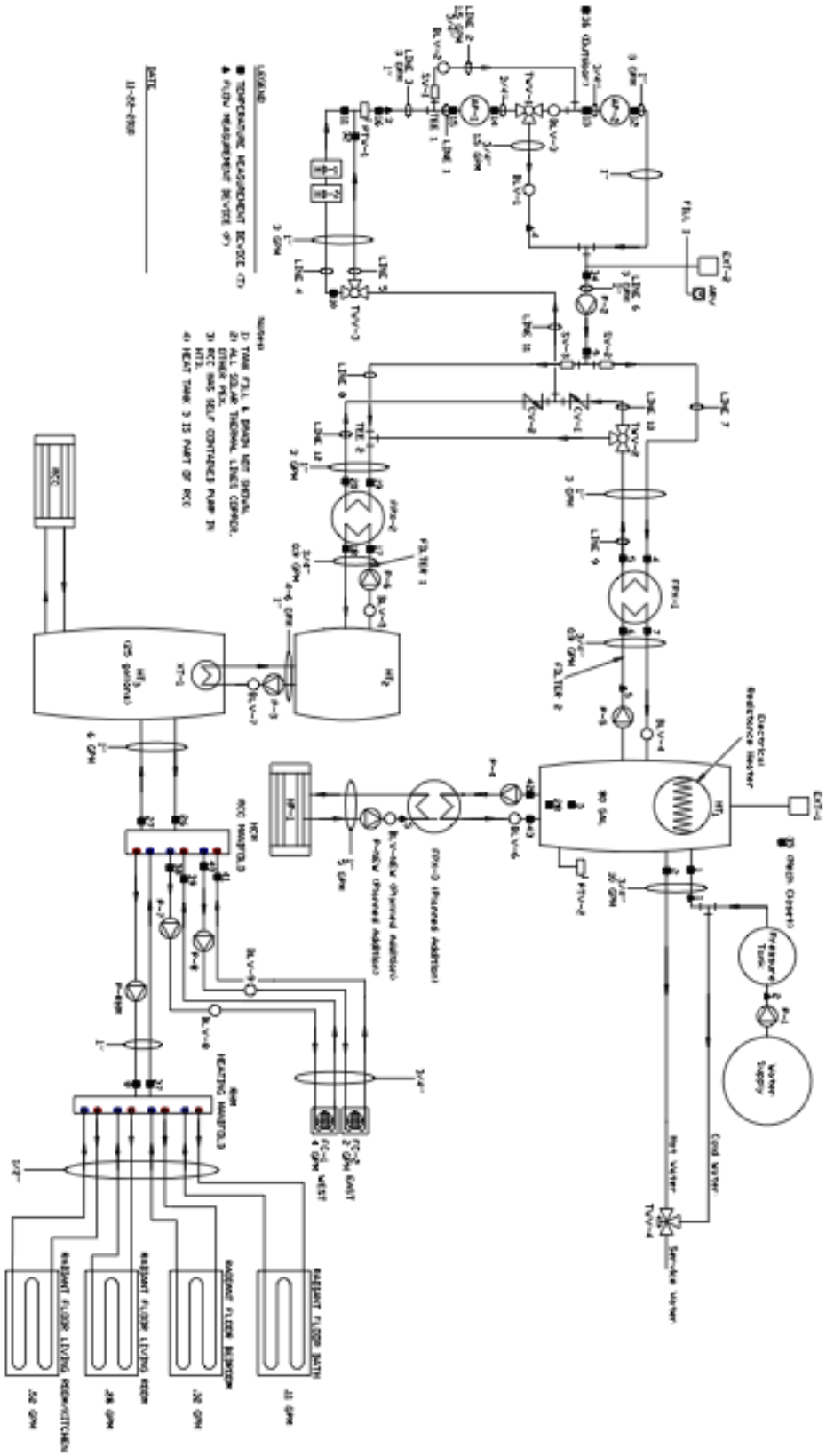

Figure 3.1 S.KYBLUE House system diagram.

Table 3.1 S.KYBLUE House system diagram notation.

AP	AP-30 Solar Collector
TWV	Three Way Valve
BLV	Balancing Valve
SV	Solenoid Valve
PTV	Pressure & Temp. Relief Valve
HD	Heat Dissipater
ARV	Air Relief Valve
P	Pump
EXT	Expansion Tank
CV	Check Valve
FPX	Flat Plate Heat Exchanger
HT	Heat Tank

Because the house was designed for use in the Solar Decathlon where peak system performance was required, transducers were installed with methods to limit their effects on the systems. Thermocouples were attached to the outside of copper pipes and insulation was provided behind them. No additional thermocouples were added within the AP-30 solar thermal collectors so that extra holes or wires would not compromise the performance of the units. The performance of the collectors was determined by measurements of the inlet and outlet temperatures collected by T12 through T15. Flow measurements were taken at only the most critical locations to minimize the head loss of the piping systems.

Two thermocouples were attached to the outside wall of heat tank 1 beneath the tank insulation to measure the effects of stratification. T3 was attached near the bottom of the tank, and T28 was attached near the bottom of the tank. The thermocouples were placed beneath factory provided access panels of the AO Smith tank. The locations of the sensors, inlets, and outlets are indicated in Figure 3.1.

Instrumentation and Data Acquisition

The temperature measurement transducers were Omega Type K thermocouples with self-adhesive backing (SA1-K-SC) and a tolerance of the larger value of 2.0°F or 0.4% of the measured temperature for temperatures between 32 and 2282°F (Omega, 2010). The thermocouples were connected to the data acquisition equipment with Omega thermocouple extension wire (EXPP-K-20-SLE (ROHS)). The flow measurement transducers used in the solar thermal system were Omega turbine meters with pulse output (FTB-4105A-P). The flow meters output 1 pulse per gallon to the data acquisition equipment with an accuracy of ±3% of the reading for flow rates below 1.3 GPM and ±1% of the reading for flow rates between 1.3GPM and 13.2GPM (Omega, 2001). Solar radiation measurements were taken with LI-COR pyranometers (LI-200SA) paired with 147Ω resistors (2220 Millivolt Adapters). Each LI-200SA was calibrated by LI-COR against an Eppley Precision Spectral Pyranometer (LI-COR, 2005). The pyranometer used at the University of Kentucky site had the serial number PY66039 and a calibration constant of 72.97 Watts per meter squared per millivolt. The pyranometer used at the Kentucky Horse Park had the serial number PY66040 and a calibration constant of 81.73 Watts per meter squared per millivolt. The uncertainty of calibration was ± 5% (LI-COR, 2005).

Two Measurement Computing data acquisition boards (USB-2416-4AO) expanded with two expansion boards (AI-EXP32 analog input expansion modules) were used to collect the temperature, flow, and radiation data. The USB-2416-4AO is a full-speed, multiplexed 24-bit measurement system with 16 differential analog inputs or 32 single ended analog inputs (Measurement Computing, 2009). The AI-EXP32 adds 16

differential, 32 single ended, analog inputs to the USB-2416-4AO board. The combined data acquisition boards and their associated expansion boards are referred to collectively as DAQ boards. Differential analog inputs can be configured for use as thermocouple thermometers, which can connect directly to thermocouple wires without an external reference junction and convert the voltage of the thermocouple wires to a temperature reading (Beckwith et al., 2007). Cold junction compensation is performed with four high-resolution temperature sensors located near the terminal blocks of the USB-2416-4AO and NIST linearization coefficients are implemented to convert the voltage measurement and cold junction measurement to a temperature reading (Measurement Computing, 2009). Analog differential voltage settings were implemented to read the flow meter's pulse output and the radiation sensor's millivolt output. The 60 samples per second rate was used for the data acquisition equipment. At this rate, the typical and maximum accuracy errors for type K thermocouples measured with the boards were 0.457°C (0.823°F) and 0.948°C (1.706°F) respectively (Measurement Computing, 2009). The pulse output from the flow meters was measured with the ±10 Volt analog DC voltage measurement range and the millivolt radiation sensor output was measured with the ±0.078125 Volt analog DC voltage measurement range. Details on the methods for collecting and recording data are presented in chapter 4.

The DAQ board thermocouple measurements were calibrated against an Omega CL134 Temperature Source and Measurement device. The Omega CL134 had an accuracy of ±0.7°F for type K thermocouples measuring temperatures between -256°F and 2505°F (Omega, 1998). All measured temperatures were modified by equations resulting from the calibration process. Calibration equations for each thermocouple in

the solar thermal system are provided in Appendix B along with the details of the calibration method and the associated error.

SECTION 4 – Data Collection

Data Collection

All data collection was driven by Visual Basic programs written and running in Visual Basic Studio 2008. Two separate programs running on two separate computers collected the data. An Internet connected computer downloaded forward weather forecasts from the University of Kentucky's Agricultural Weather Center, wwwagwx.ca.uky.edu, once an hour and archived them in a text file. The control computer located in the mechanical closet of the S.KY BLUE House interfaced with the DAQ boards via a Visual Basic program to gather data about the operation of the solar thermal system and store it in a text file.

The Visual Basic control program running on the control computer read all of the terminals of the DAQ boards every second. Every minute, the thermocouple and pyranometer measurements from the last 60 seconds were averaged and stored in a text file. After September 16, 2010, the total number of pulses output by flow meters 3 and 5 were recorded in the text file each minute. The flow rate for a period of time in gallons per minute was calculated by subtracting the number of pulses at the beginning of the period from the number of pulses at the end of the period and dividing the difference by the period length in minutes. Counter data was inspected to ensure continuous system operation during the periods considered for the calculation of the flow rates.

Prior to September 16, 2010, the pulse output from flow meter 2 was totaled for 30-minute intervals by the control program and the total was divided by 30 to obtain flow

rate measurements in gallons per minute. These 30-minute intervals occurred once an hour. While pulses were being totaled, the flow rate from the previous 30-minute interval was stored in the data text file. The flow rates stored in the text file were verified and adjusted by visual measurements taken from the flow meters at different times during daily system operation. The visual measurements were taken with a stop watch, a visual dial on the flow meter which completed one revolution for every gallon of water that traveled through the meter, and the totalizer reading on the flow meter which reported the total number of gallons that had ever traveled through the meter.

During the Solar Decathlon, an Istec FlowGuard balancing valve with an integrated, spring-loaded variable-area flow meter was used instead of flow meter 5. The dual purpose balancing valve was chosen to avoid additional the head losses associated with a separate flow measurement device. On July 21, 2010, flow meter 5 was installed to increase the accuracy for the flow measurement. Prior the September 16, 2010, flow meter 5 was read visually.

Four primary variable categories were used to control the data collection process: variables to hold instantaneous measurements read from the data acquisition terminals, variables to hold totals of the instantaneous measurements, variable to hold averaged measurements, and counter variables. Figure 4.1 displays a shell of the code used for data collection and data logging.

```
Control Computer Clock signals Passage of a Second to Second_Timer in Visual
Basic Studio 2008
        Second_Counter=Second_Counter + 1
        TC_Instant = Current Value of DAQ thermocouple terminal
        Rad_Instant = Product of Current Value of Voltage from DAQ
                      pyramometer terminal and conversion factor with units of
                      (Watts/square meter/millivolt)
        Last_Pulse_Voltage = Pulse_Voltage
```

```
Pulse_Voltage = Value of Voltage from DAQ flow meter pulse terminal
IF (Pulse_Voltage > Last_Pulse_Voltage) THEN
        Flow_Pulse_Counter = Flow_Pulse_Counter + 1
END IF
TC_Total = TC_Total + TC_Instant
Rad_Total = Rad_Total + Rad_Instant
IF (Second_Counter  = 60) THEN
        TC_Average = TC_Total/60
        Rad_Average = Rad_Total/60
        Output (TC_Average, Rad_Average, Pulse_Flow_Counter) to text
          File
        TC_Total = 0
        Rad_Total = 0
END IF
```

Figure 4.1 Outline of the data collection and logging code.

System Operation

The solar thermal system flow rates were set at the beginning of each day when the system was started. In order to determine the collection capability of the solar thermal system in all weather condition for modeling, the system ran from morning to evening on all the days of data collection instead of being controlled by the temperature differential between the collector and the storage tank. All relationships between flow rate, cloud cover, and storage tank temperature were of interest. Thus, typical solar thermal system control, which would have limited system operation to periods with energy collection rates above a set threshold, was avoided for data collection. The conditions surrounding periods of low energy collection rates, temperature equilibrium, and energy loss were also of interest.

During July 2010, the solar thermal system was started manually in the morning and stopped manually in the evening by switching pumps 2 and 5 on and off. Water

draws were conducted periodically at night. The number of gallons removed from heat tank 1 was measured with an Omega FTB-4105A-P connected to the shower in the S.KY BLUE House bathroom during the draws and recorded in a notebook. The temperature of the water withdrawn from the tank was measured with thermocouple 2 on the outlet of heat tank 2 as well as with a type K thermocouple attached to a digital multimeter.

During September and October of 2010, the control computer switched the solar thermal system on in the morning and off in the evening by sending signals to relays tied to pumps 2 and 5. Because of a limited water supply at the Horse Park during September and October, water draws were no longer conducted in the evenings. Instead, the system was operated during the night with the path to the heat dissipaters open to remove heat from heat tank 1. During some periods with high collection, the heat dissipaters path was open during the day as well.

SECTION 5 – Variability Associated with Short-Term Forward Weather Forecasts

5.1. Variability Associated with Cloud Cover Forecasts and the Prediction of Solar Radiation

Kentucky MESONET (2011) records the daily total horizontal radiation received at various counties in the state of Kentucky in megajoules per meter squared. A sensitivity analysis was performed to calibrate the clearness number (C_N) and coefficients A and B from the Perez Model (Equation 2.19) for Fayette County. The predicted horizontal radiation was calculated from equation 2.19 with GHI_{clear} calculated with equation 2.25 for the total clear sky radiation incident on a horizontal surface. The calculations were performed in Microsoft Excel and C_N, A, and B were varied to obtain

the smallest difference between the predicted daily horizontal radiation and the value recorded by Kentucky MESONET. The tables resulting from the sensitivity analysis can be found in Appendix D.

A random set of data from July and October containing days of varying radiation levels was used for the calibration; the absolute difference between the prediction of daily total radiation incident on a horizontal surface and the measured value from Kentucky MESONET (2011) for the day was summed for all of the days in the calibration set. The values of C_N, A, and B which minimized the absolute difference between the predicted and measured radiation incident on a horizontal surface were chosen as the values for these constants for Lexington, KY. The local values for Lexington, Kentucky were determined to be:

CN = 0.95,

A = 0.80, and

B = 1.8.

These constants were used with a separate set of validation data from July through November of 2010 to evaluate the use of Equations 4 and 6 to predict daily radiation from 1, 12, 24, 36, and 48 hour weather forecasts from the University of Kentucky Ag Weather Center, www.agwx.ca.uky.edu.

Table 5.2.1 displays the average of the absolute difference between the prediction of daily total radiation incident on a horizontal surface and the measured value from Kentucky MESONET (2011). Table 5.2.2 shows the average absolute difference divided by the average daily measured radiation incident on a horizontal surface for the month.

Table 5.2.1 Average of the absolute difference between the daily prediction of daily total radiation incident on a horizontal surface and the measured value from Kentucky MESONET (2011)

	July	September	October	November
n (Days)	12	4	14	6
Average Daily Horizontal Radiation (Btu/ft^2)	2000	1715	1290	897
Standard Deviation of Daily Horizontal Radiation (Btu/ft^2)	577	104	363	393
Predictors:				
1 Hour Forecast	217	46	286	78
12 Hour Forecast	173	58	338	206
24 Hour Forecast	231	57	411	235
36 Hour Forecast	242	90	520	253
48 Hour Forecast	262	92	676	276
Average Of Measured Radiation for the Month	403	77	963	322

Average Absolute Differences in Btu/ft^2

Table 5.2.2 Average of the absolute difference between the daily prediction of daily total radiation incident on a horizontal surface and the measured value from Kentucky MESONET (2011) divided by the monthly average radiation received on a horizontal surface

	July	September	October	November
n (Days)	12	4	14	6
Average Daily Horizontal Radiation (Btu/ft^2)	2000	1715	1290	897
Standard Deviation of Daily Horizontal Radiation (Btu/ft^2)	577	104	363	393
Predictors:				
1 Hour Forecast	10.9	2.7	22.2	8.7
12 Hour Forecast	8.7	3.4	26.2	23.0
24 Hour Forecast	11.5	3.4	31.8	26.3
36 Hour Forecast	12.1	5.3	40.3	28.2
48 Hour Forecast	13.1	5.4	52.4	30.8
Average Of Measured Radiation for the Month	20.1	4.5	74.7	35.9

Average Absolute Differences Divided by Monthly Averages expressed as Percentages

The daily predicted and measured total radiation incident on a horizontal surface along with the monthly average are presented in Figures 5.2.1 through 5.2.4.

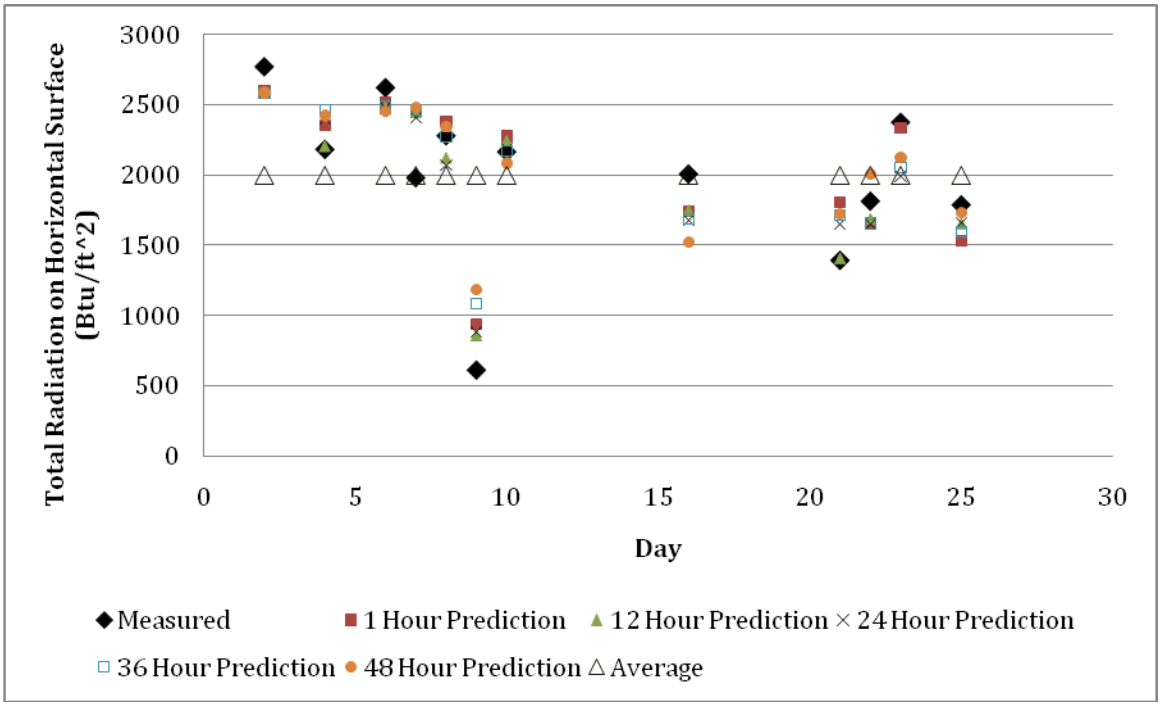

Figure 5.2.1 Daily predicted, measured, and average radiation incident on a horizontal surface for July 2010 validation data

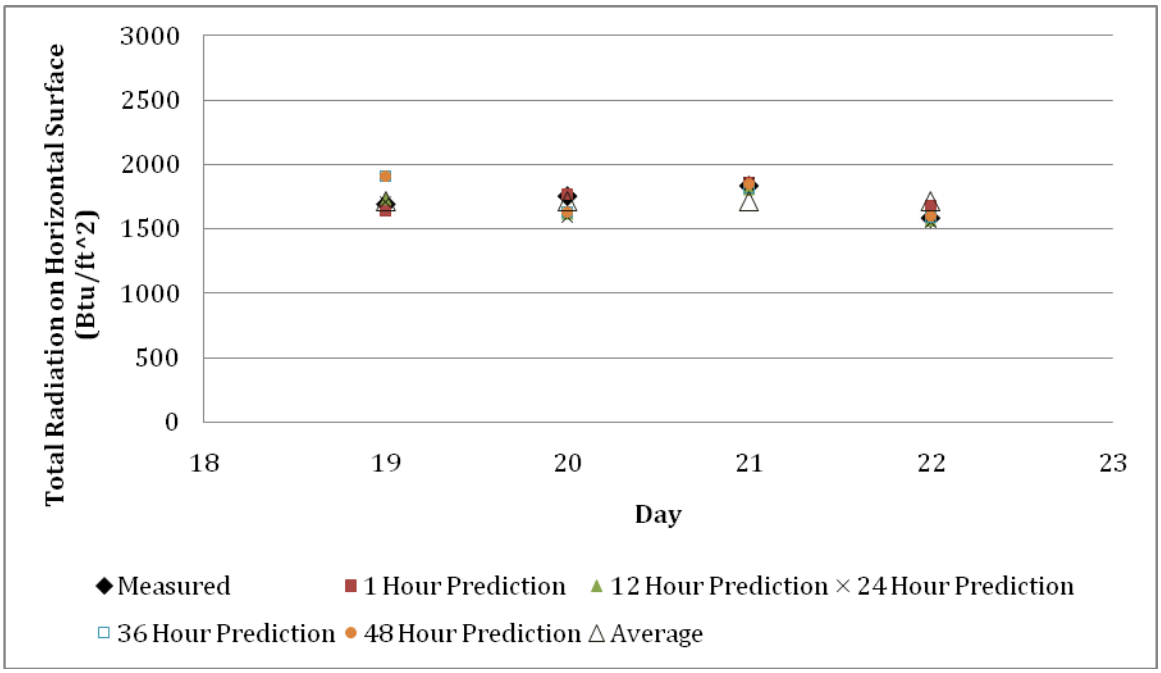

Figure 5.2.2 Daily predicted, measured, and average radiation incident on a horizontal surface for September 2010 validation data

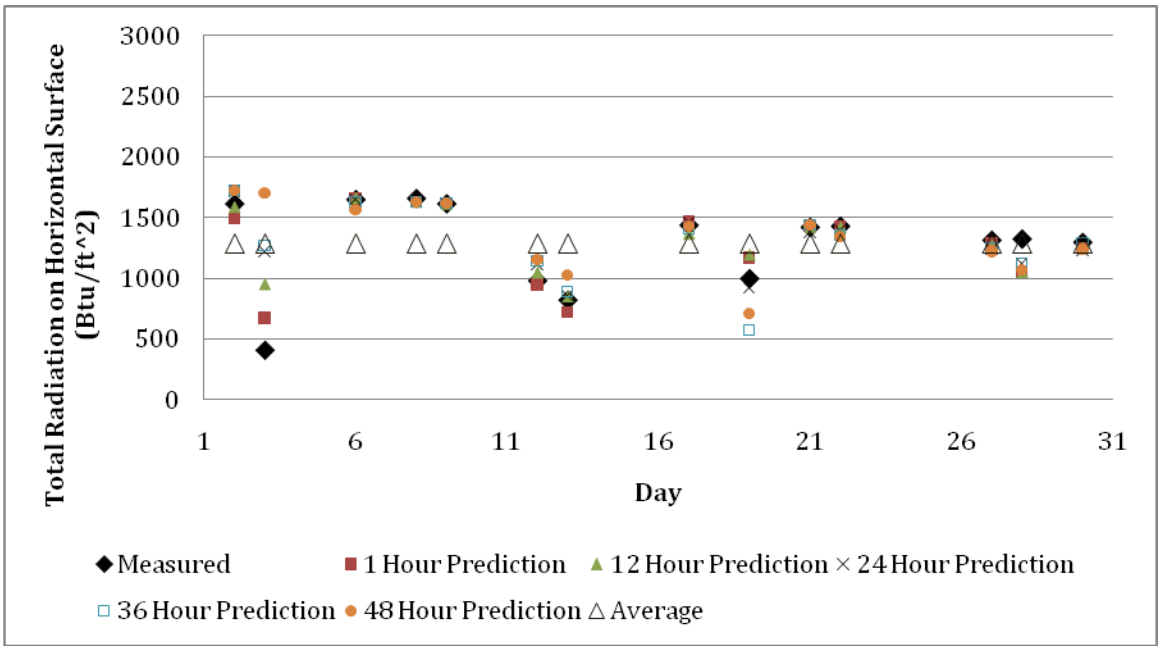

Figure 5.2.3 Daily predicted, measured, and average radiation incident on a horizontal surface for October 2010 validation data

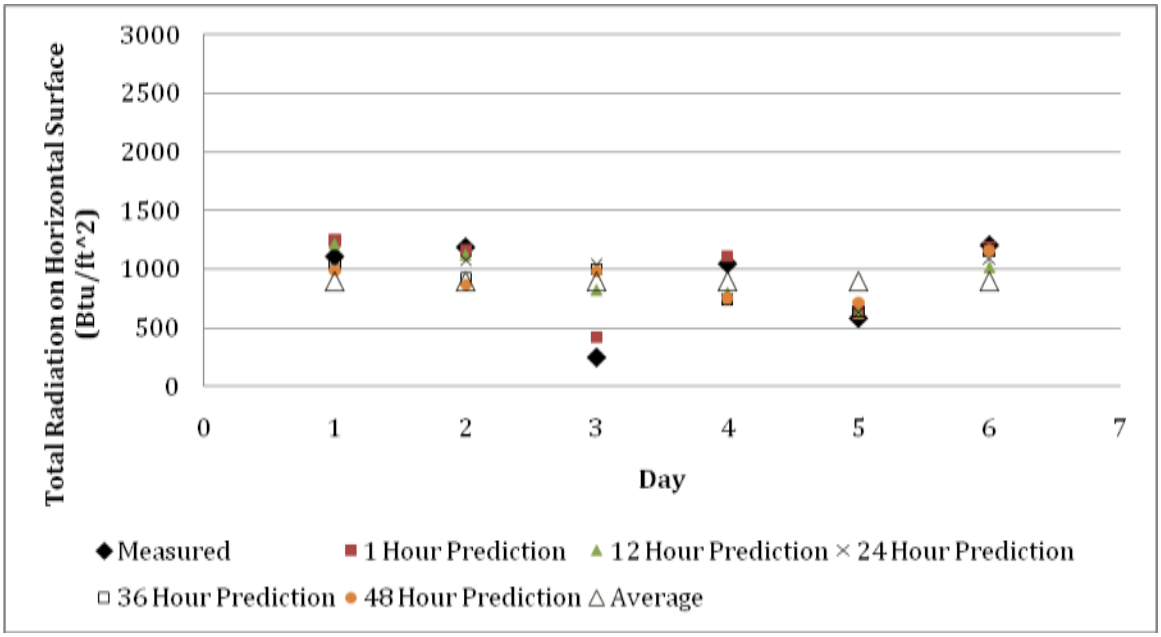

Figure 5.2.4 Daily predicted, measured, and average radiation incident on a horizontal surface for November 2010

Linear Regression was used to assess the fit of the models based on cloud cover forecasting and the ASHRAE clear sky model as well as modeling based on the monthly average. Figures 5.2.5 through 5.2.10 show the regression graphically and Table 5.2.3 summarizes the results.

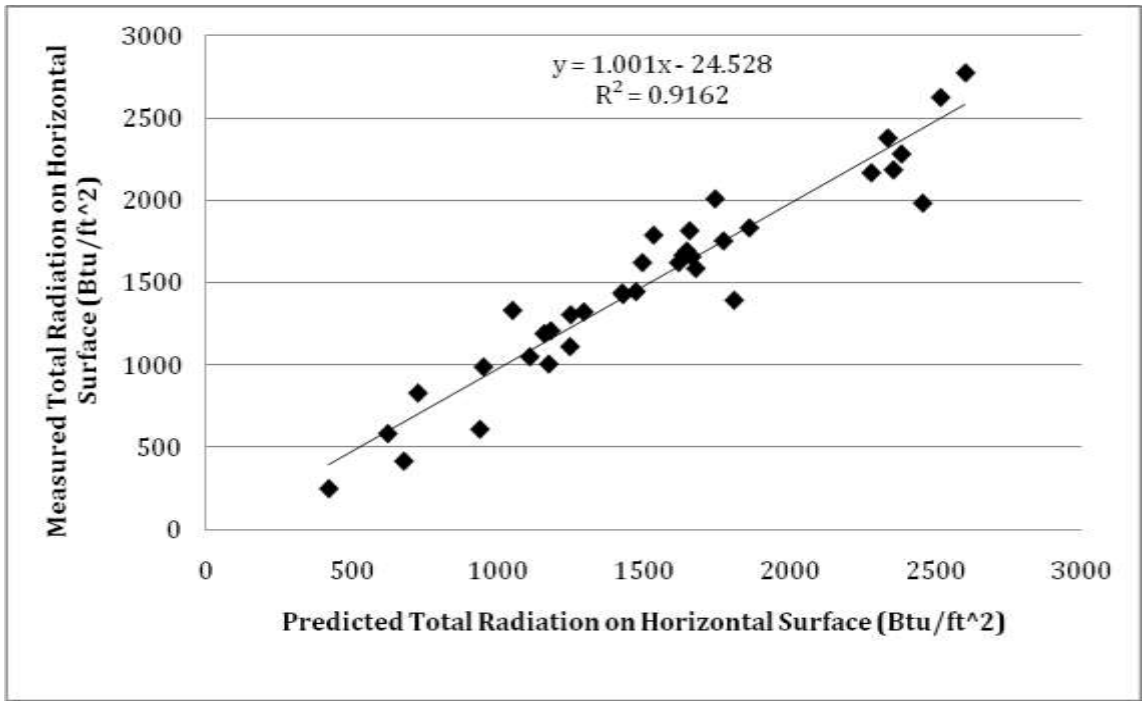

Figure 5.2.5 Measured daily total radiation incident on a horizontal surface verses the 1 hour prediction value for July through November 2010 Validation Data

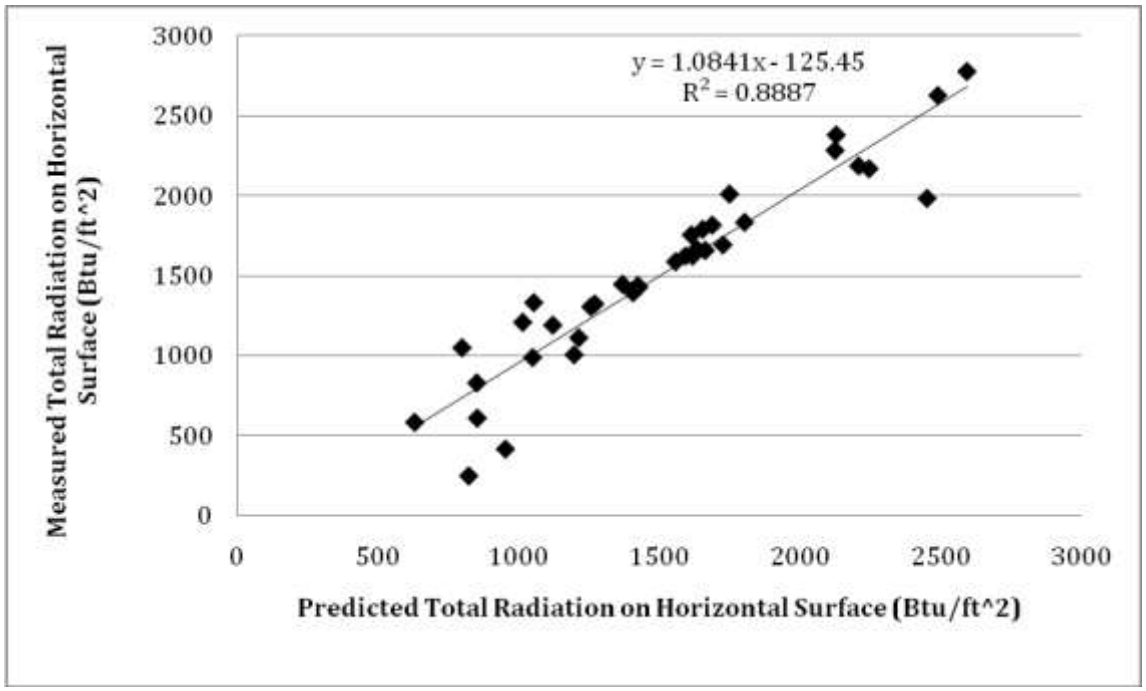

Figure 5.2.6 Measured daily total radiation incident on a horizontal surface verses the 12 hour prediction value for July through November 2010 validation data

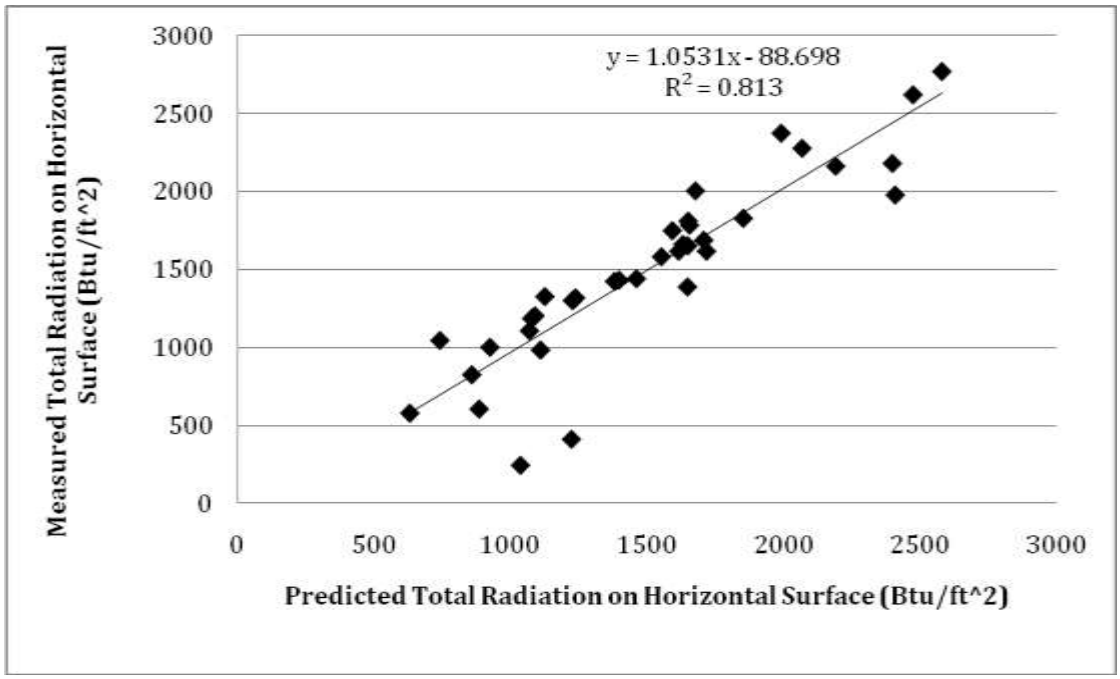

Figure 5.2.7 Measured daily total radiation incident on a horizontal surface verses 24 hour prediction value for July through November 2010 validation data

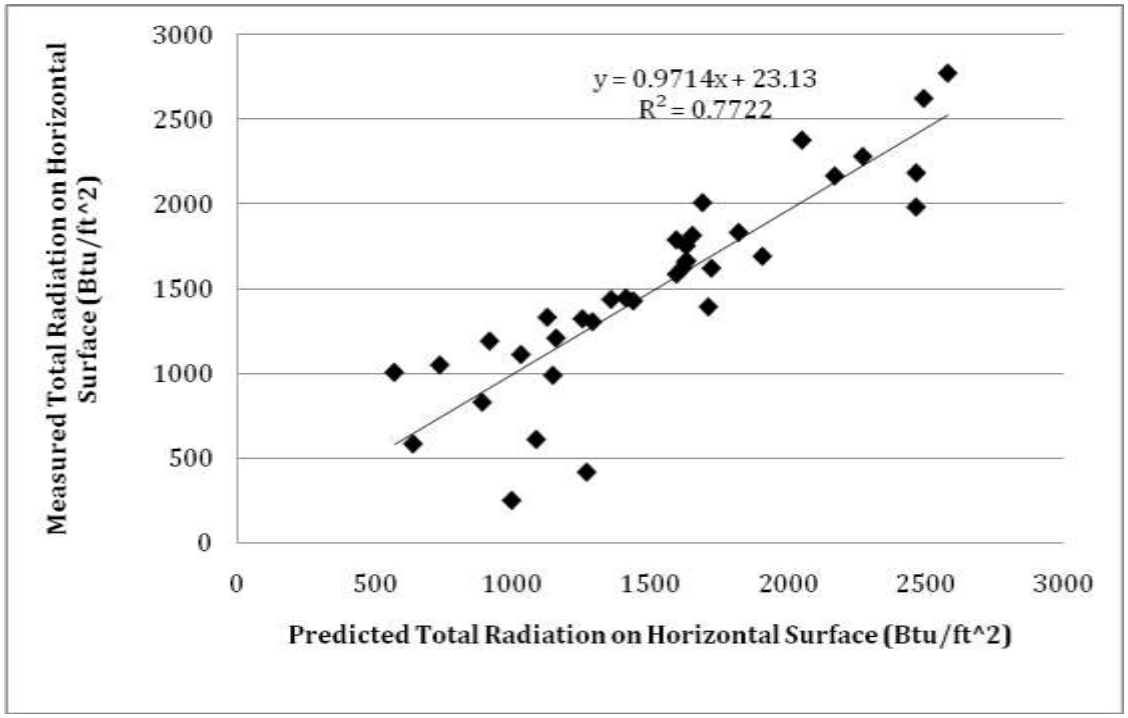

Figure 5.2.8 Measured daily total radiation incident on a horizontal surface verses 36 hour prediction value for July through November 2010 validation data

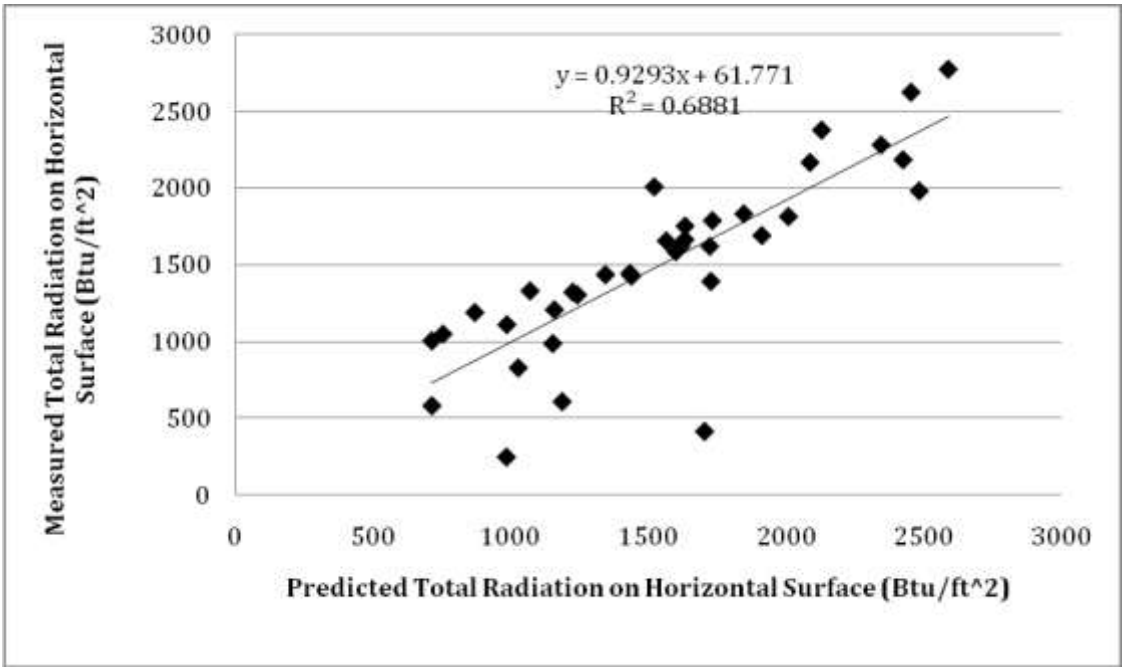

Figure 5.2.9 Measured daily total radiation incident on a horizontal surface verses 48 hour prediction value for July thorough November 2010 validation data

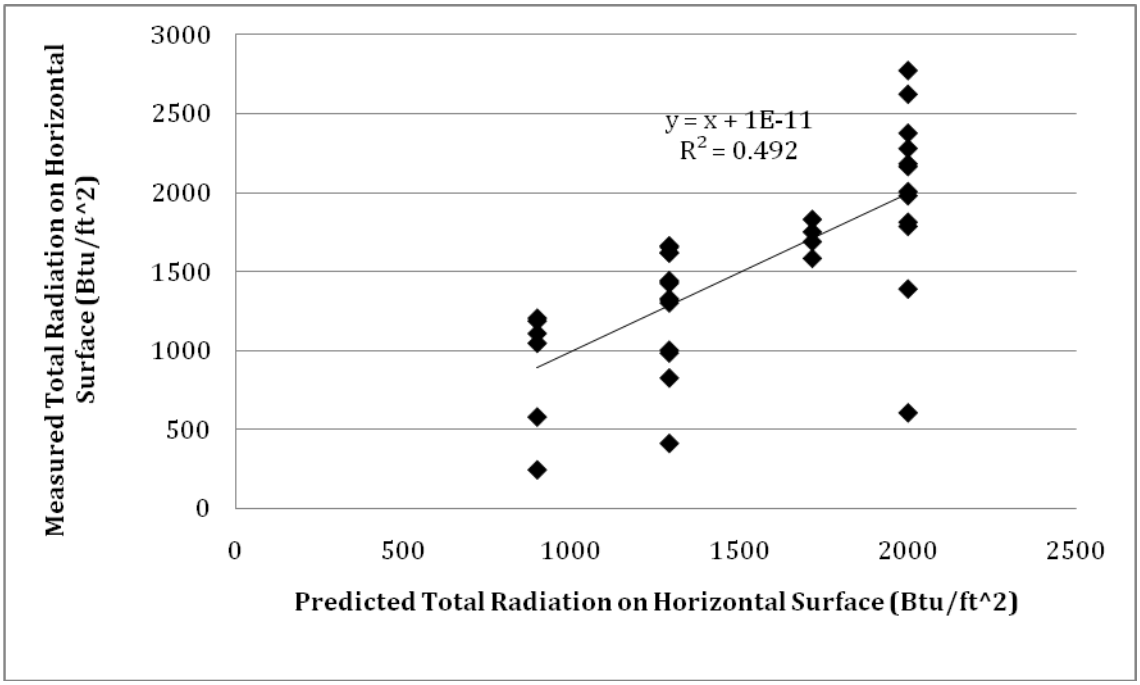

Figure 5.2.10 Measured daily total radiation incident on a horizontal surface verses the monthly average of the value for July through November 2010 validation data

Table 5.2.3 Variation in the measured daily total radiation incident on a horizontal surface explained by modeling on weather forecasts and the average value

Predictor	Percentage of Variation in Measured Daily Horizontal Radiation Explained by Predictor
1 Hour Forecast Prediction	91.6
12 Hour Forecast Prediction	88.9
24 Hour Forecast Prediction	81.3
36 Hour Forecast Prediction	77.2
48 Hour Forecast Prediction	68.8
Average Daily Horizontal Radiation for the Month	49.2

SECTION 6 – Determination of Important Factors

The Solar Thermal Collector

The literature review indicated mass flow rate through the collectors, solar insolation, temperature difference between the collector and the ambient air, and the angle of incidence of the suns rays as important factors in modeling evacuated tube heat pipe solar thermal collectors. The collector operation data collected in July, September, and October was analyzed to determine the significance of these factors in modeling the solar thermal collectors. The energy collected in the two hour period between 11:00 and 13:00 Solar Time, one hour before and after solar noon, was examined to determine the significance of each of the identified factors in modeling the collectors. The only factor not examined by this investigation was the variance of the angle of incidence throughout the day. For a set time window, only the seasonal variation in incidence angle can be examined.

To conduct a meaningful comparison, some of the measured parameters were standardized. The rate of energy transferred by the collector was calculated from the temperature measurements taken at the inlet and outlet of the two collectors operating in series and the mass flow rate of the liquid through the collectors

$$q_{Collectors} = 8.3\dot{m}_3\left(T_{12} - T_{15}\right) \qquad (6.1)$$

where; $q_{Collectors}$ = Rate of energy transfer $\left(\frac{Btu}{\min}\right)$.

Equation 6.1 was implemented for each minute of operation and the total heat transferred by the collector for the two-hour period was calculated

$$Q = \sum_{i=1}^{n=120} q_{Collector,i}\left(\Delta t_i\right) \qquad (6.2)$$

where; Q = energy transferred by collectors (Btu),

Δt = change in time (minute).

Because the collectors were mounted on a vertical wall and encased with decorative trim, shading impacted the amount of energy collected. The trim was modeled as an overhang and fin network so that the un-shaded collector area could be calculated.

To account for the effect of shading, Q was divided by the average un-shaded collector area for the two-hour time period calculated. Shading was more drastic during July than during September and October because the sun was higher in the sky; Table 6.1 displays the impact of adjusting the energy transferred by the collectors for un-shaded area.

Table 6.1 Solar insolation, energy transferred by collectors, and energy transferred per unit collector area between 11:00 and 13:00.

Date	I Btu/hr x ft^2	Q Btu	Q/Area Btu/ft^2
7/14/10	129.6	4386	73.2
7/15/10	144.7	5457	90.7
7/16/10	123.8	4467	73.9
7/19/10	124.8	5076	82.7
7/20/10	119.6	4674	75.8
7/22/10	111.3	2829	45.4
7/23/10	128.7	3450	55.1
7/27/10	84.2	2493	39.0
9/18/10	209.9	19035	246.6
9/19/10	170.7	18534	239.5
9/20/10	192.3	20125	259.6
9/21/10	212.1	20318	261.6
9/22/10	201.7	16087	206.6
9/23/10	181.6	12939	165.9
9/24/10	211.6	14433	184.7
9/25/10	227.5	18873	241.0
9/26/10	65.9	6862	87.5
9/27/10	8.3	-1265	-16.1
10/1/10	242.5	14791	186.9
10/2/10	229.8	16203	204.4
10/3/10	21.6	1777	22.4
10/4/10	52.9	3040	38.2
10/5/10	234.0	14969	187.9
10/6/10	239.3	16594	208.0
10/7/10	241.2	15172	189.8
10/8/10	248.8	21917	273.9
10/9/10	245.6	16210	202.3
10/10/10	242.9	15167	188.9

The mass flow rate of the transfer fluid through the collectors was directly measured by flow meter 3 in GPM. The solar radiation incident on the collectors used for the comparisons was the average value of the insolation measurements taken every minute for the two-hour period and was reported in Btu/hr x ft^2. To determine the temperature difference between the ambient temperature and the collector for the two-hour period, temperature 36 was subtracted from temperature 15 for each minute and the difference

for the period were averaged. The average incidence angle for the period was considered for the comparisons. The longitudinal and transversal IAMs were determined for each minute by linear interpolation based on the solar altitude angle and the surface solar azimuth respectively. The IAMs for each minute were averaged to determine the IAMs for the period. The transversal IAM is related to the change in the surface solar azimuth, which changes with time of day. Because the two-hour period occurred at the same time each day, the effects of the longitudinal and total IAMs were the focus for the significance tests. The insolation modified by the longitudinal IAM and the total IAM for the period were calculated by multiplying the average IAMs by the average insolation for the period.

APPENDIX A – Randomization

Performance and Weather data was randomly separated into calibration and validation groups. To ensure that each group contained data representative of each defining condition, the daily performance data was first grouped into the twelve categories listed in table A.1. A random number was assigned to each day. Some days only had partial data available. Half of the full days of data and half of the partial days of data within each group were assigned to the calibration group and half were assigned to the validation group. The full and partial days with the lower random numbers were assigned to the calibration group. If a group contained an odd number of days, the extra day was assigned to the calibration group. For some days, only weather forecast data was collected. Those days were grouped by amount of radiation received according to Kentucky MESONET (2011) and separated into the calibration and validation groups

with random numbers by the same method the performance data was separated. Table A.2. lists the days assigned to the calibration and validation groups.

Table A.1. Solar Thermal Performance

High Radiation	P-2 High Speed	HD On
		HD Off
	P-2 Low Speed	HD On
		HD Off
Medium Radiation	P-2 High Speed	HD On
		HD Off
	P-2 Low Speed	HD On
		HD Off
Low Radiation	P-2 High Speed	HD On
		HD Off
	P-2 Low Speed	HD On
		HD Off

Table A.2. Calibration and Validation Groups

Model Calibration		Model Validation	
Dates	Daily Radiation (Btu/ft^2)	Dates	Daily Radiation (Btu/ft^2)
7/2/10	2747.8	7/3/10	2774.3
7/4/10	2448.4	7/5/10	2184.2
7/6/10	2316.3	7/7/10	2624.5
7/12/10	2457.2	7/8/10	1981.6
7/13/10	1646.9	7/9/10	2281.1
7/14/10	713.4	7/10/10	607.7
7/15/10	1981.6	7/11/10	2166.6
7/16/10	2369.1	7/17/10	2008.0
7/18/10	1999.2	7/22/10	1391.5
7/19/10	1981.6	7/23/10	1814.3
7/20/10	2157.8	7/24/10	2377.9

7/21/10	1691.0	7/26/10	1787.9
7/25/10	2413.2	9/20/10	1691.0
7/27/10	1400.3	10/3/10	1620.5
7/28/10	1435.6	10/4/10	413.9
9/21/10	1752.6	10/7/10	1655.8
9/22/10	1831.9	10/9/10	1664.6
9/23/10	1585.3	10/10/10	1620.5
10/5/10	590.1	10/13/10	986.4
10/6/10	1558.9	10/14/10	827.9
10/8/10	1620.5	10/18/10	1444.4
10/11/10	1576.5	10/20/10	1004.0
10/12/10	1514.8	10/22/10	1426.8
10/15/10	1541.3	10/23/10	1435.6
10/16/10	1541.3	10/28/10	1321.1
10/17/10	1523.6	10/29/10	1329.9
10/19/10	1303.5	10/31/10	1303.5
10/21/10	1444.4	11/2/10	1109.7
10/24/10	1171.4	11/3/10	1189.0
10/25/10	1118.5	11/6/10	581.3
10/26/10	572.5		
10/27/10	378.7		
10/30/10	1321.1		
11/1/10	1259.4		
11/4/10	246.6		
11/5/10	1048.1		
11/7/10	1206.6		
11/8/10	1180.2		

APPENDIX B- Simple Linear Regression

Simple linear regression is utilized to evaluate the performance of forecasts and models and for model and equipment calibration. Microsoft Excel is implemented to generate the linear regression model of the form

$$\hat{Y} = b_0 + b_1 X \qquad \text{(A.1)}$$

where; $\hat{Y}$ = model prediction for quantity of interest dependent on input variable,

X= independent variable that provides the basis of the prediction,

b_0= coefficient which estimates the y-intercept of the model,

b_1 = coefficient which estimates the slope of the model.

Assuming the error involved in observing the dependent variable is normally and independently distributed with a mean value of 0, the variance in the dependent variable is the same for all values of the independent variable, the independent variables are know without error, and errors are the only factor prohibiting the model from fitting observed data, the variance of the errors can be estimated

$$s_E^2 = \frac{\sum\left(Y - \hat{Y}\right)^2}{(n-2)} \qquad \text{(A.2)}$$

where; s_E^2 = estimated variance of errors,

Y = value of the dependent variable at X,

$\hat{Y}$ = value of the model at X,

n = number of data points used to build the model

(Ostle, 1963).

The variance associated with predicting a single dependent value (Y) for a given independent value (X) is estimated

$$s_{\hat{Y}}^2 = s_E^2\left[1 + \frac{1}{n} + \frac{\left(X - \overline{X}\right)^2}{\left(\sum X^2 - \frac{\left(\sum X\right)^2}{n}\right)}\right] \qquad \text{(A.3)}$$

where; $s_{\hat{Y}}^2$ = estimated variance for an individual prediction of Y at X,

$\overline{X}$ = average of the values of the independent variable

(Ostle, 1963). The estimated variance for an individual prediction is used with at t-table to construct confidence intervals. The width of the intervals increases with the distance of the independent variable from its mean value.

When Y is observed, the unknown X variable may be determined with the equation

$$\hat{X} = \frac{(Y_0 - b_0)}{b_1} \qquad \text{(A.4)}$$

where; $\hat{X}$ = predicted value of the independent variable,

Y_0 = observed value of Y at which $\hat{X}$ is predicted

(Ostle, 1963).

The upper and lower limits of $\hat{X}$ are determined

$$\left.\begin{matrix}\hat{X}^+ \\ \hat{X}^-\end{matrix}\right\} = \bar{X} + \frac{b_1(Y_0 - \bar{Y})}{D} \pm \frac{ts_E}{D}\sqrt{B(Y_0 - \bar{Y})^2 + D\left(\frac{n+1}{n}\right)} \qquad \text{(A.5)}$$

where; $\bar{Y}$ = average of the values of the dependent variable,

t = t-value for confidence level where the degrees of freedom are n-2,

$$B = \frac{1}{\left(\sum X^2 - \frac{(\sum X)^2}{n}\right)},$$

$$D = b_1^2 - t^2 s_E^2 B$$

(Ostle, 1963).

APPENDIX C- Thermocouple Calibration

The Measurement Computing USB-24164AO Data Acquisition (DAQ) boards' terminals used to measure the type K thermocouples were calibrated against an Omega CL134 Temperature Source and Measurement device. To collect the calibration data, the solar thermal system temperature was held in high, medium, and low temperature ranges.

Four DAQ board temperature measurements (Y) were taken with each thermocouple and three measurements were taken with the Omega CL134. Those

measurements were collected with the following process: two consecutive measurements were taken with the DAQ boards; three consecutive measurements were taken with the Omega CL134; and two final consecutive measurements were taken with the DAQ boards. DAQ board measurements were 1 minute averages of 60 measurements collected every second. The three measurements taken with the Omega CL134 were averaged and the average was treated as the Standard (X) in the Equation A.1. The precision error associated with the Omega CL134 measurements that comprised X was assumed to be negligible for calculations; however, it is reported in the form of a standard deviation. Each measured Y was treated as a replication (n).

The four Y measurements associated with each X at each temperature level were plotted in Excel and regression methods were implemented to determine b_0 and b_1 from Appendix A. Figure C.1 displays the regression line with its associated R^2 value for the calibration of thermocouple 1 (T1).

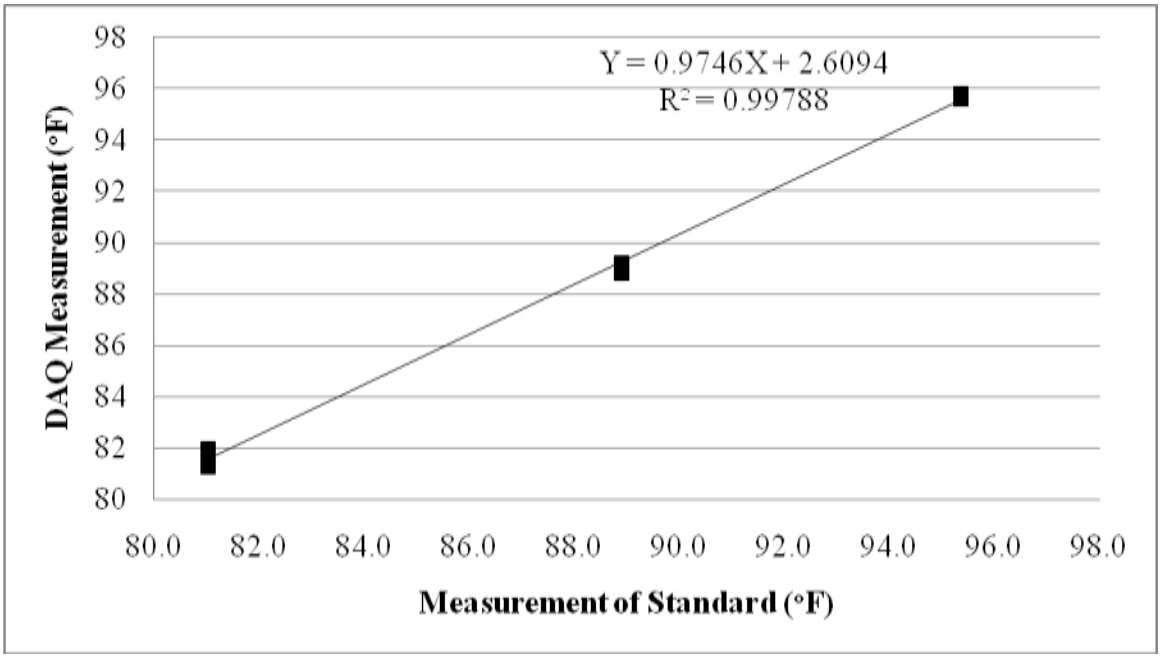

Figure C.1 DAQ Measurement (Y) verses the measurement of the Standard (X) for TC 1.

Equation A.3 was implemented to determine $\hat{X}$ from the data acquisition measurements. $\hat{X}$ was treated as the measured thermocouple temperature for all calculations. The 95% confidence interval associated with the calibrated measurements was calculated with Equation A.4. The size of the confidence interval increased with an increase of the distance between $\hat{X}$ and $\overline{X}$. The $\hat{X}$ values and the magnitudes of their 95% confidence intervals at high, average, and low values of Y_0 are presented in Table B.1 for each thermocouple. Figure B.2 displays the 95% confidence interval for T1 at different values of Y_0.

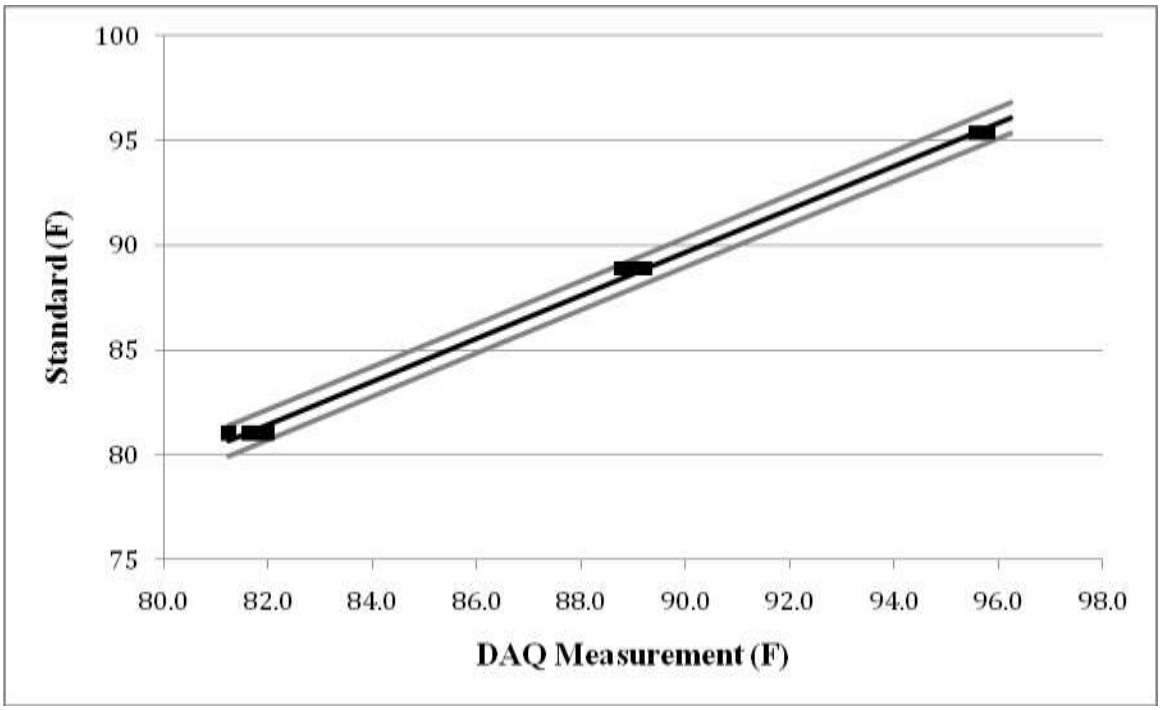

Figure B.2 Estimated Standard, $\hat{X}$, with 95% confidence interval verses DAQ Measurement, Y_0.

APPENDIX D- Radiation Sensitivity Analysis with Calibration Data

Table D.1 Sum of the absolute difference between the predicted radiation incident on a horizontal surface and the measured radiation as detailed in Section 5.2 for $C_N = 1$ with varying values of A and B (Btu)

Clearness Number :1		(Differences in Btu)											
		Exponent (B)											
		1	1.1	1.2	1.3	1.4	1.5	1.6	1.7	1.8	1.9	2	2.1
A	0.95	8191	6930	5974	5303	4880	4513	4344	4282	4348	4480	4688	4874
	0.94	7963	6715	5801	5173	4759	4407	4276	4226	4330	4495	4705	4890
	0.93	7734	6510	5638	5044	4639	4317	4209	4199	4339	4526	4722	4905
	0.92	7508	6321	5491	4915	4519	4248	4142	4209	4347	4533	4739	4921
	0.91	7280	6135	5344	4786	4402	4180	4116	4217	4354	4553	4756	4936
	0.9	7051	5950	5197	4656	4309	4144	4094	4228	4364	4572	4773	4963
	0.89	6823	5766	5050	4530	4238	4120	4082	4237	4378	4592	4790	4998
	0.88	6596	5597	4903	4445	4188	4094	4090	4246	4394	4612	4809	5035
	0.87	6379	5440	4766	4391	4145	4070	4102	4256	4409	4631	4826	5072
	0.86	6178	5284	4692	4338	4111	4046	4113	4265	4430	4650	4862	5129
	0.85	5978	5178	4627	4286	4078	4020	4124	4274	4453	4669	4913	5186
	0.84	5813	5095	4564	4234	4044	4018	4134	4283	4474	4693	4973	5242
	0.83	5699	5013	4499	4182	4011	4019	4145	4292	4497	4740	5033	5299
	0.82	5603	4930	4435	4130	3983	4018	4156	4301	4536	4804	5093	5356
	0.81	5506	4847	4371	4077	3957	4019	4168	4320	4579	4867	5153	5413
	0.8	5409	4764	4309	4038	3950	4019	4181	4361	4623	4932	5214	5475
	0.79	5313	4683	4247	4003	3951	4025	4214	4407	4687	4995	5273	5545
	0.78	5217	4602	4185	3968	3952	4055	4247	4454	4755	5064	5346	5632
	0.77	5121	4523	4123	3932	3967	4098	4294	4521	4850	5155	5432	5729
	0.76	5028	4451	4078	3941	4018	4161	4355	4610	4944	5245	5519	5825
	0.75	4961	4399	4044	3984	4069	4224	4415	4709	5039	5337	5610	5922

Table D.2 Sum of the absolute difference between the predicted radiation incident on a horizontal surface and the measured radiation as detailed in Section 5.2 for $C_N = 0.97$ with varying values of A and B (Btu)

Clearness Number :0.97		(Differences in Btu)											
		Exponent (B)											
		1	1.1	1.2	1.3	1.4	1.5	1.6	1.7	1.8	1.9	2	2.1
A	0.95	8993	7734	6651	5785	5143	4655	4263	3997	3827	3801	3868	3968
	0.94	8758	7526	6478	5641	5012	4536	4154	3927	3767	3786	3873	3983
	0.93	8523	7318	6303	5501	4887	4419	4062	3856	3739	3791	3879	3998
	0.92	8295	7110	6130	5361	4764	4302	3989	3792	3737	3797	3884	4012
	0.91	8073	6902	5956	5221	4641	4202	3916	3764	3739	3802	3888	4027
	0.9	7853	6694	5785	5081	4517	4111	3882	3735	3742	3808	3893	4042
	0.89	7632	6507	5637	4941	4411	4049	3853	3719	3744	3814	3902	4057
	0.88	7410	6323	5489	4804	4335	4001	3822	3716	3748	3820	3912	4071
	0.87	7190	6140	5341	4700	4281	3954	3791	3713	3750	3825	3924	4086
	0.86	6969	5956	5200	4633	4226	3909	3760	3710	3752	3831	3940	4101
	0.85	6747	5785	5118	4566	4171	3877	3730	3709	3755	3837	3957	4134
	0.84	6530	5673	5041	4497	4115	3844	3722	3706	3758	3842	3973	4189
	0.83	6373	5586	4963	4430	4061	3812	3715	3703	3762	3849	4007	4244
	0.82	6227	5501	4886	4363	4006	3780	3707	3706	3764	3871	4046	4299
	0.81	6105	5416	4808	4301	3950	3747	3700	3709	3773	3904	4104	4354
	0.8	6012	5331	4731	4242	3895	3735	3692	3712	3801	3936	4162	4409
	0.79	5918	5246	4653	4182	3850	3727	3685	3732	3828	3969	4220	4464
	0.78	5824	5161	4576	4122	3810	3718	3693	3757	3855	4019	4278	4520
	0.77	5732	5077	4499	4063	3770	3714	3711	3781	3887	4089	4350	4596
	0.76	5638	4992	4422	4004	3756	3740	3749	3829	3947	4176	4435	4677
	0.75	5552	4921	4364	3971	3789	3780	3794	3881	4021	4263	4520	4758

Table D.3 Sum of the absolute difference between the predicted radiation incident on a horizontal surface and the measured radiation as detailed in Section 5.2 for C_N = 0.95 with varying values of A and B (Btu)

Clearness Number :0.95		(Differences in Btu)													
		Exponent (B)													
		1	1.1	1.2	1.3	1.4	1.5	1.6	1.7	1.8	1.9	2	2.1	2.2	2.3
A	0.95	9610	8293	7208	6324	5605	5009	4528	4125	3866	3681	3609	3634	3662	3754
	0.94	9380	8089	7016	6163	5475	4885	4417	4035	3799	3636	3609	3635	3670	3764
	0.93	9150	7884	6833	6002	5344	4760	4306	3956	3732	3623	3610	3636	3679	3775
	0.92	8919	7681	6663	5851	5215	4636	4212	3885	3690	3617	3611	3636	3686	3785
	0.91	8689	7477	6493	5714	5084	4517	4124	3829	3663	3610	3612	3636	3694	3796
	0.9	8459	7273	6323	5577	4953	4416	4045	3798	3651	3605	3613	3638	3702	3807
	0.89	8227	7070	6153	5439	4823	4323	3999	3767	3645	3597	3614	3638	3710	3824
	0.88	7997	6866	5983	5301	4710	4270	3952	3735	3638	3593	3615	3638	3718	3853
	0.87	7768	6672	5831	5164	4639	4218	3906	3704	3630	3592	3616	3645	3726	3883
	0.86	7543	6492	5686	5075	4576	4166	3866	3680	3677	3589	3617	3650	3735	3927
	0.85	7326	6312	5562	5005	4512	4113	3832	3672	3617	3590	3617	3656	3767	3975
	0.84	7109	6146	5484	4936	4449	4061	3798	3663	3610	3592	3618	3665	3818	4023
	0.83	6901	6018	5408	4867	4385	4009	3765	3654	3603	3593	3619	3693	3869	4071
	0.82	6729	5885	5332	4797	4322	3960	3731	3646	3597	3594	3632	3725	3920	4120
	0.81	6584	5852	5257	4728	4258	3910	3720	3638	3588	3600	3656	3774	3971	4167
	0.8	6465	5768	5180	4658	4195	3862	3708	3629	3582	3622	3682	3822	4020	4215
	0.79	6346	5685	5104	4590	4138	3826	3697	3621	3599	3643	3708	3871	4071	4264
	0.78	6251	5602	5028	4521	4082	3790	3686	3627	3617	3664	3753	3920	4122	4312
	0.77	6160	5519	4953	4451	4025	3775	3683	3640	3635	3685	3800	3973	4183	4376
	0.76	6068	5436	4877	4382	3969	3764	3695	3661	3667	3725	3872	4052	4259	4450
	0.75	5978	5353	4805	4323	3928	3796	3729	3700	3713	3789	3946	4131	4336	4524

REFERENCES

Al-Sanea, Sami A., M. F. Zedan, and Saleh A. Al-Ajlan. 2004. Adjustment factors for the ASHRAE clear-sky model based on solar-radiation measurements in Riyadh. *Applied Energy*. Vol. 79: 215-237.

ANSI/ASHRAE. 1986 (RA 1991). *Standard 93. Methods of Testing to Determine the Thermal Performance of Solar Collectors*. Atlanta: American Society of Heating, Refrigerating and Air-Conditioning Engineers, Inc.

Apricus. 2006. *Apricus Solar Hot Water*. < http://www.apricus.com/>.

ASHRAE. 2004. *ASHRAE Handbook HVAC Systems and Equipment*. Ch 33: Solar Energy Equipment. Atlanta, GA: American Society of Heating, Refrigerating and Air-Conditioning Engineers, Inc.

ASHRAE. 1999. *ASHRAE Handbook Heating, Ventilating, and Air-Conditioning Applications*. Ch 32: Solar Energy Use. Atlanta, GA: American Society of Heating, Refrigerating and Air-Conditioning Engineers, Inc.

ASHRAE. 1972. *ASHRAE Handbook of Fundamentals*. Ch 22: Air Conditioning Cooling Load. New York, NY: American Society of Heating, Refrigerating and Air-Conditioning Engineers, Inc.

Beckwith, Thomas G., Roy D. Marangoni, and John H. Lienhard V. 2007. Mechanical Measurements. 6th ed. Upper Saddle River, NJ: Pearson Education, Inc.

Bohren, Andreas and Walter Gubler. 2004. *Test Report No. C632LPEN*. Rapperswil: Institut für Solartechnik SPF.

Chi, S. W. 1976. *Heat Pipe Theory and Practice: A Sourcebook*. Washington: Hemisphere Publishing Corporation, McGraw-Hill Book Company.

Candanedo, Jose A. and Andreas K. Athienitis. 2010. Investigation of Anticipatory Control Strategies in a Net-Zero Energy Solar House. *ASHRAE Transactions*.

Dinçer, Ibrahim, and Marc A. Rosen. 2002. *Thermal Energy Storage Systems and Applications*. West Sussex: John Wiley & Sons, Ltd.

Duffie, John A. and William A. Beckman. 2006. *Solar Engineering of Thermal Processes.* 3rd ed. Hoboken: John Wiley & Sons, Ltd.

Gul, M.S. and Muneer, T. 1998. Models for Obtaining Solar Radiation from Other Meteorological Data. *Solar Energy* 64, 99-108.

Incropera, Frank P., David P. DeWitt, Theodore L. Bergman, and Adrienne S. Lavine. 2007. *Fundamentals of Heat and Mass Transfer*. 6th ed. John Wiley & Sons, Inc.

iTouchMap.com. 2010. Latitude and Longitude of a Point. <iTouchMap.com/latlong.html>.

Kasten, F. and Czeplak, G. 1980. Solar and Terrestrial Radiation Dependent on the Amount and Type of Cloud. *Solar Energy* 24, 177-189.

Kentucky MESONET. 2011. The Commonwealth's Official Source for Weather and Climate Data. <www.kymesonet.org/index.html>.

Lane, Tom. 2004. *Solar Hot Water Systems: Lessons Learned, 1977 to Today*. Energy Conservation Services of North Florida Inc.

Lee, Gwi-Hyun. 2008. Domestic Hot Water System Using Evacuated Tubular Solar Collector. ASABE Paper No. 083576. St. Joseph, Mich.: ASABE.

LI-COR, 2005. LI-COR Terrestrial Radiation Sensors Instruction Manual. Lincoln, NE: LI-COR, INC.

Machler, M. A. and M. Iqbal. 1985. "A Modification of the ASHRAE Clear Sky Irradiation Model." *ASHRAE Transactions*, Vol. 91, Part 1A: p. 106.

McQuiston, Faye C., Jerald D. Parker, and Jeffrey D. Spitler. 2005. *Heating, Ventilating, and Air Conditioning Analysis and Design*. 6th ed. John Wiley & Sons, Inc.

Measurement Computing. 2009. USB-2416-4AO USB-based Multi-function I/O module User's Guide. Norton, MA: Measurement Computing Corporation.

Muneer, T. 2004. *Solar Radiation and Daylight Models*. 2nd ed. Burlington: Elsevier Butterworth-Heinemann.

Ng, K. C., C. Yap, and T. H. Khor. 2000. Outdoor Testing of Evacuated-Tube Heat-Pipe Solar Collectors. *Journal of Process Mechanical Engineering*. Vol 214: Part E.

Omega, 1998. Series CL134 Temperature Source/Measure User's Manual.

Omega, 2001. FTB-4000 and FTB-5000 Series Turbine Meters for Water Operator's Manual.

Omega, 2010. Omega Engineering, Inc. <http://www.omega.com/>.

Ostle, Bernard. 1963. *Statistics in Research*. 2nd ed. Ames: The Iowa State University Press.

Papadopoulos, Agis M. 2003. "Active Solar Heating and Cooling of Buildings." *Solar Thermal Technologies for Buildings the State of the Art*. Ed. M. Santamouris. London: James & James (Science Publishers) Ltd. 17-35.

Perez, Richard, Kathleen Moore, Steve Wilcox, David Renné, and Antoine Zelenka. 2007. Forecasting solar radiation – Preliminary evaluation of an approach based upon the national forecast database. *Solar Energy*. Vol 81: 809-812.

Schnieders, Jürgen. 1997. Comparison of the energy yield predictions of stationary and dynamic solar collector models and the models' accuracy in the description of a vacuum tube collector. *Solar Energy*. Vol 61: 179-190.

SPF. 2010. *SPF-InfoCD User Manual Collector Catalogue*. Rapperswil: Institut für Solartechnik SPF. Available through: <www.solarenergy.ch>.

SRCC. 2010. Certified Solar Collector: Apricus Inc. AP-30. SRCC. Cocoa, FL: Solar Rating and Certification Corporation. Available at: <www.solar-rating.org>. Accessed 2 February 2010.

SRCC. 1994. Methodology for Determining the Thermal Performance Rating for Solar Collectors. Document RM-1. Cocoa, FL: Solar Rating and Certification Corporation.

Threlkeld, J. L. and R. C. Jordan. 1958. "Direct Solar Radiation Available on Clear Days." *ASHRAE Transactions*, Vol. 64: p. 45.

Threlkeld, J. L. 1963. "Solar Irradiation of Surfaces on Clear Days." *ASHRAE Transactions*, Vol. 69: p. 24.

KREC PUBLICATIONS / PRESENTATIONS:

Publications

1. *25x'25 Roadmap for Kentucky: Charting Kentucky's Renewable Energy Future*. Louisville: University of Louisville, 2008.

2. *Kentucky Forum*: *Carbon Sequestration Through Agriculture and Forestry Management Summary*. Louisville: University of Louisville, 2009.

Presentations

The Project Director (PD), Cam Metcalf, along with representatives from the Kentucky Department for Energy Development and Independence, presented KEEPS Mentor awards to each of the eight pilot program participants, highlighting their individual contributions to the program at the 32nd Governor's Conference on the Environment on October 6, 2008.

The Project Director (PD), Cam Metcalf, presented the KEEPS program to representatives from the Ohio Valley Educational Cooperative at the University of Louisville on October 29, 2008.

The Project Director (PD), Cam Metcalf, presented the KEEPS program to members of the Kentucky School Plant Management Association at their annual conference held in Lexington, Kentucky on October 30, 2008.

The Project Director (PD), Cam Metcalf, presented the KEEPS program to members of the Kentucky School Board Association at their Winter Conference on December 13, 2008.

The Project Director (PD), Cam Metcalf, presented the Energy Management Process to KEEPS schools at the KEEPS Energy Management Workshop in Georgetown, Kentucky on February 24th, 2009.

The Project Director (PD), Cam Metcalf, presented the Energy Management Process to KEEPS schools at the KEEPS Energy Management Workshop in Cave City, Kentucky on February 26th, 2009.

The Project Director (PD), Cam Metcalf, presented at the 5th National 25x'25 Summit in Washington, DC on March 31st, 2009. Fifty-six leaders from around the United States learned how KREC formed, organized and began to advance renewable energy and energy efficiency in the Commonwealth.

The Project Director (PD), Cam Metcalf, presented the KEEPS Program at the 3rd Energizing Kentucky Conference in Lexington, KY on April 16th.

The Project Director (PD), Cam Metcalf, presented the Energy Management Process to KEEPS schools at the KEEPS Energy Management Workshop for Schools at Morehead State University, Morehead, Kentucky on September 12, 2009.

The KEEPS Coordinator, Technical Services Program Manager and Energy Efficiency Engineer presented the Energy Management Process to KEEPS schools at the KEEPS Energy Management Workshop for Schools at Kentucky Dam State Park, Gilbertsville, KY on September 22, 2009.

The Project Director (PD), Cam Metcalf, spoke on energy efficiency and conservation at the 33rd Governor's Conference on the Environment on October 1, 2009.

The KEEPS Coordinator spoke on the KEEPS program and energy teams at the Green Revolution Youth Conference on October 19, 2009.

The Project Director (PD), Cam Metcalf, presented a KEEPS program update and facilitated a KEEPS program round table discussion at the KSPMA (Kentucky School Plant Managers Association) conference on October 29th and 30th, 2009.

The Project Director (PD), Cam Metcalf, presented "Priorities for Kentucky," a review of Kentucky's renewable energy and energy priorities, before the Senate standing committee on Natural Resources and Energy on March 10, 2010.

The Project Director (PD), Cam Metcalf, gave a lecture for the University of Louisville's Green Engineering class on January 20, 2010.

The Energy Efficiency Engineer gave a lecture for the University of Louisville's Green Engineering class on January 27, 2010.

The Project Director (PD), Cam Metcalf, presented at the Kentucky Waste Water Operators Association in Louisville, Kentucky on April 14, 2010.

The Project Director (PD), Cam Metcalf, presented at the Kentucky SEN (Save Energy Now) workshop in Richmond, Kentucky on April 15, 2010.

The Project Director (PD), Cam Metcalf, spoke about the KEEPS program and energy teams at a Kentucky Association of School Business Officials Spring Conference on May 7, 2010.

The Project Director (PD), Cam Metcalf, presented at the 2010 National Environmental Summit in Orlando, Florida, May 24 - 27, 2010.

The Project Director (PD), Cam Metcalf, presented at the Hardin County Kentucky Recycling Committee on June 7, 2010.

The Project Director (PD), Cam Metcalf, and KREC Program Coordinator, Robert Hash, presented at the KREC Quarterly Meeting in Lexington on June 24, 2010.

The Project Director (PD), Cam Metcalf, presented at the KEEPS/KSBA training workshop for newly hired School Energy Managers on July 7, 2010.

The Project Director (PD), Cam Metcalf, served as a co-moderator, along with DEDI, for the "Wind Energy Webinar in Kentucky" webinar on July 23, 2020.

The Project Director (PD), Cam Metcalf, presented at the annual North American Hazardous Materials Management Association (NAHMMA) conference in St. Petersburg, Florida on July 27, 2010.

The Project Director (PD), Cam Metcalf, presented at the Economic Development through BioEnergy Symposium in Morehead, Kentucky on August 12, 2010.

KREC Public Information Officer (PIO), Dennis Smith staffed the KREC booth for the Eastern Kentucky University BioEnergy Field Day, held on September 9, 2010 in Richmond, Kentucky.

KREC Program Coordinator, Don Douglass, presented at the Economic Development through BioEnergy Symposium on September 23, 2010 in the Big Sandy Area Development District.

The Project Director (PD), Cam Metcalf, presented at the KREC Quarterly Meeting in Frankfort, Kentucky September 30, 2010

The Project Director (PD), Cam Metcalf, presented at the Economic Development Forum on Renewable Energy in Kentucky on the campus of Berea College on November 17, 2010

KREC Public Information Officer (PIO), Dennis Smith staffed the KREC booth for the National Farm Machinery Show in Louisville KY - February 16-17, 2011.

The Project Director (PD), Cam Metcalf participated with an exhibit and public information materials at the Conn Center for Renewable Energy Research at the University of Louisville statewide workshop on March 13-15, 2011.

The Project Director (PD), Cam Metcalf, presented at the KREC Quarterly Meeting in Louisville, Kentucky March 30, 2011.

The Project Director (PD), Cam Metcalf, presented at the Bluegrass ADD workshops in Lexington, Kentucky April 7, 2011.

The Project Director (PD), Cam Metcalf, presented at Sustainability Applied 2011 event in Windsor, Onatrio, Canada June 10, 2011.

The Project Director (PD), Cam Metcalf, presented at the KREC Quarterly Meeting in Louisville, Kentucky June 29, 2011.

APPENDIX 1

Organizational Chart for KREC and

Core Team Members (Currently)
(Revised April, 2011)

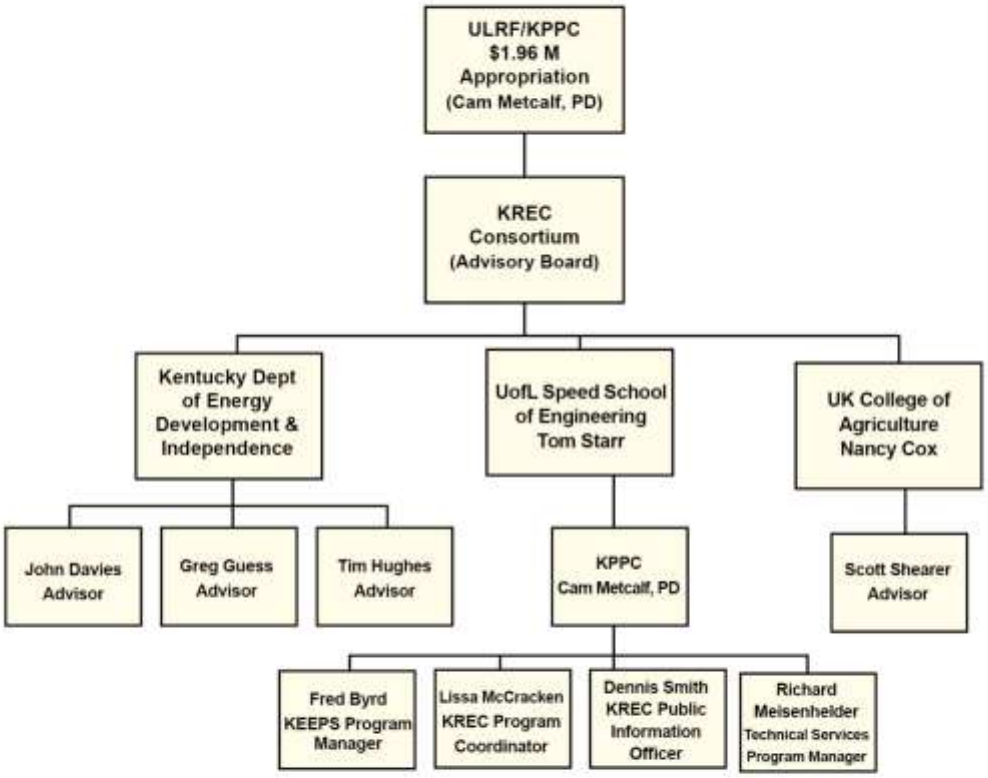

APPENDIX 2

KREC Facebook Page

APPENDIX 3

KREC Quarterly Meeting

PNC Room, Papa John's Cardinal Stadium
June 29, 2011 – 11:30 a.m. to 3:00 p.m.

AGENDA

11:30 – 11:40	Welcome/ Introduction	Cam Metcalf
11:40 – 12:00	Lunch Buffet	
12:00 – 12:30	Keynote speaker	Dr. Sue Nokes – UK
12:30 – 1:00	Research Presentations	Vijay Singh – UK Eric Berson/Keith Davis – UofL
1:00 – 1:15	Break & Visit Posters	
1:15 – 2:15	Research Presentations (continued)	Keith Sharp – UofL Mahendra Sunkara – UofL Paul Ratnasamy – UofL Mark McGinley – UofL
2:15 – 2:30	25x'25 Update	Brent Bailey – National 25x'25
2:30 – 3:00	Closing Remarks poster reviews/questions	Cam Metcalf